Geological Society Engineering Geology Special Publication No. 20

Coastal Chalk Cliff Instability

Edited by
R. N. Mortimore & A. Duperret

Published by The Geological Society

Coastal Chalk Cliff Instability

Society book reviewing procedures

The Society makes every effort to ensure that the scientific and production quality of its books matches that of its journals. Since 1997, all book proposals have been refereed by specialist reviewers as well as by the Society's Books Editorial Committee. If the referees identify weaknesses in the proposal, these must be addressed before the proposal is accepted.

Once the book is accepted, the Society has a team of Book Editors (listed above) who ensure that the volume editors follow strict guidelines on refereeing and quality control. We insist that individual papers can only be accepted after satisfactory review by two independent referees. The questions on the review forms are similar to those for *Quarterly Journal of Engineering Geology and Hydrogeology*. The referees' forms and comments must be available to the Society's Book Editors on request.

Although many of the books result from meetings, the editors are expected to commission papers that were not presented at the meeting to ensure that the book provides a balanced coverage of the subject. Being accepted for presentation at the meeting does not guarantee inclusion in the book.

More information about submitting a proposal and producing a Special Publication can be found on the Society's web site: www.geolsoc.org.uk.

It is recommended that reference to all or part of this book should be made in one of the following ways:

MORTIMORE, R.N. & DUPERRET, A. (eds) 2004. *Coastal Chalk Cliff Instability.* Geological Society, London, Engineering Geology Special Publications, **20**.

BROSSARD, J. & DUPERRET, A. 2004. Coastal chalk cliff erosion: experimental investigation on the role of marine factors. *In*: MORTIMORE, R.N. & DUPERRET, A. (eds) 2004. *Coastal Chalk Cliff Instability.* Geological Society, London, Engineering Geology Special Publications, **20,** 109–120.

Geological Society Engineering Geology Special Publication No. 20

Coastal Chalk Cliff Instability

EDITED BY

R.N. MORTIMORE
University of Brighton, UK

and

A. DUPERRET
Université du Havre, France

2004
Published by
The Geological Society
London

THE GEOLOGICAL SOCIETY

The Geological Society of London (GSL) was founded in 1807. It is the oldest national geological society in the world and the largest in Europe. It was incorporated under Royal Charter in 1825 and is Registered Charity 210161.

The Society is the UK national learned and professional society for geology with a worldwide Fellowship (FGS) of 9000. The Society has the power to confer Chartered status on suitably qualified Fellows, and about 2000 of the Fellowship carry the title (CGeol). Chartered Geologists may also obtain the equivalent European title, European Geologist (EurGeol). One fifth of the Society's fellowship resides outside the UK. To find out more about the Society, log on to www.geolsoc.org.uk.

The Geological Society Publishing House (Bath, UK) produces the Society's international journals and books, and acts as European distributor for selected publications of the American Association of Petroleum Geologists (AAPG), the American Geological Institute (AGI), the Indonesian Petroleum Association (IPA), the Geological Society of America (GSA), the Society for Sedimentary Geology (SEPM) and the Geologists' Association (GA). Joint marketing agreements ensure that GSL Fellows may purchase these societies' publications at a discount. The Society's online bookshop (accessible from www.geolsoc.org.uk) offers secure book purchasing with your credit or debit card.

To find out about joining the Society and benefiting from substantial discounts on publications of GSL and other societies worldwide, consult www.geolsoc.org.uk, or contact the Fellowship Department at: The Geological Society, Burlington House, Piccadilly, London W1J 0BG: Tel. +44 (0)20 7434 9944; Fax +44 (0)20 7439 8975; E-mail: enquiries@geolsoc.org.uk.

For information about the Society's meetings, consult *Events* on www.geolsoc.org.uk. To find out more about the Society's Corporate Affiliates Scheme, write to enquiries@geolsoc.org.uk.

Published by The Geological Society from:
The Geological Society Publishing House
Unit 7, Brassmill Enterprise Centre
Brassmill Lane
Bath BA1 3JN, UK

(*Orders*: Tel. +44 (0)1225 445046
Fax +44 (0)1225 442836)
Online bookshop: http://bookshop.geolsoc.org.uk

British Library Cataloguing in Publication Data
A catalogue record for this book is available from the British Library.

ISBN 1-86239-150-5

ISSN 0267-9914

Typeset by Servis Filmsetting Ltd, UK
Printed by Antony Rowe, UK.

Distributors

USA
AAPG Bookstore
PO Box 979
Tulsa
OK 74101-0979
USA
Orders: Tel. +1 918 584-2555
Fax +1 918 560-2652
E-mail bookstore@aapg.org

India
Affiliated East-West Press PVT Ltd
G-1/16 Ansari Road, Daryaganj,
New Delhi 110 002
India
Orders: Tel. +91 11 2327-9113
Fax +91 11 2326-0538
E-mail affiliat@nda.vsnl.net.in

Japan
Kanda Book Trading Company
Cityhouse Tama 204
Tsurumaki 1-3-10
Tama-shi, Tokyo 206-0034
Japan
Orders: Tel. +81 (0)423 57-7650
Fax +81 (0)423 57-7651
Email geokanda@ma.kcom.ne.jp

Contents

Introduction 1

MORTIMORE, R.N., LAWRENCE J., POPE, D., DUPERRET, A. & GENTER, A. Coastal cliff geohazards in weak rock: the UK Chalk cliffs of Sussex 3

DUPERRET, A., GENTER, A, MARTINEZ, A. & MORTIMORE, R.N. Coastal chalk cliff instability in NW France: role of lithology, fracture pattern and rainfall 33

GENTER, A., DUPERRET, A., MARTINEZ, A., MORTIMORE, R.N. & VILA, J-L. Multiscale fracture analysis along the French chalk coastline for investigating erosion by cliff collapse 57

MORTIMORE, R.N., STONE, K.J., LAWRENCE J. & DUPERRET, A. Chalk physical properties and cliff instability 75

WILLIAMS, R.B.G., ROBINSON, D.A., DORNBUSCH, U., FOOTE, Y.L.M., MOSES, C.A. & SADDLETON, P.R. A sturtzstrom-like cliff fall on the Chalk coast of Sussex, UK 89

MITCHELL, S.B. & POPE, D.J. Prediction of nearshore wave energy distribution by analysis of numerical wave model output: East Sussex coastline, UK 99

BROSSARD, J. & DUPERRET, A. Coastal chalk cliff erosion: experimental investigation on the role of marine factors 109

WOLTERS, G. & MÜLLER, G. The propagation of wave impact induced pressures into cracks and fissures 121

DORNBUSCH, U., MOSES, C.A., ROBINSON, D.A. & WILLIAMS, R.B.G. Laboratory abrasion tests on beach flint shingle 131

COSTA, S., DELAHAYE, D., FREIRÉ-DIAZ, DI NOCERA, L., DAVIDSON, R. & PLESSIS, E. Quantification of the Normandy and Picardy chalk cliff retreat by photogrammetric analysis 139

DAIGNEAULT, M., BOUCHARDON, J.-L. & GUY, B. Coastal cliff erosion vulnerability on the Canadian east coast (Baie des Chaleurs area): a multi-parameter visualization tool 149

Index 169

Contents

Introduction 1

MORTIMORE, R.N., LAWRENCE J., POPE, D., DUPERRET, A. & GENTER, A. Coastal cliff geohazards in weak rock: the UK Chalk cliffs of Sussex 3

DUPERRET, A., GENTER, A, MARTINEZ, A. & MORTIMORE, R.N. Coastal chalk cliff instability in NW France: role of lithology, fracture pattern and rainfall 33

GENTER, A., DUPERRET, A., MARTINEZ, A., MORTIMORE, R.N. & VILA, J-L. Multiscale fracture analysis along the French chalk coastline for investigating erosion by cliff collapse 57

MORTIMORE, R.N., STONE, K.J., LAWRENCE J. & DUPERRET, A. Chalk physical properties and cliff instability 75

WILLIAMS, R.B.G., ROBINSON, D.A., DORNBUSCH, U., FOOTE, Y.L.M., MOSES, C.A. & SADDLETON, P.R. A sturtzstrom-like cliff fall on the Chalk coast of Sussex, UK 89

MITCHELL, S.B. & POPE, D.J. Prediction of nearshore wave energy distribution by analysis of numerical wave model output: East Sussex coastline, UK 99

BROSSARD, J. & DUPERRET, A. Coastal chalk cliff erosion: experimental investigation on the role of marine factors 109

WOLTERS, G. & MÜLLER, G. The propagation of wave impact induced pressures into cracks and fissures 121

DORNBUSCH, U., MOSES, C.A., ROBINSON, D.A. & WILLIAMS, R.B.G. Laboratory abrasion tests on beach flint shingle 131

COSTA, S., DELAHAYE, D., FREIRÉ-DIAZ, DI NOCERA, L., DAVIDSON, R. & PLESSIS, E. Quantification of the Normandy and Picardy chalk cliff retreat by photogrammetric analysis 139

DAIGNEAULT, M., BOUCHARDON, J.-L. & GUY, B. Coastal cliff erosion vulnerability on the Canadian east coast (Baie des Chaleurs area): a multi-parameter visualization tool 149

Index 169

Geological Society, London, Engineering Geology Special Publications

About this title

Geological Society, London, Engineering Geology Special Publications 2004; v. 20; p. NP
doi:10.1144/GSL.ENG.2004.020.01.13

Geological Society Engineering Geology Special Publication No. 20

Coastal Chalk Cliff Instability

Edited by

R. N. Mortimore & A. Duperret

Most of the rocky coastlines around the world are subject to active erosion processes. Because of the growing hazard to local communities from coastal cliff retreat, it is necessary to investigate where, when and how cliffs collapse. The results of these studies are vital for the planners and local authorities responsible for safety and access to cliffs and beaches. This volume focuses on the coastal chalk cliffs of the English Channel, where a multidisciplinary approach has been used to understand active coastal cliff recession.

The book is organized around three main themes: the geological factors controlling cliff instability, the marine parameters influencing coastal erosion and the use of some new tools for hazard assessments.

This volume will be of use to academics and professionals working on rocky shores, with an interest in sedimentary geology, stratigraphy, tectonics, geomorphology, engineering geology, coastal engineering and GIS.

Cover illustration:
Coastal chalk cliff collapse (about 8000 m^3 of chalk rocks) observed on 29 March 2002 at Fécamp (Seine-Maritime, NW France).
Photograph by Anne Duperret.

Geological Society, London, Engineering Geology Special Publications

Introduction

R.N. Mortimore and A. Duperret

Geological Society, London, Engineering Geology Special Publications 2004; v. 20; p. 1-2
doi:10.1144/GSL.ENG.2004.020.01.01

Introduction

R.N. Mortimore[1] & A. Duperret[2]

[1] Applied Geology Research Unit, School of the Environment, University of Brighton, Moulsecoomb, Brighton BN2 4GJ, UK

[2] Laboratoire de Mécanique, Physique et Géosciences, Université du Havre, BP 540, 76 058 Le Havre cedex, France

In 1998 a European funded research programme ROCC (Risk of Cliff Collapse) was initiated by a team from France and the UK because of the growing hazard to local communities from chalk cliff retreat. Could the *where*, *when* and *how* of cliff collapses be answered and could the rate and scale of cliff retreat be modelled more accurately? Such answers are vital to the planners and local authorities responsible for the safety and access to cliffs and beaches. The primary research area is the eastern English Channel, where in northeast France there is 120km of Chalk coast, and in southeast England 40km in Sussex and a similar length in Kent. The research programme brought together geologists and engineers from BRGM, the University of Le Havre and the University of Brighton in partnership with the regional governments of the Somme, Seine Maritime, southeast England and their constituent local authorities. This book, representing several years of previous and concurrent research on the engineering geology of chalk and coastal processes, is the outcome of that research programme and allied work.

It was fortuitous that several other chalk investigations were coming to completion prior to ROCC starting. These formed a foundation on which to build the investigations. In particular, a refined Chalk lithostratigraphy with practical application to mapping and detailed correlation, was finally accepted by a joint stratigraphic committee of the Geological Society and the British Geological Survey in September 1999 (Mortimore 1986; Bristow *et al.* 1997; Rawson *et al.* 2001). This meant that a consistent set of lithological units and terms could be used for both coastlines (e.g. Mortimore 2001; Duperret *et al.* 2002). This stratigraphy and associated sedimentological studies proved to be a vital framework for analysing the tectonic structure, fracture characteristics and types of cliff failure in the Chalk. Similarly, the CIRIA *Engineering in Chalk* (Lord *et al.* 2002) begun in 1992, contained a methodology agreed by industry for describing and classifying the engineering characteristics of the chalk which was applied to the cliff investigations. In addition, Hutchinson (2002) had completed a review of major cliff collapses in the northwest European chalk and this and his previous work formed a further foundation to the ROCC studies.

ROCC has been concerned with more than just the geology or the mechanics of cliff failure. The ROCC team was multidisciplinary made up of geologists from the Universities of Brighton (Mortimore, De Pomerai & Lawrence) and Le Havre (Duperret & Martinez) and the French Geological Survey, Bureau de Recherches Géologiques et Minières BRGM (Genter); geophysists from BRGM (Watremez & Gourry); rock mechanics from BRGM and Brighton (Gentier & Stone); coastal engineers from Le Havre (Brossard) and Brighton (Mitchell & Pope) and a GIS specialist from BRGM (Laville). Pierre Watremez (BRGM, Brest) was one of the driving forces behind the ROCC Project.

The papers contained in this special publication (authors in bold type below) were presented at the International Conference on *Coastal Rock Slope Instability: Geohazard and Risk Analysis* held at the Université du Havre 30–31 May 2001. In addition to the work of the ROCC team, papers included other European funded research work on coastal processes such as marine erosion rates BERM Project (Beach Erosion on the Rives Manche)). The Conference included a field excursion to study the coastal chalk cliffs of Upper Normandy in which local communities participated.

The book is organized into three sections: the first deals with the primary geological controls on cliff instability; the second part looks at specific marine influences on coastal erosion of weak rock cliffs; in the third part some particular tools that may be used to investigate coastal cliff erosion are presented.

Geological factors controlling cliff instability hazards

Notwithstanding the wide range of studies brought together by the ROCC programme the basic geology and the range of cliff instability hazards had to be identified first. Because of the different lengths of coastline (120km in France, 40km in England) and the short period of funding for the project (two years) a different approach was adopted for the two coastlines. In the UK detailed hazard mapping was possible at a scales of 1:500 to 1:10000 (summarized in **Mortimore** *et al.*). In France, however, the mapping scale was at 1:100000.

From: MORTIMORE, R. N. & DUPERRET, A. (eds) 2004. *Coastal Chalk Cliff Instability*. Geological Society, London, Engineering Geology Special Publications, **20**, 1–2. 0267-9914/04/$15.00

The factors controlling cliff failures and the resulting types, scales and volumes of failures were measured in the field (**Duperret** *et al.*). The rock mass character was investigated in detail both in the field and by analysis of oblique aerial photographs to establish the role of different scales of fracturing on cliff instability (**Genter** *et al.*). At the same time it was necessary to investigate the physical properties of the chalk material that might have an influence on mechanisms of chalk cliff collapse (**Mortimore** *et al.*).

One paper concentrates on a particular aspect of chalk cliff failure: the potentially large rock avalanches on the Seven Sisters investigated from historical records (**Williams** *et al.*).

Marine parameters influencing coastal erosion

Mitchell & Pope investigate the role of wave energy dispersion in the inshore area from numerical analyses. In contrast, **Brossard & Duperret** have carried out laboratory flume experiments on wave energy distribution on beaches and on the base of the cliffs. A further aspect of wave impact on the cliffs is the role of fractures and cracks in the cliffs on the wave impact induced pressure propagation investigated by **Wolters & Muller**.

Flint gravel beaches are an important component of chalk coastlines and **Dornbusch** *et al.* analyse the rate of abrasion of different types of flint gravel to obtain an idea of the residence time of beach materials along different parts of the chalk coastline.

Other tools for hazard assessments

Calculating cliff-line retreat is approached in several ways and is important for planners. **Costa** *et al.* use aerial photogrammetry to quantify the cliff-line retreat on the French coast over a 30-year period. **Daigneault** *et al.* propose an interesting new way of identifying the most important factors where multiple processes are involved in coastal cliff erosion. Their case study is from the Canadian east coast.

In the UK a ROCC database was established at the University of Brighton (Applied Geology Research Unit) which provided information for local authorities on the sources of information including aerial and other photographs, professional reports and papers and the details of the geology and cliff failures. The database includes all the results from the ROCC and associated investigations. In addition, a GIS programme was used to develop detailed topographic and geology maps for hazard identification and for wrapping aerial photographs onto the maps. This is also included with the ROCC database. In France a GIS programme was used as a tool for identifying particular hazards based on the geology, topography and the volumes and scales of failures identified from historical records and current studies.

Bringing together the different approaches to geology and engineering from quite different cultures was a major benefit. The ROCC team worked together throughout on both sides of the English Channel so that each person contributed equally to the studies published here. This was a genuine team effort, which is reflected in the multiauthorship of the papers.

References

BRISTOW, C. R., MORTIMORE, R. N. & WOOD, C. J. 1997. Lithostratigraphy for mapping the Chalk of Southern England. *Proceedings of the Geologists' Association*, **109**, 293–315.

DUPERRET, A., MORTIMORE, R. N., POMEROL, B., GENTER, A. & MARTINEZ, A. 2002. L'Instabilité des Falaises de la Manche en Haute-Normandie. Analyse Couplée de la Lithostratigraphie de la Fracturation et des Effrondements. *Bulletin d'Information des Géologues du Bassin de Paris*, **39**, 5–26.

HUTCHINSON, J. N. (2002). Chalk flows from coastal cliffs of northwest Europe. *In*: DE GRAFF, J. V. & EVANS, S. G. (eds) *Catastrophic Landslides: Occurrence and Effects*. Geological Society of America, Reviews in Engineering Geology, **14**, 257–302.

LORD, J. A., CLAYTON, C. R. I. & MORTIMORE, R. N. 2002. *Engineering in Chalk*. Construction Industry Research and Information Association CIRIA Publication C574.

MORTIMORE, R. N. 1986*a*. Stratigraphy of the Upper Cretaceous White Chalk of Sussex. *Proceedings of the Geologists' Association*, **97**, 97–139.

MORTIMORE, R. N. 2001. *Report on mapping of the Chalk Channel coast of France from Port du Havre-Antifer to Ault, June-September 2001*. Bureau de Recherches Géologiques et Minières (BRGM) BP 6009 – 45060, Orléans cedex 2, France

RAWSON, P. F., ALLEN, P. & GALE, A. S. 2001. The Chalk Group – a revised lithostratigraphy. *Geoscientist*, **11**, 21.

ROCC database and GIS *www.bton.ac.uk/environment/ROCC*

Coastal cliff geohazards in weak rock: the UK Chalk cliffs of Sussex

R.N. Mortimore[1], J. Lawrence[1], D. Pope[1], A. Duperret[2] & A. Genter[3]

[1] Applied Geology Research Unit, School of the Environment, University of Brighton, Brighton BN2 4GJ, UK

[2] Laboratoire de Mécanique, Faculté des Sciences et Techniques, Université du Havre, 25 rue Phillipe Lebon, BP 540, 76058 Le Havre cedex, France

[3] Bureau de Recherches Géologiques et Minières (BRGM) BP 6009 – 45060 Orléans cedex, France

Abstract: Geohazards related to chalk coastal cliffs from Eastbourne to Brighton, Sussex are described. An eight-fold hazard classification is introduced that recognizes the influence of chalk lithology, overlying sediments and weathering processes on location, magnitude and frequency of cliff collapses. Parts of the coast are characterized by cliffs of predominantly a single chalk formation (e.g. Seven Sisters) and other sections are more complex containing several Chalk formations (Beachy Head). Rock properties (intact dry density or porosity) and mass structure vary with each formation and control cliff failure mechanisms and scales of failures. The Holywell Nodular Chalk, New Pit Chalk and Newhaven Chalk formations are characterized by steeply inclined conjugate sets of joints which lead to predominantly plane and wedge failures. However, the dihedral angle of the shears, the fracture roughness and fill is different in each of these formations leading to different rock mass shear strengths. In contrast the Seaford and Culver Chalk formations are characterized by low-density chalks with predominantly clean, vertical joint sets, more closely spaced than in the other formations. Cliff failure types range from simple joint controlled conventional plane and wedge failures to complex cliff collapses and major rock falls (partial flow-slides) involving material failure as well as interaction with discontinuities. Other hazards, related to sediments capping the Chalk cliffs, include mud-slides and sandstone collapses at Newhaven, and progressive failure of Quaternary Head and other valley-fill deposits. Weathering, including the concentration of groundwater flow down dissolution pipes and primary discontinuities, is a major factor on rate and location of cliff collapses. A particular feature of the Chalk cliffs is the influence of folding on cliff stability, especially at Beachy Head, Seaford Head and Newhaven. A new classification for cliff collapses and a new scale of magnitude for collapses are introduced and used to identify, semi-quantify and map the different hazards.

Climate (and climate change) and marine erosion affect the rate of development of cliff collapse and cliff-line retreat. This was particularly evident during the wet winters of 1999–2000–2001 when the first major collapses along protected sections of coastline occurred (Peacehaven Cliffs protected by an undercliff wall; Black Rock Marina the Chalk cliffs and the Quaternary Head). It is the geology, however, that controls the location and scale of erosion and cliff failure.

Introduction

Instability of coastal cliffs is an increasing cause for concern for many local authorities and government agencies with coastlines to manage. This paper presents some of the results of investigations into the Risk of Cliff Collapse (ROCC) along the coast of the English Channel from Eastbourne to Brighton (40km) in Sussex. The detailed results are presented elsewhere as a hazard map at a scale of 1:15000, and supporting ROCC Database (Mortimore *et al.* 2001*a*) as a contribution to managing this coastline.

In England, Chalk forms extensive cliff lines along the coast from Yorkshire to Devon. Inland, chalk cliff and slope instability along rail and road cuttings and quarry faces, is a significant aspect of ground engineering (e.g. Williams 1990). Hutchinson (1971, 1988*b*; 2002) and Middlemiss (1983) investigated Chalk coastal cliff stability in Kent. Hutchinson established the presence of two types of Chalk cliff failure, the Joss Bay Type (Hutchinson 1971) and the occurrence of Chalk flows (Hutchinson 1983; 2002). Middlemiss (1983) recognized regional patterns in the rock structure as an important component of cliff failure mechanisms. Compared to Kent, Sussex Chalk cliffs contain a more complex geology and over a relatively short distance of 40km the entire Late Cretaceous succession of rocks is exposed. This succession begins with the Gault Formation (clay) at the base of the cliffs at Beachy Head followed westwards by all the Chalk to the basal beds of the Culver Chalk Formation between Newhaven and Peacehaven (Figs 1 & 2). In places these cliffs are capped by Palaeogene sediments (sands and clays), Quaternary Clay-with-flints and loess (a metastable silt). Elsewhere only a thin veneer of topsoil covers periglacially fractured chalk. Each of the geological formations has its own impact on the types and scales of cliff slope geohazards present and are, in terms of lithology, fracture style and range of stratigraphy, different to the Kent coast examples. Each Chalk formation also imparts a special character to the shape (geomorphology) of the cliffs (Figs 2–4).

The highest cliffs in the entire investigation of the French and English coastlines occur at Beachy Head (>160m) and the lowest points are truncated valleys, some reaching

From: MORTIMORE, R. N. & DUPERRET, A. (eds) 2004. *Coastal Chalk Cliff Instability*. Geological Society, London, Engineering Geology Special Publications, **20**, 3–31. 0267-9914/04/$15.00

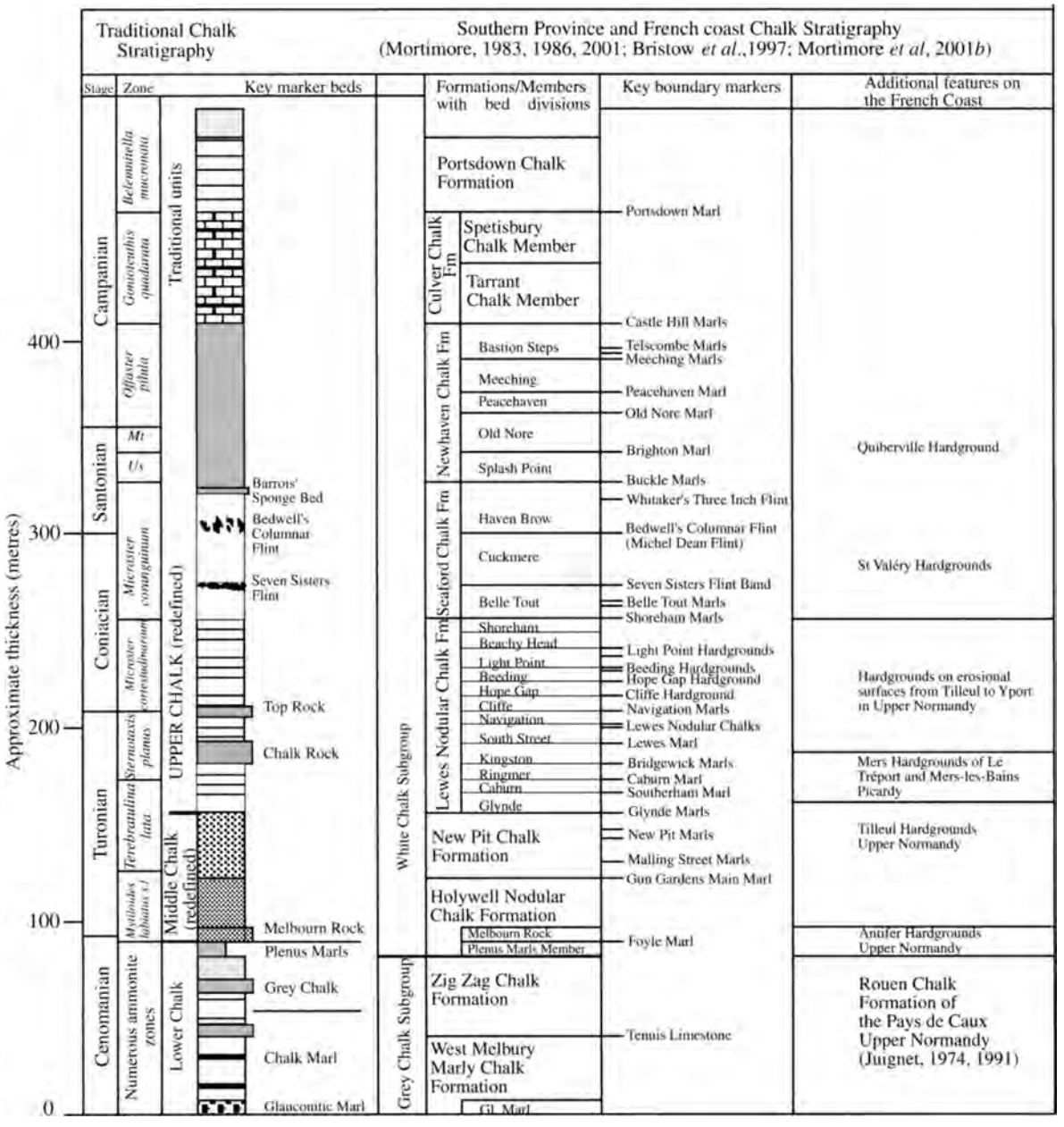

Fig. 1. Chalk lithostratigraphic units (Subgroups, Formations and Members) are those for mapping purposes on the INTERREG II ROCC Project.

sea-level, where chalk has been deeply degraded by Quaternary weathering and alteration. Slope deposits, hillwash and valley-fill deposits (Head) cover the degraded Chalk. Cliff height is another important factor in the development of cliff failures in terms of scale of collapses and run-out at the base of the cliff.

Each block of Chalk coastline (Fig. 2) exists in the form it does because of geological tectonic structures (folds and faults). The high cliffs at Beachy Head, capped by the Seaford Chalk Formation, are raised to that level on the axis of the Beachy Head Anticline (Figs 2, 3 & 5). The same horizons of flint seen at the top of Beachy Head in the Seaford

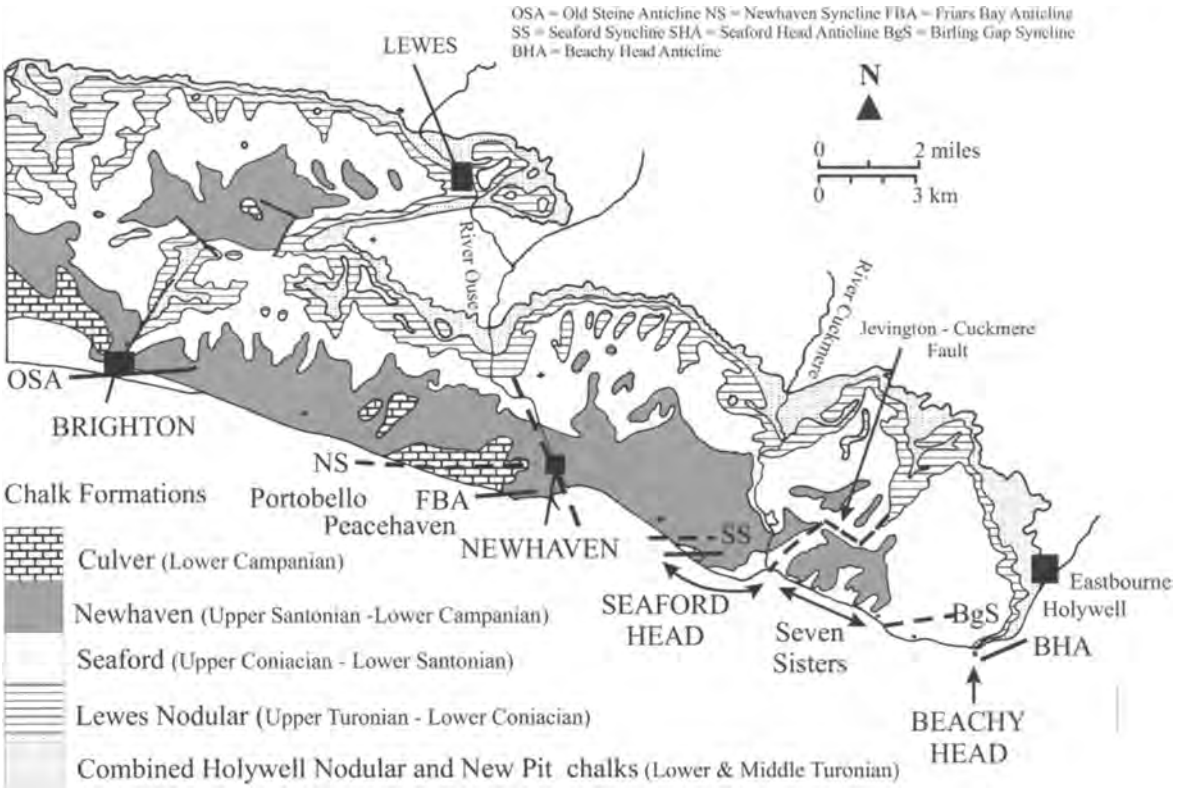

Fig. 2. Map of the Chalk formations in the East Sussex Chalk Downs and coastal cliffs.

Chalk Formation are at beach level at Birling Gap in the core of the Birling Gap Syncline. The Seaford Head Anticline again brings the Seaford Chalk to the top of the cliff at the Castrum and younger Newhaven and Culver Chalk formations are present in the cliffs northwestward at Seaford in the core of the Seaford Syncline (Fig. 2). A further complementary set of folds, the Friar's Bay Anticline and Newhaven Syncline, control the distribution of Chalk formations and overlying Palaeogene sediments on the cliffs at Newhaven and Peacehaven. Towards Black Rock at Brighton older beds in the Newhaven Chalk Formation are brought into the cliffs on the Old Steine Anticline (Fig. 2). The changing dip of strata and the change in types of chalk present in the cliffs caused by these tectonic folds has a marked effect on styles and scales of cliff failures.

Major strike-slip faults control the position of the main river valleys of the Cuckmere (Jevington Fault) and the Ouse (Newhaven Fault) which separate the Eastbourne, Seaford and Brighton Chalk blocks respectively (Fig. 2). These strike-slip faults have an impact on smaller-scale fracturing in the Chalk in turn, controlling primary modes of cliff failure.

Cliff slope geohazards are defined in Tables 1 and 3. This paper is concerned with the first aspect, *hazard identification*, as a basis for hazard analysis and risk determination and/or evaluation.

The scale or magnitude of hazards varies depending on the type of chalk or overlying deposits (lithology), the rock structure (folds, faults, joints) and the height of the cliffs. To assist in the evaluation of potential hazards a magnitude scale has been agreed for both sides of the Channel (Table 2). The volume of debris produced by a cliff fall is also used to assess the potential for chalk flows. Cliff collapses are frequently fracture controlled in terms of particular points of marine erosion, weathering and the scale and style of cliff failures. Both engineering rock mass data (scan-line surveys) and major types of fracture distribution in the Chalk of both coasts of the Channel have been investigated (Mortimore *et al.* 2001*a*, *b*; Genter *et al.* 2004). The types of cliff collapse and their possible triggers are further investigated (Duperret *et al.* 2004).

Hazards have been divided into nine classes (Table 3) based on the analyses of historical and recent observations of cliff failures made along the coastlines of England and France. These nine classes are mapped onto the coastline in a GIS format (ROCC Database) and the data related to the

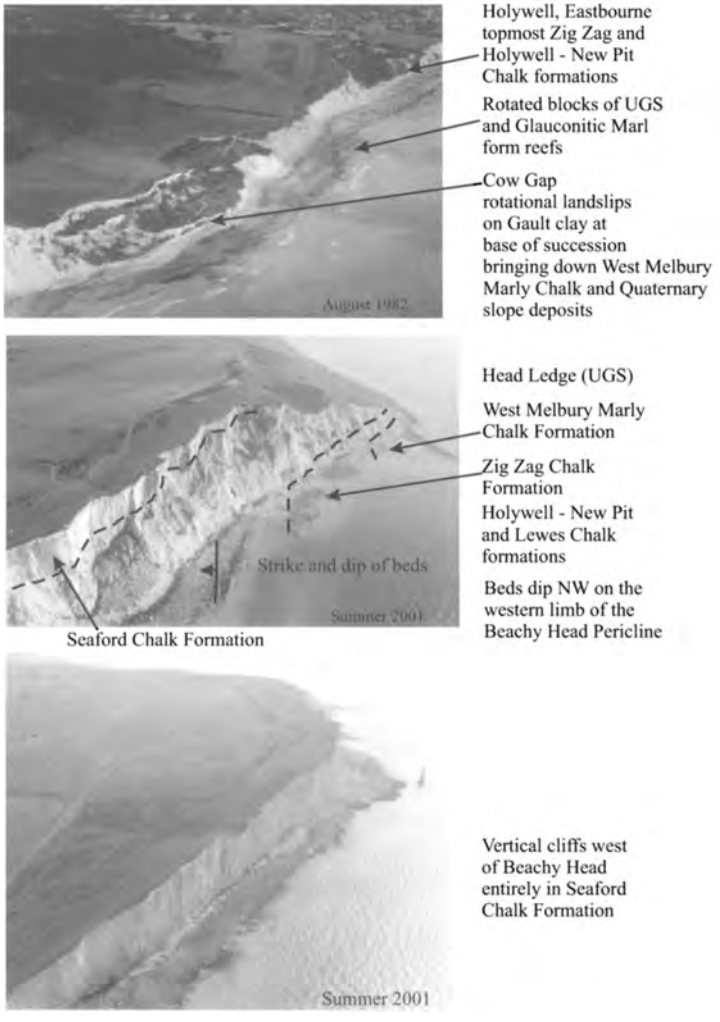

Fig. 3. Cliff geomorphology at Beachy Head related to structural setting and geological formations present (photographs R.N. Mortimore).

hazards is held in an ACCESS database developed by the authors and now held by the relevant local authorities (Mortimore *et al.* 2001*a*).

Methods of investigation

Mapping was carried out by physically walking the coast sections, photographing and drawing sketches of the cliffs, locating key features on a 1:10000 scale map, and checking the stratigraphy using key litho- and biostratigraphical marker beds. Rock mass data (scan-line surveys); the volume and details of failures, failure surfaces, weathering features were all noted. Each site was recorded several times over a three-year period to record the changes that had taken place. Photographic, historical and rock mass records have been stored in digital form in the ROCC database.

A generalized stratigraphy (Fig. 1) shows the lithostratigraphic units used in this paper and on the ROCC project for both sides of the Channel. These are the units now used for mapping the Chalk of the southern UK and along the coast of northern France. These lithostratigraphic units also define changes in physical properties and rock mass character of the Chalk which, in turn, influence rock slope stability and aquifer properties. There are local features of the lithology on the French coast (Mortimore 2001*a*) that also influence cliff instability.

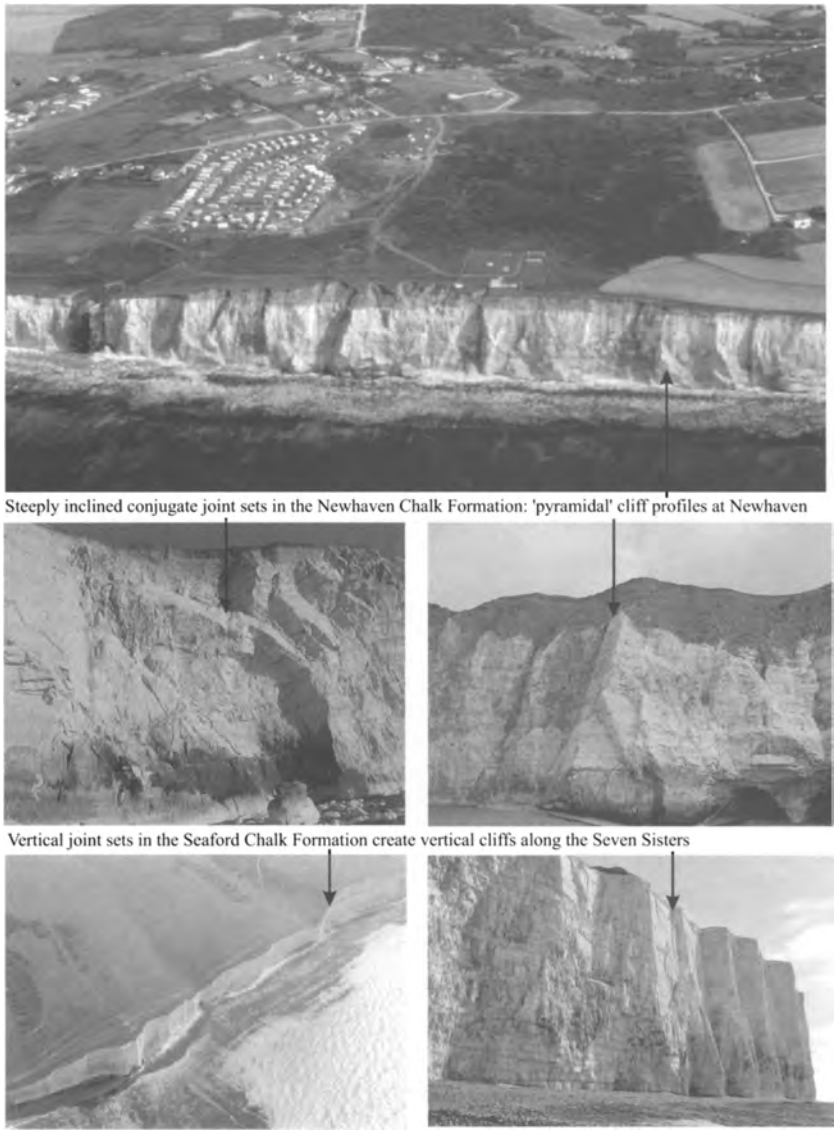

Fig. 4. Contrasting coastal geomorphology in the Seaford and Newhaven Chalk formations.

The cliff collapse geohazards

Each section of cliff contains geohazards specific to that site as well as more general hazards. Specific hazards are generally related to lithology, style of fracturing and cliff height and include types of rock slope failure. General hazards include continuous spalling of small fragments. The rate at which a hazard develops is partly related to rates of marine erosion at the base of the cliff, partly to weathering and exposure of the face to rainfall and frost events, and partly to the type of material capping the cliff. Coast protection appears to slow the rate of hazard development but seems not to completely eliminate it. In this paper we summarize the results from the 17 separate geohazard sections along the Sussex coast between Eastbourne and Brighton defined by Mortimore *et al.* 2001*a* (Table 4). Each type of failure is described in the sequential order given in Table 3 and compared or contrasted with failures from the Kent and French Chalk coasts.

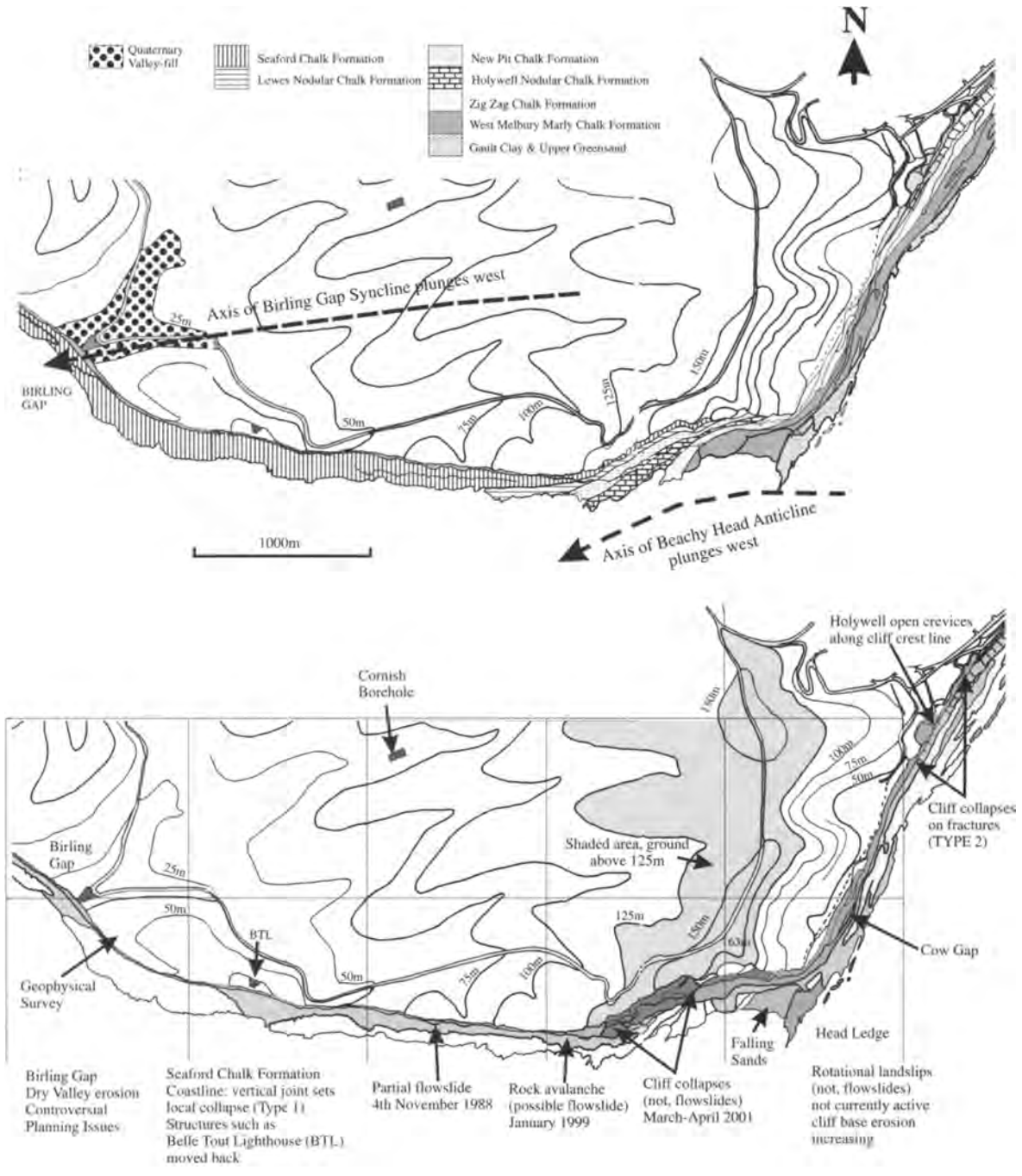

Fig. 5. Sketch map of the geology, cliff height and location of main collapse hazards between Eastbourne and Birling Gap (Beachy Head).

Table 1. *Cliff slope geohazards and risk*

The questions	*The process*
What type of cliff failure can occur and/or what can go wrong?	Hazard identification
How likely is a failure or how likely is it to go wrong?	Hazard analysis
What are the associated risks?	Consequence analysis
What are the risks?	Risk determination
Are the risks acceptable and can they be reduced?	Risk evaluation

Table 2. *Classification of the scale of Chalk cliff failures (Magnitude)*

Magnitude scale for cliff collapses	*Typical volume of rock involved (m^3)*
1	<1
2	1–10
3	10–100
4	100–1000
5	1000–10000
6	10000–50000
7	50000–100000
8	100000–500000

Cliffs with one or two Chalk formations (Hazard Class 1)

Several sections of Chalk cliffs such as the Seven Sisters, most of the cliffs between Newhaven and Brighton and cliffs at Holywell, Eastbourne, are primarily made of a single Chalk Formation. The rock mass character of the formation has a strong control on the cliff failure mechanisms. Other sections such as cliffs immediately west of Beachy Head Lighthouse, Seaford Head and Telscombe Cliffs contain two formations each imposing a special character to the rock mass and cliff failure mechanisms.

Simple vertical collapses: Seaford Chalk Formation; Seven Sisters Type (Class 1a)

The simplest cliff failures are vertical collapses where one Chalk formation with a predominant set or sets of joints controls the type and scale of failures. Except for the basal Belle Tout Beds which contain marl seams, the Seaford Chalk Formation is very pure, perhaps the most homogeneous of all the Chalk formations. This leads to a regular fracture pattern with two predominant near-vertical joint directions (sets) controlling the shape of the cliff line (Figs 3 & 4; Mortimore 2001*b*). Failure involves the progressive opening of the joints (a tension crack) sub–parallel to the cliff face (Figs 6 & 7). Eventually the increasing load of the failing stack of chalk overcomes the shear strength of the remaining chalk attached to the joint surface at some point down the tension crack. This point can usually be identified after the failure by the extensive 'powder' of chalk fines where the chalk must have failed explosively. Frequently, the failure surface extends vertically down to the base of the cliff (a vertical slab). In some cases marine undercutting and progressive 'bottom–up' vaulting failure along joints can be seen as part of the cause (Fig. 8), in other cases there is no notch or undercutting by marine erosion (Fig. 7). The width of such failures varies from a few metres to up to 100 m involving 100 m^3 to 100000 m^3 of rock. Lateral boundaries are frequently controlled by fractures perpendicular to the cliff face or faults. The eastern boundary tends to be joint controlled whereas the western boundary is controlled by the simple thinning of the failure wedge caused by the main joint set being subparallel to the cliff face.

The run-out of debris indicates that the collapse retains a crude stratigraphy although the run out can be very limited (e.g. a few metres, (Figs 6b & 7). Hence these collapses start out as a toppling failures (e.g. DeFreitas & Watters 1973) but end up as a slide with the basal beds ending furthest out from the base of the cliff. Many variants on this basic theme have been observed including bottom-up cliff failures and failures localized to the top of the cliff only (Fig. 8).

Sections of the Sussex coast illustrating the Seven Sisters type of failure include the cliff section northwestwards of Beachy Head, combining the Lewes Nodular Chalk and Seaford Chalk formations (Figs 3 & 6a). Here the cliff tends to collapse progressively bottom-up in the Lewes Chalk and top-down in the Seaford Chalk. The Lewes Chalk contains many surfaces along which overbreak occurs (e.g. marl seams) leaving local overhanging features similar to Veulettes (Fig. 8). Where the entire cliff collapses (i.e. both the Lewes and Seaford chalks fail together), then large rockfalls develop (e.g. the 4 November 1988 fall which failed from the 92 m high point on the cliff, Fig. 5). Only the upper beds of the Lewes Chalk are present at this point at the base of the cliff, overlain by Seaford Chalk.

In the Beachy Head to Birling Gap cliffs northwest of the 92 m point at Shooters Bottom (Fig. 6b), the cliffs are entirely in the Seaford Chalk formation and the northerly dip of strata is very gentle into the core of the Birling Gap Syncline. Cliff collapses here develop along the predominantly vertical joints sets. One joint set is subparallel to the cliff direction and these joints open from the top down. These types of failure typically yield 10000–50000 m^3 of material (Magnitude 6). Occasionally larger cliff collapses occur, particularly where local faults and the joint sets combine and these create collapses involving 50000–100000 m^3 of material (Magnitude 7 failures).

The Seven Sisters are composed primarily of Seaford Chalk Formation with a capping of Newhaven Chalk on the highest hills (Mortimore 1997). The typical vertical fracture sets in the Seaford Chalk, and its pure white composition, give a special character to the Seven Sisters (Fig. 4). Several faults are also present and these are usually the locus of solution widening and sediment-filled cave systems. Consequently, the faults also bound failures in the cliff. The very

Table 3. *Classification of Chalk cliff collapse hazards*

Hazard	*Description*	*Typical example*
1. Cliffs with single strata		Seven Sisters, Seaford Chalk Friars Bay, Newhaven Chalk
1a Simple vertical collapses	Vertical fracture sets control style of failure and height of cliff controls magnitude; limited run-out at base of cliff	Belle Tout to Cuckmere (Seven Sisters)
1b Plane and wedge collapses	Loose rock collapses controlled by complex system of conjugate joint sets: sometimes within part of cliff, others involve entire cliff	Holywell Nodular Chalk, Eastbourne Newhaven Chalk, Friars Bay
1c Large rock falls involving entire cliff (partial flow slides) Magnitude 5–7	Cliff collapse leads to long run-outs in which stratigraphic integrity of blocks is retained	Beachy Head to Belle Tout and Seven Sisters
2. Cliffs with more than one type of chalk formation		Beachy Head
2a Staged failure	Failure at top of cliff partly toppling partly sliding	Highest parts of Beachy Head
2b Staged failure	Failure of central mass mainly by complex multiple plane and wedge failures	Central part of Beachy Head
2c Staged failure	Failure at base of cliff by plane, wedge and complex rock interactions on fault zones	Base of highest parts of Beachy Head
3. Spalling of chalk and flint	Volume of debris related to weathered state of chalk	Occurs everywhere
4. Rotational slides	Weak mudstone strata at base of cliff beneath the Upper Greensand and Chalk and	Cow Gap, Eastbourne
5. Mudslides from top of cliff	Mudstone formations capping the cliffs	Castle Hill Newhaven
6. Toppling of sandstone from cliff top		Palaeogene sandstones at Castle Hill, Newhaven
7. Washouts of karst fills		Seaford Head
8. Slope failures in dry valley-fills or related rocks	Related to weathered state of and material (e.g. Head etc)	Birling Gap; Black Rock, Brighton

Table 4. *Features geologically mapped on the English Channel Coast from Eastbourne to Brighton*

Stratigraphy	*Structure/geomorphology*	*Geohazard*
Lithostratigraphic units based primarily on Juignet, 1974; Mortimore 1983, 1986; Mortimore & Pomerol, 1987, 1988; 1996; Bristow *et al.* 1997; Mortimore *et al.* 2001*b*	1. Style of fracturing in each unit of the Chalk	Hazards related to the cliff top (includes variable deposits on the cliff top of Tertiary and Quaternary sediments and Sarsen stones and karst or calcrete).
	2. Faults and fault zones	
Biostratigraphic marker beds, zones and stages as applied to the Chalk (Birkelund *et al.*, 1984; Mortimore, 1986; Mortimore & Pomerol, 1987; Rawson *et al*; 1996; Mortimore *et al.* 2001*b*)	3. Cliff top profiles;	Hazards related to the cliff face primarily controlled by rock structure and lithology with consequent control on karst development.
	4. Extent of dissolution and karst development	
	5. Valley profiles	
	6. Groundwater as springs in the beach platform and as emanations from the cliffs.	Hazards related to processes at the base of the cliff including marine erosion and undercutting related to styles of fracturing leading to different forms and sizes of cave.

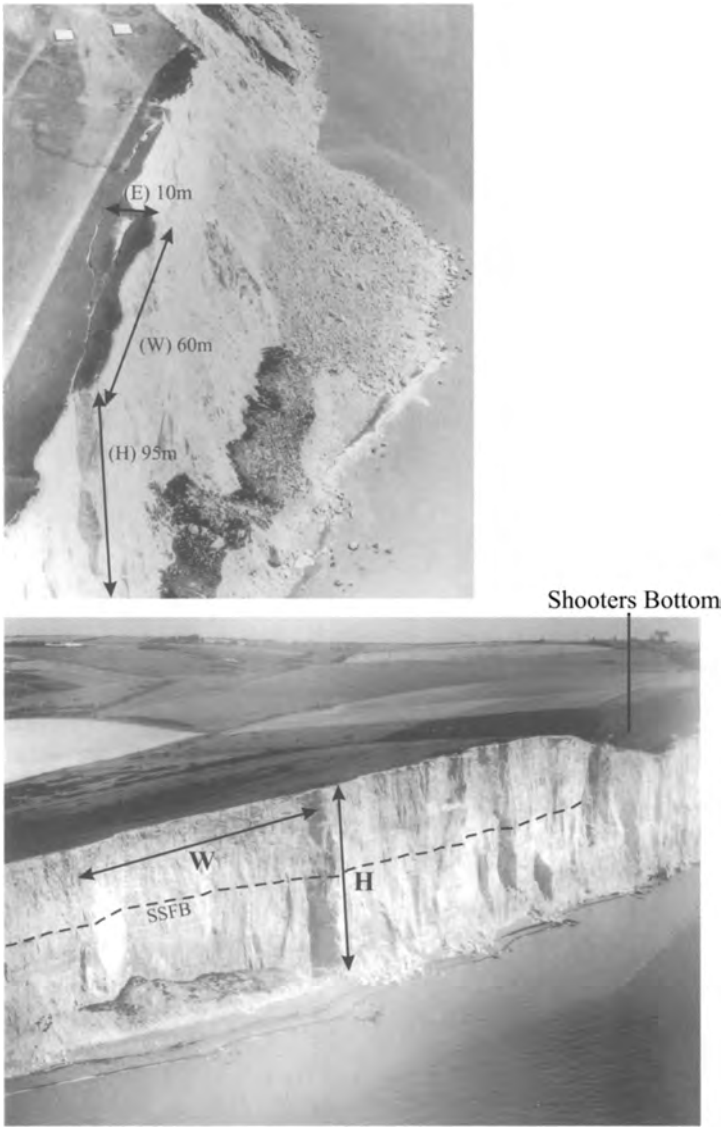

Fig. 6. Cliffs between Beachy Head and Belle Tout lighthouses, 1956, illustrating the style and scale of failures in cliffs primarily in Seaford Chalk Formation (H=75–80m; W=100m; E=3–7m); SSFB=Seven Sisters Flint Band (Photographs published with permission of Simmons Aerofilms).

highest points of the cliff containing Newhaven Chalk have steeply inclined conjugate fractures at these topmost levels proving the continuity of stratabound fracture systems in the Chalk. Similarly, the Belle Tout Beds containing the Belle Tout Marls (basal part of the Seaford Chalk), contain steeply inclined, widely spaced, conjugate joint sets (e.g at the base of the cliff at Cuckmere Haven). The predominantly vertical fracture sets produce vertical cliff collapses (Fig. 6, magnitude 3–5). Where faults and joints combine, larger-scale failures occur (magnitude 6–7). Spalling of small fragments of chalk and flint is common.

The evidence from the vertical cliff collapses is that top-down failures are controlled by opening joints that start out as topples but end up as slides with stratigraphic order retained in the debris run-out. Bottom-up failure debris tends to be less organized.

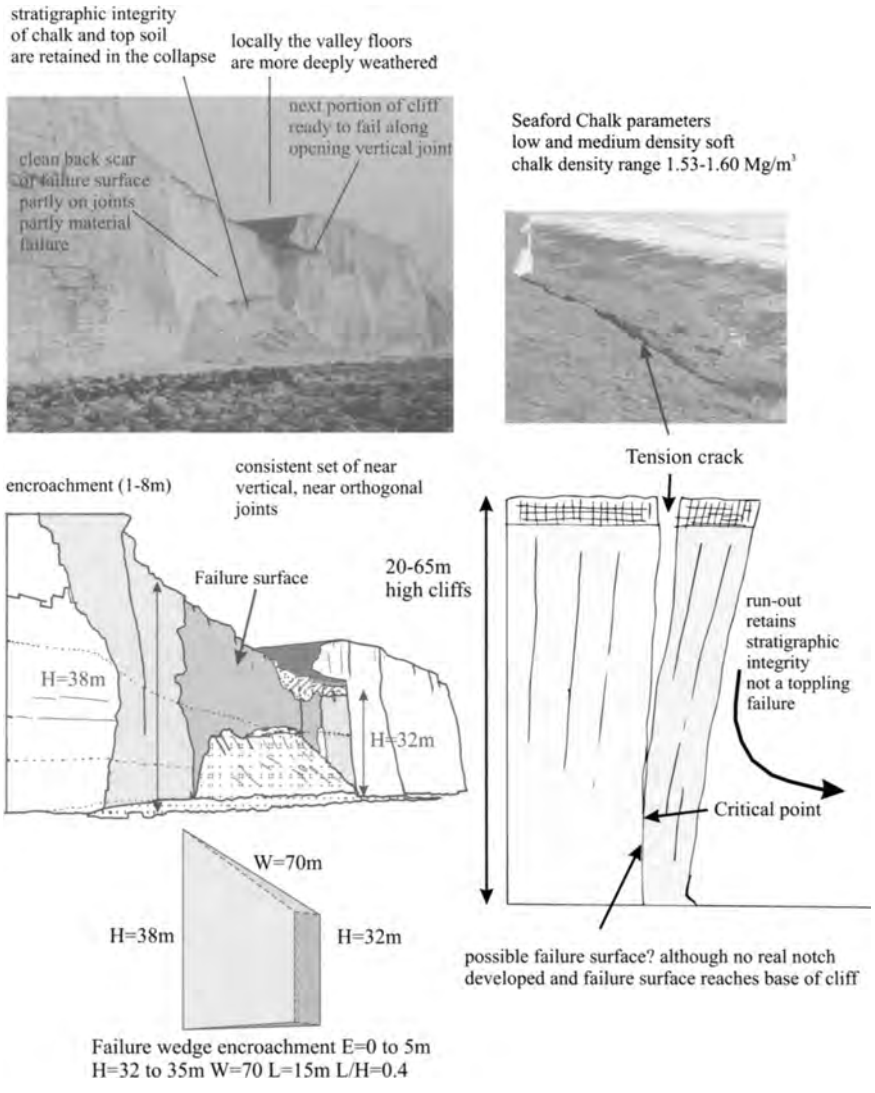

Fig. 7. Seven Sisters Type of cliff failure: simple vertical collapse along vertical joint sets and limited run-out at base of cliff. The critical point is the location of the final rupture at some depth along the failure surface (joint) where the stress (weight of chalk mass) overcomes the strength of the chalk (Magnitudes 2–5) (photographs R. N. Mortimore).

Plane and wedge failures: Holywell Nodular Chalk Formation, Holywell cliffs, Eastbourne (Holywell Type)
Several Chalk formations (Holywell Nodular, New Pit, parts of the Lewes Nodular and the Newhaven Chalk formations, Figs 9–11) are characterized by steeply inclined conjugate joint sets which contrast with the Seaford Chalk vertical fracture sets. The first of these formations is exposed in cliffs at Holywell, Eastbourne. Here the cliffs are partly protected by groynes and 'beach' at the eastern end of the section (Fig. 5). This protection does not reduce the hazard created by cliff collapses but does potentially reduce marine erosion rates. Although the cliffs are relatively low (*c.*35 m, Fig. 10), the hazards include continuous collapse in a relatively loose rock mass.

Potential wedge and plane failures are the major geohazards on the 300 m long section from Holywell Café to just south-west of Holywell Quarry. Failures are released along slickensided, conjugate shear planes which frequently dip out of the cliff face (daylight) at critical angles (i.e. dip angle $>50°$ exceeds the friction angle $<40°$; Fig. 10). The loose rock mass

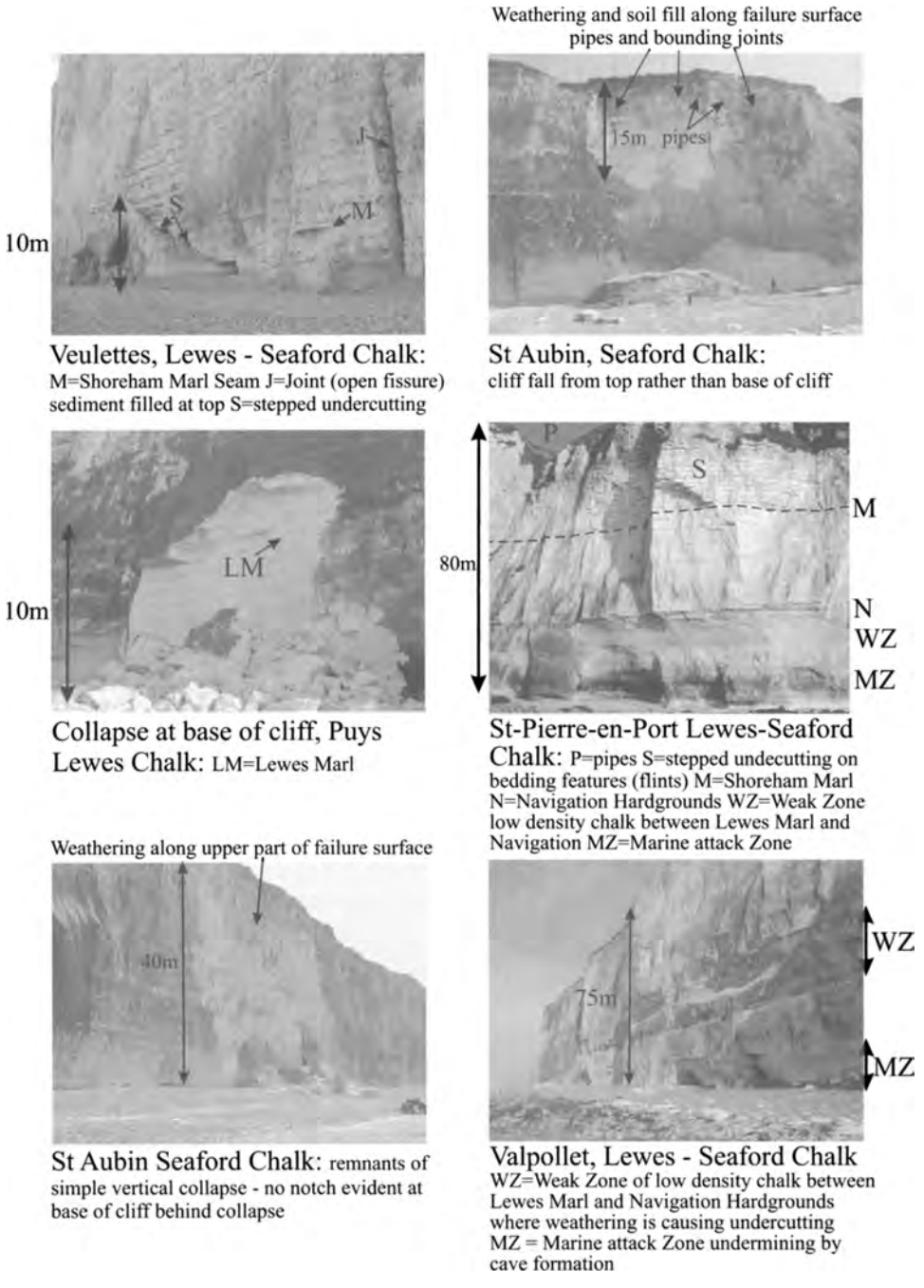

Fig. 8. Simple, vertical cliff collapses related to lithology, weathering and marine undercutting (photographs R.N. Mortimore).

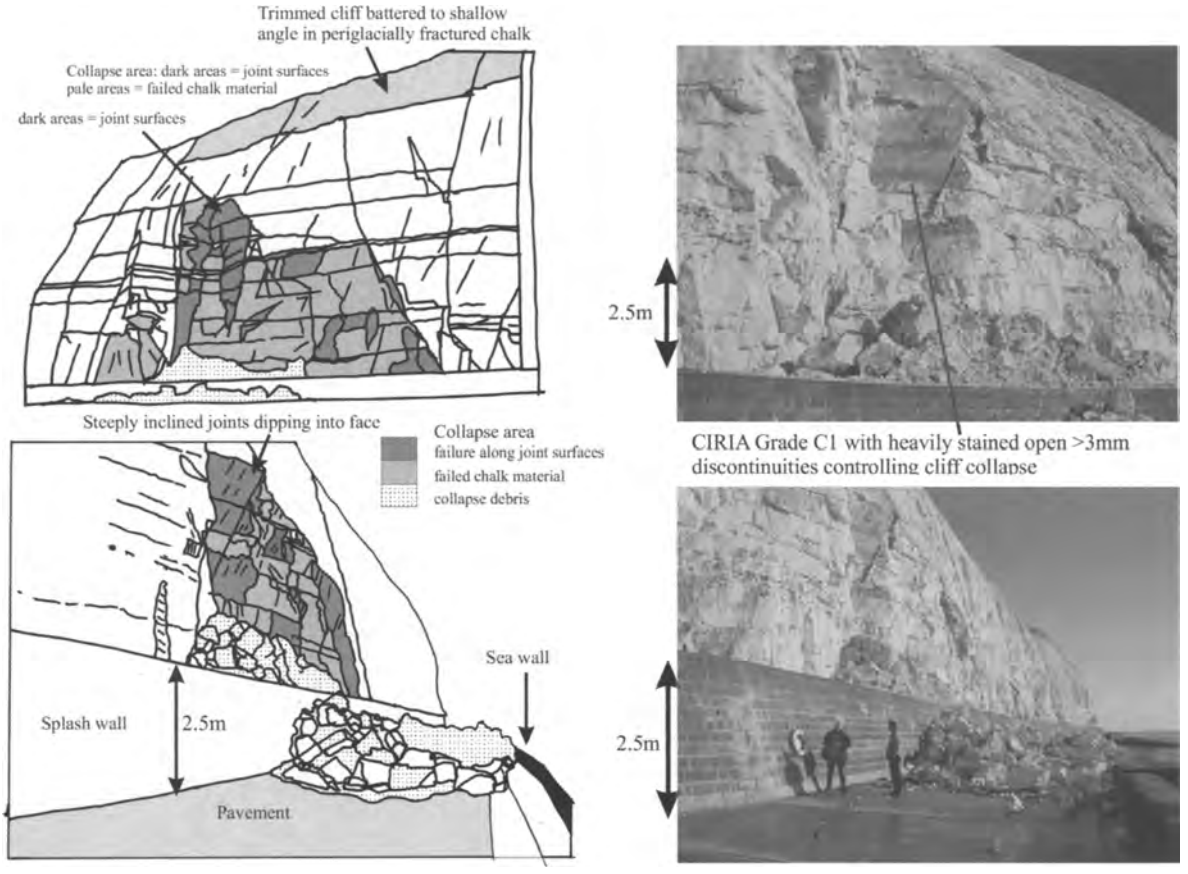

Fig. 9. The Peacehaven Cliffs failure on the protected coastline during the winter 2000–2001 was in Newhaven Chalk Formation with inclined conjugate joint sets with slickensided, polished surfaces. These joints dip in all directions but in this instance are dipping into the face. The failure surface is a combination of release along these joints, bedding planes (marl seams) and material failure (photographs R.N. Mortimore).

here reduces cohesion to zero and facilitates failures. Failures involve several tonnes of rock on each occasion (Table 4).

The 400 m of cliffs farther to the southwest are more irregular and instability is either caused by large masses failing in the Holywell Chalk or gradual creep and collapse within the Grey Chalk Subgroup. Local spalling of chalk blocks is a feature but not as frequent as other sections of coast (usually weather-controlled e.g. thaw after a sharp frost).

Water emanating from the top of the Plenus Marls and fractures in the immediately overlying Melbourn Rock are a feature of this section and are a cause of continuous movement of rock along fracture planes. Marine erosion exploits these weakness zones. Open conjugate joints are a feature of the top of the cliff northeast of the Pinnacle and these are continuously on the move. These gaping fractures are the source of future collapses.

The Holywell style of fracturing is characteristic of this formation across the main part of the Anglo-Paris Basin (e.g. at St Martin Plage, France, Fig. 11) and the type, scale and magnitude of failures are similar everywhere.

In the overlying New Pit Chalk Formation, inclined conjugate joint sets are also a feature but this formation is less nodular and the joints are smoother. In the upper part of the New Pit Chalk in beds including the Glynde Marls, the frequency of inclined joints increases leading to extensive collapse (e.g. at Lewes, Senneville and St Martin Plage, Fig. 11).

Even where the Holywell and New Pit Chalk formations are steeply dipping as at Compton Bay, Isle of Wight (dip 70° north), the same fracture style is present and is a major control on the local cliff stability (Barton 1990).

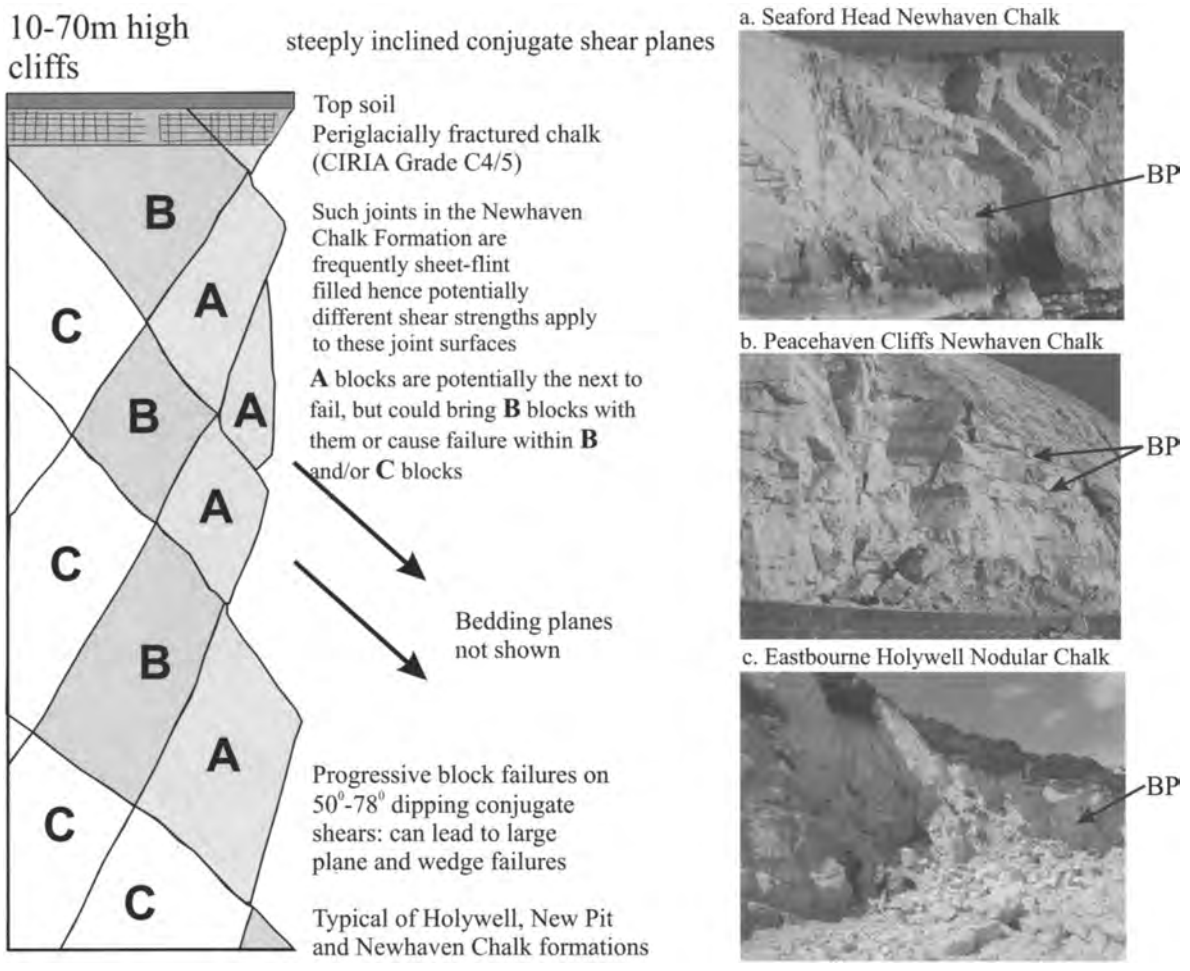

Fig. 10. Holywell and Peacehaven Type cliff collapses: failures initiated within the cliff face are as common as failures initiated at the base of the cliff. Simple marine erosion is not the explanation for these failures which can occur on protected coastlines as well as unprotected coastlines (schematic). BP, Bedding Plane (usually a marl seam) (photographs R.N. Mortimore).

Newhaven Chalk Formation plane and wedge failures, Newhaven to Brighton Cliffs: The Peacehaven Type

In contrast to the Seaford Chalk forming the Seven Sisters the cliffs at Peacehaven (and between Newhaven and Brighton) are primarily in the Newhaven Chalk Formation. The style of fracturing in the Newhaven Chalk, with steeply inclined (60°–70° dipping), slickensided, polished surfaces, produces a very different style and magnitude of cliff failure (Figs 9–11). Slides along fracture surfaces that have progressively lost shear strength through weathering are common. The complex, three-dimensional interaction of the blocks (only represented in 2D in Fig. 10) locks the cliff together (e.g. Corbett 1990). Loosening of the interlocking blocks over time and failure of chalk within blocks leads to complex failure surfaces (Fig. 9). Failures can be progressive, working either 'bottom-up' or 'top-down'. In some cases, release of blocks can occur within the central part of a cliff face with no prior bottom or top failure (Fig. 10). Trimming of the cliff face can assist in reducing the frequency of failures but will not eliminate them.

The encroachment into the cliff of the Peacehaven type failures is closely related to particular fractures being present at the top of the cliff (Fig. 10 inset, a) and to the height of the cliff. The magnitude of failures of the Peacehaven type is cliff height dependent but is rarely of the same order as the Seven Sisters Type. The blocks in such failures are generally larger than in the Seven Sisters Type of failure. Hutchinson (2002) records the failure of about 10 000 tonnes which broke

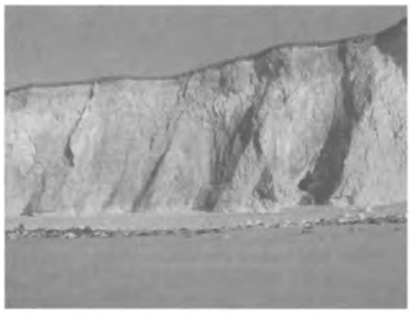

Quiberville, Newhaven Chalk, steeply inclined conjugate joints (pyramidal structure)

Quiberville, Newhaven Chalk, slickensides on steeply inclined conjugate joints (dip into face)

Veules-les-Roses, Newhaven Chalk, steeply inclined conjugate joints (pyramidal structure)

St Martin Plage, New Pit Chalk, steeply inclined conjugate joints (pyramidal structure)

Senneville-sur-Fécamp, uppermost New Pit Chalk, Glynde Marls, steeply inclined conjugate joints and water flowing along Glynde Marl 1

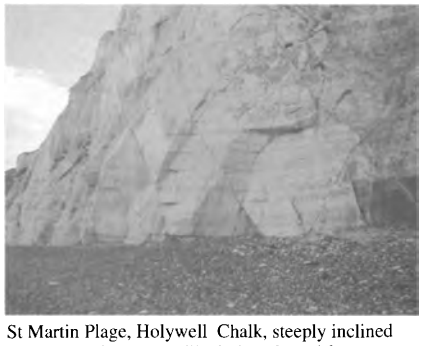

St Martin Plage, Holywell Chalk, steeply inclined conjugate joints. Note dihedral angle and frequency of joints compared to New Pit Chalk above

Fig. 11. Chalk formations with inclined conjugate joint sets on both sides of the English Channel (photographs R.N. Mortimore).

the Newhaven to Brighton road in 1891 (Geikie 1893) and the large fall with a 10 m encroachment in Friars Bay in 1899 described by Rowe (1900). These historical records suggest that large cliff collapses involving Newhaven Chalk are possible (but are probably not chalk flows in Sussex).

Cliff sections exhibiting the Peacehaven Type of failure include Castle Hill to Old Nore Point, Newhaven. Steeply inclined, conjugate, slickensided and frequently sheet-flint filled fractures typical of the Newhaven Chalk Formation are present at Old Nore Point and in the adjacent cliffs (Fig. 4). These fracture sets give the cliffs a roughly 'pyramidal' character with caves forming at the boundaries between pyramids and along the fractures. Eastwards, as the Culver Chalk Formation becomes the predominant lithology, the fractures are more vertical, less frequent and the chalk cliffs have a smoother, more vertical profile.

Wherever Newhaven Chalk is present in the cliffs of the eastern English Channel (e.g. Veules-les-Roses and Quiberville, France, Fig. 11) the same style of inclined conjugate fractures and similar slope failures occur.

Complex cliff failures combining several Chalk formations: Beachy Head: Failure Type (2a–c)

Whereas the Joss Bay, Seven Sisters, Holywell and Peacehaven types of cliff failure described above involve either one or two types of chalk lithologies, Beachy Head and similar very high cliffs in France, involve several different types of Chalk (Figs 5 & 12). The cliffs may fail in their entirety leading to huge collapses or parts of the cliff can fail independently of other parts, mechanisms of failure being closely related to material and rock mass properties of individual chalk lithological units. Seven Sisters Type failures characterize the high, Seaford Chalk towers at Beachy Head, whereas the basal parts of the cliff are controlled by Holywell Type failures. Progressive eating into the base of the cliff can lead to the higher chalk becoming unstable. Most very large failures have, however, concentrated close to the point of Beachy Head eitherside of the Lighthouse (Figs 5, 13 & 16). This is where the New Pit, Lewes and Seaford Chalks occupy the cliffs. This suggests that there is a strong lithological as well as height control on very large cliff failures.

A particular feature of Beachy Head is the impact the debris run-outs from very large cliff falls has on the hydrodynamic regime and rates of marine erosion elsewhere on this section of coast. In the past, local authorities have had to blast larger blocks of chalk to assist removal of the debris by the sea and reduce marine erosion scour on the eastward side of failures.

The Beachy Head sections are in two parts, the first dominated by the Grey Chalk Subgroup from Head Ledge to Gun Gardens and the second from Gun Gardens westwards to Beachy Head formed of the White Chalk Subgroup (Figs 1, 5 & 13). The change of direction in the Chalk cliffs west of Head Ledge brings younger chalk formations progressively to the base of the cliff on the north-dipping limb of the Beachy Head Anticline (Figs 2 & 5). Although this dip

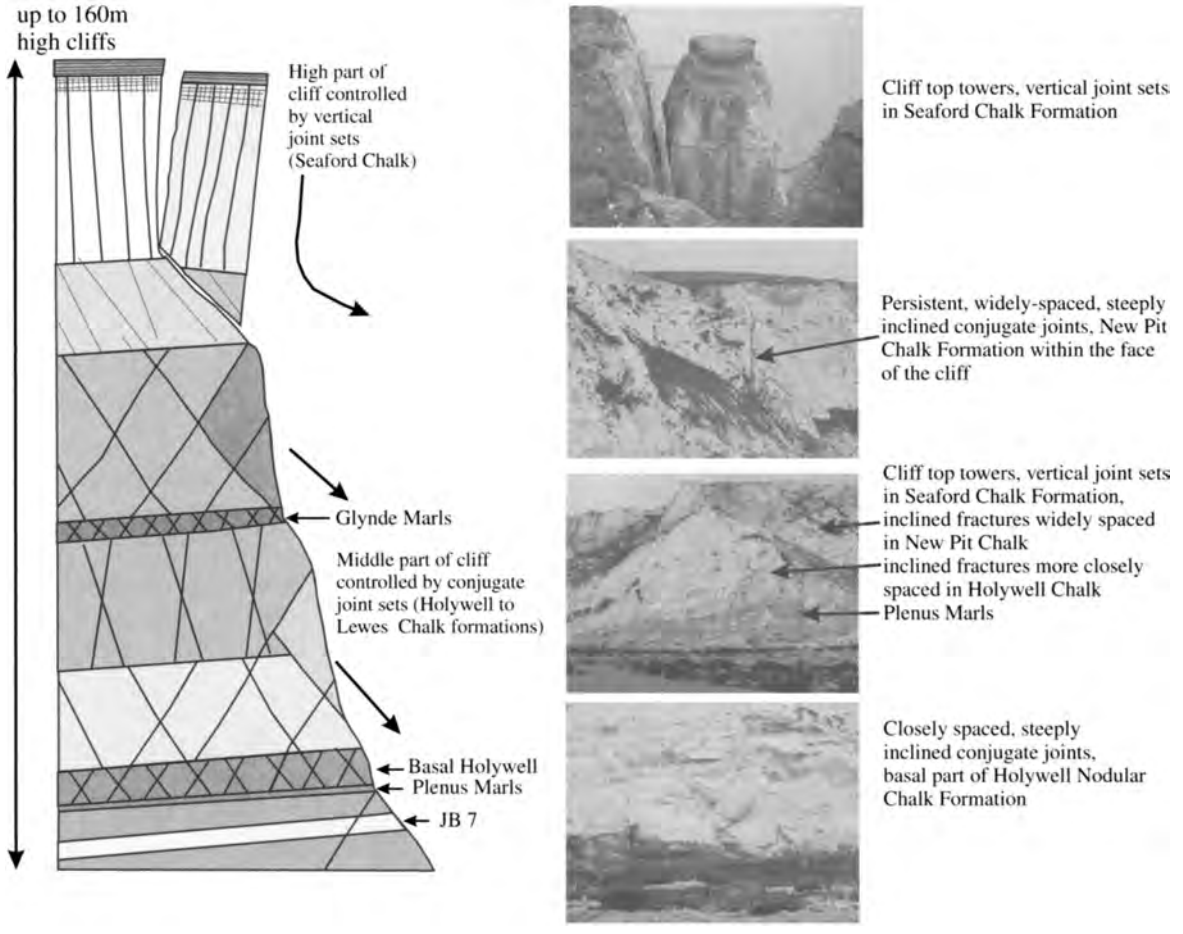

Fig. 12. Beachy Head: complex type cliff failures involving more than two Chalk formations (photographs R.N. Mortimore).

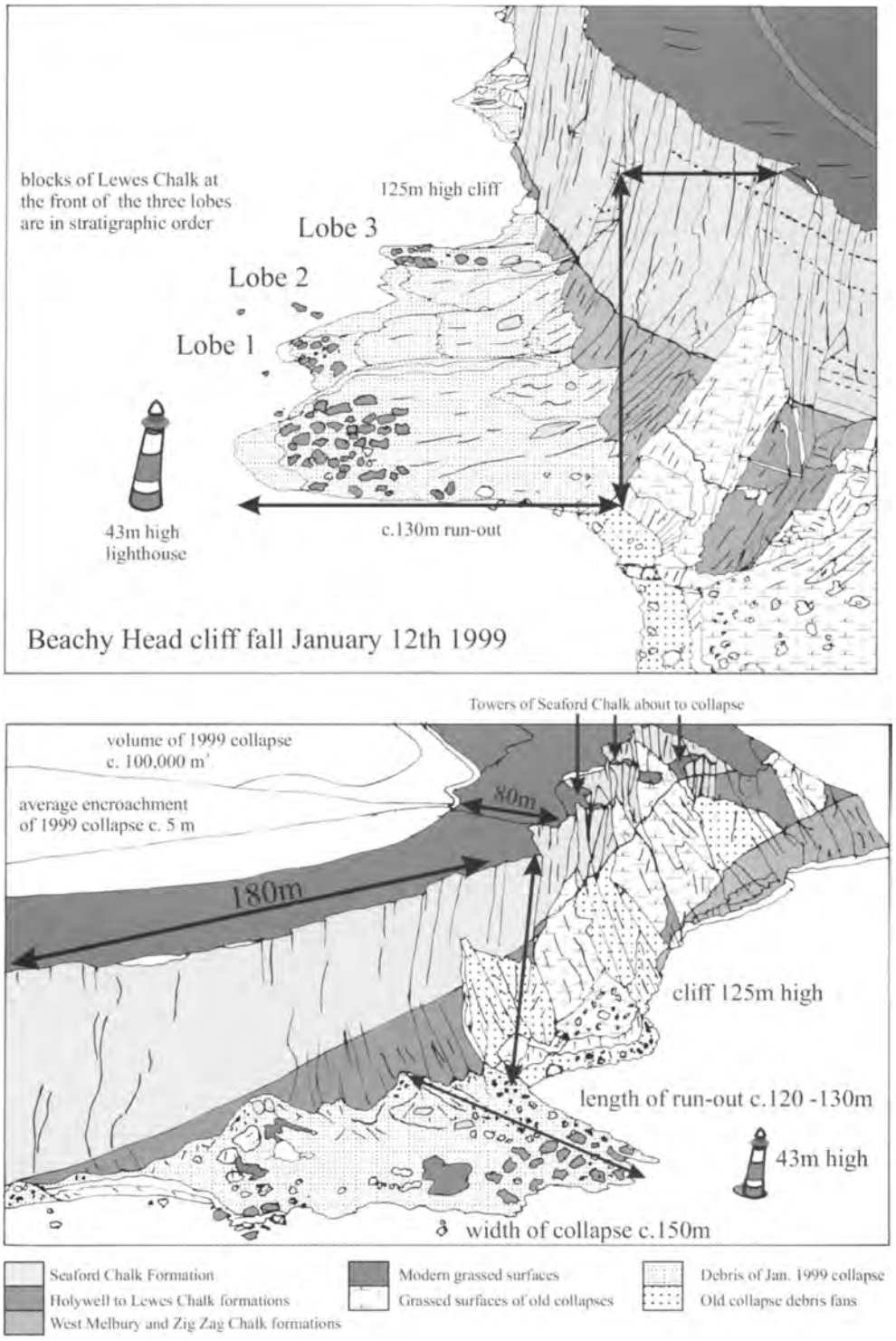

Fig. 13. The January 1999 cliff collapse at Beachy Head.

continues towards Beachy Head Lighthouse and Birling Gap, there is a marked change in the geology and associated slope hazards at Gun Gardens (Fig. 5).

Because of the height of the cliffs (55–125 m) several lithostratigraphic units of chalk are present but these change laterally from east to west (Figs 3, 5 & 13). Several faults are present in this section of cliff and these have a marked impact on the position and scale of slope failures.

In the first, easterly part of the Beachy Head cliffs, a long, wide wave-cut platform is bounded on the east by Head Ledge (Upper Greensand, Fig. 5) and on the west by an old very large rock fall which cuts across the Plenus Marls. Sand covers the part of the platform comprising the softer West Melbury Marly Chalk Formation. The back-cliff is partially covered by debris of marly chalk which, being more fine-grained, washes away relatively quickly. Less frequent falls of massive Zig Zag and Holywell Nodular Chalk formations form large boulder masses at the base of the slope.

Rock falls of larger blocks are more common westwards, derived from the harder, more massive bands in the Zig Zag Chalk (Jukes-Browne Bed 7) and the Holywell Nodular Chalk Formation.

Style and magnitude of slope failures in the cliff face are closely related to the different Chalk formations. In the West Melbury and Zig Zag Chalk formations, irregular masses of rock break away partly by failure within the material and partly as a result of joint control. In the high cliff, the Holywell Nodular Chalk Formation, characterized by steeply inclined conjugate joint sets, yields large slab and wedge failures and these slide across the lower slopes collecting other loose material on the way (Figs 12–14). The cliff degradation is progressive, sometimes working from the bottom-up, other fractures open from the top down. A slope cycle of decay, beginning with a base of slope failure, appears to take a year or more to work up the cliff. More massive failures involving the whole cliff are rare and appear to be localized to faults and fault zones of more fractured rock.

In section two, the cliffs from Gun Gardens to Beachy

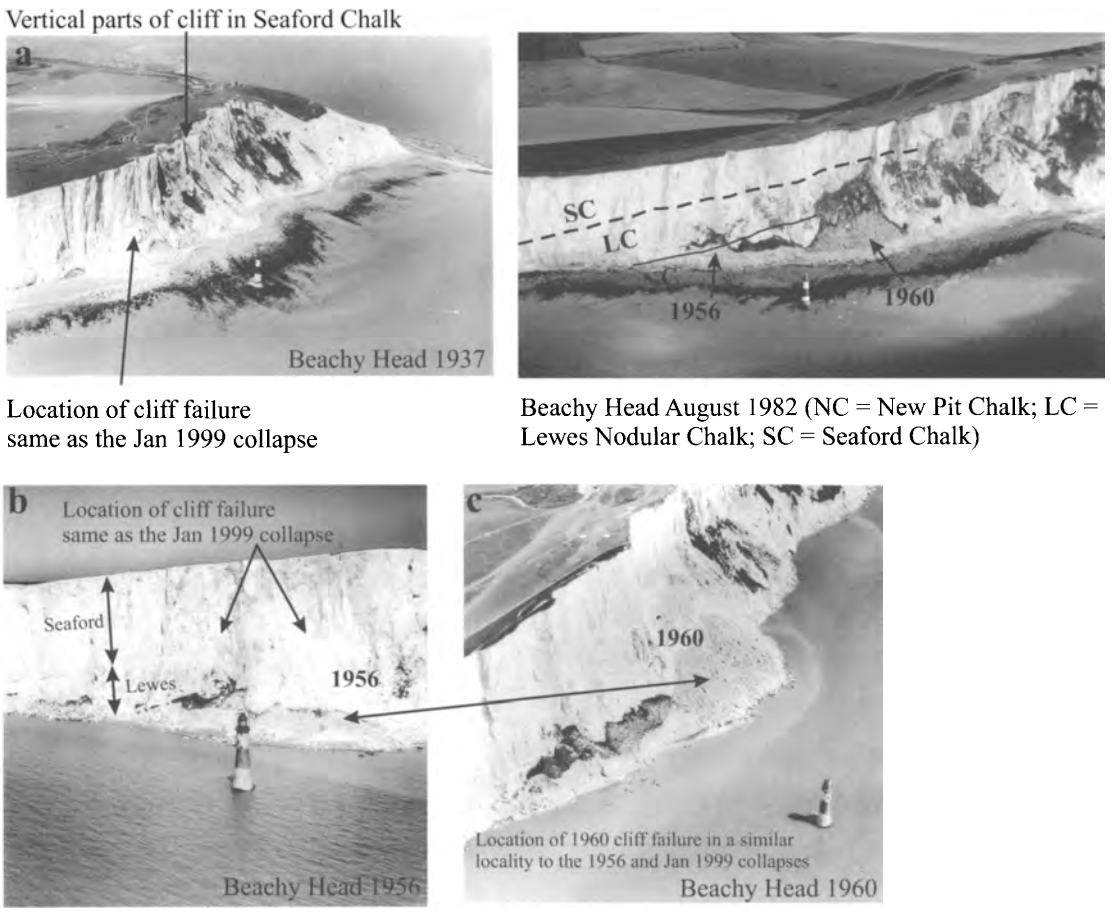

Fig. 14. Frequency and location of large rock falls at Beachy Head. Photographs (a) to (c) published with permission of Simmons Aerofilms. Photo (d) R.N. Mortimore.

Head Lighthouse (Figs 5, 12 & 13) are the highest and geologically most complex along the entire Sussex coastline. Large and small cliff failures are common. Big rock falls with a modest element of flow occurring perhaps once every 10–40 years.

Although Gun Gardens to the Lighthouse is an east–west section, the northwesterly dip brings each formation to beach level in turn. At the base of the cliff on the east side of this section are the Plenus Marls (*c.*8 m thick, Fig. 12). These marls are the basal unit of the White Chalk Subgroup overlain by the tough rugged beds of the Melbourn Rock and the abundant shell beds in the higher part of the Holywell Nodular Chalk Formation. The middle part of the cliff comprises the New Pit Chalk and Lewes Nodular Chalk formations (Figs 12 & 13). The uppermost sections forming vertical cliffs are composed of Seaford Chalk Formation (Figs 12 & 13). Patches of Clay-with-flints and small dissolution pipes are present on the highest parts of the cliff (Fig. 12). Opposite Beachy Head Lighthouse, old and new cliff collapses have covered the upper beds of the New Pit and lower part of the Lewes Nodular Chalk formations.

The fracture characteristics of each Chalk formation are a fundamental control on the cliff failure mechanisms at Beachy Head (Fig. 12). The Plenus Marls act as a break between the more massively bedded and very widely spaced fractures in the Zig Zag Chalk Formation below and the more intensely fractured Holywell Nodular Chalk above. The intensity of fracturing is greatest in the basal few metres of Holywell Chalk above the Plenus Marls. Steeply inclined, conjugate, slickensided and clay-smeared joints are a feature of the Holywell and New Pit Chalk formations. The dihedral angle is more obtuse in the Holywell and more acute in the New Pit Chalk formations respectively giving different factors of safety in the two units.

The northerly dip brings the hard, gritty parts of the Holywell Nodular Chalk Formation into the wave-cut platform west of Gun Gardens where it forms a rocky platform on which the Lighthouse is built. The only protection afforded to the base of the cliff is from the debris of cliff falls.

At Gun Gardens, where the basal Holywell Nodular Chalk Formation is present at the base of the cliff, major plane and wedge failures are common (Fig. 12). A conspicuous fault with a 10 m displacement and intense fracture zone is the locus of regular cliff collapses in this part of the section. Old scars of former major failure surfaces involving thousands of tonnes of rock (Magnitude 6) incorporating New Pit, Lewes and Seaford Chalk (i.e. the entire cliff) are present in the New Pit Chalk Formation. However, blocks of chalk from the New Pit Formation are not generally found in the smaller-scale collapses on the beach. This suggests that large-scale failures occur infrequently, but when they do occur they involve the whole cliff and an element of chalk-flow (e.g. Figs 13 & 14).

During 2000–2001 there were regular collapses from the towers at the top of the cliff in the Seaford Chalk Formation. The towers disintegrated on their way down the slope, producing debris aprons that have covered most of the exposures at the base of the cliff. It appears that a cycle of cliff decay beginning with undercutting, bottom-up collapse and weathering at the top leads to a major collapse. The debris from such a large collapse protects the base of the cliff from further erosion for some years (maybe up to 40 years) before the cycle starts again. However, parts of the cliff, particularly the towers at the top controlled by vertical fracture sets in the Seaford Chalk Formation (Fig. 12) may act independently and continue to move and fail on a regular basis. This can be seen in the ground movements on the crest-line of the cliff as well as cracks opening in the ground some distance behind the cliff edge.

A change in the cliff direction takes place opposite the lighthouse from broadly east–west to northwesterly between the Lighthouse and Birling Gap (Fig. 5). This change of direction reflects the end of the influence of the stronger Holywell Nodular Chalk Formation, which passes out to sea at the Lighthouse, and the increasing influence westwards of the weaker Seaford Chalk Formation. The strata dip brings each bed of the Lewes Nodular Chalk Formation to beach level in turn along this coastline. The overlying, softer, pure white Seaford Chalk Formation containing several conspicuous flint bands is brought down from the top of the cliff at Beachy Head to beach level just east of the old Belle Tout Lighthouse and then forms the entire cliff westwards to Birling Gap.

With this change in chalk strata forming the cliff there is an associated change in fracture style and consequent cliff profile (Fig. 12). East of the Lighthouse the top 10–20 m comprising Seaford Chalk is vertical. Below, in the New Pit and Lewes Chalk formations, the inclined joints produce an inclined cliff profile (60–70°). The vertical fractures predominate to the west as the Seaford Chalk dips down in that direction to form the cliff.

Large, old cliff collapses protect the base of the cliff opposite the Lighthouse. Large falls appear to take place about every 10–40 years either side of this point at Beachy Head (Figs 13 & 14). Marine erosion has a natural direction of attack along the west side of the harder beds of Holywell Nodular Chalk into the softer and weaker New Pit Chalk Formation. Numerous old cliff collapses, ranging from small vertical failures to large cliff collapses, litter the wave-cut platform from the Lighthouse to Birling Gap. Harder beds within the Lewes Nodular Chalk Formation form local small cliffs or reefs in the foreshore platform. There is little protection from beach and the base of the cliff, where exposed, develops a local 'notch'.

The cliffs range in height from over 125 m at Beachy Head to less than 15 m at Birling Gap (Fig. 5). In general the cliffs are between 50–100 m high. A spectacular cliff collapse on 12 January 1999 opposite Beachy Head Lighthouse happened near the beginning of the ROCC programme (Fig. 13). According to Hutchinson (2002), this failure extended at least 180 m along the crest, taking a slice generally less than 10 m wide. The run-out was low, the L/H value from Abney level readings is about 1.45. This section of coast is less complex than the preceding section, being predominantly

Seaford Chalk Formation. However, immediately to the west of the lighthouse is a heavily faulted zone of chalk. The faults form near-vertical planes with strongly developed subhorizontal slickensides. The zone is associated with deep weathering marked by solution widened fissures filled with brown-orange coloured Quaternary sediment-fills. A cave system has been explored within this complex zone (Mortimore 1997). This faulted and weathered chalk zone is the locus of the January 1999 cliff collapse and former collapses in 1937, 1956 and 1960 (Fig. 14) and is a continuing zone of weakness in the cliff. Major cliff collapses at and to the west of Beachy Head are related, therefore, to a combination of marine erosion along a gully in the weaker New Pit Chalk, special fracturing and fissure development associated with deep weathering, fracture style, the height of the cliffs as well as chalk lithologies.

Large chalk falls close to the South Foreland, Kent, also occurred in a combination of Lewes and Seaford Chalk formations (Fig. 15). However, the behaviour of the debris is different, involving a greater extent of chalk flow creating a surrounding 'ridge' of larger blocks on the seaward side of the run-out (Fig. 15). Mortimore *et al.* (1990) illustrated the consistently lower density of the Chalk in Kent compared with Sussex, supporting Hutchinson's suggestion that the extent of run-out and any flow is porosity dependent.

Historical failure 1961 L/H = 1.3 a low chalk flow

Large cliff falls at the South Foreland East Kent are in the same arrangement of Chalk formations, Seaford at top and Lewes at the base, as the Jan. 1999 failure at Beachy Head but in higher porosity (lower density) chalk

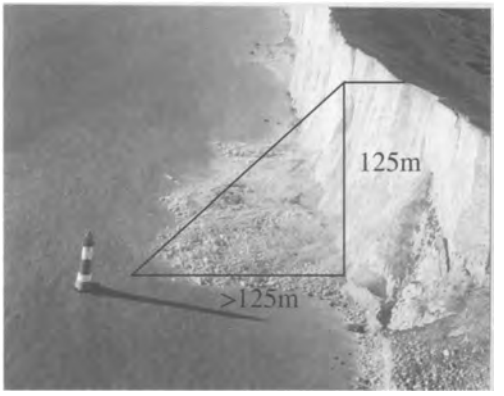

Further large cliff falls at the South Foreland East Kent 1st Feb.2001, were 150m long15m encroachment >100,000 tonnes and in the same place as the 1961 fall. (Photograph published with permission of Simmons Aerofilms)

Beachy Head cliff collapse January 1999: L/H = 1.0 to 1.05 i.e. not a chalk flow

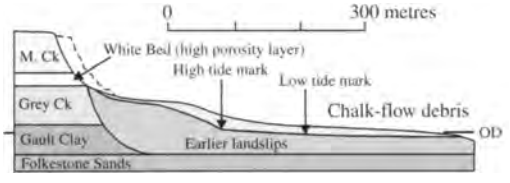

Section of the "Great Fall" of December 1915 at Folkestone Warren (Modified from Osman 1917; Hutchinson 1988) Similar chalk-flows are recorded from Møns Klint Denmark, Jan. 1952, 500m run-out (Rasmussen 1967) and Rügen, Germany, 1958, 120m and 150m run-out (Hurtig 1959) (see Hutchinson 1988, 2002)

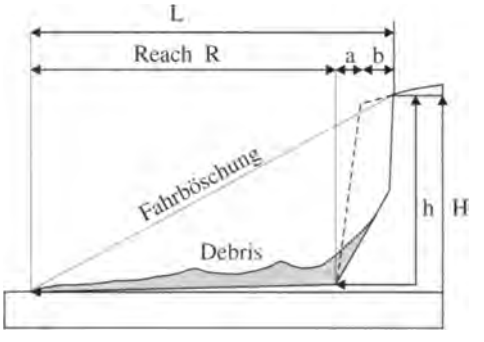

Fig. 15. Chalk flows and large rock-falls (geometrical from Hutchinson, 1988a); the Beachy Head (Sussex) cliff collapse, January 1999 and the South Foreland cliff collapse (Kent), 1961.

Rotational landslides: Cow Gap, Eastbourne (Hazard Class 4)

Rotational landslips form the low cliffs at Cow Gap on the eastern side of Beachy Head and extend from Head Ledge in the southwest to a point some 500 m northeast of the steps (Figs 3 & 5). Evidence from the rate at which the steps at Cow Gap have to be replaced or repaired suggests that marine erosion of cliff toe-weight and undercutting of the cliff could reactivate old slips.

Rotational landslips have stacked up the various beds into a series of displaced slices which dip steeply northwest on the southern flank of the Beachy Head Anticline. The landslipping is facilitated by the Gault, a dark grey marine clay formation, which occupies the base of the cliff and foreshore. Within the rotational slips the 6 m thick Upper Greensand forms northwest-dipping reefs. The Glauconitic Marl Member at the base of the Chalk Group also forms reefs which incorporate the basal beds of the West Melbury Marly Chalk Formation. These low cliffs and the associated landslips provide unique exposures in beds that are poorly exposed anywhere else in Sussex.

Observations indicate that the West Melbury Marly Chalk Formation, which predominates in this section of cliff, tends to fail in irregular masses rather than being fracture controlled. Towards Head Ledge, the stronger beds of the Upper Greensand and Glauconitic Marl allow more vertical, low cliffs to develop. Failures in these rocks tend to yield large ($>1\,m^3$) blocks.

The tough Upper Greensand forming Head Ledge forms a reef extending out to sea and marks the change in direction of the cliffs. The Ledge also marks a change in sediment type forming the beach, sand to the west and flint gravel to the east, perhaps an indication of change in erosion rates as well.

The material forming the cliff top includes periglacially weathered chalk from former valley slopes and floors as well as sections of Grey Chalk Subgroup. There is no data on rates of movement on these old landslips.

Mudslides from cliff-top: Newhaven Castle Hill (Hazard Class 5)

At Castle Hill, on the west side of Newhaven Harbour, where the Culver Chalk is present, the Chalk cliffs are protected and few failures occur. The main hazard here comes from the overlying Palaeogene deposits (Fig. 2). Mud-slides have built up aprons of material at the base of the cliff adding further protection from marine erosion. During wet weather (and particularly during the wet winter of 2000–2001) extensive mud-slides and landslides developed. These created several types of hazard. First, the sheer volume and speed of failures is potentially dangerous to those on the beach area. Secondly, the mud-slide deposits at the base of the cliff, when wet and unconsolidated, are traps for the unwary (see detailed geology in Mortimore 1997; Mortimore *et al.* 2001*a* and ROCC Database).

In addition to mud-slides, large blocks of sandstone collapse regularly onto the beach below, creating a further hazard. These tend to be of small volume (Magnitude 1–2) but have a significant impact.

Landslips, with numerous back scars of inactive and active landslides, are present in a zone behind the cliff edge. Progressive collapse of the Palaeogene deposits along this cliff top will eventually bring structures and buildings that are currently close to the cliff line into a vulnerable zone.

Influence of karst features: Hope Gap to the Castrum, Seaford Head (Hazard Class 7)

Karst features, particularly vertical dissolution pipes, are a feature of Chalk. However, on the Sussex coast these are primarily confined to Chalk formations close to the feather edge of overlying Palaeogene deposits at Seaford Head, Newhaven and at Portobello, Telscombe Cliffs. At Seaford Head a combination of a southerly dip of strata and the presence of the Jevington Fault brings Lewes Nodular Chalk Formation into the cliffs on the west side of Cuckmere Haven (Fig. 2). Dissolution pipes become progressively better developed (Fig. 16) and more influential on cliff stability along the crest-line of the cliff from east (Hope Gap) to west (the Castrum). The section exposed is almost parallel to the strike direction, hence the same beds are present along the cliff, except where faults locally offset the stratigraphy. However, the cliff becomes higher from east to west (from 30 to >75 m high), preserving younger Chalk and creating a greater hazard in areas with more extensive dissolution pipes. Unlike the Seven Sisters, caves have formed along the primary fractures at the base of the cliff. The cave roofs are supported by stronger bands of rock in the Lewes Nodular Chalk Formation. The detailed geology is described in Mortimore (1997) and Mortimore *et al.* (2001*b*).

Regular cliff collapses involving parts of the cliff and/or the entire cliff are primarily fracture controlled (Fig. 16). Steeply inclined conjugate fractures and faults are a predominant feature of the rock mass in this section, in the Lewes Nodular Chalk Formation. Cliff failures take the form of vertical collapse, collapse associated with inclined fractures (plane and wedge) or a combination leading to large rock falls. There is no evidence of chalk flows. In contrast, large blocks are common, related to the more massively bedded, stronger, Lewes Nodular Chalk. Bedding features such as marl seams and sheet flints act as overbreak horizons creating complex block failures. Many of the plane failures involve sliding on a pre-existing fracture surface and failure of the cliff material giving the cliff profile a 'buttressed' and sometimes overhanging profile (Fig. 16). Vertical 'flake' failures are also present involving vertical slabs of rock extending up much of the cliff, opening top-down, many are fissured (opened by dissolution) and frequently filled with post-Chalk sediments. In other areas slabs work bottom-up, breaking away along bedding features, initiated by marine erosion at the base.

Spalling from 'pipes' and the Clay-with-flints is particularly evident on the western part of this section. These pipes

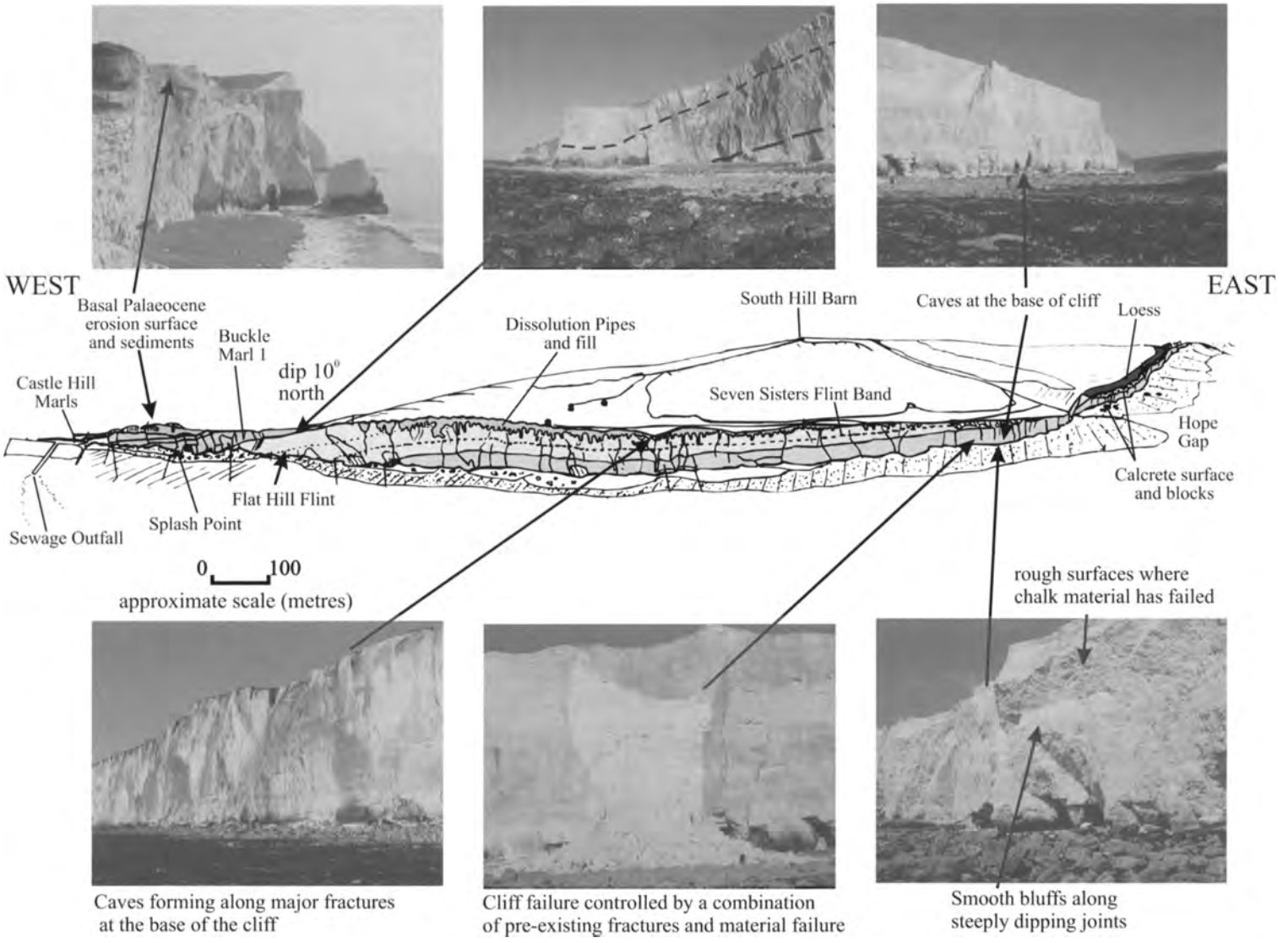

Fig. 16. Sketch geology of the Chalk cliffs at Seaford Head in the Upper Lewes Nodular Chalk, Seaford Chalk, Newhaven Chalk and Culver Chalk formations and the distribution of dissolution pipes.

create an extra hazard along the cliff top in two ways. During storms fragments of loose material are blown inland as a shower of shards. Pipes also contain metastable silt and clay that can collapse unexpectedly, particularly when wet. The same metastable material fills fractures enhancing failures of blocks of chalk.

Slope failures in dry valley-fills and related rocks: Quaternary processes and sediments: dry valleys, river terrace deposits and the Brighton Raised Beach (Hazard Class 8)

The cliff line from Eastbourne to Brighton truncates a number of dry valleys. These valleys are generally low points giving public access to the foreshore where any hazard related to instability, however small, is important to public safety. Two sites are of particular importance, Birling Gap and Black Rock, Brighton.

Birling Gap (Figs 5 & 13) exhibits the typical slope hazards associated with low-level dry valleys in the Chalk cliffs truncated and left 'hanging' by modern cliff marine erosion. Details of erosion rates and cliff retreat are contained in the ROCC Database (Mortimore *et al.* 2001*a*). Birling Gap probably formed by a combination of river erosion, subsequently enhanced by periglacial processes during the Quaternary. The surrounding bedrock is entirely Seaford Chalk Formation. As the axis of the dry valley is approached from each side the chalk is progressively degraded to a fragmented mass set in a putty-chalk matrix. The maximum degradation occurs beneath the floor of the valley and may extend several tens of metres below the cliff base. The degraded chalk is succeeded upwards by a very irregular layer containing coarse flint gravel reworked into involutions (presumed to be caused by ice churning during the cold, wet episodes of the Quaternary). Much of this degraded, poorly consolidated and ice-churned sediment is metastable (on wetting it looses shear strength and can fail easily, e.g. Fookes & Best 1969). Some of the cliff slope failures at Birling Gap are documented in the reports referenced in the *ROCC Database*. Collapses from the dry-valley altered chalk and Quaternary sedimentary fill are generally small (1–10 m^3; Magnitude 1–2), but continuous throughout the year, particularly in wet stormy weather.

Hope Gap, with the steps to the foreshore, is also formed in a dry valley (the confluence of two valleys, Mortimore 1997). The Chalk is intensely fractured on the west side and degraded beneath the valley. Valley-fill comprising solifluction, hill wash and loess covers the degraded chalk below. Rates of erosion in these low cliffs (<30 m high) vary depending on the state of weathering of the chalk. The weakest point is in the dry valley at Hope Gap and this is where most rapid erosion is taking place, leading to collateral cliff collapse.

On the east side of Hope Gap an ancient river terrace of the River Cuckmere is covered in a brown loessic soil (Fig. 16). Extensive dissolution piping into the chalk extends down from the 'loess' surface to the base of the cliff. The surrounds to the pipes are calcreted and flints are cemented to these surfaces. Remnant pipes form 'wells' on the shore platform. Sheet flints in the cliff and in the shore platform chalk are also zones of fragmentation and recementation. Collapse of the metastable loess and the pipe-fills are the major cliff hazards. Undercutting of the upper cliff by marine erosion eventually leads to release of the very large, calcreted chalk blocks and overlying loess.

Apart from Beachy Head, perhaps the most famous part of the entire Sussex coastline is the Black Rock Raised Beach and the Brighton Elephant Beds, which are exposed at the extreme western end of the Sussex Chalk white cliffs. These beds are part of the overall SSSI and an SSSI in their own right. The undercliff walk beneath these Marina sections is designed to provide access to the cliffs for the public and students. Many reports have been written on the cliff stability (see ROCC database).

Each sedimentary component of the geology has its own geotechnical properties. The Chalk wave-cut platform underneath the raised beach is solid, relatively unweathered CIRIA GRADE B/C 2/3 chalk. The degree of fracturing will affect the ability of this unit to drain freely. The altitude of the platform is usually given as 8.8 m aod (Shephard-Thorn & Wymer 1977, p. 64). Hutchinson & Millar (1998) found it to be 8.63 m aod.

The famous Brighton Raised Beach rests on the Chalk Platform and abuts against the Ancient Cliff-Line. Shephard-Thorn & Wymer (1977, p. 64) record a maximum altitude of 11.9 m aod for this deposit (i.e. 2–3 m thick) compared with the 12.3 m aod measured by Hutchinson & Millar (1998). The Raised Beach comprises well-rounded flint gravel (comparable to the present Brighton Beach on the west side of the Marina) with some sand and shell debris. Exposures in this part of the section during construction of the Marina illustrated a thin deposit of wind-blown sand on top of the beach. The flint-gravel beach deposit is locally weakly cemented by material washed down from overlying deposits but is, in general, a freely draining unit.

Above the Raised Beach are the 'Head' deposits, up to 20 m thick. These have been divided into three units by Shephard-Thorn & Wymer (1977, p. 64 and fig. 21): (i) a lowest unit comprising coarse chalk debris (ii) a middle unit of yellowish brown chalk solifluction deposits; (iii) a coarser solifluction deposit containing sarsen stones, ironstones and flint with cryoturbation involutions at the very top. Hutchinson & Millar (1988) identified and surveyed five immature palaeosols in this Head, which should permit its more precise datings and subdivision. These 'Head' deposits contain a matrix of fine silt (a form of Brickearth) which is likely to be *metastable* in the sense of Fookes & Best (1969). On wetting, these deposits lose shear strength and become unstable. This is probably a cause of failures in these deposits during the winter of 2000–2001.

Not all the deposits in the Quaternary section of the Brighton Marina cliffs will be unstable in the same way or to the same degree. Further work is required to develop a conceptual model of individual units as well as the interaction of the units as a whole.

Table 5. *Summary of geohazards for specific sections of the Sussex Chalk coastline. * Frequency is estimated, based on a very short time interval of study of two years and limited historical records*

Section	*Cliff height (m)*	*Geology*	*Rock Mass Character*	*Main Geohazards*	*Frequency**	*Magnitude*
1. Holywell Cliffs Eastbourne	35	ZZC, HNC	PM irregular joints HNC Inclined conjugate joint sets	HC wedge and plane failures Water on PM Open gulls at cliff top	1 per month	1–5
2. Cow Gap	10–30	Gault, UGS, WMMC	Gault stiff fissured clay UGS, massive widely-spaced joints. WMMC cyclic marl – limestone beds	Ancient rotational landslips Possible reactivation Small-scale spalling and local collapse	unknown	1–3
3. Beachy Head A	55–125	WMMC, ZZC, HNC, NPC, LNC, SC	WMMC Cyclic bedding ZZC massive HNC NPC conjugate joint sets, different angles of shearing	1.Complex failures: 2.SC Towers collapse 3.HNC, NPC, LC wedge and plane failures 4.Total cliff collapse	Each winter and after heavy rain 10–40yr	1–7 7–8
4. Beachy Head B	125–160	NPC, LNC, SC	Complex interaction, vertical joint sets above, inclined conjugate below	1.Total cliff collapse 2.BCC 1 per 10 yrs 3.SST each winter and after heavy rain	10–40yr Each winter	6–8 5–6
5. Seven Sisters	20–100	SC, NC	Vertical joint sets; faults	1.SST 2.FS	Each winter 10yr	3–7
6. Seaford Head		LNC, SC, NC, CC, Pal.	Complex interactions of pipes, vertical joints, conjugate joints, faults and strata dip	1.LNC blocky collapses 2.SC vertical joints and fissures with pipe fills 3.Faults and vaulted collapses 4. Pal. spalling	Each winter and after heavy rain	1–6
7. Newhaven	30–60	NC, CC, Pal.	Loose to medium dense sands, weak clays CC vertical joints NC conjugate joint sets	Mudslides, rock falls	after heavy rain irregular	1–6
8. Peacehaven	20–40	NC, CC	CC vertical joints and pipes NC conjugate joint sets	Wedge and plane failures (PT)	Each winter and after heavy rain	1–5
9. Black Rock	30	Raised Beach Head deposits	Loose gravels and sands, metastable silt, brickearth and loess	Inundation collapse of Head deposits	Each winter and after heavy rain	1–5
10. Dry valleys	10–25	Head deposits Degraded chalk	Weakly cemented CIRIA Grade Dm or Dc Chalk	Regular spalling	Each winter and after heavy rain or storms	1–3

UGS, Upper Greensand; WMMC, West Melbury Marly Chalk; ZZC, Zig Zag Chalk; PM, Plenus Marls; HNC, Holywell Nodular Chalk; NPC, New Pit Chalk; LNC, Lewes Nodular Chalk; SC, Seaford Chalk; NC, Newhaven Chalk; CC, Culver Chalk: Pal, Palaeogene; SST, Seven Sisters Type; BCC, Big Cliff Collapse

Discussion

In this paper the hazards related to cliff stability along the coast of Sussex between Eastbourne and Brighton have been identified and partially quantified (Table 5). The coastline has been divided for descriptive purposes into different hazard regions based on a combination of geology (lithology, structure, weathering), cliff height and presence or absence of coast protection works. Within each hazard zone an estimate of the magnitude of failures has been made based on direct observation and historical records. At four localities (Beachy Head, Birling Gap, Newhaven – Peacehaven and Black Rock) more detailed work has been carried out on the rock mass character to provide a standard for particular

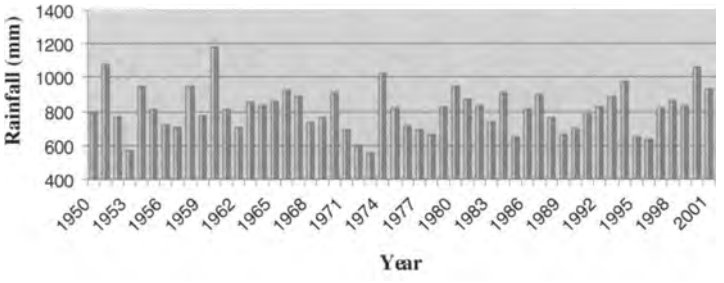

Fig. 17. Annual rainfall for Eastbourne, 1950–2001. Data compiled with permission from records held by Eastbourne Borough Council.

lengths of coast (data in the ROCC database). There are places where vulnerable properties or structures are present. In places marine erosion is the direct cause of distress to structures (e.g. Cuckmere Haven). In other cases, weathering, long wet periods or extreme inundation events are a cause (Kent, Hutchinson 1971; Black Rock, Brighton; Newhaven Harbour Heights, Beachy Head cliff collapses, Fig. 17). In many places, coast protection works have not eliminated rock slope failures (e.g. Peacehaven Cliffs) and the role of beach material as a protection against erosion is ambiguous (e.g. Birling Gap).

Classification of cliff collapses

Many classifications have been proposed for slope failures. The most widely used is that of Varnes (1978). However, the range of chalk slope failures identified required a separate system (Tables 4 & 5). In addition, the work of Hutchinson (1971, 1988, 2002) on chalk slope failures was recognized as being of particular importance. Hutchinson recognized what can be termed his *Joss Bay type failures* (Fig. 18) and he described numerous *chalk flows* developed from the Chalk cliffs of Europe (1983, 1988, 2002). During this study we have confirmed that Hutchinson's Joss Bay Type failures, and occasional falls with some element of chalk flow, also occur on the Sussex coast. However, the Chalk geology of the Sussex coast is much more complex than in Kent and consequently there are other types of slope failure that need to be considered when constructing a hazard map.

The Joss Bay Type of Cliff Collapse

Hutchinson's (1971) Joss Bay Type of chalk cliff failure involved development of a wave-cut notch, followed by a vertical tension crack and then a failure surface dipping out of the cliff at 64°–67°. The failure surface was freshly slickensided and the whole cliff was involved in the collapse. Nearly 2 m of encroachment (the 'bite') was recorded. The tension crack developed predominantly, and the failure surface partly, through pre-existing joints and other discontinuities, as a result of progressive marine erosion at the base of the cliff (development of the notch). Middlemiss (1983) illustrated the strong influence of pre-existing joints on cliff instability on the Kent coast and Hutchinson (1971, p.4) had noted similar joint controls on other failures in the Thanet Chalk. Hutchinson also indicated the possibility of the failure planes following a complex network of minor joints and that the magnitudes of these types of failure depended on the cliff height.

Another possible factor controlling the style of the Joss Bay failure is the lithology of the different types of chalk involved. The change from the inclined failure plane to the vertical tension joint occurs just above Barrois' Sponge Bed (Fig. 18). This sponge bed is a continuous surface of originally hardened (mineralized) sea-floor. It forms the boundary marker between the Seaford and Margate chalks, a change from chalk below with regular flint bands to Margate Chalk (Fig. 1; Mortimore 1997) with very sparse flint and a differ-

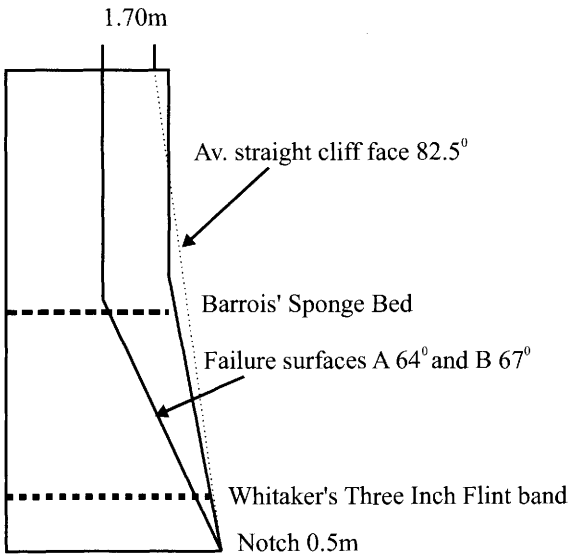

Fig. 18. Joss Bay Type failure in Seaford Chalk Formation, Isle of Thanet, which involves both joint and material failure (modified from Hutchinson 1971).

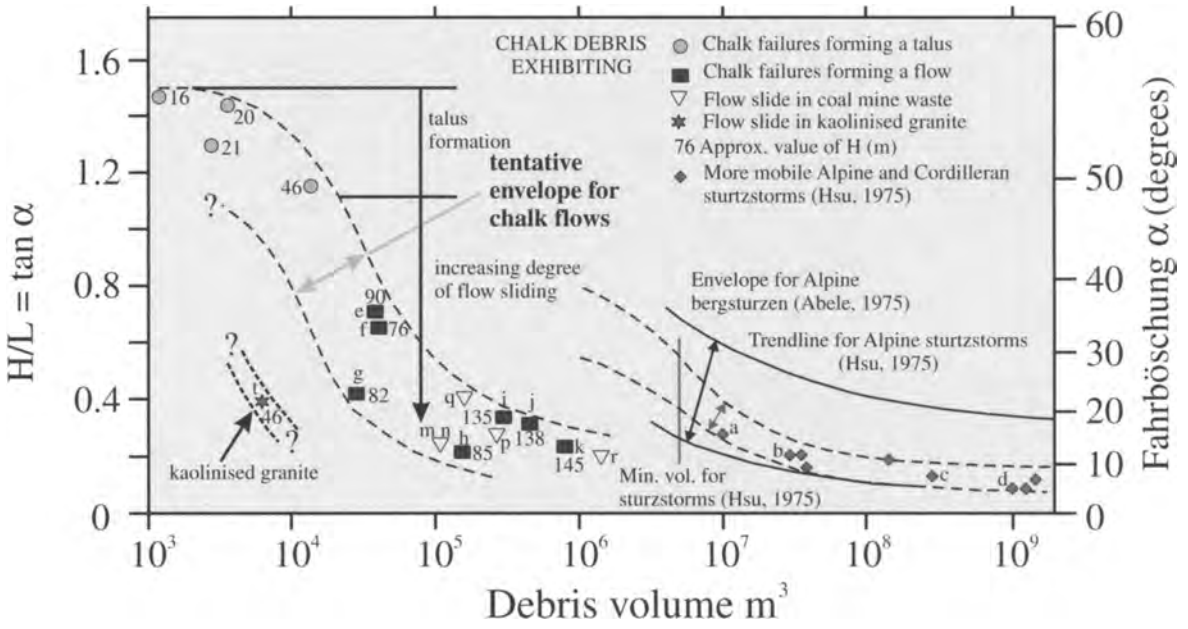

Fig. 19. Chalk flow slides and large rock falls in England. East Kent: Shakespeare Cliff (1909, 1912); f, h, St. Margaret's Bay (1910, 1905); i,j, Abbot's Cliff (1988, 1911); k, Folkestone Warren (1915). Note prior to 1988 no flow slides were recorded in Sussex chalk. Three large rock falls with an element of flow have been recognized: 1, Beachy Head January 1999; 2, between Beachy Head and Belle Tout, 1988; 3, between Birling Gap and Cuckmere Haven, 1914 (105 000 m^3) and 1925 (266 100 m^3) Hutchinson 2002. Several other large rock falls include Beachy Head, February 1813 (235 000 m^3), March 1848 (105 000 m^3) 140 m wide, 15 m encroachment, March 1853, 1862; Summer 1956 at the Head; June 1960 at the Head; Autumn 1960 a large fall east of the Head (Gilbert 1964); Seaford Head 15 July 1986 90 m wide and 15 m encroachment; Friars Bay 1899 (Rowe 1900) 'a great fall of chalk'; February 1891 (10 000 tonnes) broke the cliff-top road between Brighton and Newhaven (Geikie 1893); South Foreland, Kent, 1960 and 2001. Data (supplemented) from Hutchinson (1988*a*, 2002).

ent texture. It is uncertain how this lithological change affected the cliff failure mechanism but it may well be a factor in the distribution of fracture styles and frequencies. Barrois' Sponge Bed may also act locally as a surface for perched water.

Joss Bay type failures are not common on the Sussex and French coasts; however, this may reflect the tectonic structure of the Sussex and French chalks which imparts a much more profound fracture control on slope failures.

Chalk flows

Hutchinson (1988*a*, 2002), also recognized flow-slides in chalk (chalk flows) along many parts of the Chalk coasts of Europe. These are giant slope failures in which the debris runs seawards from the base of the cliff for up to six times the cliff height. This contrasts with 'normal collapses' which produce an essentially conical apron of debris at the base of the slope (Fig. 19). Chalk flows occur where cliffs exceed about 30 m in height and are composed of high porosity ($n>$ about 40%). Hutchinson thus believes that a mechanism of impact collapse is operating, principally as the falling rock hits the shore platform, the saturated or near-saturated chalk pores being crushed and excess pore-water pressures generated. These transform the debris into a flow slide and lead to its large run-out. This mechanism, absent in low porosity Alpine rock avalanches, for instance, means that the run-outs of chalk flows can match those of rock avalanches at debris volumes two orders of magnitude smaller. The geometrical definitions for flow slides are shown in Figure 15. Chalk flows vary considerably in run-out. Hutchinson (2002) subdivides them on a basis of L/H values into chalk flows of low (L/H = 1.3 − 2.5), moderate (L/H = 2.5 − 3.5) and high (L/H = 3.5 − 5 or 6) run-out. A feature identified during the ROCC investigation is the stratigraphic distribution of blocks within the debris run-out and a tendency for large blocks to be emplaced in the front of the run-out. Stratigraphic integrity is broadly retained, with the oldest beds from the base of the cliff (and the place where the largest blocks of chalk are displaced) having travelled farthest out. This corresponds with Heim's (1932) observations in the Alps.

Hutchinson (2002) found the greatest concentration of high run-out chalk flows to be on the Kent coast (Hutchinson 1988*a*), while on the Sussex coast, though there are big chalk falls with elements of flow, run-outs tend to be more restricted (e.g. Beachy Head (Jan 1999) had an L/H value of about 1.45, a chalk flow of low run-out). Hutchinson ascribes this difference in chalk flow behaviour to the generally lower porosites (higher densities) of the Sussex Chalk cliffs (e.g. Mortimore *et al.* 1990, fig.3).

Deep 'grooves' cut into the chalk wave-cut platform beneath a collapse debris fan were regularly observed during the ROCC investigations, particularly in the higher porosity French chalks where an element of flow had occurred during a cliff collapse. Such grooves indicate considerable friction at the base of a flow. The properties (porosity/density and degree of saturation) of the chalk in the wave-cut platform may also be a determining factor in the development of chalk flow slides and may control the extent of the run-out of a flow.

Other types of cliff hazard

In addition to the major types of cliff failure, smaller-scale 'slabbing' of the cliffs is common. Spalling of flint and small blocks of chalk is a continuous hazard. This is particularly common where periglacially weathered chalk is present (e.g. Black Rock, Mortimore *et al.* 2001*a*). Failures in material overlying the Chalk, including mud–slides (Newhaven 2001) and disintegration of Quaternary deposits (Black Rock Marina), are on a smaller-scale than the big chalk collapses but are a particular hazard as they occur in areas of active public access.

Influence of folding: Seaford Head and Portobello

At Seaford Head from the Castrum to Splash Point (Fig. 16) the cliff line changes to a more northerly direction as the influence of the Seaford Head Anticline becomes apparent (beds dip 10° north, see details in Mortimore 1997, Mortimore *et al.* 2001*b*).

Towards Splash Point there is a marked change in the bedding structure of the Chalk with the entry of marl seams in the Newhaven Chalk Formation. Associated with this change in lithology is a marked change in fracture style from joints perpendicular to bedding in the Seaford Chalk to steeply inclined, conjugate sets of slickensided joints in the Newhaven Chalk Formation. These joints create surfaces for large plane and wedge failures (Fig. 4). However, the 10° dip to the north provides a different orientation for these fractures compared to the Newhaven Chalk in the cliffs between Newhaven and Brighton and hence a different factor of safety against failure.

The cycle of cliff decay is different in the section between Splash Point and the old timber groyne compared to Seaford Chalk sections such as the Seven Sisters and much of Seaford Head. Following cliff failure along one of the major inclined shear fractures, erosion eventually breaks through the fracture surface and only minor spalling occurs for a while (may be a number of years). Eventually, another major inclined fracture daylights in the cliff face and continued erosion and weathering leads to another major plane or wedge failure. Evidence from historical records and photographs suggests that this cycle may take 1 to 5 years depending on the climatic conditions and frequency of fractures. No chalk flows are known from this section.

Although Palaeogene sediments are present resting unconformably on the top beds of the Culver Chalk Formation along the crest of part of the cliff, the 10° dip north prevents major sliding over the cliff. In contrast, at Newhaven, mudslides and collapses of sandstone are common (Fig. 11) and the dip is near-horizontal or to the south out of the cliff.

Portobello lies in the axial centre of the Newhaven Syncline, the structurally lowest point on the cliffs between Newhaven and Brighton. In the core of the Syncline here is the most complete (if only partial) Culver Chalk Formation, exposing beds up to just above the Lancing Flint Band (Fig. 12; Mortimore *et al.* 2001*b*). As there is no *in situ* sub-Palaeogene erosion surface preserved here it must be assumed that even more Culver Chalk was once present. On this coastline, therefore, the depth of sub-Palaeogeone erosion into the Chalk is greatest at Newhaven and least at Portobello, reinforcing the angular nature of this unconformity and the nature of the plunge of the overall tectonic structure westwards. In the centre of the Newhaven Syncline immediately on the east side of Portobello are remnants of Palaeogene and Quaternary sediments in degraded, heavily weathered chalk which also has dissolution pipes.

The weaker degraded, highly weathered chalk in the core of the valley at Portobello is eroding most rapidly, requiring the cliff-top path and protective fence-line to be moved back regularly.

Cliff collapse magnitude and frequency

A magnitude scale for Chalk cliff collapses has been developed. The volume of material involved in each type of failure was estimated by measuring the length, width and height of collapse debris. Bulking effects have been considered and are based on measurements of Chalk earthworks bulking factors (Jenner & Burfitt 1975; Hutchinson 1988*b*, 2002; Lord *et al.* 2002). Unpublished bulking factors used in chalk landscaping works for different chalk units are included in Mortimore *et al.* (this volume). Hutchinson (1988*a*) has shown how important volume is in terms of potential scale of a slope hazard.

A frequency of occurrence of a particular hazard is required for a risk analysis. The two year ROCC programme was not sufficiently long to provide an accurate record of frequency of cliff failures for all types of hazard (Table 5). Historical records have been used to illustrate the increased occurrence of failures during periods of high rainfall (ROCC Database; also see Duperret *et al.* 2004; Fig. 17). However, more observations are required before a reliable frequency analysis can be carried out.

Until recently, most analyses of the Sussex cliffs were concerned with rate of cliff retreat. This is an estimate of erosion rate based on historical records of cliff-line positions. Whilst cliff-line retreat is an important factor, the location, magnitude and frequency of particular types of cliff failure are of more immediate importance to planners and engineers (Table 5). The length and width of cliff involved in a collapse has been analysed (presented in Duperret *et al.* 2004).

Marine erosion and climatic factors

An understanding of the impact of marine erosion rates and climatic conditions is required for a fully integrated risk management policy for the coastline.

A basic assumption with cliff erosion is that a notch forms at the base of the cliff where marine wave attack is concentrated (e.g. Hutchinson 1971). Failure results from unloading at the base of the cliff with a fracture progressively developing 'bottom-up'. As indicated above there are many more types of processes than this operating in Chalk cliffs. There are places where a notch develops but this tends to be in hard chalk such as occurs on the Isle of Wight. On the coasts of Sussex and France marine erosion exploits the different lithological and fracture characteristics of the chalk to create caves of different shape and size (e.g. Duperret *et al.* 2002). Locally, some caves may develop into isolated stacks (such as Splash Point at Seaford Head). Marine undercutting may, therefore, take the form of a notch or a cave.

The 'exceptionally' wet winter of 2000–2001 (Fig. 17) illustrated the scale of failures that can occur even where cliffs are protected. These failures ranged from joint controlled failures at Peacehaven Cliffs and Black Rock to the mud-slides and ravelling of the cliff at Newhaven and Black Rock respectively. Major cliff collapses at Beachy Head in 1960 and 1999–2001 (Fig. 14) show a close relationship with rainfall data for Eastbourne (Fig. 17).

Marine erosion and weathering due to rainfall, frost and storms will influence the rate at which a particular hazard develops. If these factors are going to change in the future (e.g. a sea-level rise might produce a critical wave impact level or increased rainfall or storm events may accelerate cliff failures of all types) then these need to be modelled (e.g. Mitchell & Pope 2004).

Influence of coast protection works

A particular feature of this study is the recognition that coastal protection works against wave attack will, of themselves, not eliminate slope failures in the Chalk. The various phases of the Peacehaven Coast Protection Works between Peacehaven Steps and Telscombe Cliffs were constructed between 1978 and 1984. As a result, the cliffs in this entire section (nearly 4 km) are protected from wave attack at the base of the cliff. The cliff height is relatively uniform from high points around 35 m on interfluves to low points below 25 m in the intervening small dry valleys. The sea wall and undercliff walkway were constructed to protect the most vulnerable properties in Peacehaven, which in many cases, are within 10–20 m of the cliff edge.

The Chalk geology of these cliffs is dominated by the Newhaven Chalk Formation. However, the continuing strata dip northwards takes older beds of Newhaven Chalk below beach level and brings in the basal beds of the Culver Chalk Formation. The Culver Chalk is present along the entire cliff line westwards to Portobello.

The feather-edge of the Palaeogene deposits gets closer to the cliff edge northwestwards as the dip brings younger deposits to lower levels in the axis of the Newhaven Syncline. This leads to the presence of dissolution pipes (e.g. Argent 1981; Mortimore *et al.* 1990; Lawrence 2001).

It has been a surprise to see significant cliff failures occur in this protected section of coastline during the wet winter of 2000–2001. The failures involved up to 100000 tonnes of rock that had to be cleared from the undercliff walk (Magnitude 5–6). These were typical Newhaven Chalk Formation failures, controlled by steeply inclined fractures and involving some material failure within chalk blocks (Figs 9 & 10). The chalks were weathered (heavily iron-stained fractures) and the failures were located in areas of cliff that had not been trimmed back, removing potential failure blocks.

The inference from the style and scale of cliff failures on this protected section of coast during 2000–2001 is that it takes 15–20 years after cliff trimming for weathering to loosen the rock mass sufficiently to allow cliff failures to develop. Once the process starts it is likely to continue. Hence the hazard frequency is likely to increase with time. The final trigger was heavy rainfall.

Regular spalling of small fragments of chalk and flint is a continuous hazard on this undercliff.

The entire cliff section from Saltdean in the east to Black Rock in the west is protected by a sea wall, groynes and, in part, by a beach replenishment programme. The undercliff walk is regularly used for recreational purposes (walking, bicycle riding, disabled access) and even small falls are, therefore, a hazard. The beds of Chalk continue to rise towards Brighton on the southern limb of the Old Steine Anticline. As this is a protected section of coastline, major cliff failures were not expected. However, during the winter 2000–2001 several collapses occurred in the *in situ* chalk cliffs behind Black Rock Marina, Brighton. In addition, numerous small fragments of chalk and flint from both the *in situ* chalk cliff and the degraded valley-fill material have fallen onto the undercliff pavement and the access pathways. Like the Peacehaven cliff failure, the Brighton Marina failures were related to the structure of the Newhaven Chalk, the length of time the cliffs have been weathering since they were trimmed and the severe wet weather. The scale of failures were of Magnitude 2–5. Areas that are potentially going to fail are those where full face trimming has not been complete, where overhangs are developing and where the main fractures daylight in the cliff at a critical dip angle and strike direction.

Conclusions

The first stage of a risk management programme for the Chalk cliffs of Sussex, that of hazard identification in terms of type and scale (magnitude) of slope failure (Table 5) has been accomplished during the INTERREG II ROCC investigations. Each section of cliff along the 40km of coast has been mapped and described in terms of its geohazards and the underlying geology that controls that hazard. Details of this work are held by local authorities (Mortimore *et al.* 2001*a*); only a summary of this work is given here. The results of the investigation indicate that the geology determines the type of rock mass in terms of material strength and fracture style and persistence. The weakest materials are those in the Seaford and Culver Chalk formations. These two formations are characterized by vertical fracture sets. In contrast, the Holywell, New Pit and Newhaven Chalk formations are characterized by numerous marl seams and inclined conjugate shear joints. The dihedral angle of the shears, however, varies consistently in each unit. The shear strength of fractures also varies depending on fracture fill. The common sheet-flint fill of joints in the Newhaven Chalk will have a different shear strength compared to the clay-filled, polished surfaces in the Holywell and New Pit Chalk formations.

The geology, particularly the relationship of bedding dips on folds (anticlines and synclines), also determines the way in which failures develop. For example, the dip north of beds of Newhaven Chalk at Seaford Head creates a different orientation for the same style of fractures in nearly horizontally bedded Newhaven Chalk at Newhaven. Hence the critical angle for failure planes will vary according to dip of strata. The same dip north at Seaford prevents the Palaeogene deposits from collapsing over the edge of the cliff in contrast to the way these same deposits readily form mudslides at Newhaven.

The Chalk cliff hazards range from simple plane and wedge failures in low-cliffs (e.g. at Peacehaven and Eastbourne), through to the complex failures in high cliffs such as Beachy Head. Each part of the cliff contributes to the overall hazard. The wave-cut platform may increase or reduce the rate of cliff erosion at the base of the cliff depending on the material present and the amount of protection in terms of beach present. The properties of the chalk forming the wave-cut platform (e.g. porosity or density and friction) may be a factor in controlling flow-slide generation and run-out distance. The complexity of geology in the main cliff face and the degree of weathering, presence of dissolution pipes and Palaeogene deposits on the cliff top are all factors considered in this study.

Location, magnitude and frequency of particular types of cliff failure are considered to be more important than calculations of generalized rates of cliff-line retreat when dealing with the vulnerabilty of properties and users of particular parts of the coastal cliff-line. Magnitude and frequency analyses of cliff collapses have been carried out over a limited period to provide a preliminary magnitude scale, frequency of occurrence and identification of the locations of particular types of cliff failure.

The ROCC investigation has begun the process of identifying the cliff collapse hazards, understanding the processes and integrating some of the information necessary for a risk management programme. This work needs to be carried to its conclusion.

Acknowledgements. This work has been undertaken as part of INTERREG II project ROCC funded by the European Union. We have received enormous support from our local councils particularly Brighton and Hove City Council; Lewes District Council; Wealden District Council; English Nature; The Environment Agency; The National Trust and Southern Water. We are particularly grateful to the Environment Agency, Southern Water and Bob Seago (University of Brighton) for some of aerial photographs of the Sussex coastline used in this paper. Climate data was obtained from the Meteorological Office. The British Geological Survey and the Ordnance Survey provided digital format maps for the GIS and ROCC Database and have also been immensely supportive throughout the research programme.

Although this paper concerns the Chalk cliffs of Sussex only, it is part of a wider study with our French colleagues of the coast of France and England. We acknowledge the wonderful teamwork developed with the French that allowed us to complete the ROCC programme in such a short time (two years) and we have gained great benefit from each of our different experiences and methodologies.

We are very grateful for the constructive criticisms and comments of referees, particularly from Professor John Hutchinson, which have greatly improved the manuscript.

References

ARGENT, K. C. 1981. *The Location and Investigation of Swallow Holes in Chalk Using Geophysical Methods*. BSc Thesis, University of Brighton.

BARTON, M. E. 1990. Stability and recession of the chalk cliffs at Compton Down, Isle of Wight. In. BURLAND, J. B., MORTIMORE, R. N., ROBERTS, L. D., JONES, B. L. & CORBETT, B. O. (eds). *Chalk. Proceedings of the International Chalk Symposium, Brighton Polytechnic, 1989*. 541–544. Thomas Telford, London.

BIRKELUND, T., HANCOCK, J. M., HART, M. B., RAWSON, P. F., REMANE, J., ROBAZYNSKI, F., SCHMID, F. & SURLYK, F. 1984. Cretaceous stage boundaries – proposals. *Bulletin of the Geological Society of Denmark*, **33**, 3–20.

BRISTOW, R., MORTIMORE, R. N. & WOOD, C. J. 1997. Lithostratigraphy for mapping the Chalk of southern England. *Proceedings of the Geologists' Association*, **109**, 293–315.

CORBETT, B. O. 1990. Slip in chalk cliffs at Brighton. *In*: BURLAND, J. B. MORTIMORE, R. N., ROBERTS, L. D. & JONES, D. L. (eds) *Chalk*. Thomas Telford, London, 527–531.

De FREITAS, M. H. & WATTERS, R. J. 1973. Some field examples of toppling failure. *Géotechnique* **23**, 495–514.

DUPERRET, A., GENTER, A., MORTIMORE, R. N., DELACOURT, B. & DE POMERAI, M. 2002. Coastal rock cliff erosion by collapse at Puys, France: the role of impervious marl seams within the chalk of NW Europe. *Journal of Coastal Research*, **18**, 52–61.

DUPERRET, A., GENTER, A., MARTINEZ, A. & MORTIMORE, R. N. 2004. Coastal chalk cliff instability in NW France: the role of chalk lithology, fracture pattern and rainfall. *In*: MORTIMORE,

R. N. & DUPERRET, A. (eds) *Coastal Chalk Cliff Instability*. Geological Society, London, Engineering Geology Special Publication, **20**, 33–55.

FOOKES, P. G. & BEST, R.1969. Consolidation characteristics of some Late Pleistocene periglacial soils of east Kent. *Quarterly Journal of Engineering Geology*, **2**, 103–128.

GEIKIE, A. 1893. Text–book of Geology (3rd edn). Macmillan, London, New York.

GENTER, A., DUPERRET, A., MARTINEZ, A., MORTIMORE, R. N. & VILA, J-L. 2004. Multiscale fracture analysis along the French chalk coastline for investigating erosion by cliff collapse. *In*: MORTIMORE, R. N. & DUPERRET, A. (eds) *Coastal Chalk Cliff Instability*. Geological Society, London, Engineering Geology Special Publication, **20**, 57–74.

GILBERT, R. 1964. Changing face of Beachy Head. *Eastbourne Gazette*, Eastbourne, 12th August, p. 21.

HEIM, A. 1932. Bergsturz und Menschenleben. *Beiblatt zur Vierteljahrsschrift der Naturforschenden Gesellschaft in Zürich*, No. 20, **Jahrg. 77**, 1–218.

HUTCHINSON, J. N. 1971. Field and Laboratory Studies of a fall in Upper Chalk cliffs at Joss Bay, Isle of Thanet. *Roscoe Memorial Symposium, Cambridge University, 1971*, Henley-on-Thames; G.T. Foulds & Co. Ltd, 692–706.

HUTCHINSON, J. N. 1983. *Engineering in a Landscape*. Inaugural lecture, 9 October, 1979. Imperial College, London.

HUTCHINSON, J. N. 1988*a*. General Report: Morphological and geotechnical parameters of landslides in relation to geology and hydrogeology. *In*: BONNARD, C. (ed.). *Landslides*. Balkema, Rotterdam, **1**, 3–35.

HUTCHINSON, J. N. 1988*b*. A small-scale check on the Fisher-Lehmann and Bekker – Le Hevre cliff degradation models. *Earth Surface Processes and Landforms*, **23**, 913–926.

HUTCHINSON, J. N. 2002. Chalk flows from the coastal cliffs of north-west Europe. Geological Society of America. *Reviews in Engineering Geology*, **15**, 257–302.

HUTCHINSON, J. N. & MILLAR, D. L. 1998. Survey of the interglacial Chalk cliff and associated debris at Black Rock, Brighton. *In: The Quaternary of Kent and Sussex: Field Guide*. Murton, J. B. *et al.* (eds). Quaternary Research Association, London, 135–146.

JENNER, H. N & BURFITT, R. H. 1975. *Chalk: An Engineering Material*. Paper read to a meeting of the Southern Area of the Institution of Civil Engineers at Brighton, Sussex on Thursday 6th March 1975.

JUIGNET, P. 1974. La transgression crétacée sur la bordure orientale du Massif Armorican, Aptien, Albien, Cénomanien de Normandie et du Maine. Le stratotype du Cénomanien. Thèse, Université de Caen.

LAWRENCE, J. 2001. Depressions adjacent to the cliff top behind numbers 9 and 11 Neville Road, Peacehaven. Report for Lewes District Council. 16/04/2001.

LORD, J. A., CLAYTON C. R. I. & MORTIMORE, R. N. 2002. *Engineering in Chalk*. Construction Industry Research and Information Association. CIRIA, **C574.**

MIDDLEMISS, F. A. 1983. Instability of Chalk cliffs between the South Foreland and Kingsdown, Kent, in relation to geological structure. *Proceedings of the Geologists' Association*, **94**, 115–122.

MITCHELL, S. B. & POPE, D. J. 2004. Prediction of nearshore wave energy distribution by analysis of numerical wave output: East Sussex coastine, UK. *In*: MORTIMORE, R. N. & DUPERRET, A. (eds) *Coastal Chalk Cliff Instability*. Geological Society, London, Engineering Geology Special Publication, **20**, 99–107.

MORTIMORE R. N. 1978. The stability of the Chalk cliffs between Newhaven and Brighton. Report for East Sussex County Engineers Department, Site Investigation Unit.

MORTIMORE, R. N. 1983. The stratigraphy and sedimentation of the Turonian – Campanian in the Southern Province of England. *Zitteliana*, **10**, 27–41.

MORTIMORE, R. N. 1986. Stratigraphy of the Upper Cretaceous White Chalk of Sussex. *Proceedings of the Geologists' Association*, **97**, 97–139.

MORTIMORE, R. N. 1997. *The Chalk of Sussex and Kent*. Geologists' Association Guide No. 57.

MORTIMORE, R. N. 2001*a*. *Report on Mapping of the Chalk Channel coast of France from Port du Havre-Antifer to Ault, June-September 2001*, Bureau de Recherches Géologiques et Minières (BRGM), 27th September 2001.

MORTIMORE, R. N. 2001*b*. Chalk: a stratigraphy for all reasons. The Scott Simpson Lecture. *Proceedings of the Ussher Society, Geoscience in south-west England*, **10**, 105–122

MORTIMORE, R. N. & LAWRENCE, J. 2001. Collapse of Chalk coastal cliffs below Peachaven, 500m west of Peachaven Steps. Report for Lewes District Council, 12/01/2001.

MORTIMORE, R. N. & POMEROL, B. 1987. Correlation of the Upper Cretaceous White Chalk (Turonian to Campanian) in the Anglo-Paris Basin. *Proceedings of the Geologists' Association*, **98**, 97–143.

MORTIMORE, R. N., POMEROL, B. & FOORD, R. J. 1990. Engineering stratigraphy and palaeogeography of the Chalk of the Anglo-Paris Basin. In. BURLAND, J. B., MORTIMORE, R. N., ROBERTS, L. D., JONES, B. L. & CORBETT, B. O. (eds). *Chalk. Proceedings of the International Chalk Symposium, Brighton Polytechnic, 1989*. 47–62. Thomas Telford, London.

MORTIMORE, R. N., LAWRENCE, J. & POPE, D. 2001*a*. Geohazards on the UK Chalk Cliffs of Sussex. Final Report. INTERREG II. Espaces Rives-Manche East Sussex/Seine Maritime/ Somme, December 2001.

MORTIMORE, R. N., WOOD, C. J. & GALLOIS, R. W. 2001*b*. *British Upper Cretaceous Stratigraphy*. Geological Conservation Review Series, No. 23, Joint Nature Conservation Committee, Peterborough.

MORTIMORE, R. N., STONE, K. J., LAWRENCE, J. & DUPERRET, A. 2004. Chalk physical properties and cliff instability. *In*: MORTIMORE, R. N. & DUPERRET, A. (eds) *Coastal Chalk Cliff Instability*. Geological Society, London, Engineering Geology Special Publication, **20**, 75–88.

OVE ARUP. 1976. Black Rock Interchange. Site Investigation Report.

RAWSON, P. F., DHONDT, A.V., HANCOCK, J. M. & KENNEDY, W. J. 1996. Proceedings of the Second International Symposium on Cretaceous Stage Boundaries Brussels 8–16 September 1995. *Bulletin de l'Institut Royal des Sciences Naturelles de Belgique, Sciences de la Terre*, **66**-supplement.

ROWE, A. W. 1900. The Zones of the White Chalk of the English coast. I–Kent and Sussex. *Proceedings of the Geologists' Associa*tion, **16**, 289–368.

SHEPHARD-THORN, E. R. & WYMER, J. J.1977. *South-East England and the Thames Valley*. International Unioin of Quaternary Research (INQUA) X Congress 1977. Guidebook for Excursion A5. INQUA 1977.

WILLIAMS, R. E. 1990. Performance of highway cuttings in chalk. *In*: BURLAND, J. B., MORTIMORE, R. N., ROBERTS, L. D., JONES, B. L. & CORBETT, B. O. (eds). *Chalk. Proceedings of the International Chalk Symposium, Brighton Polytechnic, 1989*. 469–476. Thomas Telford, London.

Coastal chalk cliff instability in NW France: role of lithology, fracture pattern and rainfall

A. Duperret[1], A. Genter[2], A. Martinez[1] & R. N. Mortimore[3]

[1] Laboratoire de Mécanique, Physique et Géosciences, Université du Havre, BP 540, 76 058 Le Havre cedex, France

[2] BRGM (French Geological Survey), 3 avenue Claude Guillemin, BP 6009, 45060 Orléans, France

[3] Applied Geology Research Unit, University of Brighton, Moulsecoomb, Brighton, BN2 4GJ, UK

Abstract: Coastal retreat has been studied along 120km of French Channel chalk coast from Upper Normandy to Picardy. During the investigation period, 1998–2001, 55 significant collapses were recorded. Of these 5.5% were very large-scale, 34.5% large-scale, 34.5% medium-scale and 25.5% small-scale collapses. Observations indicate that the larger the collapse size the greater the coastal cliff retreat. Four types of cliff failure were observed: (1) vertical failures in homogeneous chalk units; (2) sliding failures where two superimposed chalk units were present; (3) wedge and plane failures mainly recognized in the UK in formations with stratabound fractures; (4) complex failures in cliffs with more than one style of fracturing. Rainfall in relation to the timing of cliff collapse indicates two periods that trigger a collapse. The first occurs about one month after heavy rainfall within poorly fractured chalk and the second occurs when a dry period is interrupted by sharp rainfall in cliffs with major karst features (pipes etc). Medium to small-scale cliff collapses were, in some cases, caused by marine erosion at the base of the cliff creating a notch. A key factor controlling the type of collapse is the lithostratigraphic unit, while the extent of the collapse scar may be controlled by fracture type.

Coastal cliff erosion in Upper-Normandy and Picardy

Long-term mean erosion rates of coastal chalk cliffs of the English Channel are roughly similar in France and UK, with 0.23 m/year on the French chalk coast (Costa 2000) and 0.27 m/year on the East Sussex chalk coast (Dornbusch *et al.* 2001). These recent studies as well as those by May (1971) in UK and Prêcheur (1960) in France have focused on calculating the long-term average erosion rates on the Channel chalk cliffs. Based on analysis of vertical photographs of the French coast, acquired between 1939 and 1995, Costa (2000) shows that long term mean erosion rate is variable in space, with three main coastal sections having various rates varying from 0.1 to 0.5 m/year. Similar results were obtained for the East Sussex chalk coast, with a comparison of Ordnance Survey maps surveyed in 1870 and 1990, where four main coastal sections with values from 0.01 to 0.70 m/year have been identified (Dornbusch *et al.* 2001). Furthermore, as shown on the California rocky coast, more erosion occurs over a time scale of several years during period of severe storms or tectonic activity, than occurs during decades of 'normal' weather or tectonic quiescence (Kuhn & Shepard 1983; Griggs 1994; Hapke & Richmond 1999). Thus, the coastal cliff retreat could be highly episodic in time, with various short-term mean erosion rates.

Recent field evidence presented in this paper shows that chalk cliff retreat is mainly governed by sudden collapses involving a complete vertical section of cliff, rather than a continuous retreat of the whole coastline. Little work has been devoted to the analysis of processes responsible for the collapses of the chalk seacliffs, and this led to the European scientific project, ROCC (Risk Of Cliff Collapse) reported herein. The main goal of the ROCC project is to identify the critical parameters leading to chalk coastal cliff collapses, and to evaluate the impact of those parameters and their interaction in such rock mass movements. The ROCC project focused on Upper Normandy and Picardy chalk coasts in France, from Le Tilleul to Ault (120km long) and on East Sussex chalk coast, from Brighton to Eastbourne (40km long), in UK (Fig. 1).

The evolution of a cliff from stability toward failure, depends on changes present in the rock mass (lithology, fracture pattern), and processes acting within the rock mass (degree of water saturation, water movement) caused by external agencies of subaerial and marine origin. Field observations indicate a wide range of variation within cliff failure type, in relation to the chalk lithology and the fracture pattern of coastal chalk cliffs, which could influence the spatial distribution of collapses.

The aim of this paper is to determine the main types of chalk cliff failures on the French coast and to discuss the processes leading to collapse. The paper presents (1) a synthetic description of the chalk cliff characteristics (stratigraphy, lithology, fracture pattern); (2) a detailed analysis of the chalk cliff collapses observed on the French coastline; (3) the various chalk cliff failure types in relation to chalk lithology and fracture pattern, and a discussion on (4) the triggering mechanisms of chalk cliff collapse.

From: MORTIMORE, R. N. & DUPERRET, A. (eds) 2004. *Coastal Chalk Cliff Instability*. Geological Society, London, Engineering Geology Special Publications, **20**, 33–55. 0267-9914/04/$15.00

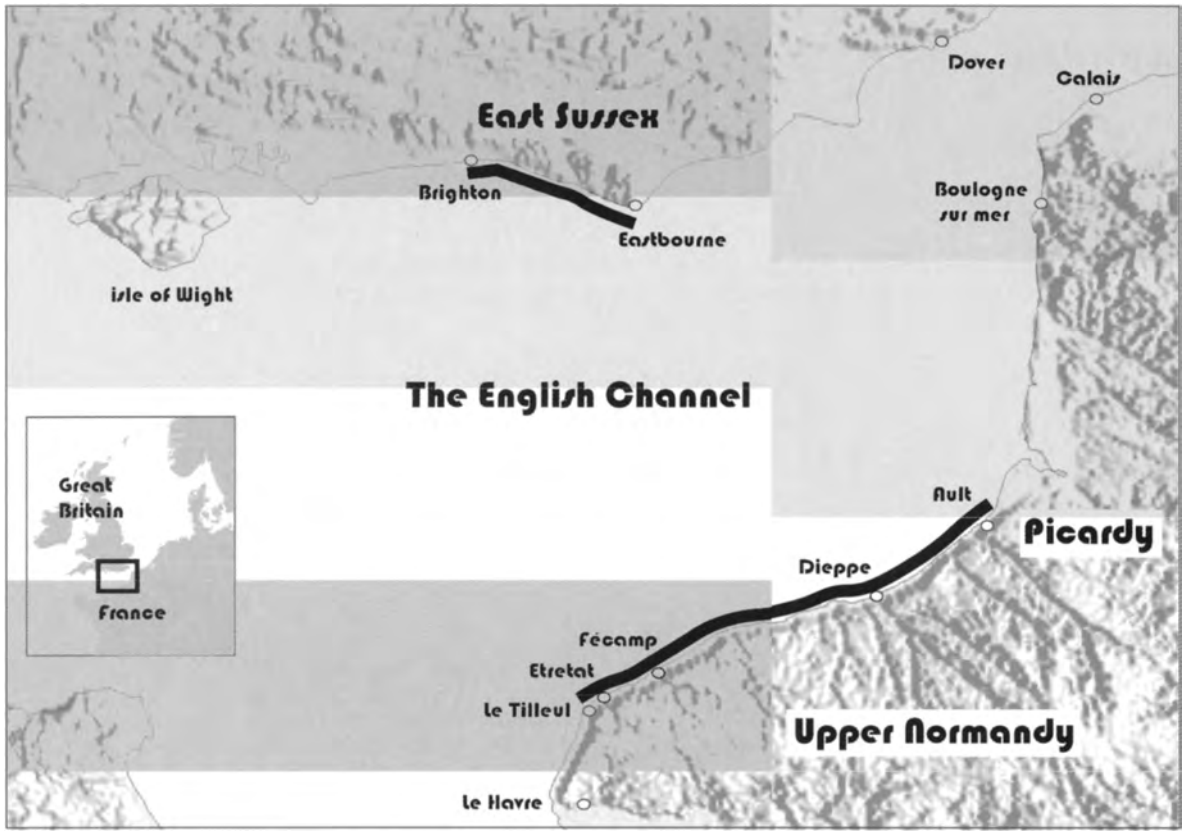

Fig. 1. Location of the study area along the coast of the English Channel. The thick line is the area investigated by the ROCC project.

Lithostratigraphy of the chalk cliffs

The Upper Cretaceous Chalk cliffs of the eastern English channel range in age from the Cenomanian (98 Ma) to lower Campanian (80 Ma) in age (Mégnien & Mégnien 1980; Mortimore & Pomerol 1987). The same lithostratigraphic divisions can be recognized and applied to both English and French coasts. These divisions are closely linked to the physical properties of the chalk and are thus well adapted to engineering purposes (Mortimore *et al.* 1990; Mortimore 1993 2001*b*) and for understanding the mechanical behaviour of the chalk during cliff collapse.

Chalk unit stratigraphy

On the French coast from Le Tilleul to Ault (120 km long), the chalk cliffs are made of six different formations, from the Upper Cretaceous: Craie de Rouen (Middle to Upper Cenomanian), Holywell Nodular Chalk (Lower Turonian), New Pit Chalk (Lower to Middle Turonian), Lewes Chalk (Middle Turonian to Middle Coniacian), Seaford Chalk (Middle Coniacian to Middle Santonian) and Newhaven Chalk (Upper Santonian to Lower Campanian) (Mortimore & Pomerol 1987; Mortimore 2001*a*), whereas on the English coast of East Sussex, from Brighton to Eastbourne (40 km long), the cliffs contain eight chalk formations; the succession is completed by one more younger unit: the Culver Chalk (Lower Campanian) and two more older units: the West Melbury Chalk (Lower to Middle Cenomanian) and the Zig Zag Chalk (Middle to Upper Cenomanian). The craie de Rouen corresponds to the combined West Melbury and Zig Zag Chalk formations in UK (Mortimore 1983). Two simplified geological sections are produced from field observation on the chalk outcrops at twenty locations selected on each part of the Channel (Fig. 2): the greater diversity of chalk units on the English coast results from more folding in Southern England than in Northwest France. Fold axes are generally NW–SE across the AngloParis basin becoming WNW–ESE along the coast of England (Mortimore & Pomerol 1997).

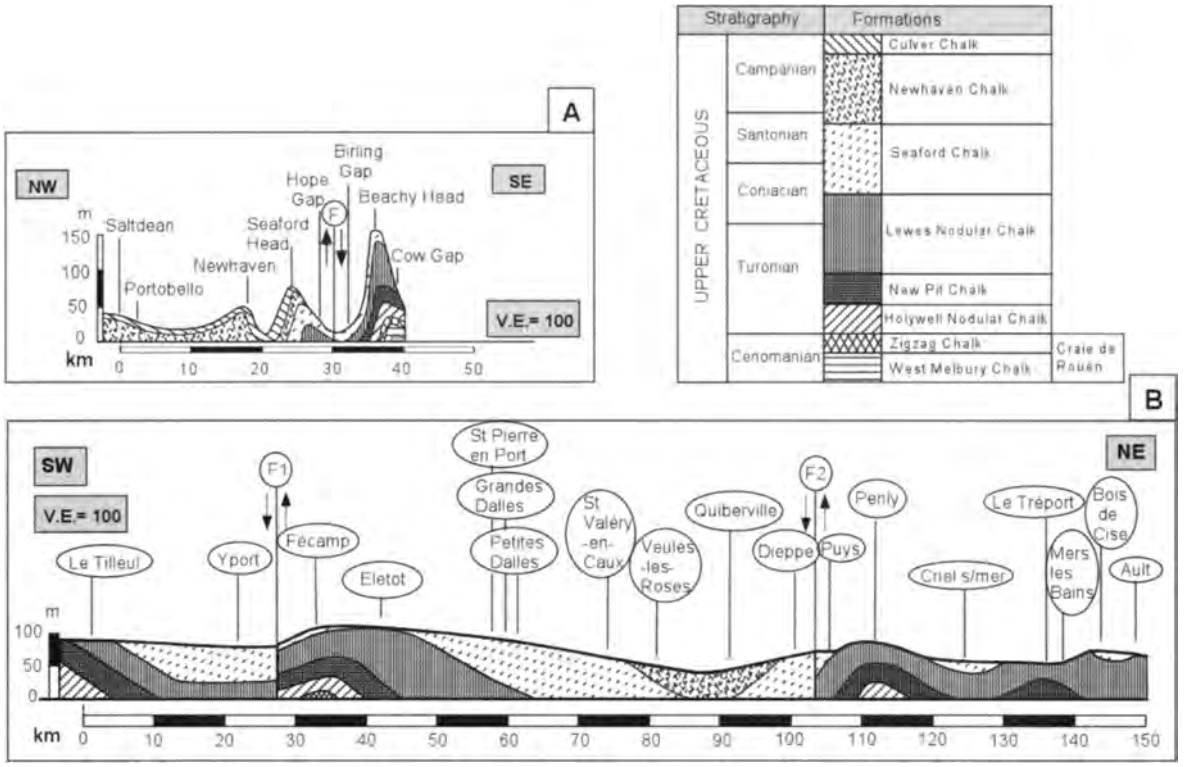

Fig. 2. Geological cross sections of chalk outcrops from each part of the English Channel, using the lithostratigraphic scale, correlated with the stratigraphic scale of Upper Cretaceous age (Mortimore 1986). A. Simplified cross section on the East sussex coast (40km long), England, from NW to SE. F, fault; B, simplified cross section on the Upper-Normandy and Picardy coasts (120km long), France, from SW to NE; F1, Fécamp Lillebonne fault; F2, Bray fault; V.E., vertical exaggeration.

Chalk lithology in Upper-Normandy and Picardy

Each chalk unit has its own lithological and geotechnical characteristics. Both the chalk type and the marl content as well as flint band occurrence within a given chalk unit induce different geotechnical properties (Mortimore 1983, 2001; Mortimore *et al.* 1990; Bristow *et al.* 1997; Duperret *et al.*, 2002*a*). Some chalk units contain numerous marl seams (New Pit Chalk and Newhaven Chalk formations), other are nodular (craie de Rouen, Holywell and Lewes Nodular Chalk formations), whereas the Seaford Chalk formation is more homogeneous and contains bands of large flints (Fig. 3). Differences when compared to the UK are the presence of the Cenomanian craie de Rouen with numerous flint bands in Upper Normandy (Juignet 1974) in contrast to the West Melbury Marly Chalk and Zig Zag Chalk formations of Beachy Head in Sussex. The Holywell Nodular Chalk is a nodular and massive chalk, with few flint bands, which contains many flaser marls and abundant *Mytiloides* shell debris layers. There is no Plenus Marls at the base of the Holywell Nodular Chalk Formation in Upper Normandy. The New Pit Chalk is a massively bedded chalk with conspicuous marl seams and regular flint bands. The New Pit Chalk Formation contains numerous flint bands in cliffs to the south of Fécamp but is flintless northwards at St Martin-plage, north of Dieppe. The Lewes nodular Chalk is a nodular yellowish coarse chalk, including soft, marly bands and nodular hardgrounds, with regular flint layers. The Lewes Nodular Chalk Formation contains dolomitic layers to the south of Fécamp which are absent northwards. The Seaford Chalk is a white chalk with conspicuous bands of large flints. The Newhaven Chalk is a marly chalk, with numerous marl seams and regular but few flint bands.

Vertical distribution of chalk units in Upper-Normandy and Picardy

A lithostratigraphic map of the 20–100m high cliffs along the French coast was constructed (Mortimore 2001*a*), using the scheme devised in Southern England (Mortimore 1983, 1986). The synthetic map of chalk unit distribution exposed on the French cliffs indicates the different chalk succession

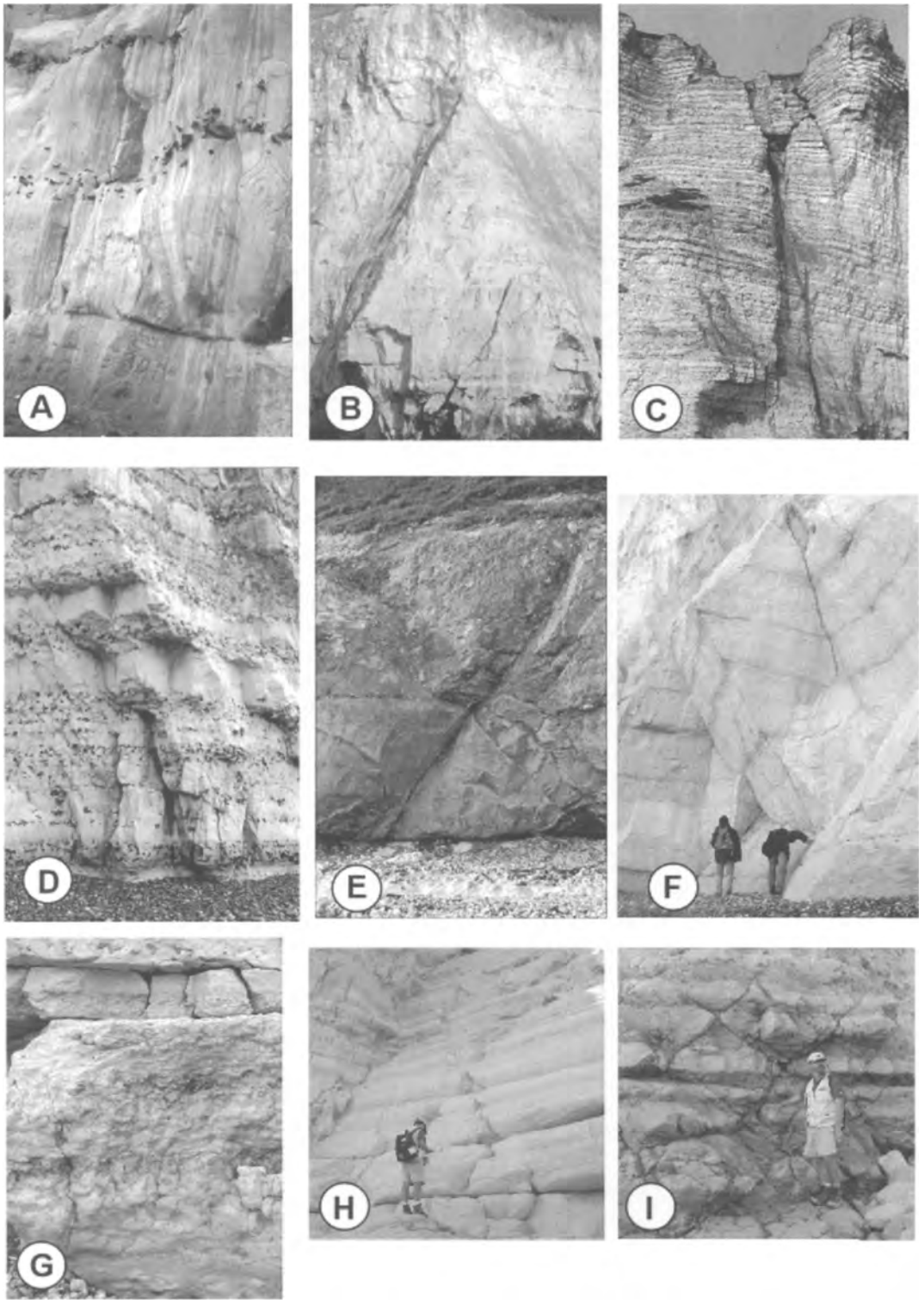
A
B
C
D
E
F
G
H
I

present on a vertical cliff section (Fig. 4). About 45% of the analysed coastline length exposes one lithostratigraphic unit: 15% Lewes Nodular chalk Formation at five locations between Dieppe and Ault; 20% Seaford Chalk Formation between Veulettes sur Mer and Veules-les-Roses; 10% Newhaven Chalk Formation between Veules-les-Roses and Quiberville. About 50% of the analysed coastline contains two Chalk formations in the cliff face of which the majority (40%) comprises Lewes and Seaford Chalk formations whereas the combination of Seaford and Newhaven Chalk formations represents only 4% of the cliff line (between Quiberville and Pourville). The remaining 6% of coastline combines the New Pit and Lewes Chalk formations between Le Tréport and Mers-les-Bains. Only 4% of the coastline combines three Chalk formations represented by the Holywell, New Pit and Lewes chalks and only 1% combines five chalk units, the cap Fagnet section at Fécamp (Craie de Rouen to Seaford Chalk formations).

Fracture patterns in the chalk cliffs

A key geological parameter with a significant role in coastal cliff collapse is the occurrence of a pre-existing fracture network. As noted by Middlemiss (1983) on the chalk cliffs of Kent (UK), cliff collapses are mainly controlled by pre-existing fractures. The more intense the fracturing the more frequently collapses are likely to occur. However, this simple empirical relationship is not systematic, probably because the natural fracture properties and the interaction with other parameters could be complex. In the upper Cretaceous chalk of the Anglo-Paris basin, the fracture style is linked either to chalk lithology, or to tectonics. Fracture systems embedded within chalk correspond to two major systems: (1) the existence of the stratigraphical tectonic concept defined in the UK by Mortimore (1979), where some lithostratigraphic Cretaceous chalk units show an earlier fracture pattern called here stratabound fractures; (2) the existence of fracture network related to the post-sedimentary structural evolution of the Anglo-Paris basin, called here non-stratabound fractures (Genter *et al.* 2004). The various types of fracture described by Genter *et al.* (2004) are illustrated including stratabound fractures typical of the Holywell Nodular Chalk Formation (Fig. 3F), New Pit Chalk Formation (Fig. 3E) and the Newhaven Chalk Formation (Fig. 3B), whereas non-stratabound fractures are shown in Figures 3C, 3D and 5.

Fig. 3. The chalk units present along the coastline of France (Upper-Normandy and Picardy) and England (East Sussex), from field observations and previous synthetic works (Mortimore & Pomerol 1987; Bristow *et al.* 1997). A, Culver Chalk: chalk with some flint bands; B, Newhaven Chalk: marly chalk, with numerous marl seams and regular but few flint bands; C, Seaford Chalk: white chalk, from very soft to medium hard with conspicuous bands of large flints; D, Lewes Chalk: a nodular yellowish coarse chalk, including soft, marly bands and nodular hardgrounds, with regular flint layers; E, New Pit Chalk: massively bedded chalk with conspicuous marl seams; F, Holywell Chalk: nodular and massive chalk, with few flint bands; G, Craie de Rouen: very hard nodular chalk with glauconitic and phosphatic hardgrounds and flint bands; H, Zigzag Chalk comprises two sub-units. The upper unit consists on firm, pale-grey to off-white, blocky chalk, whereas the lower unit is a gritty, silty chalk; I, West Melbury Chalk: buff, grey and off-white marly chalk, with local beds of hard chalk.

In the framework of the ROCC project, more than 2000 fracture orientation measurements were made on the chalk cliffs of the Channel, at 24 sites in France (Upper-Normandy and Picardy). Measurements were made both on the vertical cliff face and on the flat beach platform. This combination of measurements provided data on fractures roughly parallel to the coastline on the beach platform and fractures crossing the vertical cliff face.

Fracture data acquired on the cliff face on 16 sites evidence the N120E trend as the most significant set. On each site, one or several secondary sets may appear. Fracture data acquired on the beach platform at Le Tilleul, Eletot, Petites Dalles, Bois de Cise and Veulettes sur Mer show a N40E–60E oriented fracture set, which is rarely evident on the cliff face due to its orientation being broadly parallel to the local coastline (Genter *et al.* 2004). Acquisition of structural data from the beach platform has also shown two types of fracture pattern. One is made of joints (from 10cm to several metres lengths) organized in clusters, whereas the other one is made of isolated fractures (from several metres to one hundred metres lengths), extending into the cliff face where they correspond to normal faults or master joints.

Karstic system in Upper-Normandy and Picardy

According to Rodet (1992) and Crampon *et al.* (1993), the karst system is better developed in Upper-Normandy than in Picardy and may extend along pre-existing fractures of the chalk. On the coastal chalk cliffs, several structural types confirm the occurrence of karst: (1) vertical dissolution pipes (DP), which develop from the top of the cliff, along large-scale fractures of tectonic origin (Fig. 5). Dissolution pipes observed on the cliff face are only located south of the Bray fault in Upper-Normandy region; (2) horizontal caves may develop along sub-horizontal hardgrounds, semi-tabular flint bands, sheet flints and marl seams, as observed at Etretat, Yport, Fécamp, Veulettes sur Mer and Dieppe. These karstic systems are characterized by caves which develop along pre-existing fracture network. Open caves may correspond to the outlet of palaeo-groundwater system, as assumed by Rodet (1992) at Fécamp, but may also correspond to a sediment-filled cave system which develops upwards from a hard-ground, as at Veulettes sur Mer and to underground river fed by an overlying dissolution pipe system, as at Dieppe (Mortimore 2001*b*). (3) Active karstic spring outlets are rising at the base of the cliff or on the beach platform as 'depression' springs, such as between St Valéry-en-Caux and Veules-les-Roses (Chemin *et al.* 1992), or as karstic exsurgence at Yport

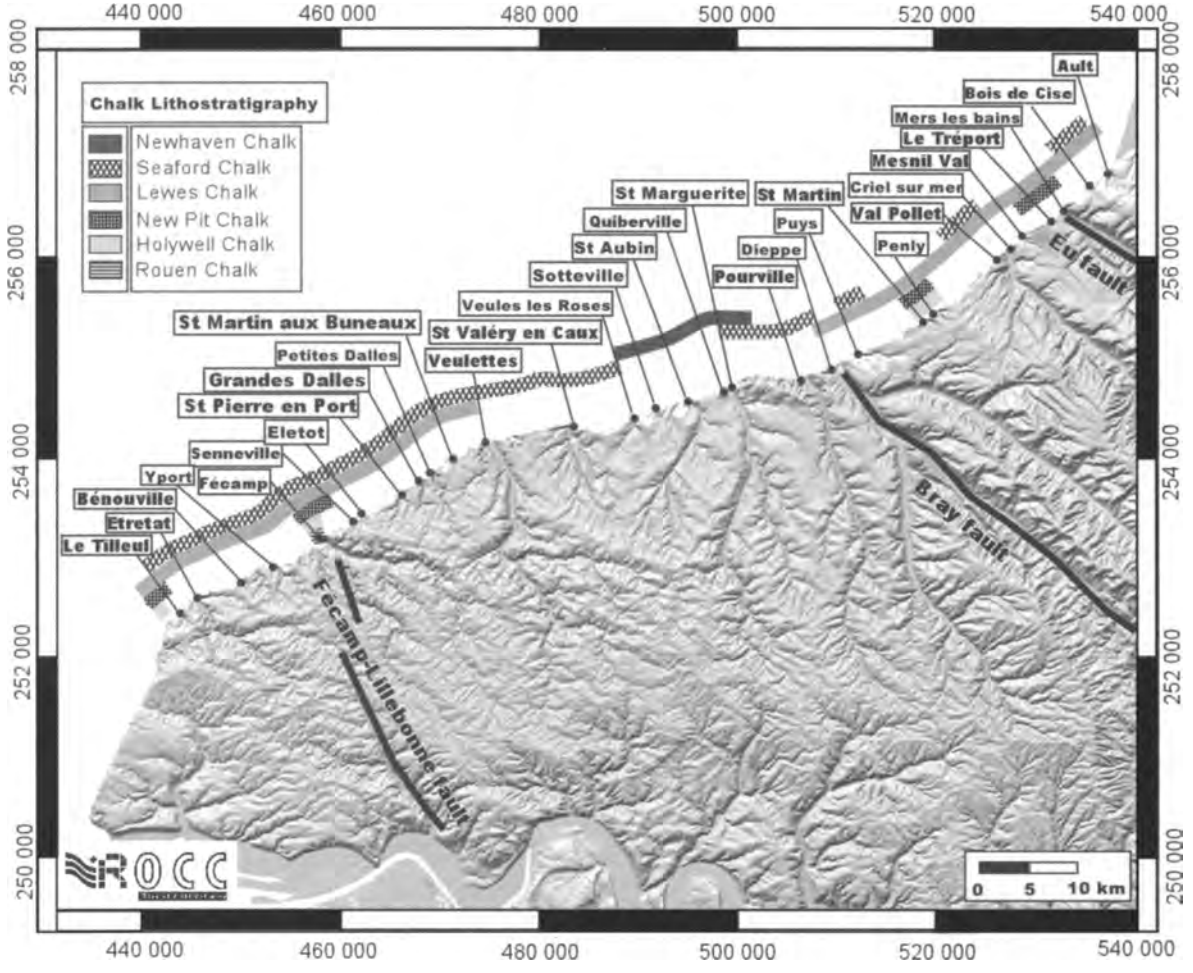

Fig. 4. Schematic lithostratigraphic chalk unit distribution along the French vertical cliffs, between Le Tilleul and Ault, adapted from Mortimore (2001*a*).

and Senneville sur Fécamp (Bassompierre & Roux 1968; Lepiller & Rodet 1971) and as spring outlets of groundwater rivers. e.g. Heurt river at Senneville sur Fécamp (Rodet 1986).

Chalk cliff collapse characteristics

Scale of chalk cliff collapses

For the last three years (from October 1998 to September 2001), a minimum of 55 collapses have been observed along the French chalk coastline and about ten collapses along the English chalk coastline. From the set of reported data on the French coastline (Table 1), we have classified the chalk cliff collapses on the basis of volumes involved: (1) very large-scale collapses, with volumes greater than 50000 m^3; (2) large-scale collapses, with volumes comprising between 10000 and 50000 m^3; (3) medium-scale collapses, with volumes ranging from 1000 m^3 and 10000 m^3, and (4) small-scale collapses, with volumes lower than 1000 m^3 (Fig. 6). From this collapse database, some correlations are made between the collapse sizes, the cliff height, the scar width, the H/L ratio of the deposit and the cliff retreat.

The observed collapsed volumes vary from 85000 m^3 (Puys) to a few m^3, with a mean volume ranging from 10000 to 50000 m^3, whereas the chalk cliff heights vary from 20 to 105 m. The highest collapsed volume was observed on 10 January 1999 at Beachy Head, UK, with 150000 m^3 of chalk debris along a 130 m high chalk cliff. The volumes of collapses show a tendency to increase with increasing cliff height (Fig. 7a). Mean volumes of subaerial non-volcanic landslides reported from the literature in various environ-

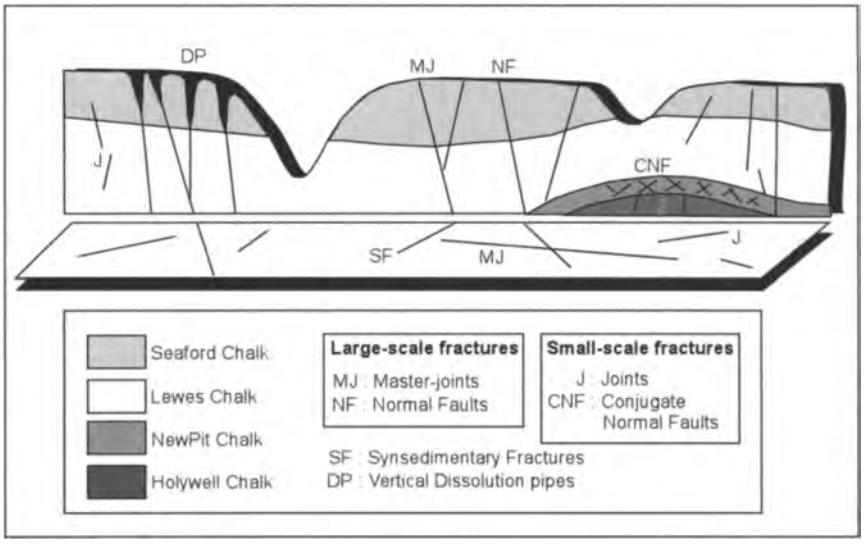

Fig. 5. Schematic sketch of fractures type observed on the French chalk cliff face and on the beach platform.

ments vary from $10^6 m^3$ to $10^{11} m^3$ ($100 km^3$), with cliff heights varying from 300 to 3000 m (Hayashi & Self 1992). Chalk cliff collapses range in subaerial non-volcanic landslides of small volume (10 to $10^5 m^3$) due to the small heights of the cliffs (20–130 m).

Method of volume estimation for a chalk cliff collapse

The volume estimation of each collapse has been calculated from field measurements and photograph analysis (Table 1). Field measurements have been performed on the scar (height, *H* and width, *W*) and on the length of the deposit (*L*). In most of the cases, the direct estimation of scar retreat is not possible, due to the lack of data before the collapse. The cliff height (*H*) measured on the cliff is compared with the height given by the topographic maps of the French Geographical Institute (IGN). The height of the distal part of the deposit has been deduced from photograph analysis, by comparison with the measured height of the cliff. However, the real volume of collapsed rocks is always lower than the estimated volume, due to the large amount of void spaces occurring between the collapsed blocks. The real volume can be estimated using a bulking factor. Estimations on non-volcanic dry landslides give a bulking factor of 30% (Hadley 1960), whereas estimations on volcanic landslides, with large entire slumped blocks, such as the Mt St Helens landslide, have shown a bulking factor of 20% (Voight 1983). A bulking factor of 16% has been observed in Lewes chalk earthworks where only low or no compaction occurred (Lord *et al.* 2001). An overall bulking factor of 20% is assumed herein for all the chalk cliff collapses on the coast.

The scar retreat has been only calculated for collapses extending all over the cliff height that represent 85% of the reported collapses. It is thus assumed that the scar height is equal to the cliff height (*H*). The calculated scar retreat (*R*) is deduced from the volume of the deposit (*V*), the height of the scar (*H*) and the width of the scar (*W*) with the relation: $R = V / H*W$.

Very large-scale collapses

Very large-scale collapses represent 5.5% of the reported collapses. One typical example has been reported at Beachy Head (10 January 1999), with an estimated volume of $150000 m^3$ of debris (Fig. 6B) and three other collapses occurred in France: at Puys (17 May 2000), with $85000 m^3$ of debris (Fig. 6A) (Duperret *et al.* 2002*a*) ; at Veulettes s/Mer (March 2001), with $63000 m^3$ of chalk debris (Fig. 6C); at Grandes Dalles (15 July 2001), with $60000 m^3$ of debris. The failure scars extend over the entire cliff height. The debris fans of the collapses may have a lobate shape which is derived from debris avalanche processes, as suggested by the H/L ratio of 0.68 for the Beachy Head collapse, of 0.63 for the Grandes Dalles collapse and 0.50 for the Puys collapse. In contrast, at Veulettes sur Mer, the deposit has a conical shape and a very short runout (H/L ratio of 1.1). The debris mass is restrained to the toe of the cliff and covers 70% of the cliff face surface. The magnitude of cliff retreat has been determined by comparison with previous photographs for the two collapses and reaches 17 m at Beachy Head and 12.5 m at Puys (Duperret *et al.* 2002*b*). For the very large-scale collapses, the calculated cliff retreat varies from 8 to 12 m deep (Fig. 7b).

Very large-scale collapses are located on cliffs with a height greater than 50 m and their scars always extend over the entire cliff height. They present very large scars, with

Table 1. *ROCC database of the reported collapses on the French Chalk coastline between 1998 and 2001, with the characteristics of each collapse: date of occurrence, location, run-out: L in m, cliff height; H in m, H/L ratio. Scar wide: W in m, calculated cliff retreat in m, collapse type, collapse extension on the cliff face and remarks*

No	*DATE*	*LOCATION*	*Runout: L (m)*	*Cliff height: H (m)*	*H/L ratio*	*Scar wide: W (m)*	*Volume (m^3)*	*Cliff retreat (m)*	*Collapse type*	*Collapse extension on the cliff*	*Remarks*
1	Oct-98	Ault N	undefined	undefined	undefined	undefined	1,000	undefined	undefined	all the cliff height	
2	Nov-98	Le Tilleul	25	80	3.20	30	1,200	0.50	vertical	all the cliff height	
3	17-Jul-99	Veules les Roses N	95	50	0.53	95	24,000	5.05	sliding	all the cliff height	Low tide
4	25-Aug-99	Pourville sur Mer N	undefined	undefined	undefined	undefined	7,700	undefined	undefined	all the cliff height	DDE source
5	Dec-99	Les Petites Dalles N	20	80	4.00	50	5,200	undefined	vertical	2/3 of lower cliff	
6	Dec-99	Les Petites Dalles N	30	80	2.67	30	7,200	undefined	undefined	2/3 of lower cliff	
7	25-Feb-00	Puys S	undefined	undefined	undefined	undefined	4,200	undefined	undefined	all the cliff height	DDE source
8	May-00	Veules les Roses N	70	50	0.71	90	12,800	2.84	sliding	all the cliff height	
9	17-May-00	Puys N (2000)	120	60	0.50	120	85,000	11.81	sliding	all the cliff height	High tide
10	Nov-00	St Marguerite sur Mer N	10	15	1.50	30	600	1.33	undefined	all the cliff height	
11	23-Nov-00	Pourville sur Mer S	undefined	70	undefined	undefined	2,100	undefined	undefined	all the cliff height	DDE source
12	19-Dec-00	Pourville sur Mer N	undefined	70	undefined	undefined	18,400	undefined	undefined	all the cliff height	DDE source
13	Marc-01	Veulettes sur Mer S	65	65	1.00	40	16,000	6.15	vertical/sliding	all the cliff height	
14	Marc-01	Veulettes sur Mer S	45	50	1.11	150	63,000	8.40	undefined	all the cliff height	
15	15-Marc-01	St Pierre en Port S	100	90	0.90	100	48,000	5.33	sliding	all the cliff height	
16	20-Marc-01	St Pierre en Port N	60	80	1.33	80	15,000	2.34	sliding/wedge	all the cliff height	
17	Apr-01	Le Tilleul	15	80	5.33	25	600	0.30	vertical	all the cliff height	
18	Apr-01	Puys S	130	50	0.38	undefined	40,000	undefined	sliding	all the cliff height	
19	30-Apr-01	Vaucottes N	33	55	1.67	32	3,661	2.08	vertical	all the cliff height	
20	winter-spring-01	Veules les Roses	10	35	3.50	51	1,900	1.06	sliding/wedge	all the cliff height	
21	winter-spring-01	St Aubin sur Mer S	3	24	8.00	12	70	undefined	undefined	1/2 of lower cliff	
22	winter-spring-01	St Marguerite sur Mer N	24	34	1.42	28	550	undefined	undefined	1/3 of lower cliff	
23	winter-spring-01	St Marguerite sur Mer N	22	41	1.86	85	7,500	undefined	undefined	1/3 of lower cliff	
24	winter-spring-01	Quiberville S	5	32	6.40	25	150	0.19	undefined	all the cliff height	
25	winter-spring-01	Quiberville S	5	28	5.60	10	150	0.54	undefined	all the cliff height	
26	winter-spring-01	Quiberville S	4	26	6.50	25	200	0.31	undefined	all the cliff height	
27	winter-spring-01	Quiberville S	4	28	7.00	36	200	0.20	undefined	all the cliff height	
28	winter-spring-01	St Aubin sur Mer S	6	20	3.33	22	240	0.55	undefined	all the cliff height	
29	winter-spring-01	Quiberville S	5	28	5.60	20	300	0.54	undefined	all the cliff height	
30	winter-spring-01	St Aubin sur Mer S	5	25	5.00	50	400	0.32	undefined	all the cliff height	
31	winter-spring-01	Quiberville S	5	28	5.60	25	500	0.71	undefined	all the cliff height	
32	winter-spring-01	Quiberville S	10	30	3.00	95	1,500	0.53	undefined	all the cliff height	
33	winter-spring-01	St Marguerite sur Mer N	30	26	0.87	60	5,000	3.21	undefined	all the cliff height	
34	winter-spring-01	Quiberville S	50	30	0.60	60	6,000	3.33	undefined	all the cliff height	
35	winter-spring-01	St Marguerite sur Mer N	30	26	0.87	70	7,700	4.23	undefined	all the cliff height	
36	winter-spring-01	St Marguerite sur Mer N	40	26	0.65	70	7,800	4.29	undefined	all the cliff height	
37	winter-spring-01	St Marguerite sur Mer N	160	30	0.19	65	12,500	6.41	undefined	all the cliff height	
38	winter-spring-01	Quiberville S	36	33	0.92	90	15,000	5.05	undefined	all the cliff height	
39	winter-spring-01	St Marguerite sur Mer N	40	34	0.85	50	23,500	13.82	undefined	all the cliff height	

Table 1. (*continued*)

No	*DATE*	*LOCATION*	*Runout: L (m)*	*Cliff height: H (m)*	*H/L ratio*	*Scar wide: W (m)*	*Volume (m^3)*	*Cliff retreat (m)*	*Collapse type*	*Collapse extension on the cliff*	*Remarks*
40	May-June-01	St Valery en Caux N	45	65	1.44	106	24,000	3.48	vertical	all the cliff height	
41	May-June-01	St Martin plage Nord	50	80	1.60	86	32,000	4.65	complexe	all the cliff height	
42	June-01	Yport Sud (La Pucelle)	50	75	1.50	90	45,000	6.67	vertical	all the cliff height	High tide
43	Spring-01	Puys N	54	68	1.26	61	10,000	2.41	sliding	all the cliff height	
44	Spring-01	Puys N	70	60	0.86	50	14,000	4.67	sliding	all the cliff height	
45	15-Jul-01	Les Grandes Dalles S	112	70	0.63	96	60,000	8.93	sliding	all the cliff height	
46	24-Jul-01	Benouville (valleuse curé)	80	65	0.81	100	43,000	6.62	vertical	all the cliff height	
47	26–Aug-01	Yport Sud	40	70	1.75	80	32,000	5.71	vertical	all the cliff height	Low tide
48	Sep-01	Les Grandes Dalles S	10	40	4.00	10	300	undefined	vertical	2/3 of lower cliff	
49	Sep-01	Les Grandes Dalles S	25	70	2.80	45	2,500	undefined	vertical	1/2 of lower cliff	
50	27-Sep-01	Pourville N	36	40	1.11	45	3,500	1.94	undefined	all the cliff height	DDE source
51	Aug-01	Val Pollet S 2	16	65	4.06	33	845	undefined	vertical	1/3 of lower cliff	
52	Aug-01	Val Pollet S 1	50	65	1.30	70	2,800	0.62	vertical	all the cliff height	
53	spring-summer-01	Le Tréport S	54	90	1.67	72	7,776	1.20	undefined	all the cliff height	
54	spring-summer-01	Penly N	154	100	0.65	75	18,480	2.46	undefined	all the cliff height	
55	spring-summer-01	Le Tréport S	60	90	1.50	108	38,016	3.91	complexe	all the cliff height	

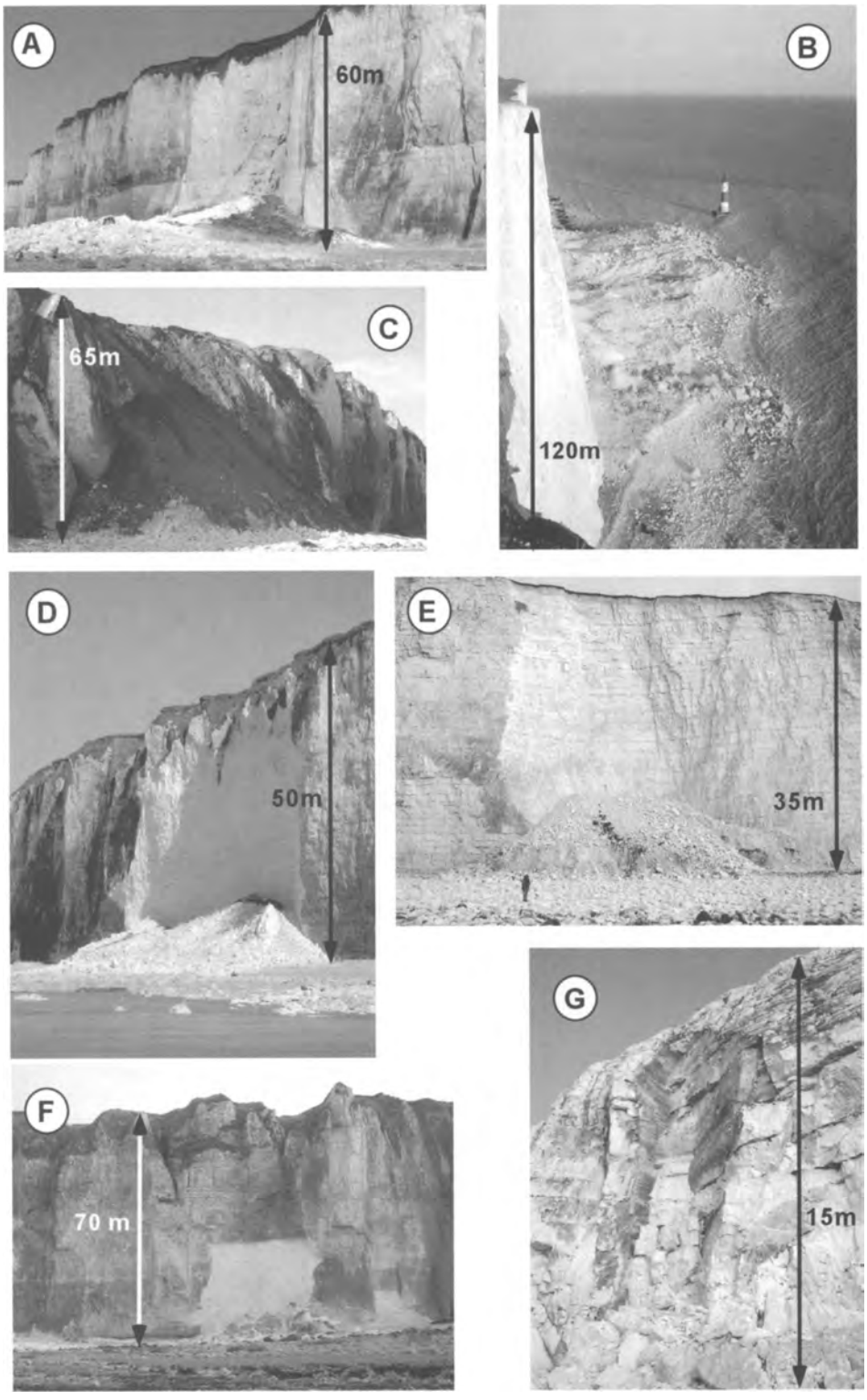
A
60m
B
120m
C
65m
D
50m
E
35m
F
70 m
G
15m

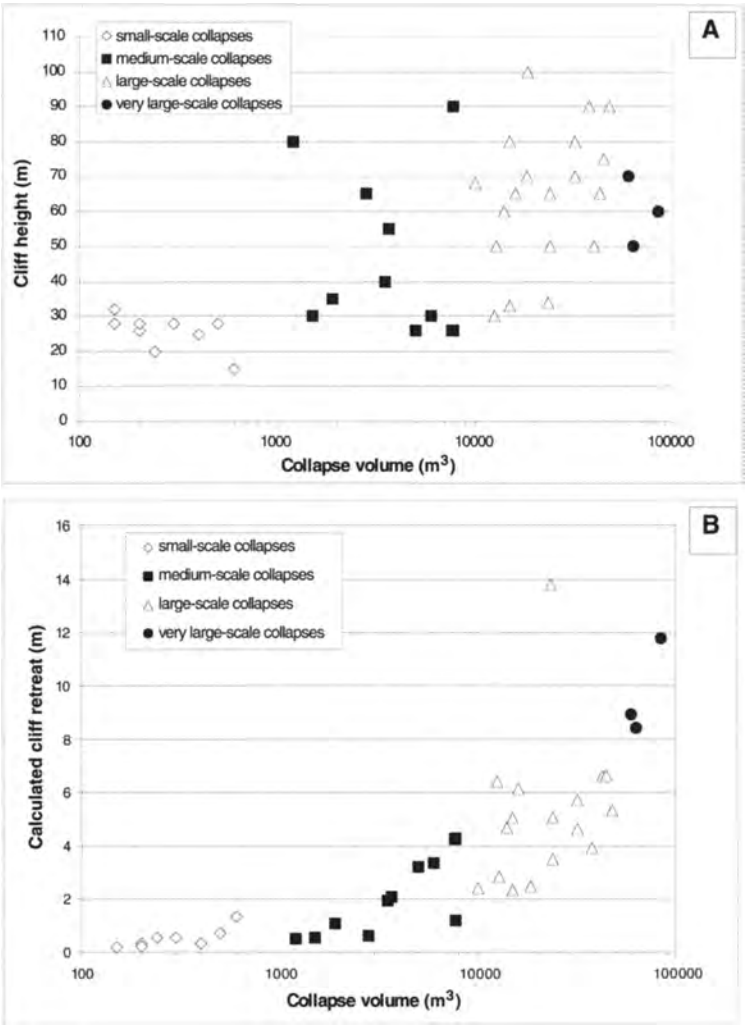

Fig. 7. A, Measured cliff height (in m) at the location of the collapse, which corresponds to the height of the collapse scar (H) versus the collapse volume (in m^3). B, Estimated cliff retreat (in m) for a measured collapse versus the collapsed volume (in m^3).

Fig. 6. Photographs of recent coastal chalk cliff collapses, both in France and UK. The various scale of chalk cliff collapses are illustrated. A, B and C are very large-scale collapses; D is a large-scale collapse; E is a medium-scale collapse; F and G are small-scale collapses. A, Puys, France, 17 May 2000, volume: 85000 m^3; B, Beachy Head, UK, 10 January 1999, volume: 150000 m^3; C, Veulettes sur Mer, France, March 2001, volume: 80000 m^3; D, St Valéry en Caux, France, spring 2001, volume: 24000 m^3; E, Birling Gap, UK, January 2001, volume: 3000 m^3; F, Grandes Dalles, France, September 2001, 2500 m^3; G, Peacehaven, 6 January 2001, volume: 250 m^3.

widths between 90 m and 150 m. These collapses are not laterally limited by large-scale transverse fractures, except at Grandes Dalles, where a small-scale vertical fracture has partially bounded the upper part of one side of the scar. Based on aerial photograph analysis, the mean space between all fracture types reported on the cliff face varies from 9 to 20 m (Genter *et al.* 2004) and the scar width of each collapse varies from 96 to 150 m. At Grandes Dalles, the very large-scale collapse crosses the NW–SE fracture set.

Large-scale collapses

Large-scale collapses represent 34.5% of the reported failures, with 19 events in France, such as at St Valéry-en-Caux

(spring 2001), with 24000 m^3 of debris chalk (Fig. 6D). Field observations illustrate that the failure surfaces extend also over the entire cliff height, but the run-out of the deposits are variable with H/L ratios varying from 0.19 at Ste Marguerite s/Mer to 1.75 at Yport, where the debris mass is restrained at the toe of the cliff. The calculated cliff retreats are between 2 to 7 m in depth (Fig. 7).

Large-scale collapses occur on cliffs greater than 30 m high. The detailed analyses of the collapses on the cliff face has shown different types of lateral boundaries. 70% of the large-scale failures are laterally bounded by near-vertical large-scale fractures, with 80% of the scars having such fractures on one side of the scar and 17% on the both sides of the scar. The large-scale collapses were limited by NW–SE fractures in a range of sizes, whereas the collapses of intermediate size (with volumes varying from 15000 to 35000 m^3) were not limited by NW–SE fractures. Based on aerial photograph observation, the mean space between fractures vary from 6.5 to 24 m, whereas the scar width of each collapse varies from 40 to 110 m. Where scars are laterally bounded, they may also cross transverse fractures.

Medium-scale collapses

Medium-scale collapses represent 34.5% of the reported collapses, with 19 collapses in France and 6 collapses in UK. Medium-scale collapses extend over the entire cliff height, such as the two collapses along the Seven Sisters in UK (January 2001), which involved about 5500 and 2000 m^3 of chalk respectively (Fig. 6E). They may also be limited to the lower part of the cliff, such as the Grandes Dalles collapse (September 2001), which involved about 2500 m^3 of material (Fig. 6F). The majority of debris is limited to the toe of the cliff, with a short run-out. H/L ratios are higher than the large and very large-scale collapses with variation from 0.6 to 3.20, with H/L ratio lower for collapses extending over the whole cliff height rather than for collapses located only in the lower part of the cliff. The calculated cliff retreat ranges from 0.5 to 4 m in depth, for collapses extending over the whole cliff height (Fig. 7).

Where medium-scale collapses extend all over the cliff height, the width of their scars is larger than 30 m and may reach 95 m wide on cliffs with heights varying from 20 m to 90 m. 65% of the medium-scale collapses are laterally limited on one side of the scar by large-scale NW–SE fractures. The collapses with the lowest sizes are not laterally limited, whereas the collapses with the larger sizes are laterally limited. The scar width varies from 30 to 95 m, and the mean space between all fracture types varies from 6.6 to 44 m.

Small-scale collapses

Small-scale collapses represent 25.5% of the reported collapses, with 14 collapses in France and 3 collapses in UK. They show a large variety of scar morphology. Scars may extend over the whole cliff height such as at Quiberville in France (150 m^3), and scars may also be located in the lower part of the cliff, such as at Peacehaven in UK (6 January 2001), where the deposit (250 m^3) has locally buried the undercliff walk of several metres width (Mortimore *et al.* 2004) (Fig. 6G). The highest H/L ratios have been measured for these collapses with values ranging from 1.50 to 7. The calculated cliff retreat is always lower than 2 m in depth (Fig. 7).

Small-scale collapses occur on cliffs of various heights for failures occurring on the lower part of the cliff. For collapses extending over the whole cliff height, they occur on cliffs varying from 15 m to 35 m in height, showing scar widths varying from 10 m to 50 m. Most of them are not laterally limited by NW–SE fractures and they generally cross them. The mean space between all types of fractures varies from 14 to 44 m.

64% of the reported chalk cliff collapses vary in size between 1000 and 50000 m^3. 26% have sizes lower than 1000 m^3 and 6% have sizes greater than 50000 m^3. The larger the collapse size, the greater the cliff retreat and the higher the cliff height. Previous work conducted on comparisons between run-out distance and landslide volume suggest that landslide spreading is essentially controlled by their own volume, and not by the height of fall (Hsü 1975; Davies 1982; Legros 2002). All the chalk cliff collapse deposits are unconfined and have H/L ratios varying from 0.19 to 7 (Table 1). Only 7% of the landslides shows H/L ratios around the value of 0.6 as it was predicted by Heim (1932). As 76% of the collapses have H/L ratios higher than 0.6, most of them present short run-outs. By considering the 7% of chalk cliff collapses with H/L ratios lower than 0.6, long run-outs have also occurred at Veules les Roses, Puys and Sainte Marguerite sur Mer.

The analyses conducted on the observed scar characteristics show a mean scar width of 60 m, with a maximum scar width of 150 m at Veulettes sur Mer and a minimum scar width of 10 m at Quiberville. The mean space between all types of fracture observed on the cliff face is about 15 m and the mean space between large-scale fractures is 27 m. There is no clear relation between the scar width or the collapse size and the mean space between fractures shown in the cliff face, because some fractures are crossed by the scars and some other fractures limit the scars (Genter *et al.* 2004). It is suggested that the lateral limit on a scar depends on the type of fracture filling. Three main situations have been recognized in the field: (1) fractures filled by flints, called synsedimentary fractures; (2) fractures filled by clays, such as normal faults or master-joints and (3) open or closed fractures, mainly represented by joints and master-joints.

Type of chalk cliff failures

Chalk cliff failure types have been determined from field observation on the both sides of the Channel. The geohazard database collected on the English coastline is presented in Mortimore *et al.* (2004). During the ROCC project, it was

rather difficult to sample systematically all the scales of collapses along the 120 km of the French studied coastline. As the analysis was concentrated on the largest collapses, some sections that may contain small-scale collapses were not documented fully. Therefore, the cliff collapse database is not exhaustive, and it is for this reason that medium to small-scale collapses which occur in the lower part of the cliff face represent only 15% of the observed collapses. A large diversity of failure types have been observed mainly for collapses involving the whole cliff height. For collapses involving only the lower part of the cliff, only one type of failure is represented. Significant collapses derived from the upper part of the chalk cliff face have never been observed within the Cretaceous chalk of the study coastline in France. However, as pointed out by Mortimore *et al.* (2004) along East Sussex coastline, failures in materials overlying the Chalk including mud-flows (Newhaven) and disintegration of Quaternary deposits (Black Rock marina) are on a smaller scale than the big chalk collapses.

Vertical failure type

Scars with a vertical slope profile have been observed within cliffs made of a homogeneous chalk unit, such as at the Seven Sisters (Mortimore *et al.* 2004) and at Saint-Valery-en-Caux (Fig. 6D), within the Seaford Chalk Formation. At the Seven Sisters, the collapsed scar is made of one regular and vertical plane with no striations. A set of closely spaced pre-existing joints with an sub-parallel orientation to the cliff face present plume-structures on their surfaces related to the joint growth. The SW border of the scar is clearly limited by a transverse master joint which crosses all the cliff height, whereas its NE border stops gradually on the cliff face. We suggest that the rupture propagates along the pre-existing joint system and stops abruptly against a transverse fracture or where the pre-existing joints are cutting the cliff face (Fig. 8A).

At the Seven Sisters, in a homogeneous section of the Seaford Chalk, the rupture is controlled by vertical small-scale joints oriented parallel to the cliff face, whereas in France such an orientation for pre-existing joints was difficult to observe. However, local observations on the beach platform may suggest a secondary fracture set oriented roughly parallel to the cliff face, as observed on the N60E coastline at Petites Dalles, where a N40E family made of joints and synsedimentary fractures has been revealed (Genter *et al.* 2004). The vertical failure is assumed to propagate along the pre-existing joint set, which is roughly parallel to the cliff face orientation.

For vertical failure types involving the lower part of the cliff only, collapse always occurs within one chalk unit. The upward extension of the scar is bounded by lithological features of the chalk, such as horizontal flint bands, marl levels or stratification. An overhang delineates the upper part of the scar, such as at Grandes Dalles within the Lewes Chalk formation (Fig. 6F).

In France, about one third of the total number of observed collapses correspond to the vertical failure type. They are mainly located within the Seaford chalk formation and within the Lewes–Seaford Chalk succession (Fig. 9). As pre-existing fractures parallel to the cliff have not been observed on scar collapses in France, we suppose that collapses occur along newly created decompression fractures, parallel oriented to the cliff.

Sliding failure type

Sliding failure type is characterized by scars with a change of slope profile. They have been observed within cliffs made of two chalk units. Sliding failure type has been described in the Seaford Chalk at Joss Bay in Kent, UK (Hutchinson 1971; Mortimore *et al.* 2004). In France, the scar-type has been described at Puys, on the collapse which occurred on 17 May 2001 (Duperret *et al.* 2002*a*) (Fig. 6A). The cliff comprises two chalk formations: the Lewes and Seaford Chalks. The scar shape presents a vertical upper part and an inclined lower part with large striations and crushed chalk. The change of slope profile is located at mid-height of the cliff and corresponds to the limit between Seaford Chalk and Lewes Chalk. Marl seams are located at the chalk unit boundary (Shoreham Marl). On-site structural analysis of the scar suggests an overall mechanism of sliding characterized by an outward tearing process without striations in the upper part of the cliff and a shearing mechanism with slickenslides and striations in its lower part. The sliding process has been confirmed by the biostratigraphic succession within the blocks of the deposit, where the original stratigraphy is retained. The scar face of the Puys collapse does not show large-scale transverse pre-existing fractures and is not bounded by fractures, giving an overall curved scar shape. However, there are some large-scale fractures in the vicinity of the Puys collapse. In NW France, the main fracture set (N120E), which is oblique to the coastline (Genter *et al.* 2004) is made of large-scale fractures from tectonic origin (normal faults and master-joints). In some cases, transverse fractures may limit the lateral extension of a scar on the cliff face, as observed on collapses reported on the same chalk unit succession at Saint-Pierre-en-Port and Grandes Dalles (Fig. 8B).

In France, about one third of the total number of observed collapses correspond to the sliding failure type. They are mainly located within the Lewes–Seaford Chalk succession and more rarely within the Seaford–Newhaven Chalk succession (Fig. 9).

Wedge and plane failure type

Where two or three fracture sets cross, some small-scale collapses may occur in the lower part of the cliff. In that case, lateral and upward extension of the scar is limited by the size and geometry of fracture sets. This failure type has been observed on the English chalk coastline, within Newhaven Chalk formation, such as at Peacehaven (Fig. 6G), where steeply inclined large-scale shear fractures occur within the cliff (Mortimore *et al.* 2004). Wedge and plane failure type is closely linked to the chalk units characterized by conjugate

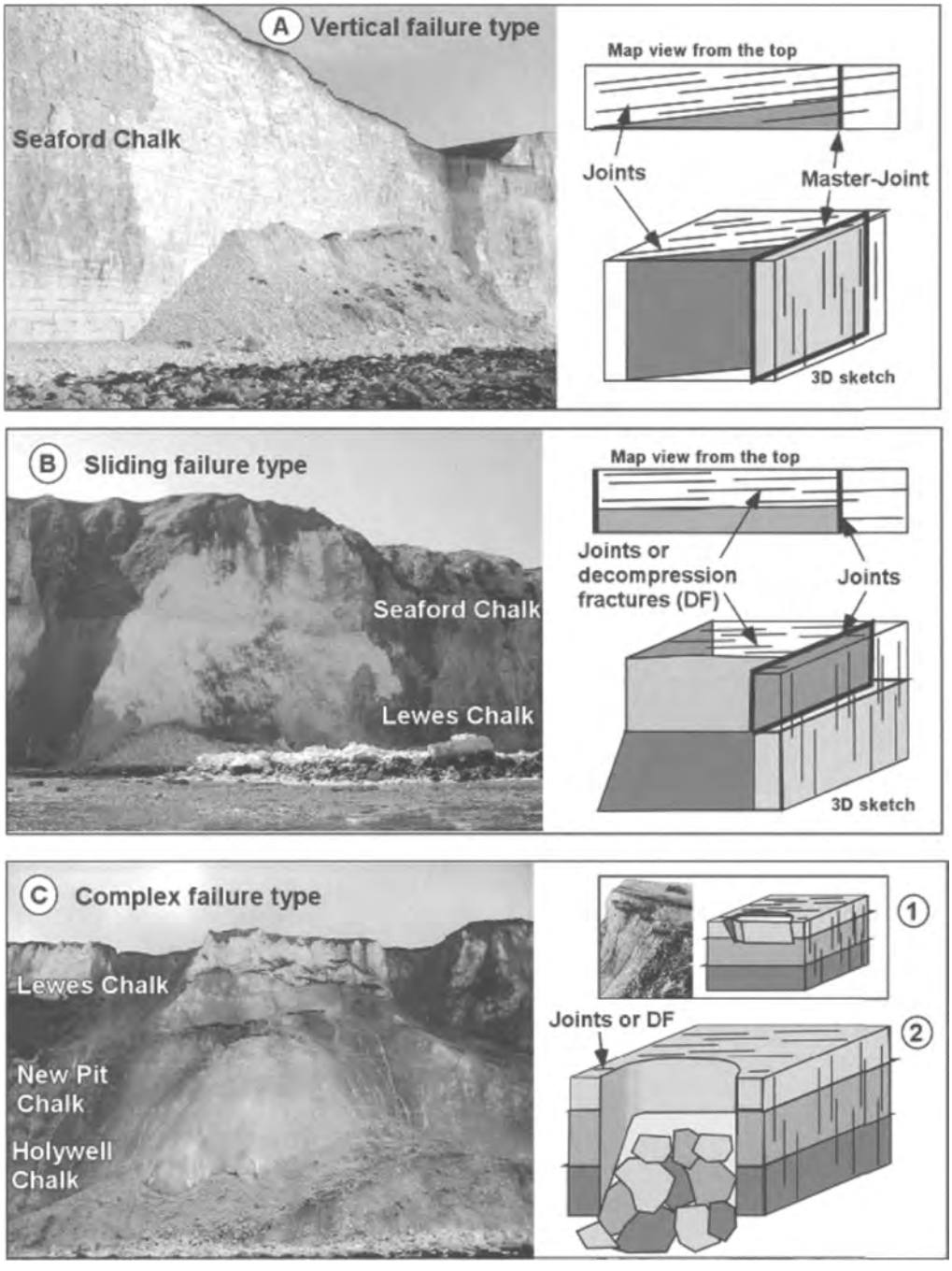

Fig. 8. Schematic bloc diagrams and photograph illustration of the main types of collapses observed on the French chalk cliffs of the English Channel. A, Vertical failure type, observed at Seven Sisters, near Birling Gap, UK. B, Sliding failure type, observed at Grandes Dalles, France. C, Complex failure type, observed at (1) Beachy Head (UK) during the first phase of failure and (2) at Penly (France), after the failure.

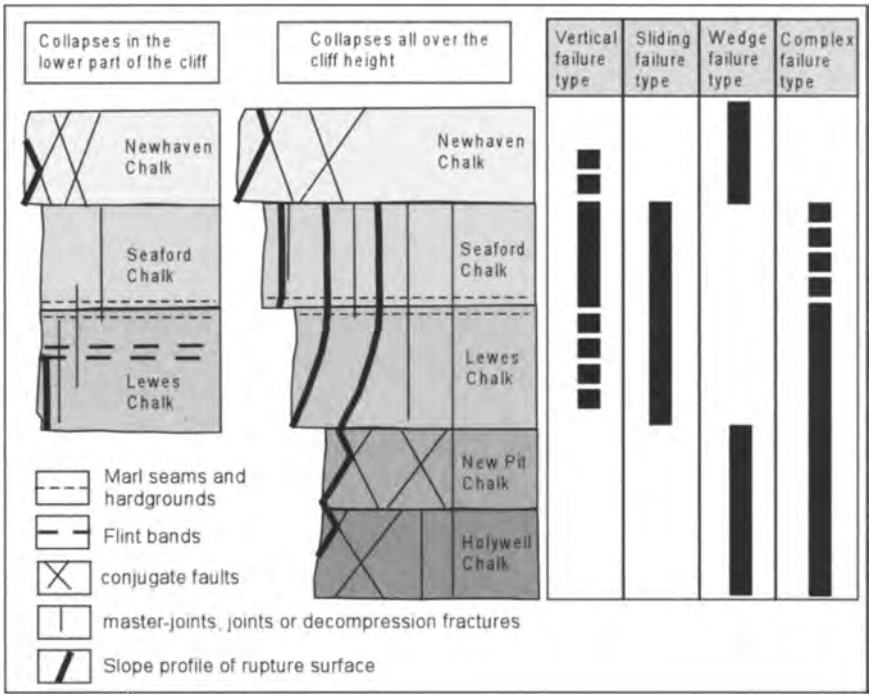

Fig. 9. Synthetic sketch of slope profile rupture surface for all chalk cliff collapses types observed on the English Channel chalk coast, in relation with the Chalk lithology and the fracture pattern.

sets of stratabound fractures, which cross each others on the cliff face, as in New Pit Chalk, Holywell Chalk and Newhaven Chalk.

On the French coastline, the wedge failure type has not been clearly identified, due to a lack of collapses involving only the chalk units with stratabound fractures. However, due to the occurrence of inclined fractures crossing a two chalk units succession, some hybrid failure types close to the wedge-plane failure type and sliding type are suspected very locally, such as at Saint-Pierre-en-Port and Veules-les-Roses.

Complex failure type

The complex failure type defined at Beachy Head (Mortimore *et al.* 2004) involves at least three different types of chalk units, which interact in a complex way. Scars present a vertical profile in the upper part of the cliff and an inclined profile with a convex shape covered by crushed chalk, in the lower part of the cliff. The vertical part is due to enlarged vertical fractures leading to a detached block within Lewes and Seaford Chalks, where fracture sets are mainly sub-vertical (Mortimore 2001*b*; Genter *et al.* 2004). The irregular inclined part contains conjugate oblique fracture sets within the New Pit Chalk and the Holywell Chalk (Fig. 8C). As observed on the field at Beachy Head (UK) (Fig. 8C-1) or at St Martin-plage, near Penly (France) (Duperret *et al.* 2002*b*), in a first step, there was a movement of large chalk blocks along sub-vertical fractures in the upper part of the cliff and in a second step, the large blocks failed down several months later. The upper part falls and breaks and drags down the pre-fractured underlying chalk, by wedge failure. These collapses have been always observed on high cliffs and they involve large and very large-scale collapses, with long run-outs.

In France, only two collapses ascribed to complex failure type have been observed at Le Tréport and Saint-Martin-plage, near Penly. At Le Tréport and Saint-Martin-plage, two and three chalk units are involved in the collapses, respectively. They correspond to New Pit-Lewes Chalk and Holywell-New Pit-Lewes Chalks (Fig. 9). The complex failure type scar is a mixing of vertical failure in the upper part and wedge failure in the lower part, with a change of slope profile at the contact between New Pit and Lewes Chalks. Complex failure types involve chalk units with fractures of tectonic origin in the upper part of the cliff and chalk units with stratabound fractures in the lower part of the cliff.

Undefined failure type

A series of collapses representing about one third of the total amount of the observed failures was not classified in the previously described. The main concern was to observe

correctly the scar face and the collapse characteristics, as they correspond to a large variety of chalk lithologies.

Failure type and cliff retreat

The collapsed volume of chalk can be estimated from each failure type of chalk cliffs deduced from field analysis. Wedge failure collapses vary between small scale and medium scale, including those collapses observed in UK. Vertical failure collapses vary between medium scale and large scale. Sliding and complex failure collapses vary between large scale and very large scale. Undefined failure types correspond to all collapse sizes. The maximum cliff retreat is due to complex and sliding failure types, with values ranging from 2 m to 12 m deep. A vertical failure induces a lower cliff retreat, with values ranging from 1 m to 7 m deep.

Chalk cliff collapses and rainfall

In order to understand the spatial and temporal relationships between collapse occurrence and triggering mechanisms, a comparative analysis between rainfall intensities and the timing of collapse is presented. This correlation was based on records collected between September 1998 and December 2001.

Fifty-five collapses of various sizes extending over the full cliff height were reported from the French chalk coastline. Of these two collapses occurred during autumn 1998, four collapses occurred in 1999, six collapses occurred in 2000, whereas during the year 2001, 43 collapses occurred, including 28 collapses with a volume greater than 1000 m^3 (Fig. 10a).

The mean annual rainfall recorded over the last 30 years at Dieppe is 803.8 mm. Annual rainfall recorded at the same place during the year 1999 is 966.2 mm, whereas 1113.6 mm were recorded during the year 2000 and 956.4 mm fall during the year 2001. Elevated rainfall of 117%, 133% and 119% were thus recorded during the years 1999 and 2000 and 2001, respectively. The sharp increase of collapses observed during the year 2001 is interpreted as being triggered by excessive rainfall that occurred over the previous 18 months.

A breakdown of the annual rainfall data into monthly means is more revealing in terms of the timing of collapses (Fig. 10b). During autumn 1998, collapses occurred in October and in November, whereas excessive rainfall was recorded in September with a value of 180% of the monthly mean. During 1999, the two main periods of high rainfall occurred at the beginning of the year, in January (180% of the monthly mean) and at the end of the year, in December (220% of the monthly mean). Whereas no collapse occurred in January, two collapses occurred in December at Petites Dalles. Furthermore, two collapses occurred in summer after five months of rainfall similar to the seasonal average: the first failure in this period was at Veules-les-Roses during the dry period of July (50% of monthly rainfall) and the second one at Pourville, in August, after a period of rainfall twice the monthly mean.

During the year 2000, elevated rainfall occurred during spring and autumn, in April (250% of the monthly mean) and in May (225% of the monthly mean). Four months later, elevated rainfall occurred in October (210% of the monthly mean) and in November (220% of the monthly means). During the year 2000, failures occurred from a few weeks to about one month after the beginning of each period of heavy rainfall. During the year 2001, 40 collapses were recorded. Unfortunately, their precise date of occurrence is poorly constrained for 25 failures observed between June and September 2001. Their fresh scars allow us to suggest an estimated time of collapse between winter and spring 2001. The comparisons between periods of rainfall and collapse have only been performed on the 15 collapses which are constrained in terms of time of occurrence. During the year 2001, an increase in the collapse frequency is observed, with events recorded each month between March and September 2001, except in May. Three periods of above average rainfall occurred in 2001: in January, March–April and in August. No collapse was observed in January, but seven collapses were reported during March with excessive rainfall (280% of monthly average) and April (180% of monthly means) 2001, and another one in August (230% of monthly mean) at Yport. However, three collapses occurred during dry periods, in June with low rainfall (only 36% of monthly average) and July (62% of monthly average) 2001. From May to July 2001, the weather was characterized by alternations of long dry periods with intervals of short heavy rainfall (Fig. 11).

Two types of temporal relationships between rainfall and collapse are suggested: (1) collapses related to heavy rainfall that occurs about one to two months after the beginning of period of heavy rainfall; (2) collapses related to a dry period after a normal rainfall period, as in summer 1999 at Veules-les-Roses or after a long dry period of three months, such as in summer 2001 at Grandes Dalles, Bénouville and Yport. Even if the period is dry, sudden rainfall over one or two stormy days leads to an increase of collapses as indicated during summer 2001.

Triggering mechanisms

The main mechanism capable of triggering cliff collapses are meteorological (rainfall, temperature), wave action (wave orientation, height, energy dispersion), cyclical tidal effects, fatigue caused by stress relief and earthquakes. These external mechanisms act on the chalk lithology and rock mass structure to trigger failures. The seismic activity reported in Upper Normandy is very low (Lambert *et al.* 1996) and appears as not really relevant on recent cliff collapses.

As suggested by Hutchinson (1971) from studies conducted on coastal chalk cliffs of the Kent (UK), the correlation between climatic factors and the incidence of falls is high and the latter are concentrated within the winter months, from October to April, with a greater influence of rainfall

during the earlier part of this period and frost during the later part. Field observations conducted on the East Sussex chalk coastline during the ROCC project has confirmed the concentration of collapses during winter months in UK (Mortimore *et al.* 2004). Even if the collapses observed on the French coast appear also to be linked to climatic factors, collapses have been recorded at all times of the year and especially during the summer in 1999 and 2001. Moreover, above average rainfall occurred at various times of the year, such as winter 1999, spring and autumn 2000, and winter, spring and summer 2001. The collapse triggering factors are thus focused on the role of groundwater within the chalk in relation with its fracture pattern.

Heavy rainfall as a triggering factor

At Puys, a collapse occurred on 17 May 2000, three weeks after damaging floods. There were two periods of intense rainfall during the third and fourth week of April and during the second week of May, which gives April and May 2000 a level of rainfall of 260% and 230% above average, respectively. We suggest that the aquifer probably reacted rapidly to the increase of rainfall. The sliding failure type is assumed to be triggered by water pressure increase on marl seams, located at the boundary between the Lewes Chalk and Seaford Chalk, at mid-height in the cliff, in an area of low fracture content (Duperret *et al.* 2002*b*) (Fig. 12a). The delay between heavy rainfall and the collapse may be explained by the low velocity of water transmission through a porous chalk, with a low fracture content (i.e. a dual porosity system). This illustrates a case of very large-scale sliding failure (85 000 m^3) induced by groundwater accumulation in a poorly fractured chalk. In the vicinity of this collapse, large-scale fractures extending over the whole cliff height cross the same chalk succession. As no collapse occurred laterally, we suspect that the excess water due to heavy rainfall may flow through well-drained fractures, avoiding water overpressure within fractured chalk in contrast to increasing water pressure in poorly fractured or non-free-draining chalk. The Puys collapse, which occurred about one month after excess rainfall, was therefore probably triggered by water pressure increase within poorly fractured Lewes–Seaford chalk at site, particularly along impervious marl seams.

Dry period as a triggering factor

A series of large-scale collapses were recorded during the summer 2001, at Yport in June, at Grandes Dalles on 15 July and at Bénouville on 24 July. These collapses occurred after a dry period of three months, disrupted by short intervals of intense rainfall events. A collapse occurred again at Yport on 27 August, after an increase of rainfall earlier in the month. All these sites present the same chalk succession as at Puys, but their fracture pattern is better developed with the occurrence of large-scale subvertical fractures extending over the whole cliff height (Fig. 12b). For instance, the fresh scars of collapses observed at Yport and Bénouville show subvertical fractures filled by clays, and dissolution pipes filled by Clay-with-flints, which develop from the top to the mid-part of the cliff. DRX pattern analysis conducted on clays sampled in a 30 cm wide subvertical fracture that bounds the large-scale collapse at Yport (Fig. 12b), has revealed iron hydroxides, quartz, crushed chalk, illite, kaolinite and mixed layer illite/smectite.

During a long dry period, mixed layer illite/smectite may contract within the pipes and favour the development of space at the contact between the chalk and the clay deposits. Such opening may favour the direct infiltration of water from rainfall and thus the deepening of the dissolution cone (Rodet 1992). The karstic fractures partially filled by clays become better drained after long dry periods disrupted by short rainfall. The vertical lengthening of dissolution pipes allows connection to pre-existing fissures and/or some impervious layers. We thus suggest that the upper part of the cliff could be well-drained due to the karstic system, whereas its lower part could also be well-drained if pre-existing fissures are open. In the case of impervious layers or clay-filled fractures, the lower part of the cliff could be undrained, favouring water overpressure. It is suggested that the process leading to collapse becomes similar to those suspected at Puys. The cyclic behaviour of vertical dissolution pipes illustrated by the alternation of dissolution and plugging, probably generates successive cycles of well-drained and undrained chalk cliffs. Experimental measurements conducted on coated and uncoated fractures surface of an unsaturated chalk exposed to short flow events (hours) of synthetic rainwater, followed by long drying periods (weeks) has shown a more pronounced erosion on the coated than on the uncoated fracture surface (Weisbrod *et al.* 1999). After a dry period, fracture apertures were found to be enlarged by the dissolution processes. The main difference compared with the Puys example is the rapid introduction of rainfall water through the dissolution pipes, which act as effective drainage fractures in the upper part of the cliff due to mixed layers I/S retraction, and conduct the excess water to the middle part of the cliff.

The large number of collapses observed during summer 2001, such as the Yport and Bénouville collapses, could be linked to the sudden introduction of rainfall through dissolution pipes filled by mixed layers I/S, following a three-month dry period. The time delay between the last short rainfall event disrupting a dry period and the rupture leading to a collapse may be of the order of one month. These collapses occurred within the fractured Seaford Chalk characterized by dissolution pipes, which acted as a complex karstic system overlying the fractured Lewes Chalk.

Marine parameters

A large number of authors (e.g. Emery & Kuhn 1982; Sunamura 1992) propose that marine parameters acting at the toe of rock cliffs are responsible for undercutting the cliff, which leads to rock-falls and other kinds of mass movements. Coastal chalk cliffs of the English Channel are subject to marine processes, such as wave action and wetting/drying

(a)

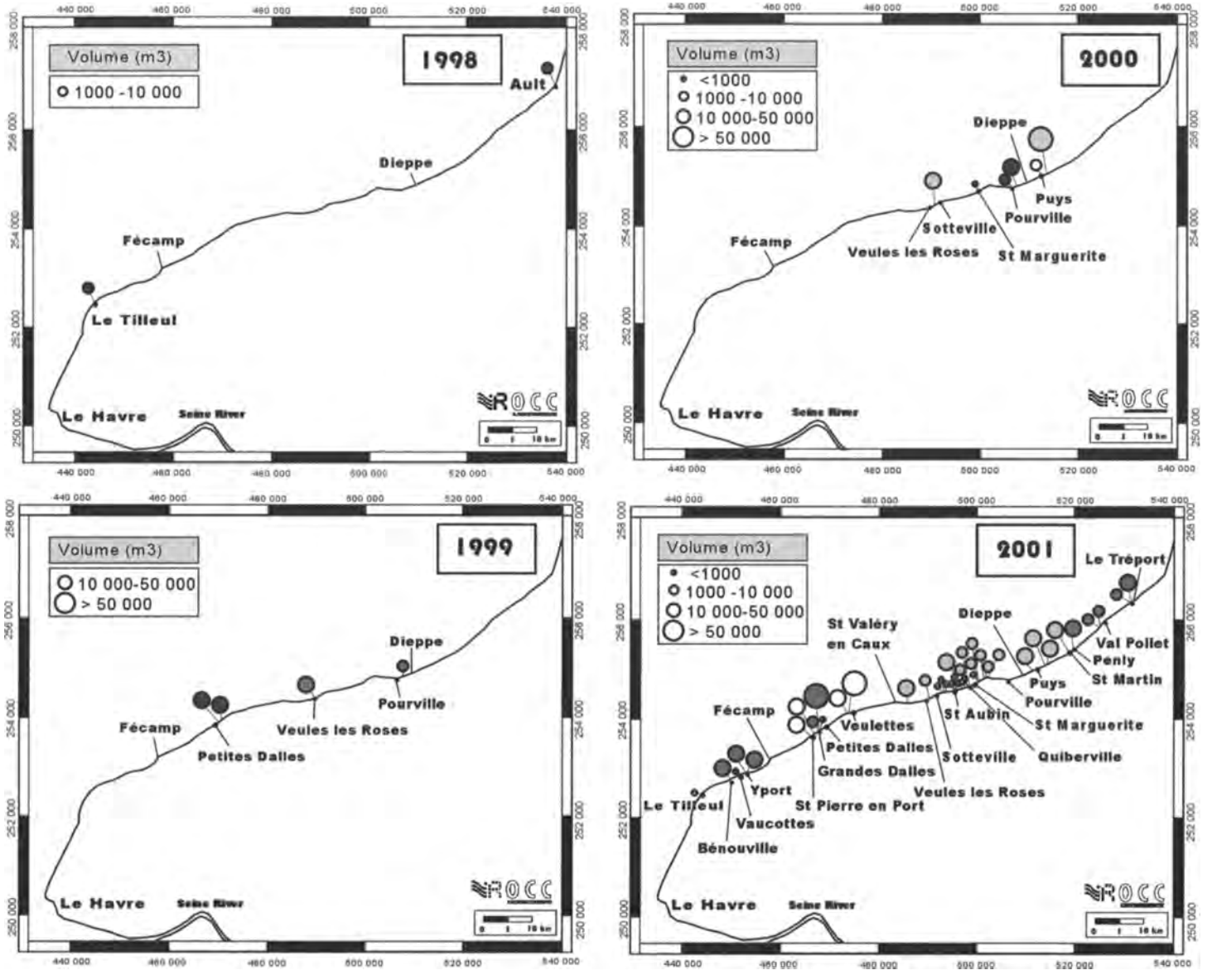
Volume (m3)
1000 -10 000
1998
Ault
Dieppe
Fécamp
Le Tilleul
Le Havre
Seine River
Volume (m3)
<1000
1000 -10 000
10 000-50 000
> 50 000
2000
Dieppe
Puys
Pourville
Sotteville
Fécamp
Veules les Roses
St Marguerite
Le Havre
Seine River
Volume (m3)
10 000-50 000
> 50 000
1999
Dieppe
Pourville
Fécamp
Veules les Roses
Petites Dalles
Le Havre
Seine River
Volume (m3)
<1000
1000 -10 000
10 000-50 000
> 50 000
2001
Le Tréport
St Valéry
en Caux
Dieppe
Val Pollet
Penly
St Martin
Puys
Pourville
St Aubin
St Marguerite
Fécamp
Veulettes
Petites Dalles
Sotteville
Quiberville
Grandes Dalles
Yport
Veules les Roses
Le Tilleul
St Pierre en Port
Vaucottes
Bénouville
Le Havre
Seine River

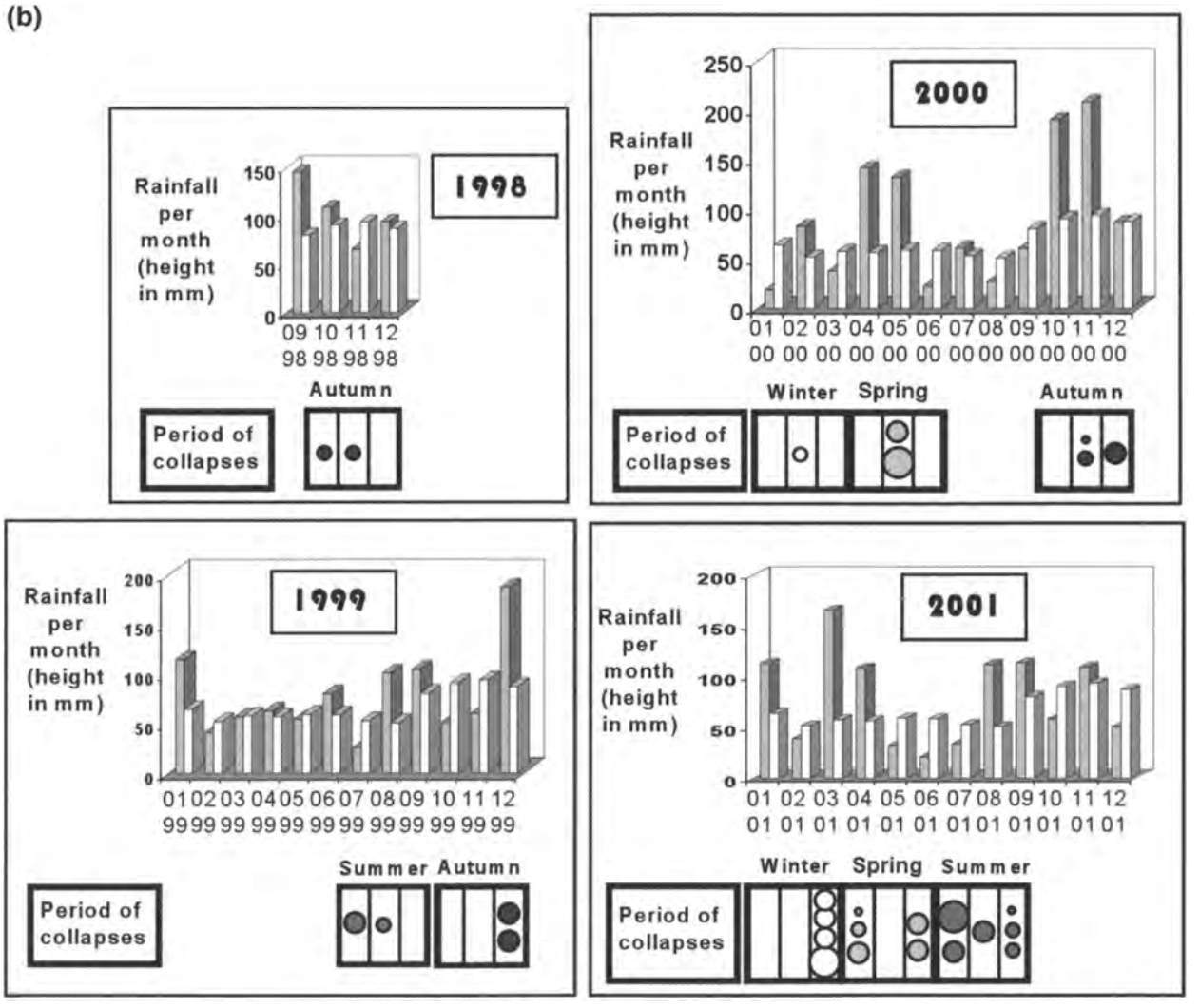

Fig. 10. (a) Collapses location on the French Chalk cliffs, between 1998 and 2001. The range of volume for each collapse is indicated by the size of its circle. The grey scale of the circles corresponds to the season of occurrence for each collapse (the same grey scale is used in the Fig. 10B): white circle is winter, light grey is summer, medium grey is spring and dark grey is autumn. (b) Pluviometric data (in mm height) recorded at Dieppe during 1998, 1999, 2000, 2001 (data from Meteofrance). Pluviometric data are reported in mm for each month of the year (grey bar) and compared with the mean monthly rainfall, calculated over a period of 30 years (white bar), versus each month of the year. The period of collapse occurrence is reported for each event.

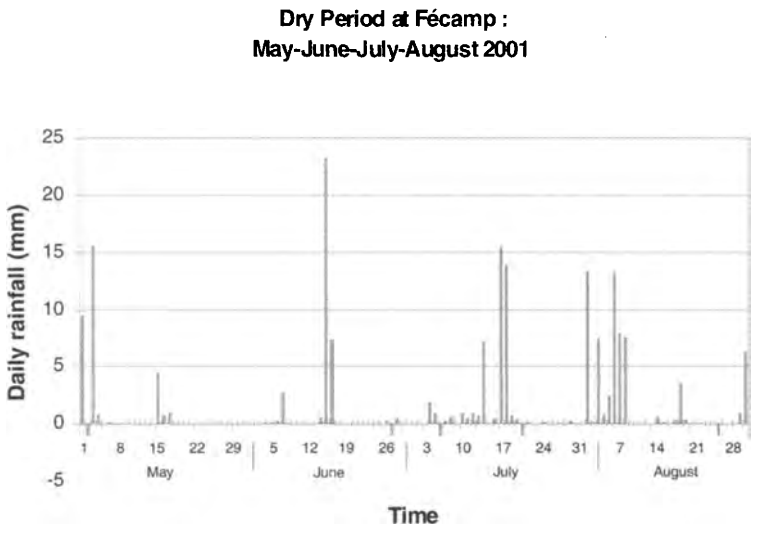

Fig. 11. Rainfall data (in mm height) reported at Fécamp during a dry period, from May to August 2001. See the alternation of dry periods and heavy rainfall.

processes. However, even if a basal erosion has been observed at some places, the observed notches are always less than one metre deep. Moreover, numerous coastal sections have no basal undercutting. Two explanations may be proposed: (1) some coastal sections of chalk cliffs are not reached by seawater during high tide, due to the occurrence of a several metres high shingle bar at the toe of the cliff, as observed at Le Tilleul (Brossard & Duperret 2004); (2) on some coastal sections, the base of the cliff is made of indurated chalk (hardground levels), which presents a higher resistance to erosive processes, as observed at Etretat and Yport within the Lewes Chalk formation (Mortimore 2001*a*).

It is suggested that only collapses limited to the lower part of the cliff are closely linked to basal notching, because the observed cliff retreat for one event is lower than one metre and the resulting collapses involved are of small and medium scales.

For most of the collapses observed on the lower part of the cliff, the top of the scar is limited by an overhang extending along a rectilinear and horizontal flint band or stratification, as observed at Petites Dalles within the Lewes Chalk (Fig. 6F). Where pre-existing joints or decompression fractures have developed parallel to the cliff face, it is suggested that basal undercutting of the cliff may favour small and medium-scale vertical slope failures. In this case, the failure does not reach the top of the cliff, but is limited upward by the lowest horizontal chalk discontinuity, such as flint bands.

Conclusion

On the coastal chalk escarpment of Upper-Normandy and Picardy, the lithological and structural context of the coastal chalk cliffs control the location and the type of the collapses. The large diversity of chalk failure types observed are mainly linked to the various geotechnical and hydrogeological properties of each chalk unit. Firstly, where the cliff face is only made of the Seaford Chalk formation, the scar shape presents a vertical slope profile. Secondly, where the cliff is made of two chalk formations, such as the Lewes Chalk and Seaford Chalk, the scar shape is nearly vertical in the Seaford Chalk formation and presents an inclined slope profile in the Lewes Chalk formation. Thirdly, where the cliff is made of a chalk unit characterized by strata-bound fractures, as in the Newhaven Chalk, the scar presents wedge-plane failure type. Finally, where the cliff is made of more than three chalk unit succession, the upper part of the scar located within the Seaford Chalk and the Lewes Chalk is vertical and the lower part of the scar is irregular shaped within the lower chalk formations (i.e. the Holywell Chalk and New Pit Chalk). In France, the two main types of chalk cliff failure observed on the coast are sliding failure type (as Puys collapse) and vertical failure type (as St-Valéry-en-Caux collapse), whereas in East Sussex (UK) wedge and plane failure types prevail over sliding failure type.

A minimum of 55 chalk collapses occurred between 1998 and 2001. The sudden increase of collapses observed during the year 2001 is interpreted as resulting from increased rainfall. The collapse triggering factors have focused on the role of groundwater within the chalk in relation to its fracture pattern. Firstly, some collapses may occur a few weeks up to about one month after heavy rainfall, as at Puys in May 2000. This occurs where a coastal cliff is composed of a poorly fractured chalk separated by some marls seams. Higher rainfall may initiate a collapse by increasing water pressure on the marl seams, which act as impervious layers (Duperret *et*

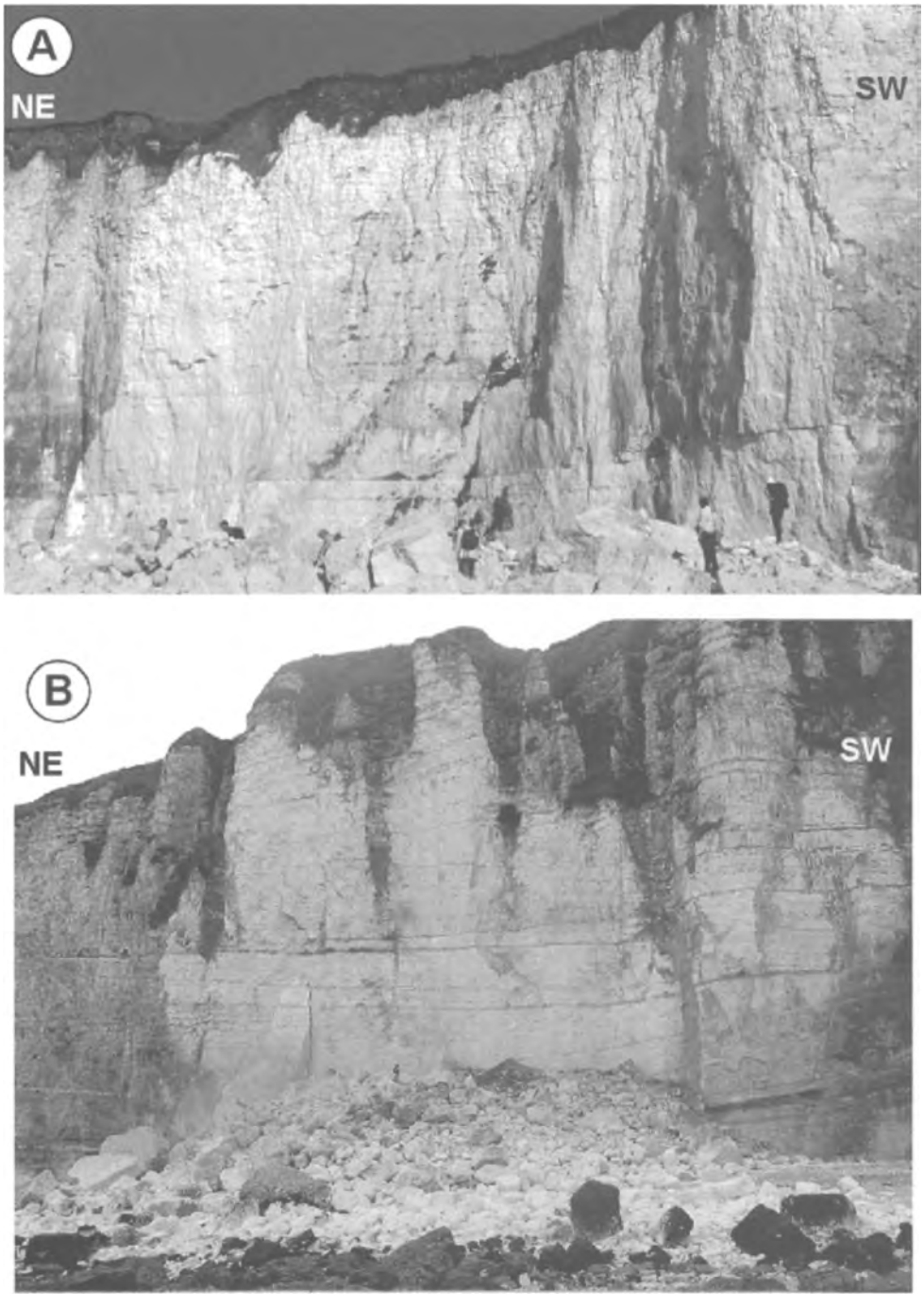

Fig. 12. A, Collapse scar at Puys (17 May 2000). The scar shows any fractures, any vertical dissolution pipes and is not bounded by fractures. The two dark horizontal levels exposing at the base of the scar are marl seams (Lewes Marl) and flint bands (Breaky Bottom Flints level) of the chalk. B, Collapse at Yport (June 2001). The scar shows vertical dissolution pipes filled by clays in the upper part of the cliff. The scar is bounded NE by a dissolution pipe and bounded SW by a large-scale oblique fracture filled by clays, with a dissolution pipe developing in its upper part. Dark horizontal levels exposing within the scar correspond to marls seams of the chalk.

al. 2002*a*). Secondly, collapses may occur during a long dry period disrupted by short-term storms, as at Grandes Dalles, Bénouville and Yport in summer 2001. This occurs where a coastal cliff is characterized by large-scale fractures filled by clays and dissolution pipes filled by Clay-with-flints, as observed in karstic environments.

Mixed layers illite/smectite may contract during long dry periods and thus favour the direct infiltration of water through the dissolution pipes, which act as well-drained fractures in the upper part of the cliff and may conduct to excess water to the middle part of the cliff. These types of collapse result from cyclic alternation of dissolution and plugging processes.

Lastly, the marine parameters which produce basal notching on the cliffs appear to have a secondary role on cliff retreat, because only notches less than one metre deep have been observed at the base of the French chalk cliffs. Basal notching may only induce medium to small scale collapses that develop in the lower part of the cliff. The occurrence of horizontal chalk discontinuities, as flint bands, limit the upward extension of the collapse.

The vertical failure type observed within homogeneous chalk is guided by joint sets roughly parallel to the cliff face fractures, as observed at Seven Sisters (UK). The magnitude of the cliff retreat is thus closely linked to the occurrence of secondary sets, made of a joint pattern, that is roughly parallel to the cliff face. In France, as observed at St-Valéry-en-Caux, secondary sets of pre-existing fractures have only been reported locally on the beach platform. We thus assume that the vertical failure type is due to newly created decompression fractures in France. Large-scale fractures transverse to the cliff face may limit the lateral expansion of a collapse, as observed at the Seven Sisters and at Saint-Pierre-en-Port, whereas some other large-scale fractures may be crossed by collapses, as observed at Yport. Such a range of behaviour may be linked to the type of fracture filling, which controls the water circulation within the chalk. Where fractures are voided, water could easily circulate through the fracture and the fracture may have a limited role on the lateral extension of a collapse. Where fractures are filled partially by clays, water may circulate or not through the fracture, depending on the wetting or drying state within the fracture. In this case, the role of the fracture on the lateral limitation of the collapse may vary with time.

Acknowledgements. The ROCC project was funded by the European community through the INTERREG II Rives-Manche community initiative (contract I99059). This research work has also been partly funded by the Centre National de la Recherche Scientifique in the framework of Programme National des Risques Naturels, through the contract PNRN 99–35–AS, by the Regional Council of Somme, the French Geological Survey (BRGM) and the University of Brighton. We thank the Maritime Direction Départementale de l'Equipement at Dieppe for providing us with additional data concerning collapses on the French coast.

We wish to thank Martin Daigneault (Saint-Etienne), Patricia Patrier (Poitiers), Said Taibi and Moulay Ghembaza (Le Havre) for RX pattern analysis, interpretation of clays RX pattern and mechanical analysis of clays samples, respectively. We also thank Bill Murphy for his constructive criticism and improvement of the paper.

References

BASSOMPIERRE, P. & ROUX, J. C. 1968. Etude hydrogéologique des fontaines d'Yport (Seine-Maritime), données acquises à la date du 15 Avril 1968. BRGM report 68 SGN 84 PNO.

BRISTOW, R., MORTIMORE R. N. & WOOD, C. J. 1997. Lithostratigraphy for mapping the chalk of southern England. *Proceedings of the Geologists' Association*, **109**, 293–315.

BROSSARD, J. & DUPERRET, A. 2004. Coastal Chalk cliff erosion: experimental investigation on the role of marine factors. *In*: MORTIMORE, R. N. & DUPERRET, A. (eds) *Coastal Chalk Cliff Stability*. Geological Society, London, Engineering Geology, Special Publication, **20**, 109–120.

CHEMIN, J., HOLÉ, J-P., PECKRE, M. & VIDARD, I. 1992. *Notice de L'atlas Hydrogéologique de la Seine-Maritime*. BRGM.

COSTA, S. 2000. Le recul des falaises du pays de Caux. *Bulletin d'Information des Géologues du Bassin de Paris*, 37, n°1, 31–34.

CRAMPON, N., ROUX, J. C., BRACQ, P., DELAY, F., LEPILLER, M., MARY, G., RASPLUS, L. & ALCAYADÉ, G. 1993. France. *In*: DOWNING, R. A., PRICE, M. & JONES, G.P. (eds) *The Hydrogeology of the Chalk of North-West Europe*. Oxford Science Publications, 113–152.

DAVIES, T. R. H. 1982. Spreading of rock avalanche debris by mechanical fluidization. *Rock Mechanics*, 9–24.

DORNBUSCH, U., WILLIAMS, R. B. G., ROBINSON, D. A. & MOSES, C. 2001. Disappearing act: Contribution of cliff erosion and in situ abrasion of flint to the shingle budget on the East Sussex coast. *European Rock Coasts 2001 Conference, Brighton, UK, 17–18 December 2001.*

DUPERRET, A., GENTER, A., MORTIMORE, R. N., DELACOURT, B. & DE POMERAI, M. 2002*a*. Coastal rock cliff erosion by collapse at Puys, France: the role of impervious marl seams within chalk of NW Europe. *Journal of Coastal Research*, **18**, 52–61.

DUPERRET, A., MORTIMORE, R. N., POMEROL, B., GENTER, A. & MARTINEZ, A. 2002*b*. L'instabilité des falaises de la Manche en Haute-Normandie. Analyse couplée de la lithostratigraphie, de la fracturation et des effondrements. *Bulletin d'information des Géologues du Bassin de Paris*, **39**, 6–26.

EMERY, K. O. & KUHN, G. G. 1982. Sea cliffs: their processes, profiles, and classification, *Geological Society of America Bulletin*, **93**, 644–654.

GENTER, A., DUPERRET, A., MARTINEZ, A., MORTIMORE, R. N & VILA, J.-L. 2004. Multiscale fracture analysis along the French chalk coastline for investigating erosion by cliff collapse. *In*: MORTIMORE, R. N. & DUPERRET, A. (eds) *Coastal Chalk Cliff Stability*. Geological Society, London, Engineering Geology Special Publication, **20**, 57–74

GRIGGS, G. 1994. California's Coastal hazards. *Journal of Coastal Research* Special Issue, n°12: Coastal Hazards, 1–15.

HADLEY, J. B. 1960. The Madison landslide. *Billings Geological Society*, 11th Annual Field Conference, 45–48.

HAPKE, C. & RICHMOND, B. 1999. Short-term episodic response of seacliffs to tectonic and climatic events: rates, failure style and spatial variability, Santa Cruz, California. *The Non-steady state*

of the inner shelf shoreline: Coastal change on the time scale of decades to millenia in the late Quaternary, PDF version of abstracts with programs, *Inaugural Meeting of IGCP Project 437, Coastal Environmental change during Sea level high-stands*. University of Hawaii, Honolulu, USA, Nov. 9–12 1999, 74–75.

HAYASHI, J. N. & SELF, S. 1992. A comparison of pyroclastic flow and landslide mobility. *Journal of Geophysical Research*, **97**, 9063–9071.

HEIM, A. 1932. *Bergusturz und Menschenleben. Fretz und Wasmuth*, Zurich, 218.

HSÜ, K. J., 1975. Catastrophic debris streams (Sturzstroms) generated by rockfalls. *Geological Society of America Bulletin*, **86**, 129–140.

HUTCHINSON, J. N., 1971. Field and Laboratory Studies of a fall in Upper Chalk cliffs at Joss Bay, Isle of Thanet. *Roscoe Memorial Symposium, Cambridge University.*

JUIGNET, P. 1974. *La transgression crétacée sur la bordure orientale du Massif Armoricain: Aptien, Albien, Cénomanien de Normandie et du Maine. Le stratotype du Cénomanien.* Thèse, Université de Caen.

KUHN, G. G., & SHEPARD, F. P. 1983. Beach processes and sea cliff erosion in San Diego county, California., *In*: KOMAR, P. D. (ed) *CRC Handbook of Coastal Processes and Erosion*. CRC Series in Marine Science, CRC Press Inc., Boca Raton, Florida.

LAMBERT, J., LEVRET-ALBARET, A., CUSHING, M. & DUROUCHOUX, C. 1996. Mille ans de séismes en France. Catalogue d'épicentres paramètres et références. *Ouest Editions, Presses Académiques*, Nantes, France.

LEGROS, F. 2002. The mobility of long-runout landslides. *Engineering Geology*, **63**, 301–331.

LEPILLER, M. & RODET, J. 1971, L'exsurgence de Senneville sur Fécamp (Seine-Maritime) par le GS-MJC-H. *Spéléo-Drack*, 3, GS-MJC Le Havre, France.

LORD, J. A. CLAYTON, C. R. I. & MORTIMORE, R. N. 2001. *Engineering in Chalk*. Construction Industry Research and Information Association (CIRIA), London.

MAY, V. J. 1971. The retreat of chalk cliffs. *Geographical Journal*, **137**, 203–206.

MÉGNIEN, C. L. & MÉGNIEN, F. 1980. Synthèse géologique du bassin de Paris. Stratigraphie et Paléogéographie, vol. I, *Mémoire du Bureau de Recherches Géologiques et Minieres n°101*, Orléans, France.

MIDDLEMISS, F. A., 1983. Instability of Chalk cliffs between the South Foreland and Kingsdown, Kent, in relation to geological structure. *Proceedings of the Geologists'Association*, **94**, 115–122.

MORTIMORE, R. N. 1979. *The Relationship of Stratigraphy and Tectonofacies to the Physical Properties of the White Chalk of Sussex*. PhD Thesis, CNAA, Brighton Polytechnic.

MORTIMORE, R. N. 1983. The stratigraphy and sedimentation of the Turonian-Campanian in the Southern Province of England. *Zittelania*, **10**, 27–41.

MORTIMORE, R. N. 1986. Stratigraphy of the Upper Cretaceous White Chalk of Sussex. *Proceedings of the Geologist's Association*, **97**, 97–139.

MORTIMORE, R. N. 1993. Chalk water and engineering geology. *In*: DOWNING, R. A. PRICE, M. & JONES, G. P. (eds.) *The Hydrogeology of the Chalk of North-West Europe*. Clarendon, Oxford, 67–92.

MORTIMORE, R. N. 2001*a*. ROCC project, Report on mapping of the chalk Channel coast of France from Port du Havre-Antifer to Ault, June-September 2001, report for BRGM.

MORTIMORE, R. N. 2001*b*. Chalk: a stratigraphy for all reasons, the Scott Simpson lecture. *Geoscience in South-west England*, **10**, 105–122.

MORTIMORE, R. N. & POMEROL, B. 1987. Correlation of the Upper Cretaceous White chalk (Turonian to Campanian) in the Anglo-Paris Basin. *Proceedings of the Geologists' Association*, **98**, 97–143.

MORTIMORE, R. N., POMEROL, B. & FOORD, R. J., 1990. Engineering stratigraphy and palaeogeography for the Chalk of the Anglo-Paris Basin. *In*: BURLAND, J. B., MORTIMORE, R. N., ROBERTS, L. D. & CORBETT, B. O. (eds) *Chalk*. Thomas Telford, London. 47–62.

MORTIMORE, R. N., LAWRENCE, J., POPE, D., DUPERRET, A. & GENTER, A. 2004. Coastal cliff geohazards in weak rock: the UK Chalk cliffs of Sussex. *In*: MORTIMORE, R. N. & DUPERRET, A. (eds.) *Coastal Chalk Cliff Stability*. Geological Society, London, Engineering Geology Special Publication, **20**, 3–31.

PRÊCHEUR, C. 1960. Le littoral de la Manche, de Sainte-Adresse à Ault. Etude morphologique. *Norois*, n° hors série, Poitiers.

RODET, J. 1986. Exploration de la rivière souterraine du Heurt (Senneville sur Fécamp, Seine-Maritime). *Spéléo-Drack*, 16, Dec. 1986, GS-MJC Le Havre, France.

RODET, J. 1992. *La craie et ses karsts*, C.N.E.K. Centre Normand d'Etude du Karst et des cavités du sous-sol, Elbeuf, France.

SUNAMURA, T. 1992. *Geomorphology of Rocky Coasts*. Wiley, Chichester.

VOIGHT, B., JANDA, R. J., GLICKEN, H. & DOUGLASS, P. M. 1983. Nature and mechanics of the Mount St Helens rockslide-avalanche of 18 May 1980. *Geotechnique*, **33**, 243–273.

WEISBROD, N., NATIV, R., ADAR, E. M. & RONEN, D. 1999. Impact of intermittent rainwater and wastewater flow on coated and uncoated fractures in chalk. *Water Resources Research*, **35**, 11, 3211–3222.

Multiscale fracture analysis along the French chalk coastline for investigating erosion by cliff collapse

A. Genter[1], A. Duperret[2], A. Martinez[2], R. N. Mortimore[3] & J-L. Vila[1]

[1] BRGM, CDG/ENE, 3 avenue Claude Guillemin, BP 6009, 45060 Orléans cedex 2, France
[2] Laboratoire de Mécanique, Physique et Géosciences, Université du Havre, 25 rue Philippe Lebon, BP 540, 76 058 Le Havre cedex, France
[3] Applied Geology Research Unit, University of Brighton, Moulsecoomb, Brighton, BN2 4GJ, UK

Abstract: Coastal cliffs of Upper Normandy and Picardy are eroded by cliff collapses of various sizes. This paper presents a multi-scale analysis of the pre-existing fractures embedded within the Cretaceous chalk. About 20 representative sites equally spaced along the 120km long coastal section were analysed and compared to a continuous structural analysis of the coast derived from aerial photographs taken in 1986. Ancient collapses interpreted on the aerial photos were compared to the pre-existing fracture content. Regional faults, pre-1986 collapse location and fracture density are spatially correlated. However, recent collapses observed on the field between 1998 and 2001 did not systematically correlate to the pre-existing fracture occurrence and therefore, there is no clear link between recent collapse and the regional faults.

Coastal cliff erosion in Cretaceous chalk

Erosion of chalk cliffs by collapse is a serious geohazard that induces coastal retreat. In order to understand the cliff collapse mechanism, a multidisciplinary research project co-funded by Europe, called ROCC (Risk Of Cliff Collapse), was carried out between 1999 and 2001. The ROCC project focused on Upper Normandy and Picardy regions in France, from Le Tilleul to Ault (120km long) and on East Sussex in UK, from Brighton to Eastbourne (40km long). Previous studies based on long period analysis suggest that the mean rate of chalk cliff erosion along the Channel coasts varies between 0.2 m/year and 0.3 m/year (May 1971; Costa 2000; Dornbursch *et al.* 2001). Recent field observations in France show that the coastal erosion is spatially and temporally variable and occurs by sudden cliff collapse that could generate significant cliff retreats of 1–10s of metres (Duperret *et al.* 2004). Cliff instability is governed by a series of parameters of different origins. Pre-existing fractures as well as lithology represent two of those parameters. In the period 1998–2001, a minimum of 55 collapses have been observed along the French chalk coastline and about ten collapses along the English chalk coastline. For example at Beachy Head in UK, a huge collapse of 150000m^3 occurred in 1999 controlled by vertical pre-existing fractures were involved (Mortimore *et al.* 2004). At Yport in France, a collapse occurred in 2001 in a fractured cliff characterized by the presence of a series of vertical fractures and of dissolution pipes (Duperret *et al.* 2004). At Puys in France, a collapse occurred on May 2000 within a very low fractured zone bounded by large-scale fractures (Duperret *et al.* 2002). From these observations, a preliminary hypothesis was suggested that fractures embedded within the Cretaceous chalk of NW France could influence cliff collapse. The aim of this paper is, therefore, to investigate the relationships that exist between fracture characteristics and cliff collapses. In order to investigate the role of fractures in cliff collapse, we: (1) analysed cliffs forming the French coast at two different scales by combining fracture characterization (attitude, density, types) on selected sites at field scale, with a continuous analysis of aerial oblique photographs of the coastline; (2) made a complete interpretation of the ancient collapses visible on aerial photographs (location, size) and then compared the results with the cliff fracture content; (3) made a comparison between pre-1986 collapses observed on aerial photographs and recent collapses observed in the field in terms of spatial distribution along the French coast. A scar is the fresh rupture surface visible on the vertical coastal cliff after a rock fall event, called here a collapse. Its state of freshness is indicated by the colour differences in the cliff. On the coastal chalk cliff, a fresh scar surface is easily detectable because the chalk colour is white. The scar width is the maximum width of the rupture surface located between the flanks of the cliff collapse. In this paper, a collapse is a generic term that describes a cliff rock fall (Dikau *et al.* 1996).

The French chalk cliffs of upper Normandy and Picardy regions represent a 3D rock mass with a horizontal distance, about 2000 times greater than the vertical height. The average cliff height is about 60m for a coastal strip of about 120km long. As pre-existing fractures are on a scale of metres to tens of metres, it was not possible to investigate them continuously at a field scale of 120km. Then, we were obliged to combine geological acquisition based on a series of control areas and a continuous information set represented by the aerial photographs. The choice of the control areas

From: MORTIMORE, R. N. & DUPERRET, A. (eds) 2004. *Coastal Chalk Cliff Instability*. Geological Society, London, Engineering Geology Special Publications, **20**, 57–74. 0267-9914/04/$15.00

was mainly due to the most accessible valleys, knowing that the cliff height is on average 50 metres in upper Normandy. About 34 zones were visited for geological characterization (lithology, stratigraphy, structural framework) and collapse data (occurrence, size, run-out, etc.). Furthermore, between St Valéry en Caux and Pourville, about 25 km in length, an exhaustive geological survey has been done along the coastal cliff foot in order to calibrate field analysis and aerial photograph interpretation. Consequently, on the French coast, 2000 pieces of data (1400 on the cliff, 600 on the beach) were acquired mainly along the coast but also on the beach platform, allowing at least a 2D characterization of the fracture pattern.

Fracture analysis at field scale

Fracture typology

In order to determine the fracture characteristics, a selection of about 20 more or less relatively equally spaced sites was investigated along the French coast (Fig. 1). As the lithology was not uniform along the coast, the analysis was conducted in different lithostratigraphic units. Based on field observations on the cliff face or in the beach platform, a fracture typology was defined. On the cliff, the fracture attitude (strike, dip) as well as their vertical extension were measured. The occurrence of shear movements such as slickensides, striation or vertical offsets of flint layers was used to determine the presence of faults. On the beach platform, fracture orientations and more local horizontal fracture traces were collected. Locally, large-scale fractures were observed both on the beach platform and on the cliff. On the cliff, the

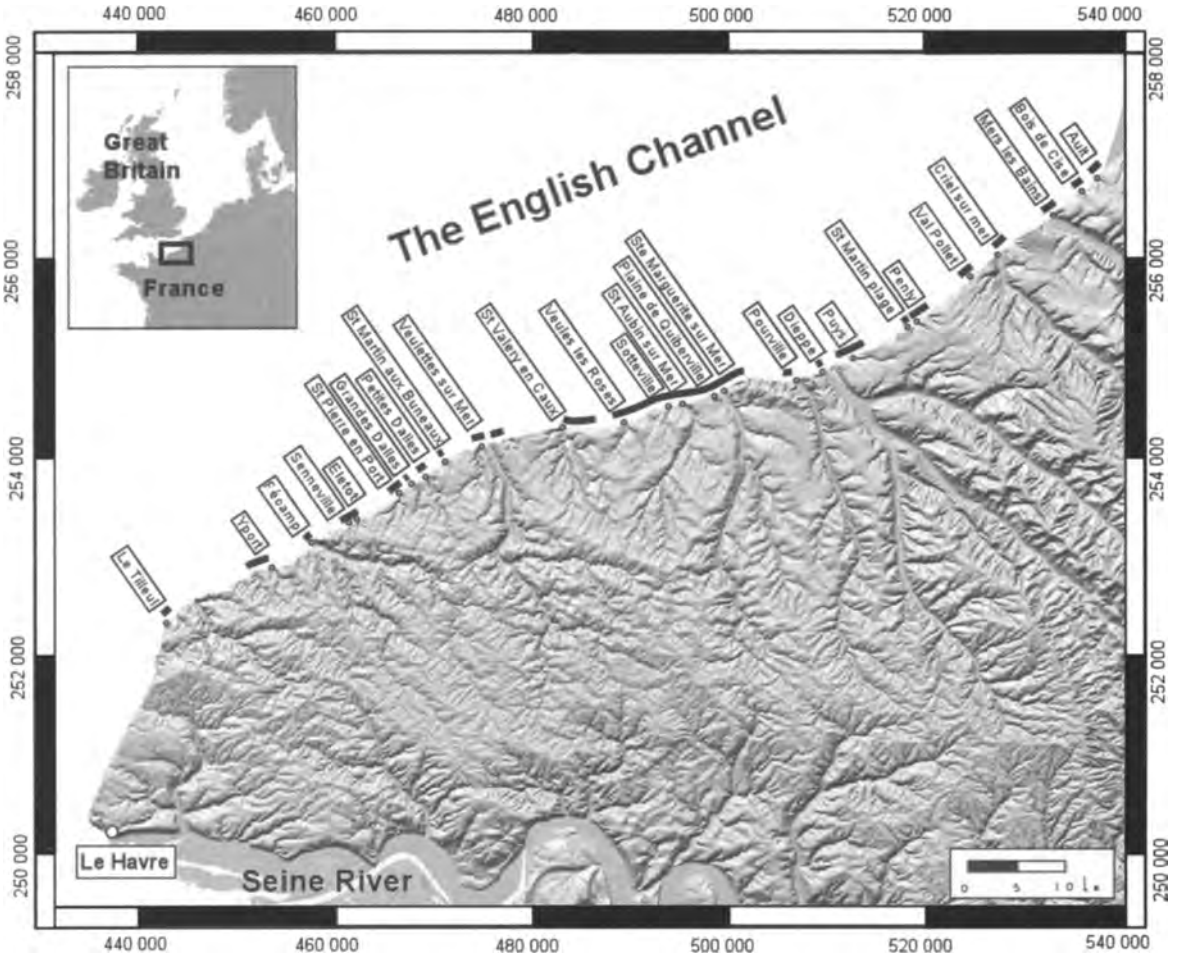

Fig. 1. Location of the fracture sites investigated at field scale, on the French coastline of Upper Normandy and Picardy.

main fracture types collected in the field were pre-existing fractures (synsedimentary fractures, strata-bound fractures, master-joints, normal faults, joints) and newly created fractures (stress release fractures). Other kinds of structures related to stratification were also recorded including flint levels or marl seams. As the French coast is gently folded, stratification represents a sub-horizontal anisotropy within the cliffs.

(1) Synsedimentary fractures are characterized by 10 mm thick filling made of flint. The presence of flint within the fracture plane is interpreted as a very early genesis for those structures in the chalk basin development. They are small-scale fractures and show a zigzag pattern characterizing low anisotropic palaeostress field conditions consistent with the basin creation. They are low dipping fractures. Locally, some vertical striations are visible indicating that they correspond to synsedimentary small-scale normal faults. They are slightly isolated at outcrop scale and do not constitute a well-organized network. (2) Strata-bound fractures correspond to small-scale normal faults well developed in a given chalk unit (Mortimore *et al.* 1990). Those fractures are also interpreted as early synsedimentary fractures. (3) Master-joints are large nearly vertical fractures that cross the whole cliff with an apparent extension of tens to hundreds of metres. They are tiny fractures whose vertical trace is underlined by a Fe-oxide coloration. As they show no indicator of movement, they were defined as master-joints. Vertical dissolution pipes of karstic origin nucleate on vertical master-joints. (4) Normal faults show typical apparent vertical offsets of cm to metric scale. In some case, vertical slickensides were observed as well as a cataclased damaged zone associated to the major fault plane. They are steeply dipping fractures. Their fracture filling was not investigated systematically but some clay minerals, iron oxides as well as carbonates could be partly sealed the normal fault planes. (5) Joints represent small-scale fractures with no indication of movement. They are isolated structures or organized in more pervasive vertical network embedded within the chalk unit. Their origin is not well constrained. (6) Stress release fractures occur in the vicinity of some valleys, e.g. where the cliff height is rather low, chalk outcrops being highly fractured. Such a network reduces progressively away from the valleys. Locally, some newly created vertical fractures parallel to the cliff face were also observed, but they were not investigated systematically. There is no stress release fractures on the beach platform.

Fracture orientation

About 2000 fracture orientation measurements were collected on the field (Table 1). The directional fracture set analysis shows a major fracture set, as well as a series of secondary sets. The nearly vertical N110–N130E fracture is the dominant set (Table 2). This set is ubiquitous through the chalk coastline except between Eletot and Senneville sur Fécamp which shows a strata-bound fracture pattern. The secondary fracture sets are characterized by a N0–20E set, a N20–30E set which occurred only at Eletot, and a N40–60E set mainly parallel to the cliff face, which is well represented on the beach platform (Tilleul, St Pierre en Port, Petites Dalles, Bois de Cise) but difficult to observe and then to sample on the cliff face (Fig. 2). The secondary N90–N100E and N160–170E sets have been observed north of Fécamp but are not well represented, whereas the N140–160E set is well represented between Fécamp and Dieppe and north of Criel sur Mer.

In the vicinity of Eletot and Senneville sur Fécamp, the fracture network has an orientation, which is not related to the regional NW–SE trend. The measurements were made in specific chalk units at the bottom of the cliff. Strata-bound fractures consisted of conjugate normal faults, with tens of metres length such as at Senneville sur Fécamp in the New Pit Chalk Formation and at Eletot in the Lower Lewes Chalk Formation where the network was more or less isotropic (Fig. 2). At Quiberville, strata-bound fractures consisted of dual conjugate normal faults with tens of metres length, giving a pyramidal morphology to the cliff face in the Newhaven Chalk Formation.

From Antifer to Ault, the coastline is mainly oriented NE–SW, whereas the dominating fracture set is oriented N120E with a certain degree of scattering (Table 2). This regional fracture set is made mainly of master-joints and normal faults. It suggests that this NW–SE fracture set could be related to a palaeostress field event oriented NE–SW active from late Cretaceous to early Tertiary times (Vandycke 1992; Vandycke & Bergerat 1992). Hibsch *et al.* (1995) suggest that the normal faulting in the late Cretaceous Chalk deposits is syn-diagenetic faulting related to compaction, inducing a radial extensional stress tensor. On the field in Upper-Normandy coastline, the normal faults show a significant N120 E directional anisotropy probably indicative of anisotropic palaeostress tensors. The compaction processes proposed by Hibsch *et al.* (1993, 1995) could have generated the isotropic small-scale normal faults observed at Eletot and Senneville sur Fécamp (Fig. 2) and qualified of stratabound fractures by Mortimore (1983). Along the upper Normandy coastline, as the N120E normal faults are not synsedimentary faults, they are not linked to compaction processes.

A comparison between fracture content on the beach platform and on the cliff face was done in several sites for minimizing the fracture sampling bias. The fracture sampling along the coast is very powerful for collecting fractures intersecting the coast but is not sufficient for characterizing what part of the fracture system could be parallel oriented to the coast. On the beach platform, fracture data were collected on profiles which are not parallel to the coast. However, as the fracture system is nearly vertical, it was rather difficult to measure fracture dips on the platforms. Then, fractures were mainly characterized by their azimuth as only their horizontal traces are visible. Moreover, along the coast, all the beach platforms are not easily accessible due to beach sediment deposits (sand, shingle). Then, only 11 sites were investigated on the beach platform for evaluating the fracture content. About 600 fractures were collected on these different horizontal accessible surfaces (Table 2). On the vertical

Table 1. *Characteristics of the sites investigated for fracture evaluation*

Investigated site	*Number of lithological units on the cliff*	*Name of the lithological units (from Mortimore, 1983)*	*Cliff orientation*	*Strucural data collected on the cliff*	*Strucural data collected on the beach platform*
Ault Nord	2	Lewes & Seaford	N40	32	0
Ault S	2	Lewes & Seaford	N40	34	0
Bois de Cise N	2	Lewes & Seaford	N45	100	123
Mers les Bains N	2	Lewes & New Pit	N50	8	0
Criel sur Mer N	2	Lewes & Seaford	N40	78	0
Criel sur Mer S	2	Lewes & Seaford	N60	29	0
Val Pollet	2	Lewes & Seaford	N50	16	0
Penly N	3	Holywell, New Pit, Lewes	N45	25	30
St Martin N	3	Holywell, New Pit, Lewes	N45	83	0
Puys N	1	Lewes	N60	61	0
Puys S	1	Lewes	N70	13	0
Dieppe S	1	Seaford	N60	17	0
Pourville S	1	Newhaven	N95	12	0
Quiberville N	1	Newhaven	N50	58	0
St Aubin sur Mer N	1	Newhaven	N70	104	0
Epineville	1	Newhaven	N65	16	0
Sotteville La Pointue	1	Newhaven	N55	93	0
Veules les Roses N	2	Seaford & Newhaven	N55	23	0
Veules les Roses S	1	Seaford	N75	21	0
St Valéry en Caux N	1	Seaford	N85	9	43
Veulettes sur Mer N	2	Lewes & Seaford	N50	10	
Veulettes sur Mer S	2	Lewes & Seaford	N90	30	85
St Martin aux Buneaux	2	Lewes & Seaford	N55	17	0
Les Petites Dalles N	2	Lewes & Seaford	N40	65	93
Les Grandes Dalles S	2	Lewes & Seaford			14
St Pierre en Port N	2	Lewes & Seaford	N40	47	32
St Pierre en Port S	2	Lewes & Seaford	N50	43	29
Eletot	2	Lewes & Seaford	N60	83	62
Senneville N	3	New Pit, Lewes & Seaford	N60	32	0
Fécamp N	4	Zig Zag, Holywell, New Pit, Lewes	N50	48	0
Yport N	2	Lewes & Seaford	N65	12	0
Yport S	2	Lewes & Seaford	N90	31	12
Le Tilleul N	3	New Pit, Lewes, Seaford	N35	159	0
Le Tilleul S	2	Holywell, New Pit	N40	24	35

cliff faces, about 1400 fractures were collected in 34 different sites. In order to minimize the sampling bias along the coast, some field works were focused on the best outcropping cliff and beach platform. For example, in Bois de Cise, 100 and 123 fractures were collected on the cliff and the platform respectively (Fig. 2). On the beach platform, the fracture system is mainly organized around two fracture sets: (1) a dominating fracture set oriented NW–SE and (2) a secondary fracture set oriented NE–SW. On the cliff face, the fracture system is more scattered around the principal fracture set oriented NW–SE. A secondary fracture set is oriented NNE–SSW. Based on this analysis, we can concluded that the main fracture system is mainly oblique to the coast and is well revealed on both the cliff and the beach platform. Parallel fractures to the coast occur but they do not correspond to a principal fracture set (Table 2).

The fracture pattern embedded within the Cretaceous chalk of upper Normandy and Picardy is characterized by (1) a dominant NW–SE vertical network of master joints and normal faults; (2) the presence of two secondary fracture sets oriented NE–SW and NNW–SSE, better sampled on the beach platform (Table 2); (3) locally, the presence of relatively isotropic conjugate small-scale normal faults developed in particular chalk units and called strata-bound fractures. The fracture network encountered within the Cretaceous chalk of Normandy has a pattern made of at least two-secant fracture sets (Fig. 3). The interpretation of aerial photos described below is used to determine the fracture density continuously along the coast.

Fracture analysis on aerial photography

A series of oblique black and white aerial photographs of the coastline taken in 1986 was available at an approximate scale of 1:5000 for an exhaustive interpretation of the cliff and its

Table 2. *Fracture dataset characteristics collected on the cliff and on the beach platform*

Site	*F1 Main fracture set on the cliff*	*F2 Main fracture set on the cliff*	*S1 Minor fracture set on the cliff*	*S2 Minor fracture set on the cliff*	*S3 Minor fracture set on the cliff*	*Dominating cliff fracture typology*	*Beach fracture typology*	*Main fracture set on the beach*	*S1 Minor fracture set on the beach*	*S2 Minor fracture set on the beach*	*S3 Minor fracture set on the beach*
Ault Nord	N120		N25	N105	N160	Fractures					
Ault S	N140	N110									
Bois de Cise N	N130		N110	N020	N155	Fractures		N120	N055		
Mers les Bains N	N110	N90				Normal faults					
Criel sur Mer N	N000					Fractures					
Criel sur Mer S	N140	N120	N155	N105		Master joints					
Val Pollet	N135					Master joints					
Penly N	N090		N015	N070		Normal faults		N080	N040	N060	
St Martin N	N120		N010	N070		Master joints	Joints				
Puys N	N110		N050			Master joints	Normal faults				
Puys S	N110					Master joints	Normal faults				
Dieppe S	N115					Joints	Master joints				
Pourville S	N130					Master joints					
Quiberville N	N110		N095	N145		Master joints	Normal faults				
St Aubin sur Mer N	N125	N140	N160			Normal faults					
Epineville	N125					Normal faults					
Sotteville La Pointue	N120					Normal faults	Master joints				
Veules les Roses N	N130					Normal faults					
Veules les Roses S	N140					Normal faults					
St Valéry en Caux N	N115	N90/ N165				Master joints	Normal faults	N130			
Veulettes sur Mer N	N135					Joints					
Veulettes sur Mer S	N110					Joints	Master joints	N120			
St Martin aux Buneaux	N130					Master joints	Joints				
Les Petites Dalles N	N120					Master joints	Joints	N120	N35	N160	N100
Les Grandes Dalles S								N60			
St Pierre en Port N	N110	N10				Master joints	Joints	N110	N10	N25	N165
St Pierre en Port S	N105		N170			Master joints	Joints	N60			
Eletot	N145		N30			Normal faults		N160	N100		
Senneville N	N140	N150	N165			Normal faults					
Fécamp N	N120	N000				Master joints					
Yport N	N110					Master joints					
Yport S	N115					Joints	Master joints	N150	N100		
Le Tilleul N	N115		N15	N165		Fractures					
Le Tilleul S	N120					Joints	Synsediment.	N40	N120	N15	N165

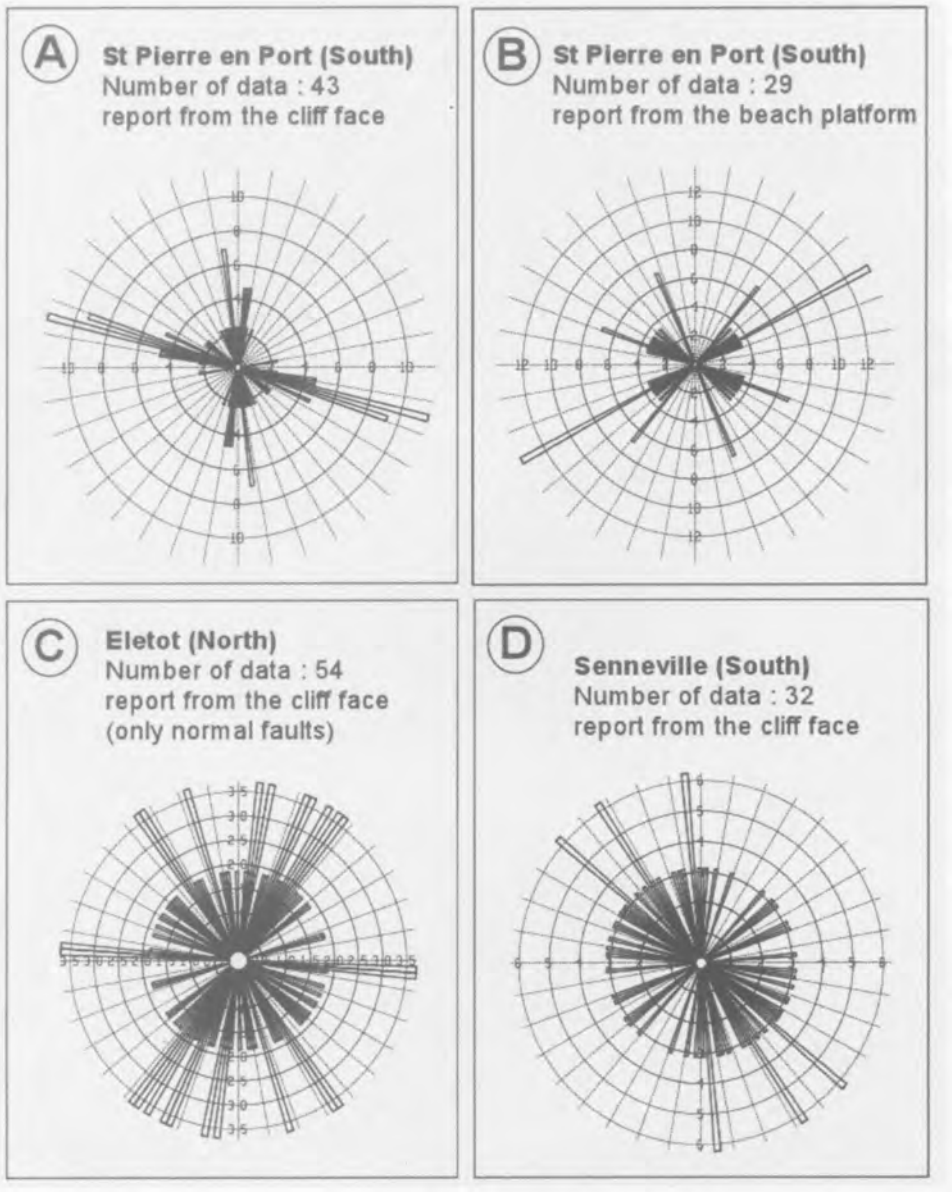

Fig. 2. Rose diagrams of fracture azimuth collected on the cliff face (A) and on the beach platform (B) at Bois de Cise. Rose diagrams of stratabound fracture azimuth collected on the cliff face at Eletot (C) and Senneville sur Fécamp (D).

beach platform. Before carrying out the photo interpretation, some corrections were applied for the oblique nature of the dataset and the problem related to the photograph shot. During the data acquisition, the horizontal distance between the aeroplane and the cliff face was not constant. As a result, some distortions occurred and the photos were mainly interpreted in their central part, for minimizing the sampling bias.

In order to generalize the local structural information collected on the selected sites, about 450 photos were interpreted (Vila 2000). An interpretative methodology was thus outlined on the best quality photographs in which several features (collapses, fractures, dissolution pipes, shingle platform, cliff limits, etc...) were analysed continuously from Antifer to Ault (Vila 2000). As the aim was to provide data for a GIS application, the following relevant layers of information derived from the photo interpretation were inte-

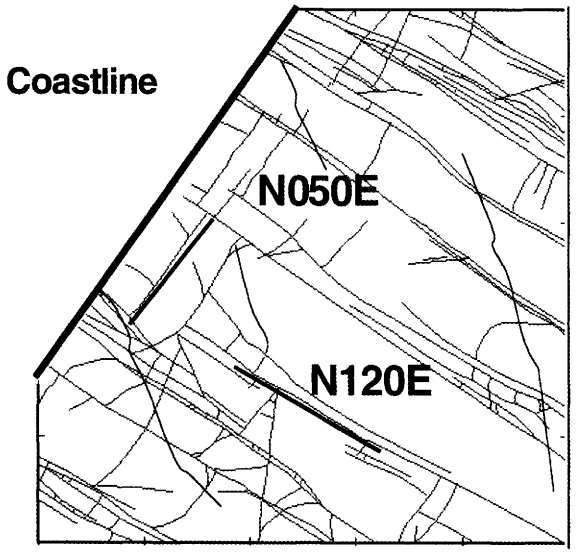

Fig. 3. Conceptual model of the fracture system embedded within the chalk of Upper-Normandy and Picardy (map view) based on field survey.

grated: (1) the fracture content visible on the cliff face, which corresponds to the fractures orthogonal to the cliff face; (2) the fracture content visible on the beach platform, which mainly corresponds to the fractures parallel to the cliff; (3) the collapse characteristics (size, location).

An example of a raw aerial photograph is presented on Figure 4. It shows the Bois de Cise area in the northern part of the French coastline. The vertical chalk cliff is very fractured and shows several parallel large-scale fractures dipping north corresponding mainly to normal faults and master-joints that cut the cliff face. At the bottom of some fractures, there are some triangle-shaped caves. At the cliff bottom, several collapses are located either in relatively low fractured zones or in highly fractured zones. They were qualified as ancient collapses or pre-1986 collapses because the aerial photographs were taken more than 15 years ago. It was not possible to clearly identify what kind of cliff collapse was involved even though a large diversity of failure collapse types is suspected in chalk cliff on both sides of the Channel (Duperret *et al.* 2004; Mortimore *et al.* 2004). For each observed ancient collapse, its horizontal extension was measured parallel to the cliff providing a collapsed width. Those collapses visible on the aerial photo did not all occur in 1986 but correspond to the cumulative erosional activity of several years of cliff collapse. Actually, it is well known that some large scale collapses are relatively old and are still visible on the beach platform such as the '*Chien neuf*' collapse located close to Senneville sur Fécamp that occurred

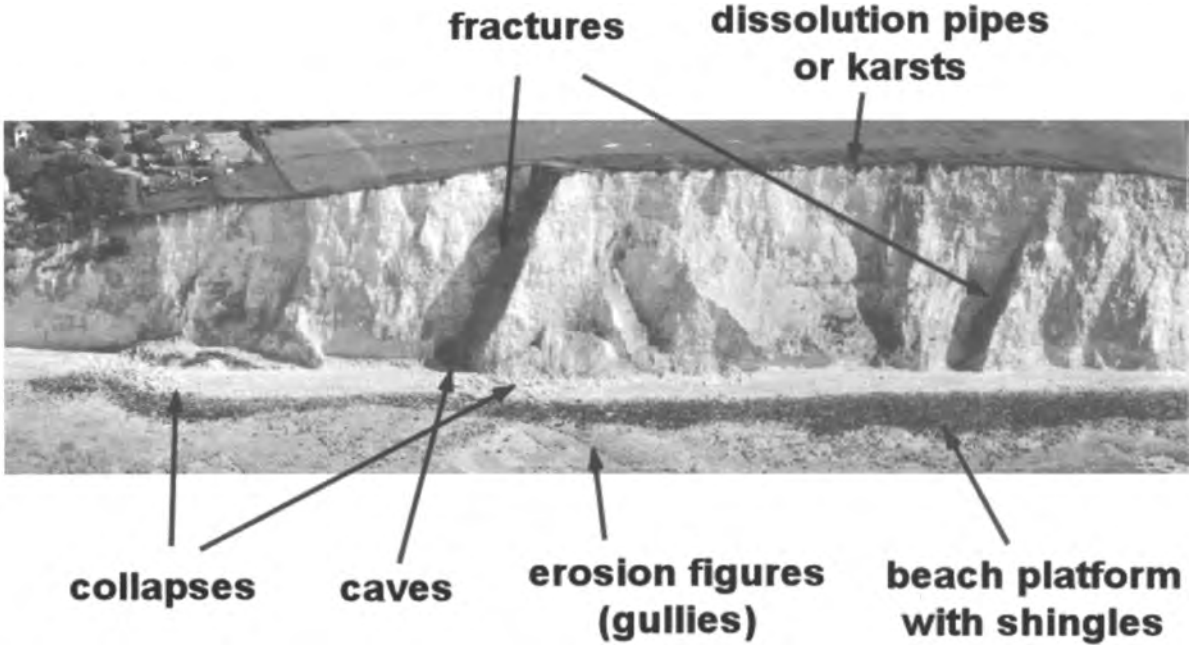

Fig. 4. Example of an oblique aerial view (shot taken in 1986) of the French coastline (on the left, Bois de Cise area), with its main features.

more than 70 years ago (Rodet 1992). On the beach platform some fractures parallel or orthogonal to the cliff face are also visible as well as some marine gullies. Even though the sampling bias related to the oblique photos occurred, the cliffs appear always more fractured than the beach platforms. This observation was also made during the field analysis. The pre-existing fractures are more visible on the cliff because the fracture fillings which are generally dark-coloured, were not eroded. On the beach platform, sea erosion takes place and the pre-existing fractures become more difficult to detect.

Calibration of aerial photo interpretation

As the aerial photographs are continuous, their calibration was necessary in order to get the best structural identification of the interpreted photo fractures and to determine the actual scale of the photographs. The structural knowledge of the field scale through the 20 equally spaced selected studied sites equally spaced was helpful in providing a better understanding of the aerial photo interpretation.

A continuous section between Pourville to St Valéry en Caux was investigated at field scale and compared with the cliff photo interpretation (Fig. 5). In this section about 25 km long, all the pre-existing fractures visible in the field were classified, measured and located (Fig. 6). Three main types of fractures were observed in the field: (1) Normal faults characterized by a N120E orientation. Secondary fracture sets oriented N–S and E–W were present preferentially between Quiberville and St Aubin where they formed conjugate networks. In terms of size, they were mainly cross-cliff fractures but the N–S and E–W fault sets were small-scale normal faults. (2) Master-joints, characterized by a dominant N110–120E orientation, were large-scale steeply dipping fractures. (3) Synsedimentary faults, which are quite isolated, showed oblique dip values ranging between 50 and 70° and E–W to NW–SE orientations. These last small-scale to medium-scale fractures were mainly filled by black flint.

As the aerial photos are oblique, it was not possible to obtain quantitative information from them about fracture orientations. However, an apparent dip value can be determined as well as their vertical extension. The lack of information about fracture orientation from the photo interpretation is not penalising because the fracture analyses carried out in the 20 different sites and continuously between Pourville and St Valéry en Caux, showed a very consistent fracture orientation around the N120E direction (Table 1). It means that the oblique photos of the coastline highlight the dominating fracture set with steeply dipping planes. The vertical extension of the fractures visible on the cliff face can also be obtained from the photographs, which is especially useful for detecting the largest fractures.

Between Pourville and St Valéry en Caux, the detailed comparison between the field data and the aerial photo interpretation indicates three main calibrating guidelines applicable at the scale of the French coastline. (1) The fracture density, e.g. the total number of fractures visible on a given horizontal distance, observed in the field or interpreted on the aerial photo shows a value in the same range of magnitude. In this case, the main fracture types visible in the field are large-scale fractures made of normal faults or master-joints which are, therefore, correctly detectable on the photographs due to their large vertical extension. (2) The fracture density deduced from aerial photo interpretation is higher than those

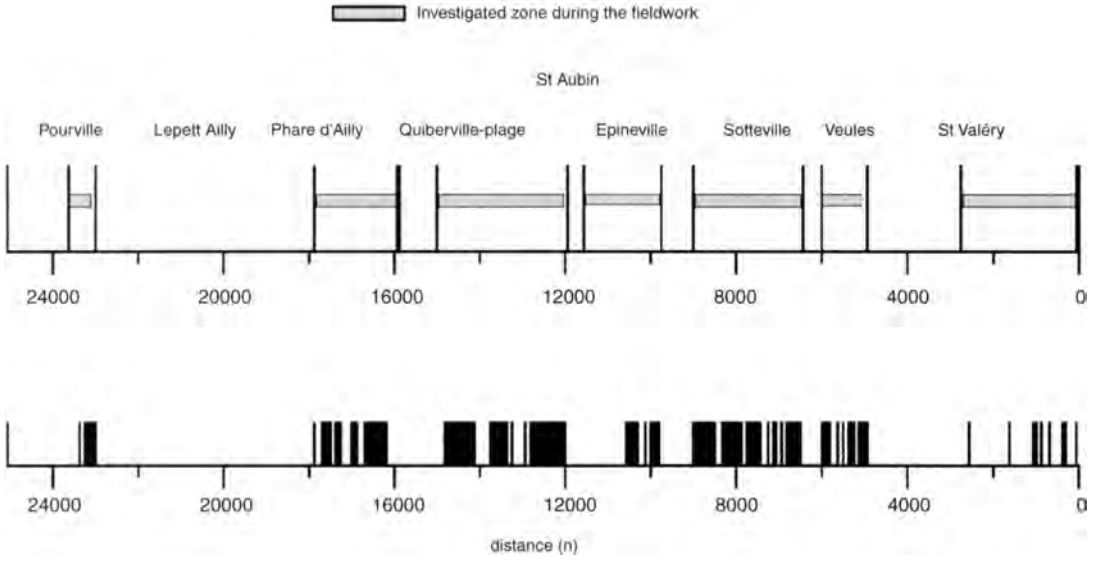

Fig. 5. Location of the detailed coastal sections analysed on the field between St Valéry-en-Caux (SW) and Pourville (NE) and fracture location.

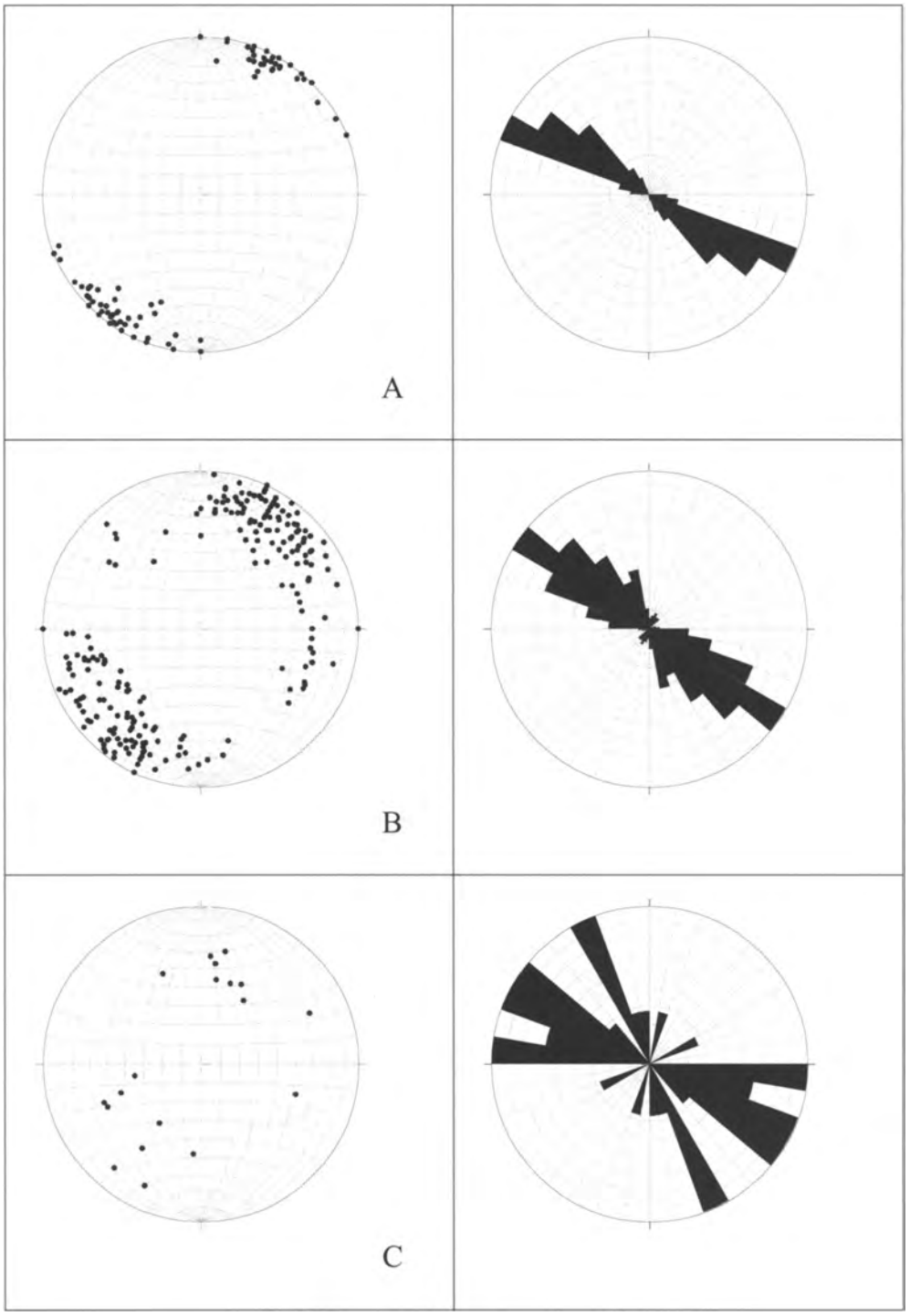

Fig. 6. Stereographical projections (Schmidt plot in lower hemisphere) of the fractures collected on the field between St Valéry-en-Caux and Pourville. A, master-joints; B, normal faults; C, synsedimentary fractures.

measured on the field. The over-estimation of the aerial photo fractures is due to the presence of small-scale to medium-scale structures that are not well constrained in terms of origin. For example, a lot of joints not well defined (induced fractures or stress release fractures) or some vertical morphological structures could be visible in some altered cliffs around Pourville. In some aerial photos, a given large-scale fracture is divided into several apparent smaller segments due to the obliquity of the photo shot leading to a slight over-estimation of the fracture density. In other places, a not well-defined vertical network of pervasively distributed joints may be revealed on aerial photos. The field evaluation has shown that these networks do not really correspond to relevant pre-existing fractures. Such structures lead to an over-estimation of the fracture content on aerial photos. (3) The fracture density deduced from aerial photo interpretation is lower than those measured on the field. In this case, inclined synsedimentary fractures filled with flint as well as some small-scale normal faults oriented N–S and E–W, were not systematically detectable on the aerial photos. There are about 15% of the field fractures which are not visible on the photos. They correspond generally to tiny synsedimentary fractures with various orientation and normal faults, parallel to the cliff, and consequently difficult to characterize even with high-resolution photos. Finally, as most of the fractures show a vertical extension higher or equal to the cliff height, the field fractures were easily detectable on the photo.

Two fracture sizes are visible on the cliffs that mainly correspond to two main groups of fracture types: the small-scale fractures (joints, synsedimentary fractures, stress release fractures, induced fractures) and the large-scale fractures (normal faults, master-joints). Generally, the small-scale fractures are more poorly sampled than the large-scale fractures, on aerial photos. Therefore, based on the aerial photograph analysis, two different fracture densities were calculated: the whole fracture density that mixes all the fractures types, called Total Fracture Type (TFT) and the large-scale fracture density that takes into account the large-scale fractures only, called Major Fracture Type (MFT).

The second goal of the calibration procedure was to determine the actual scale of the oblique aerial photographs knowing that there were some distortions on the raw aerial photos. In the field, between Pourville and St Valéry en Caux, measurements were made to provide some typical benchmarks. The horizontal distance between similar features identified both in the field and on the aerial photographs was measured, allowing checking of the actual photo-scale, which is 1:4900. This field scale calibrated value was very close to the initial scale value and allowed us to derive real fracture densities from aerial photographs.

Fracture data analysis on aerial photographs

For building the geohazard map of the coastline, it was necessary to divide the coast into adjacent sectors having a given state of fracturing. Therefore, based on aerial photo fracture evaluation of the cliff, the coast has been delineated into a series of sectors having a homogeneous fracture content with a low, average, or high fracture density (Fig. 7). Between Ault and Antifer, 63 sections with different length have been determined. In each section, the total number of fractures, the section length as well as the whole linear fracture density were calculated, knowing that the horizontal scale was calibrated in the field. The sector with the highest density of fractures was Puys with 0.172 fract./m. The sector with the lowest density of fractures was close to Penly with 0.011 fract./m. Several sectors showed a fracture density close to zero because they corresponded to areas with very low cliff height (perched valleys) or valleys (town, harbour). The average fracture density along the coast was 0.074 fract./m. As we were looking for some relationships between fracture content and cliff collapse, the fracture data were expressed as

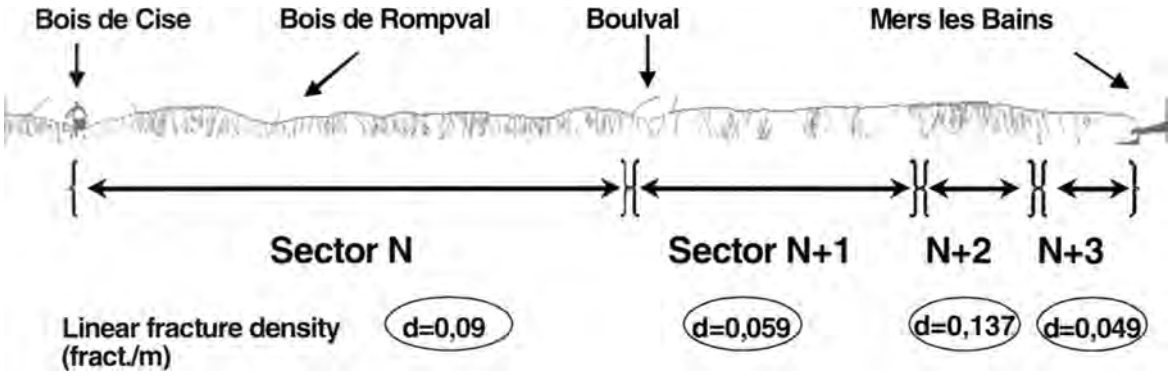

Fig.7. Example of fracture density sectoring along the cliff face. Each sector having a given fracture organization is characterized by its linear fracture density or its fracture spacing. This section is oriented NE–SW, i.e. Bois de Cise to Mers les Bains.

fracture spacings. The lower the fracture density, the higher the spacing values. For example, a fracture density of 0.02 fract./m, means that the minimum horizontal distance between two consecutive fractures, i.e. the fracture spacing calculated as the inverse of the fracture density, is 50 m.

Between Antifer and Ault, the map of the Total Fracture Types (TFT) shows some sectors with low fracture spacing, ranging from 5 to 10 m, which alternate with sectors with high fracture spacing, ranging from 50 to 100 m. 90% of the fracture spaces range between 5 and 25 m, the average value being 13 m. At regional scale, the most fractured sectors match with large-scale faults such as the Fécamp-Lillebonne fault (at Fécamp), the Bray Fault (at Dieppe) and the Eu Fault (at Mers les Bains) (Fig. 8). The length of the highly fractured coastal sections extends a few kilometres on each side of the regional faults, such as is observed between Yport and St Martin aux Buneaux. The coastal sections located south of Yport, as well as between St Martin aux Buneaux and Cap d'Ailly, and Penly and Criel sur Mer, are characterized by a low fracture content. These sections are both far away but relatively equally spaced from the major regional faults.

The map of the Major Fracture Types (MFT) which corresponds to the master-joints and the normal faults is herein compared to the TFT strip (Fig. 8). The fracture spacing varies between 7 and 182 m, the average value being 30 m. Due to the lower fracture content, the MFT strip systematically shows higher spacing values than the TFT strip, except in the north between Criel sur Mer and Ault. In this northern area characterized by the occurrence of the Eu fault, the fracture content is very high, similar for both MFT and TFT and

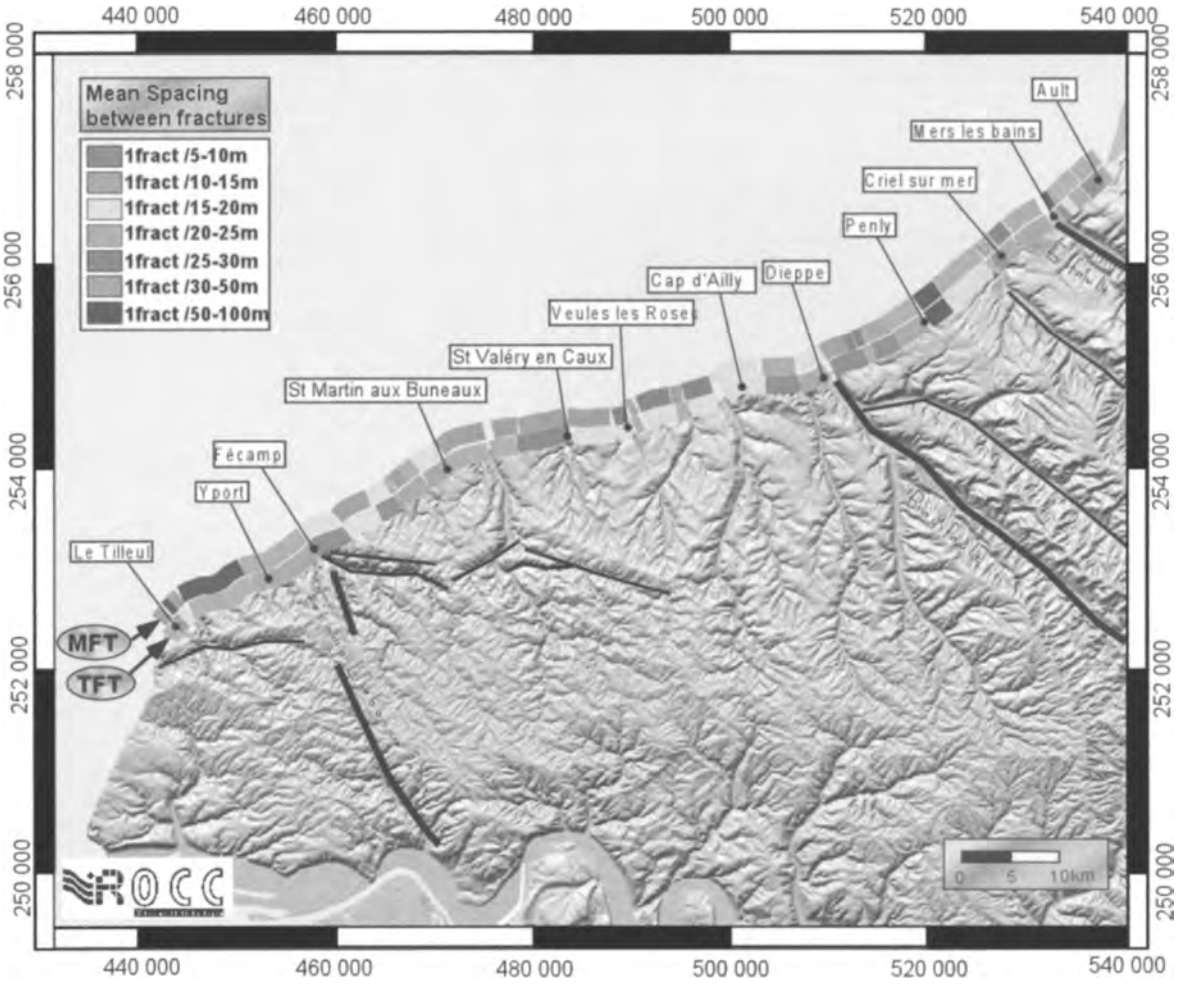

Fig. 8. Fracture density based on aerial photos, between Le Tilleul and Ault on the chalk coastline of NW France. TFT (Total Fracture Types) strip: mean fracture spacing in each coastal sectors for all the fracture types. MFT (Main Fracture Types) strip: mean fracture spacing in each coastal sectors for large-scale fractures only.

corresponds mainly to large-scale normal faults oriented N120E, checked in the field. The MFT strip shows moderate fracture content around the Bray fault. Near the Fécamp–Lillebonne fault, the MFT strip reveals very low fracture content as well as between St Martin aux Buneaux and Veules-les-Roses.

From the MFT strip, here appear to be two main domains of fracture content. Northward from the Bray fault, the high fracture density due to normal faults is indicative of a high tectonic paleo-activity, whereas southward from the Bray fault, the fracture density is lower, suggesting that normal faulting is not so well developed. At larger scale, the tectonic activity of the Bray and Eu faults is better expressed topographically by rectilinear and sharp lineaments than the Fécamp-Lillebonne fault, which shows a curved and smooth topographic signature (Fig. 8).

Pre 1986 collapse data analysis on aerial photos

Methodology

Within the 63 sections derived from the fracture analysis, the size of the collapse process was evaluated from the aerial photo interpretation. Several parameters related to the pre-1986 collapses visible in 1986 were collected or calculated:

(1) the total number of pre-1986 collapses per section (PC);
(2) the cumulative scar length (CSL) along the cliff face in each section of a given length;
(3) the percentage of pre-1986 collapsed cliff surface (PCS), which is the ratio between the cumulative scar length (CSL) divided by the length (L) of the given section;
(4) the percentage of normalized pre-1986 collapsed cliff surface, which is the ratio between PCS and the total number of pre-1986 collapse in a given section (NPCS). This ratio is given by:

$$NPCS = (CSL/L)/(PC) = PCS/PC$$

For example, in a given cliff section length, high PCS values could be interpreted as a series of small scars or an isolated huge scar representing an equivalent scar length. Low PCS values could represent the same scar population (a lot of small scars or a huge scar) but it occurs in a larger cliff section. By taking into account the percentage of cumulative collapse length per section, we calculated a normalized parameter NPCS which is not dependent of the number of collapse. For example, high NPCS values mean a cliff section with a significant tendency for collapsing whatever the number of collapse. This parameter represents a kind of collapse intensity normalized on the scar length.

Number of pre-1986 collapses per section (PC)

300 ancient collapses have been recorded from the aerial survey conducted in 1986 (Fig. 9). The average value per section is close to 7 pre-1986 collapses, with a maximum of 27 and two minima of zero. The areas with no collapse correspond to the valleys, with no significant cliff. The map of PC shows three sections with the highest concentrations of collapses, which are located southward of Criel sur Mer, westward of St Valéry-en-Caux and southward of Vaucottes, with the maximum PC southward of Criel sur Mer, between Val Pollet and Penly. The two minima are located north of St Pierre-en-Port valley and north of Dieppe up to Puys in a 50 m height cliff. The sections with high to moderate collapse concentrations do not show a preferential distribution. The PC is not related to the well-known regional faults. There is no significant concentration of ancient collapses in the vicinity of the Eu, Bray and Fécamp-Lillebonne faults (Fig. 9). On the contrary, the highest PC values are located far away from the regional faults. The number of collapses is therefore not directly related to the paleo-tectonic activity.

Percentage of pre-1986 collapsed cliff surface per section (PCS)

By ignoring the valleys, the average value of the PCS rate is 21%. The map of PCS shows three main areas, from SW to NE (Fig. 9): (1) the highest PCS values are located between Le Tilleul and Veules-les-Roses, with the maximum value (66%) located south to Fécamp; (2) the lowest PCS rates are located between Veules-les-Roses and Dieppe; and (3) north of Dieppe, PCS rates are intermediate.

The PCS is not systematically related to the location of regional faults. For the Bray and the Eu faults, there is no spatial correlation, whereas for the Fécamp–Lillebonne fault, the PCS value is rather high. The low PCS values are located far away from the regional faults.

Percentage of normalized pre-1986 collapsed cliff surface per section (NPCS)

The average value of NPCS rates is about 5%. By normalising the PCS, extreme values are reinforced and minima and maxima alternate spatially (Fig. 9). Three maxima located at Fécamp, Dieppe and Mers-les-Bains are clearly identified. The minima are located south of Yport, between St Martin aux Buneaux and Dieppe, and from Puys to Criel sur Mer.

The high NPCS values mimic the regional fault locations, whereas the low NPCS values are located far from the regional faults. The NPCS rate is the most relevant parameter for characterizing the ancient collapse intensity, because it takes into account the collapse size effect (small to large size-scar), the section dimension (horizontal length) and the number of events (i.e. number of ancient collapses).

Several points arise from this part of the study. TFT spacing distribution and NPCS values are both spatially correlated with the location of the regional faults. Fractures visible in the cliff and ancient collapses are also correlated for the maximum values. This correlation is not well constrained for the minimum and intermediate values. For example, between Dieppe and Veules-les-Roses, the NPCS values are very low whereas the TFT values are moderate. By

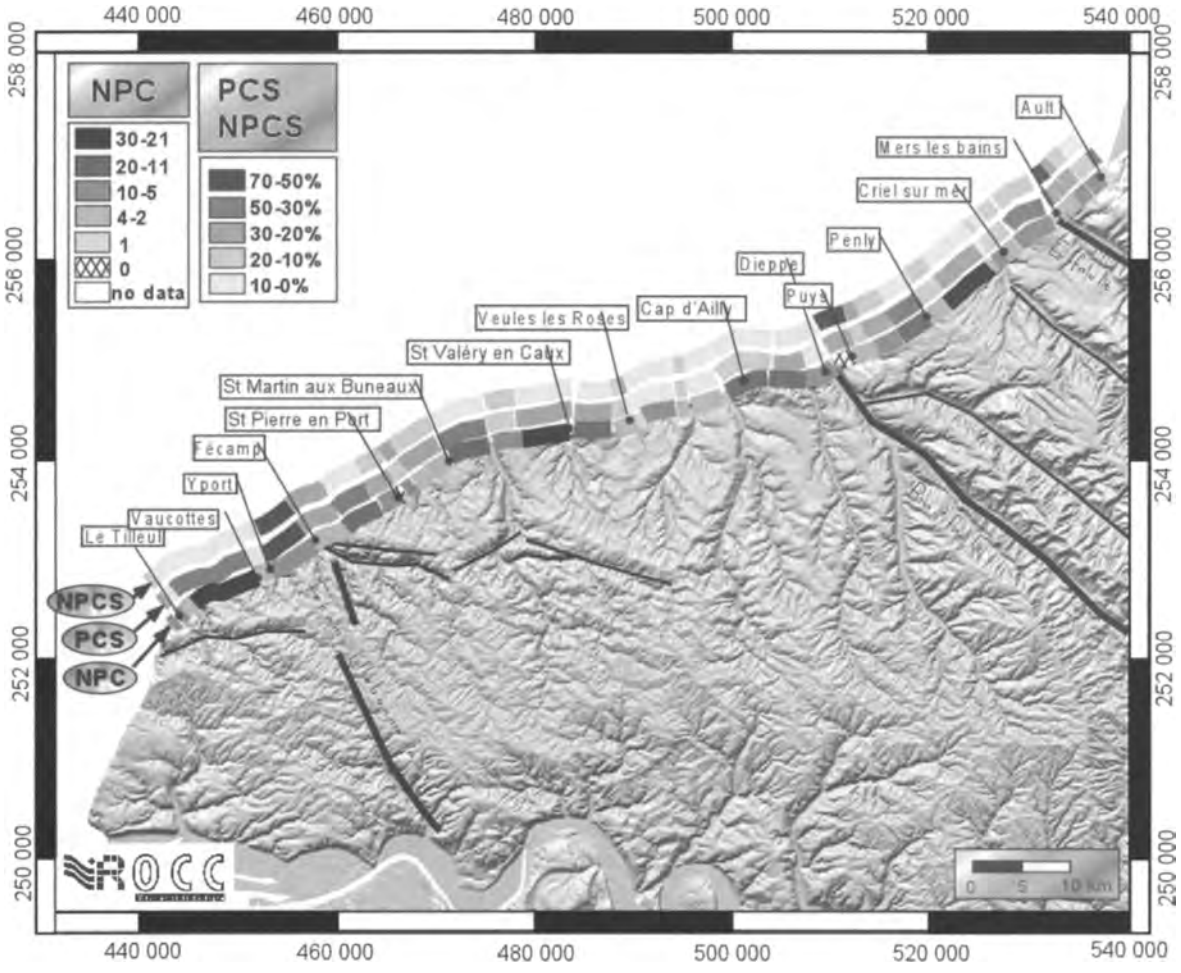

Fig. 9. Map of pre-1986 collapse data recorded in 1986 from aerial photographs, between Le Tilleul and Ault on the chalk coastline of NW France. NPC, Number of pre-1986 Collapse, in each coastal sector. PCS, Percentage of pre-1986 Collapsed Cliff Surface, per section. NPCS, Percentage of Normalized Pre-1986 Collapsed Cliff Surface, per section.

considering only the large-scale fractures (MFT), the spatial correlation between pre-1986 collapses and fractures is less clear than for the whole fracture population (MFT). At a regional scale, the pre-1986 collapse distribution derived from aerial photos and the whole fracture distribution is spatially correlated to the regional faults of Fécamp–Lillebonne, Bray and Eu.

Recent collapses analysed from field observation

Between 1998 and 2001, a minimum of 55 cliff collapses of various size has been recorded along the coastline of Upper-Normandy and Picardy (Fig. 10). About 75% of them correspond to large-scale collapses, which affect the whole cliff height. 70% of the recent collapses occurred in 2001 and are mainly interpreted as a consequence of high rainfall (Duperret *et al.* 2004). Recent collapses are not equally spaced along the coastline, some areas with high concentrations alternating with areas of low concentrations creating a clustered distribution pattern. Between Veules-les-Roses and cap d'Ailly, many collapses have been observed (mainly small-scale failures). However, the sampling of collapse data was unequal because it was not possible to record continuously the entire coastline. It is for this reason there are a lot of small-scale collapses between Veules-les-Roses and cap d'Ailly, this section being fully surveyed in the field. This is also the reason why only larger collapses are recorded everywhere else, whereas the small ones are missing.

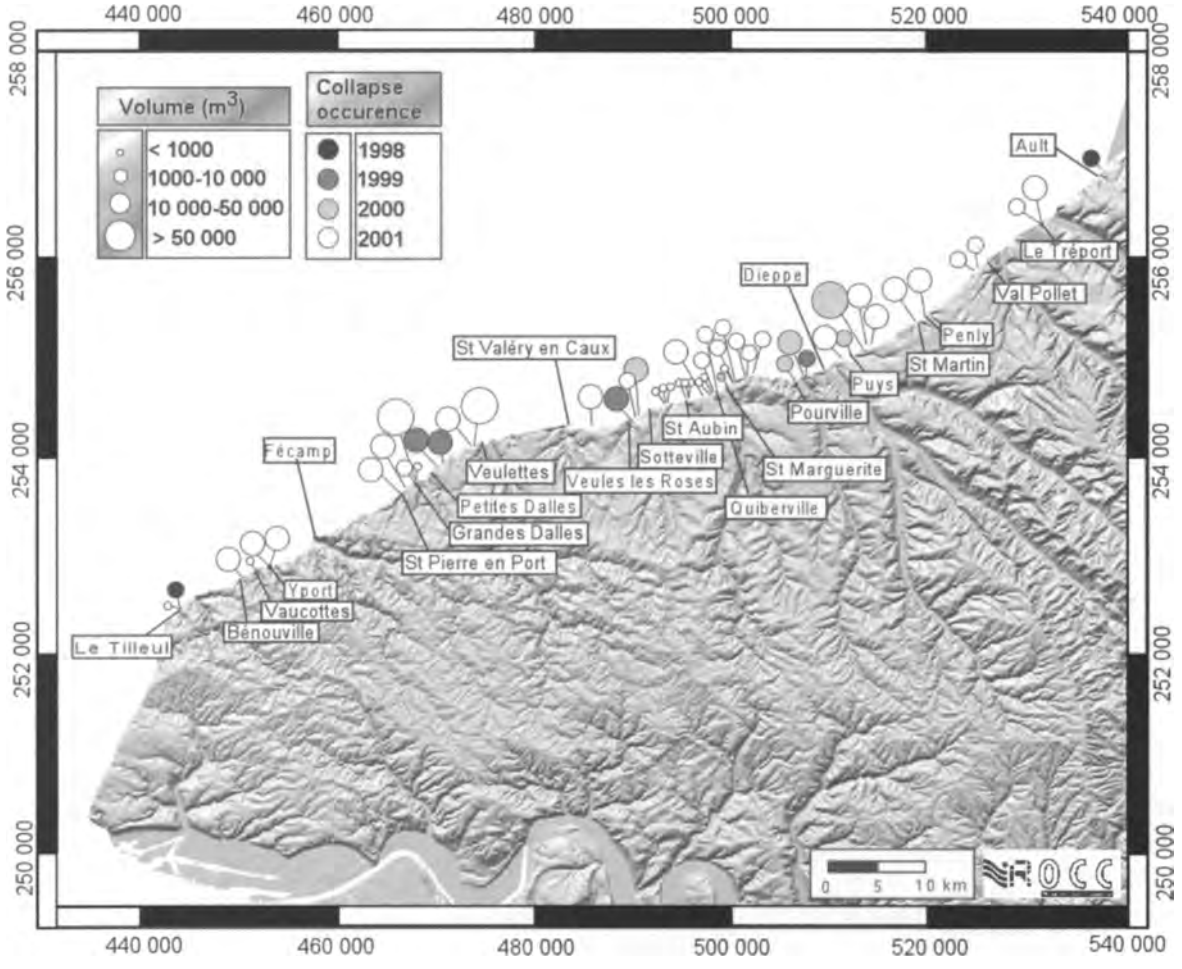

Fig. 10. Location of recent collapses recorded on the field between October 1998 and December 2001. The size of the circles is proportional to the size of the collapse. The grey scale within the circles indicates the year of collapse occurrence.

In order to evaluate the role of the pre-existing fractures on recent collapse location, the fracture content controlling or not the scar collapse, as well as those embedded within the scar, has been analysed. Based on the recent collapse database, field observations show that 40% of the collapses are not bounded laterally by pre-existing fractures, 55% are bounded by at least one fracture and 5% are bounded by two fractures. 58% of the recent collapses show no significant pre-existing fractures within the scar. Stress release fractures could exist but they were not observed. An example of a recent collapse limited by a pre-existing fracture is presented in Figure 11. As the fractures observed within the collapse are generally transverse fractures relatively orthogonal to the cliff face, we assume that they do not create the collapse trigger. They could represent either mechanical barrier by halting the lateral progression of failure scar or behave as a passive mechanical structure when they are developed inside a given scar.

The number of collapses observed on the cliff face in 1986 is six times higher than those observed during the three-year period 1999–2001. However, between St Aubin sur Mer and Quiberville, recent collapses are more numerous but they mainly correspond to small-scale collapses (Fig. 12). As this section was better sampled during the field survey, this result is not significant in terms of degree of erosion. In the other sections, small-scale collapse inventories were underestimated as well as the related degree of erosion. Actually, the collapses reported in 1986 correspond to the footprints of successive collapse events visible as scars on our photograph that may have occurred a few years before the observation, whereas collapses reported between 1998 and 2001 are better constrained in terms of time of occurrence. There is conse-

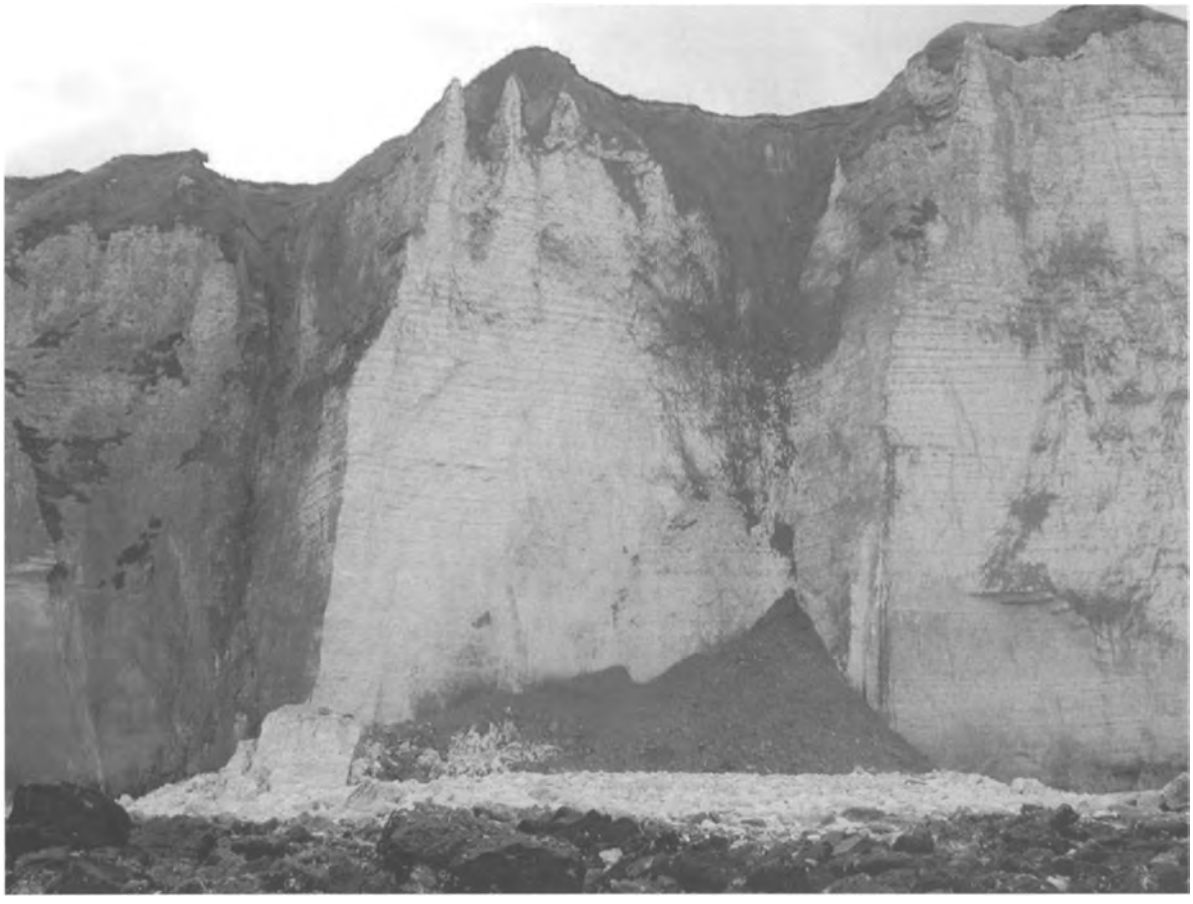

Fig. 11. Example of recent collapse at St Pierre en Port, that occurred on 15 March 2001, showing a scar bounded laterally by a pre-existing vertical fracture. The total cliff height is about 90 m.

quently a significant uncertainty for the real timing of occurrence for collapses identified on the aerial photos taken in 1986. Those photos probably contain some collapse marks, which occurred several years before 1986, increasing the pre-1986 collapse number. The coastal sections having a higher number of collapses in 1986 do not match with those defined between 1998 and 2001. For example, between Fécamp and Eletot, no collapse is observed between 1998 and 2001, whereas about 20 collapses are recorded from the 1986 aerial photographs.

The comparison between the two survey periods suggests a different spatial evolution of collapse events along the coast. The areas active in 1986 are not exactly the same as those observed in 1998–2001. The results suggest that the erosion by collapse is not continuous in space and time, but occurs suddenly at different locations and at different time periods. The absence of long-term observations reduces the accuracy of conclusions that can be drawn from this study.

Discussion

The erosion of the coastal chalk cliffs of Upper-Normandy and Picardy is mainly controlled by collapses of various sizes. From Le Tilleul to Ault, the coastline is made of three large-scale linear segments oriented N60E (from Le Tilleul to Veulettes sur Mer), N80E (from Veulettes sur Mer to Dieppe) and N50E (from Dieppe to Ault) (Fig. 13). The N60E and N50E coastal segments present the same chalk succession, whereas the N80E segment is completely different from a lithological point of view (Duperret *et al.* 2004). As the dominating fracture set observed both from regional scale, aerial photos and field observations is oriented normally to the coastline, the coast is not directly controlled by this regional fracture orientation. A secondary fracture set roughly parallel to the coastline has been observed, but only locally, and does not seem to influence the coastline orientation. Therefore, as field observation shows, the chalk cliffs

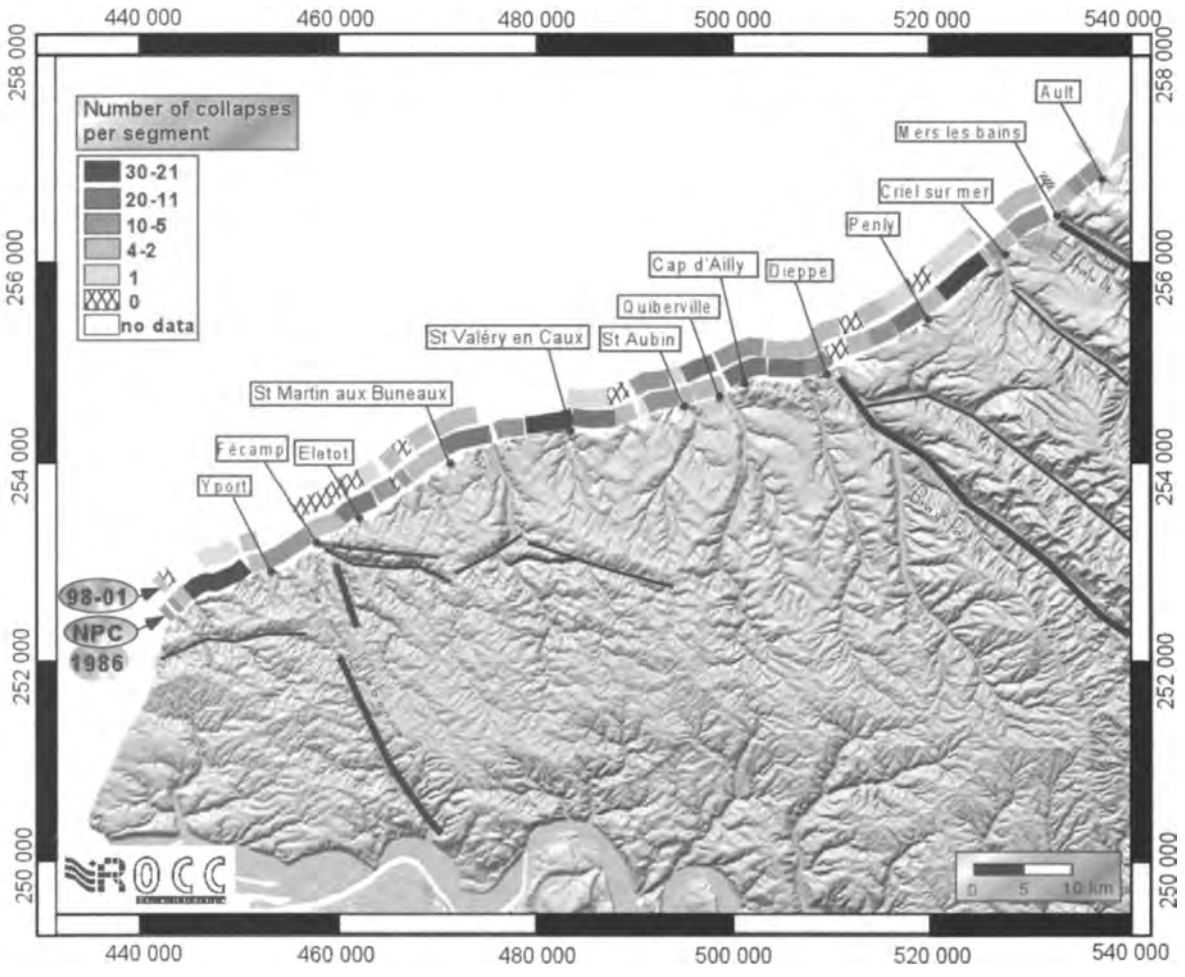

Fig. 12. Comparison between the number of pre-1986 Collapses (NPC) observed in 1986 on aerial photos and the number of collapses observed on the field between 1998 and 2001.

are not affected by a systematic fracture set parallel to the coastline and the observed collapses are not directly linked to this fracture orientation. However, we infer that stress release fractures newly created and parallel to the cliff face could be a control on some collapse mechanisms. The fractures orthogonal to the coastline are dominant, but their orientation does not tend to favour a cliff collapse, from a geometrical point of view. A part of these fractures may limit the lateral extension of the collapse on the cliff face, by forming mechanical barriers.

The erosion of the coastal chalk cliffs could be also derived from the whole fracture density. The fracture density is heterogeneously distributed along the coastline, the maxima being linked to the regional faults. As the fracture density correlates better to areas with more pre-1986 collapses than the large-scale fracture density, this suggests that the full ranges of fracture sizes are involved in the collapse process. The impact of the fracture density on the cliff collapses can be deciphered by analysing the coastal orientation in relation with the fracture content. Coastal segments with the higher fracture density are mainly oriented N60E (around the Fécamp–Lillebonne fault) and N50E (northward of the Bray fault). In that case, the coastline is roughly perpendicular to the main fracture orientation. Coastal segments with a low fracture density are mainly oriented N80E (between Veulettes sur Mer and Dieppe). In that case, there is no dominating fracture set and the orientation of the coastline could be controlled mainly by the chalk lithology (Fig. 13).

In spite of the uncertainties related to the collapse data acquisition, both from aerial photos and field measurements, the collapse datasets (1986, 1998–2001) show different responses along the coastline. The pre-1986 collapses are

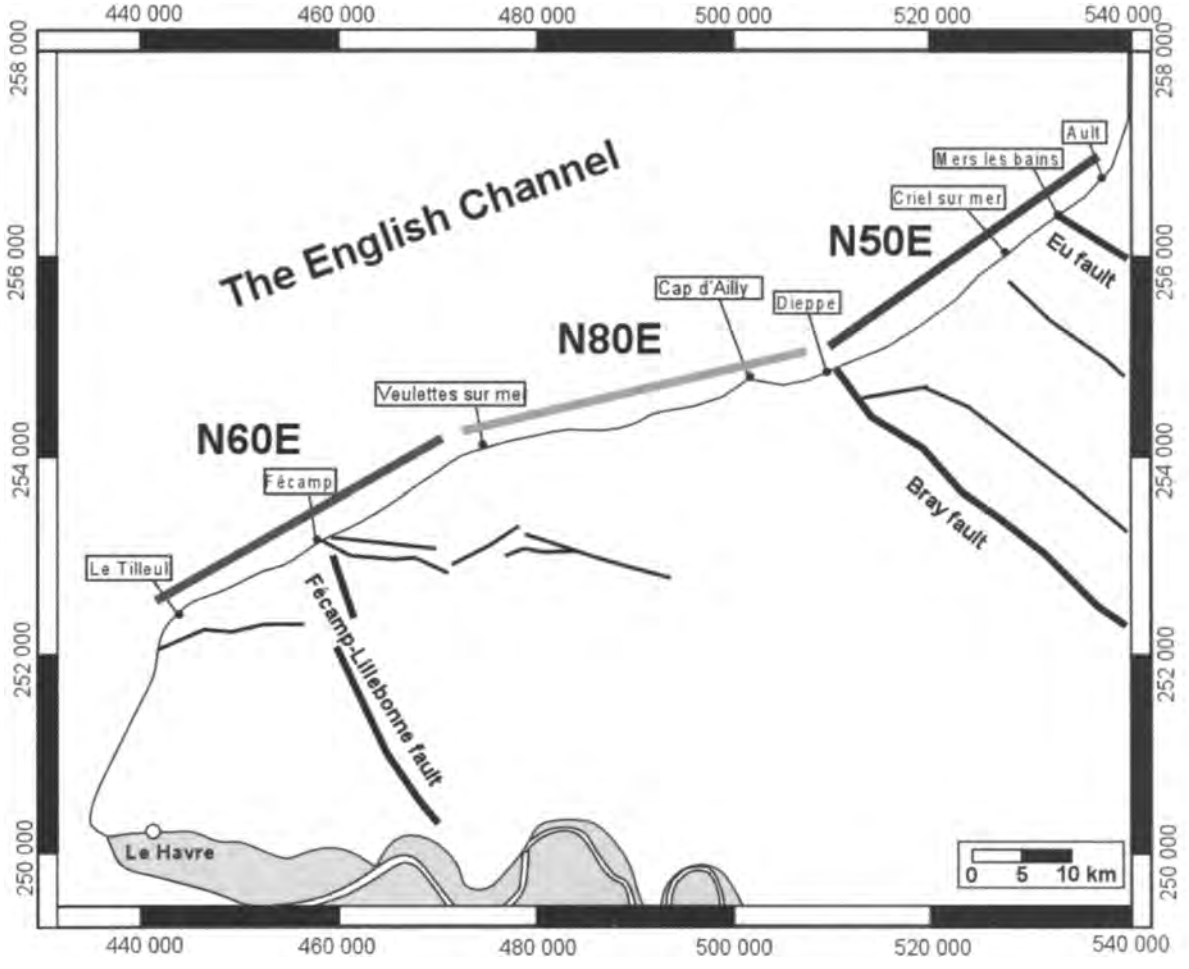

Fig. 13. Schematic sketch of the coastline orientation versus regional faults in upper Normandy and Picardy.

correlated with the regional fault location and the fracture content, whereas the recent collapses do not show the same spatial relationship with fracture content. We thus suppose that this discrepancy is due to the superimposition of some other parameters (rainfall, marine erosion, ...) or to the recent collapse sampling period, which is probably too short in relation to the long-term erosion process. The coastal erosion by collapse is difficult to measure on short-term periods (for example, three years) because cliff collapses are spatially and temporally variable and discontinuous.

The role of fractures on collapse occurrence is determined by means of observations conducted over two time periods and a multiscale fracture analysis. Some fracture characteristics (filling, aperture, rugosity, channelling) have not been investigated which could influence collapse characteristics (location, size, triggering effect). For instance, according to the nature of the fracture filling (impermeable clays, karstic network), a fracture could be well drained or undrained and consequently could influence collapse mechanism.

Conclusion

Multiscale fracture analysis, based on field survey and aerial photograph interpretation, was used to investigate erosion by cliff collapse of the Upper Cretaceous Chalk coastline of NW France. The field survey provided a control on observations derived from aerial photographs and provided a more detailed fracture and collapse data not obtainable from aerial photographs. The coastline is divided into 63 sections derived from fracture analyses within which cliff collapse processes have been evaluated. A new method of delineating the extent of cliff erosion within sections of cliff is based on total number of collapses (PC), cumulative cliff failure scar

width, percentage of pre-1986 collapsed cliff surface (PCS) and on percentage of normalized pre-1986 collapsed cliff surface (NPCS). The NPCS in particular helps identify where maxima and minima in cliff collapse erosion are located. In addition, the results of applying the NPCS to the 120 km of coastline illustrate the importance of major structural features (the major faults at Fécamp, Bray and Eu) in the location of maxima and minima. At a local scale, in contrast to the aerial photograph analyses, the field study of recent collapses suggests no systematic correlation of cliff collapse and fracture occurrence.

Fracture evaluation shows that the dominating fracture set is N120E and this corresponds mainly to normal faults roughly perpendicular to the coastline orientation. Several secondary fracture sets have been identified one of which is locally parallel to the coastline. Field observations have shown three relationships between fractures and the scars left by cliff collapses: (i) fractures limit the scar laterally; (ii) fractures are located only within the scar; (iii) no pre-existing fractures are involved in the scar.

The study also illustrates the differences in location, frequency and structural interpretation of cliff collapses between two periods of observation (pre-1986 and 1998–2001) and the need, therefore, for a long and detailed historical record of cliff collapses before final conclusions can be drawn about the mechanisms, frequency, location and size of cliff collapses.

Acknowledgements. The ROCC project was funded by the European community through the INTERREG II Rives-Manche community initiative (contract I99059). This research work has also been partly funded by the Centre National de la Recherche Scientifique in the framework of Programme National des Risques Naturels, through the contract PNRN 99-35-AS, by the Regional Council of Somme, the French Geological Survey (BRGM) and the University of Brighton. We thank the Maritime Direction Départementale de l'Equipement at Dieppe for providing us with oblique aerial photographs of the French coastline. The authors thank W. Murphy for a very helpful review.

References

COSTA, S. 2000. Le recul des falaises du pays de Caux. *Bulletin d'Information des Géologues du Bassin de Paris*, **37**, n°1, 31–34.

DIKAU, R., BRUNSDEN, D., SCHROTT, L. & IBSEN, M-L. 1996. *Landslide Recognition, Identification, Movement and Causes*. International Association of Geomorphologists, Wiley.

DORNBUSCH, U., WILLIAMS, R. B. G., ROBINSON, D. A. & MOSES, C. 2001. Disappearing act: Contribution of cliff erosion and in situ abrasion of flint to the shingle budget on the East Sussex coast, *European Rock Coasts 2001 Conference, Brighton, UK, 17–18 December 2001*.

DUPERRET, A., GENTER, A., MORTIMORE, R. N., DELACOURT, B. & DE POMERAI, M. 2002. Coastal rock cliff erosion by collapse at Puys, France: the role of impervious marl seams within chalk of NW Europe. *Journal of Coastal Research*, **18**, n°1, 52–61.

DUPERRET, A., GENTER, A., MARTINEZ, A. & MORTIMORE, R. N. 2004. Coastal chalk cliff instability in NW France: the role of lithology, fracture pattern and rainfall. *In*: MORTIMORE, R. N. & DUPERRET, A. (eds) *Coastal Chalk Cliff Stability*. Geological Society, London, Engineering Geology, Special Publications, **20**, 33–55.

HIBSCH, C., CUSHING, M., CABRERA, J., MERCIER, J., PRASIL, P. & JARRIGE, J-J. 1993. Palaeo-stress evolution in Great Britain from Permian to Cenozoic: a microtectonic approach to the geodynamic evolution of the southern UK. Basins. *Bull. Cent. Rech. Explor. Prod. Elf Aquitaine*, **17 (2)**, 303–330.

HIBSCH, C., JARRIGE, J-J, CUSHING, E. M. & MERCIER, J. 1995. Palaeostress analysis, a contribution to the understanding and geodynamic evolution: Example of the Permian/Cenozoic tectonics in Great Britain and geodynamic implications in western Europe. *Tectonophysics*, **252**, 103–136.

MAY, V. J. 1971. The retreat of chalk cliffs. *Geographical Journal*, **137**, 203–206.

MORTIMORE, R. N. 1983. The stratigraphy and sedimentation of the Turonian-Campanian in the Southern Province of England. *Zittelania*, **10**, 27–41.

MORTIMORE, R. N. 1986. Stratigraphy of the Upper Cretaceous White chalk of Sussex. *Proceedings of the Geologists' Association*, **97**, 97–131.

MORTIMORE, R. N. & POMEROL, B. 1987. Correlation of the Upper Cretaceous White chalk (Turonian to Campanian) in the Anglo-Paris Basin. *Proceedings of the Geologists' Association*, **98**, 97–143.

MORTIMORE, R. N., POMEROL, B. & FOORD, R. J. 1990. Engineering stratigraphy and palaeogeography for the chalk of the Anglo-Paris Basin. *In*: Chalk. Thomas Telford, London.

MORTIMORE, R. N., LAWRENCE, J., POPE, D., DUPERRET, A. & GENTER, A. 2004. Coastal cliff geohazards in weak rock: the UK Chalk cliffs of Sussex. *In*: MORTIMORE R. N. & DUPERRET, A. (eds.) *Coastal Chalk Cliff Stability*. Geological Society, London, Engineering Geology, Special Publications, **20**, 3–31.

RODET, J. 1992. La craie et ses karsts, CNEK. Centre Normand d'Etude du karst et des cavités du sous-sol. Elbeuf, France.

VANDYCKE, S. 1992. *Tectonique cassante et paléo-contraintes dans les formations crétacées du Nord-Ouest européen. Implications géodynamiques.* Thèse de l'Université de Paris VI.

VANDYCKE, S. & BERGERAT, F. 1992. Tectonique de failles et paléo-contraintes dans les formations crétacées du Boulonnais (France). Implications géodynamiques. *Bull. Soc. Géol. France*, **163**, n°5, 553–560.

VILA, J. L. 2000. *Étude du littoral cauchois: méthode descriptive des falaises côtières à partir des photos aériennes obliques dans l'optique de l'évaluation de leur sensibilité à l'érosion*. Rapport de DESS, Télédétection, méthodes, application, environnement. Université Pierre et Marie Curie, Paris.

Geological Society, London, Engineering Geology Special Publications

Chalk physical properties and cliff instability

R. N. Mortimore, K. J. Stone, J. Lawrence and A. Duperret

Geological Society, London, Engineering Geology Special Publications 2004; v. 20; p. 75-88
doi:10.1144/GSL.ENG.2004.020.01.05

Chalk physical properties and cliff instability

R. N. Mortimore[1], K. J. Stone[1], J. Lawrence[1] & A. Duperret[2]

[1] Applied Geology Research Unit, School of the Environment, University of Brighton, Moulsecoomb, Brighton BN2 4GJ, UK

[2] Laboratoire de Mécanique, Faculté des Sciences et Techniques, Université du Havre, 25 rue Phillipe Lebon, BP 540, 76058 Le Havre cedex, France

Abstract: Physical properties such as porosity and intact dry density (IDD) are compared with strength testing in relation to the Chalk formations in the cliffs of the English Channel. Natural moisture contents are close to saturation moisture contents for chalks with intact dry densities above 1.70 Mg/m^3. Below this IDD, the natural moisture contents show a much greater range and greater divergence from the saturation line. There is also an indication that certain types of chalk retain water at saturation level while others gain and lose water more readily. Strength tests (Point Load Index, Brazilian Crushing Strength and Uniaxial Compressive Strengths) show up to four times reductions in strength between dry (higher strength) and saturated (lower strength) samples. Absence of a strong correlation between density and strength is interpreted as resulting from either mineralogical differences in the samples and/or textural differences between different chalks. The variation in physical properties and strength in the different chalks forming the cliffs indicates the strong stratigraphical and sedimentological controls on mechanical performance of the material and mass in cliff failures.

Introduction

Physical properties, particularly density and porosity, have been used to classify chalk and provide an index of potential mechanical performance since the 1950s (e.g. Meigh & Early 1957; Carter & Mallard 1974; Fig. 1). Despite the doubt about the reliability of physical properties (e.g. Lamont-Black & Mortimore 1996), density is still the simplest way of characterizing the intact material (Warren & Mortimore 2002). Often considered to be homogeneous, the variation in physical properties even within a single block of intact chalk illustrates the complexity of the sediment, related to sedimentation, bioturbation and sea-bed diagenesis. Unless a sample is adequately described in terms of these sedimentary and diagenetic variations, few conclusions can be drawn about the variability in physical properties (e.g. Fig. 2).

There has been considerable debate about the validity of strength/density terms for the engineering description of chalk. Should density be related to chalk hardness or to chalk strength? Bowden *et al.* (2002) found that the standard strength categories used to describe rocks for engineering purposes (BS 5930: 1981, 1999) could not be applied readily to chalk and concluded that an independent chalk hardness scale was more appropriate. The results of the investigations reported herein are related to a hardness scale based on common agreement amongst many authors (Fig. 1) as well as observations on the mechanical behaviour of different chalks. The CIRIA density scale (Lord *et al.* 1994, 2002) is developed primarily for foundation design, for the confined compressive deformation of chalk and for chalk earthworks classification. With respect to chalk cliff instability, the number of density divisions required to characterize types and scales of failures may be greater (Fig. 3), but this is still being investigated.

Density and moisture contents

To test the typical range of variation in Intact Dry Density (IDD) and Natural Moisture Content (NMC) of white chalks, samples were obtained from the cliffs of Sussex and local quarries (Fig. 3; Mortimore & Fielding 1990). Natural moisture contents were measured by drying and loss of weight (BS 1377) within a few hours of sample collection (in sealed bags) to reduce moisture loss prior to testing. IDD was measured by wax-coated Archimedes displacement (BS 1377), and selected samples checked by the measurement of volume and weight of well-prepared cores (e.g. Lamont-Black & Mortimore 1996).

The results of the IDD and NMC investigations (Fig. 3) reveal several aspects of the physical properties of chalk, some of which influence the collapse of chalk cliffs.

Firstly, within any sample set from a particular locality or stratigraphic level there is a significant range of results. Some of this variation is related to the layering of the chalk. For example, within the Seaford Head East and Downend data sets, the high-density chalks (>1.95 Mg/m^3) were sampled from nodular chalk beds and hardgrounds (resulting from synsedimentary sea-floor hardening). Hard chalks (1.8–1.95 Mg/m^3) from Juggs Lane and Downend tended to be sponge nodular chalk beds. In other cases the hard and medium hard chalks included apparently pure white beds which were made of a particular type of calcareous nannofossil or beds of chalk exhibiting a greater degree of cementation than softer chalk beds (Mortimore & Fielding 1990).

From: MORTIMORE, R. N. & DUPERRET, A. (eds) 2004. *Coastal Chalk Cliff Instability*. Geological Society, London, Engineering Geology Special Publications, **20**, 75–88. 0267-9914/04/$15.00

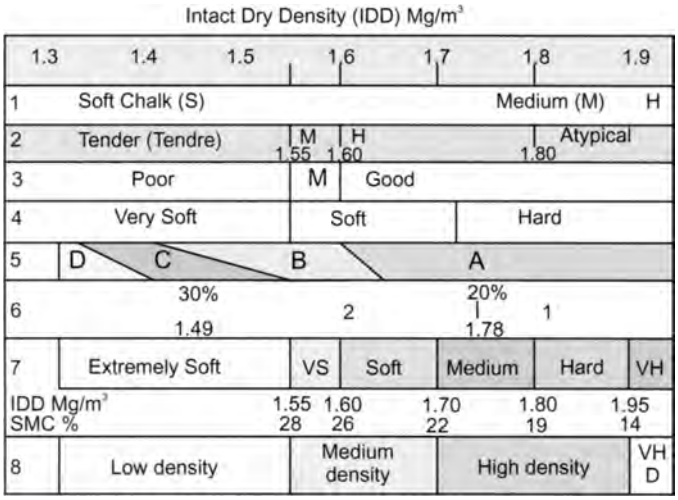

Fig. 1. Classifications used for chalk based on intact dry density (IDD) or saturation moisture content (SMC). 1. Lewis & Croney (1966); 2. Masson (1973); 3. Jenner & Burfitt (1975); 4. Clarke (1977); 5. Ingoldby & Parons (1977); 6. DTp Specifications (1986); 7. Mortimore & Fielding (1990); 8. CIRIA Lord *et al.* (2002).

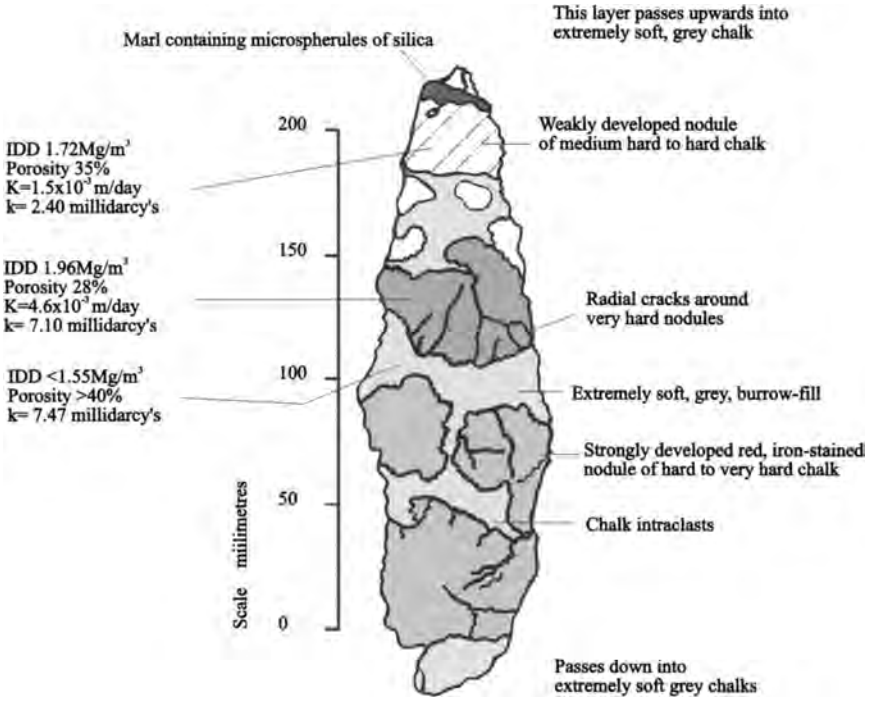

Fig. 2. Cut-slab of nodular chalk (sample N7, Beeding Hardgrounds, Shoreham Cement Works, Sussex) showing variation in hardness and porosity. K = Hydraulic conductivity (pure water at 10°C m/day); k = Intrinsic premeability to a non-reactive liquid; IDD = Intact Dry Density. (Modified from Mortimore 1979; Mortimore & Pomerol 1998).

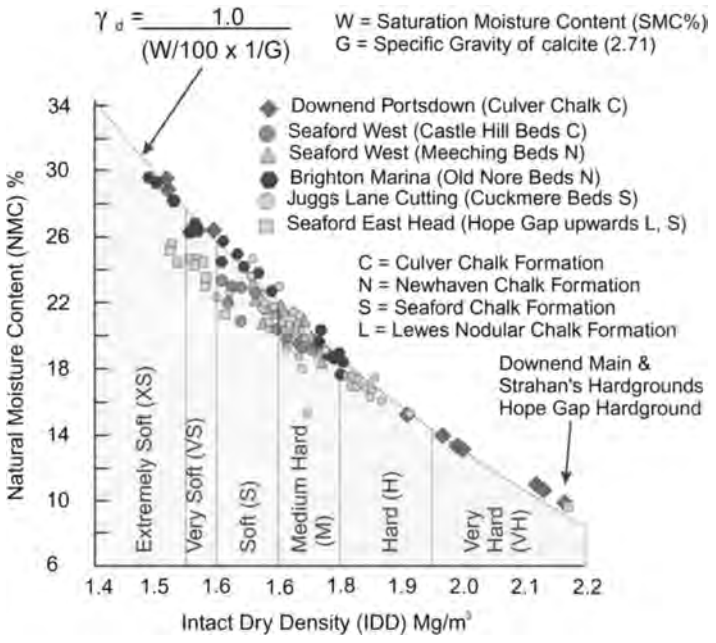

Fig. 3. Moisture contents of naturally occurring chalks from cliffs and quarry faces plotted onto the Intact Dry Density (IDD) – Saturation Moisture Conent (SMC) line (modified from Mortimore & Fielding 1990).

Chalk, whether it is a marly chalk formation at the base of the succession or a younger pure white chalk formation, exhibits a cyclostratigraphy of alternating couplets (the A and B divisions of a single bed of chalk, Mortimore 1986). This sedimentary structure will inevitably result in a continuous cyclostratigraphic variation in density/ porosity.

Secondly, the softer lower density chalks tend to show the greatest deviation from the Saturation Moisture Content (SMC) – IDD line, suggesting that these chalks can probably gain and lose water more easily than other types of chalk. An exception to this general trend is seen in the set of results from Brighton Marina (the Old Nore Beds of the Newhaven Chalk Formation). This may be related to the texture and fabric of the Old Nore Beds in terms of pore size, pore throat diameters and degree of cementation at grain contacts compared with, for example, Seaford Chalk samples of the same density. Variation in these aspects of chalk texture (Mortimore 1979; Mortimore & Fielding 1990) may influence the rate and amount of loss or gain of moisture in chalks exposed to weathering in cliff faces. IDD, texture and degree of saturation also affect the strength of the material (see below), the failure mechanism and probably the behaviour of failing material (debris mobility) in a cliff collapse.

Strength tests

Many tests have been performed on chalk in an attempt to establish a range of strength related to a particular value or category of density, porosity and field description (e.g. Mortimore 1979; Mortimore & Fielding 1990; Matthews & Clayton 1993; Bowden *et al.* 1998, 2002; Lord *et al.* 2002). As part of the investigation of chalk cliff collapses the index strength tests of intact chalk material are reviewed.

Point Load Test (PLT)

The Point Load Test (PLT) is used as an industry standard index of strength of rock (e.g. Norbury 1986). Bowden *et al.* (1998) evaluated the Point Load Test for chalk (testing intact chalk at natural moisture contents). Bowden *et al.* (1998) found that axial tests gave more consistent results and a better correlation with IDD than diametrical tests, suggesting bedding anisotropy influenced results and supporting the earlier observations of Mortimore & Fielding (1990). The samples tested by Bowden *et al.* (1998, fig. 2) were from the Newhaven Chalk Formation at Southwick Hill Tunnel (Fig. 4) and illustrated a scatter of values closely related to stratigraphic variation in the Chalk. These authors also noted that the K factor varied with Unconfined Compressive Strength (UCS), supporting the observation of Norbury (1986) and indicating that a standard K factor of 24 for chalk should not be used. Instead, the K factor should be related to UCS results, a conclusion that also applies to the testing of flint (Cummings 1999). In general, the range of PLT results indicates that white chalk falls in the range of 0.1 to 0.7 MPa tested at natural moisture contents (but see below).

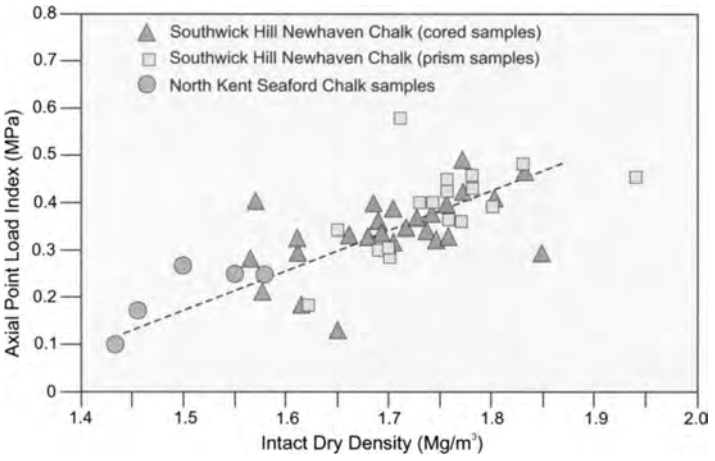

Fig. 4. Intact Dry desity compared with axial point load index (modified from Bowden *et al.* 1998).

Brazilian Crushing Strength

A problem with all chalk testing is preparation of the sample both in terms of meeting ISRM standards and performing tests at natural moisture contents. Where core is prepared either by using a rotary saw (corundum or diamond) to trim or shape samples, or where laboratory coring of blocks is used, then the moisture content is going to vary whether air flush (drying) or wet cutting or coring techniques are used. The most reliable control samples were, therefore, tested dry and saturated, the two conditions that could be adequately controlled.

There are also frequently problems in obtaining a sufficient number of cores that meet ISRM standards for PLT or UCS testing. In an attempt to overcome these problems and obtain a wider range of samples, the Brazilian Crushing Test was evaluated. This test involves splitting a disc of rock diametrically (Fig. 5). A range of size of discs and thicknesses of discs was used and these were tested dry and saturated as the two extreme conditions that could be controlled. A 38 mm diameter core was finally settled upon, and both thick and thin discs were tested. Only those results that produced a perfect diametrical split were used and tests were carried out both perpendicular and parallel to bedding. All features of the test sample were recorded before and after testing.

The results from these tests (Fig. 6) show that saturated white chalk samples, whether from thick or thin discs, rarely exceed 1 MPa and fall broadly in the same range of strength as the PLT results tested at natural moisture contents. However, many more thin discs were rejected as the samples fell apart before testing or failed in an uncontrolled manner, hence the thick disc is recommended in future testing. The correlation between Brazilian Crushing Strength and IDD is poor in the small sample set and is worse with saturated samples. The results for saturated Brazilian crushing

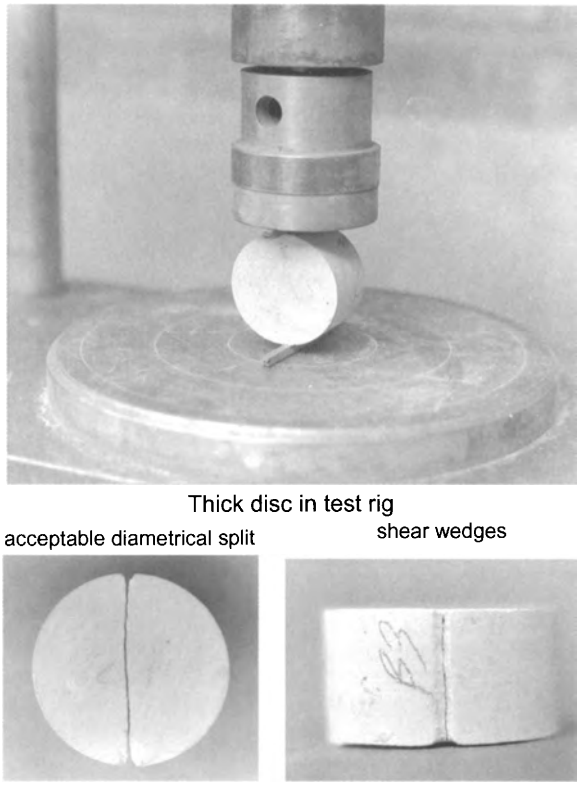

Fig. 5. The Brazilian Crushing Strength of chalk.

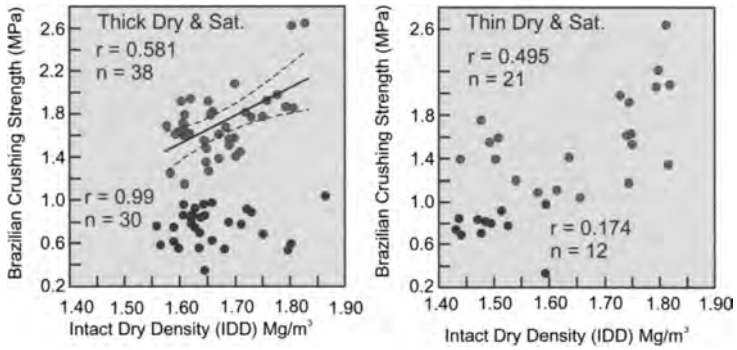

Fig. 6. The Brazilian Crushing Strength, dry and saturated, compared with intact dry density.

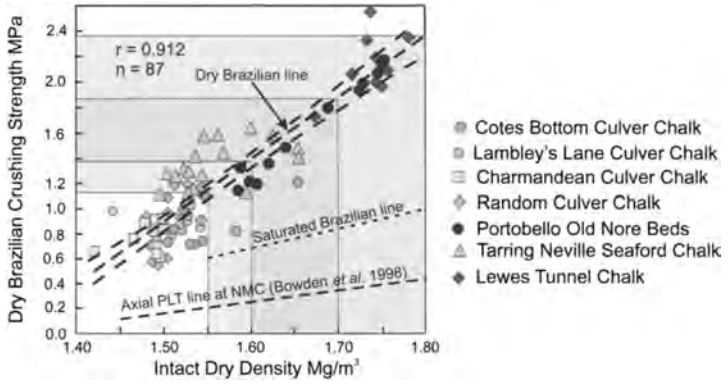

Fig. 7. Dry Brazilian Crushing Strength (thick discs) compared with Intact Dry Density for chalks from Sussex. The saturated Brazilian Crushing Strength line and the axial Point Load Test Line of Bowden *et al.* 1988 are also shown.

strengths suggest that there is up to a four times reduction in strength of chalk from dry to saturated. Some of the greatest reductions in strength are in the high density hard chalks. However, many of these hard chalks had a greater number of inhomogeneities (soft burrow-fills, cracked nodules, irregular cementation, e.g. Fig. 2) which were weakened by saturation. Hence moisture content will be a critical factor in the strength of all types of chalk involved in cliff collapses.

Further sets of samples were obtained from a wider range of sites from which, for control purposes, thick discs were prepared and tested dry. The results of these later Brazilian tests (Fig. 7) produced a better correlation with IDD and raised a number of questions. Each sample set had an individual distribution of strength in relation to density and plotted in a unique cluster about the general correlation line. This suggests that stratigraphic position (probably related to sedimentology and texture), has a profound influence on strength. Like the NMC – IDD results above (Fig. 3), the Old Nore Beds (Portobello data set) plot closest to the IDD – dry Brazilian strength correlation line, further supporting the idea that this chalk is very different mechanically to the material in the underlying Seaford Chalk Formation.

Uniaxial Compressive Strength (UCS)

Preparation of cores for UCS testing is even more difficult than samples for PLT and Brazilian tests. The numbers of samples rejected for falling outside the ISRM specifications or for failing in a non-standard manner was around 60%. Both saturated and dry samples were tested, the dry results giving the better correlation with IDD (Fig. 8). The strengths of dry UCS tests are about twice those of saturated samples (Fig. 9). These results are similar to those of Matthews & Clayton (1993). Bell *et al.* (1990) also recorded reduction in strength of chalk from dry to saturated including the generally harder, higher density varieties of chalk from Yorkshire.

A pattern of strength in relation to IDD similar to the Brazilian crushing strength emerges from the UCS results (Fig. 8). For example, the Seaford Chalk results from Tarring Neville plot on the high strength side of the correlation lines

in both the Brazilian and UCS test results whereas the Culver Chalk from Cotes Bottom plots on the low strength side of the correlation lines. An implication of this pattern is that each unit of chalk has unique intact material features that influence mechanical properties. Some of these unique features (texture) were investigated and a Texture Index developed (Mortimore & Fielding 1990).

An eight-fold difference in intact material dry strength between PLT or Brazilian strength results and the UCS results is evident.

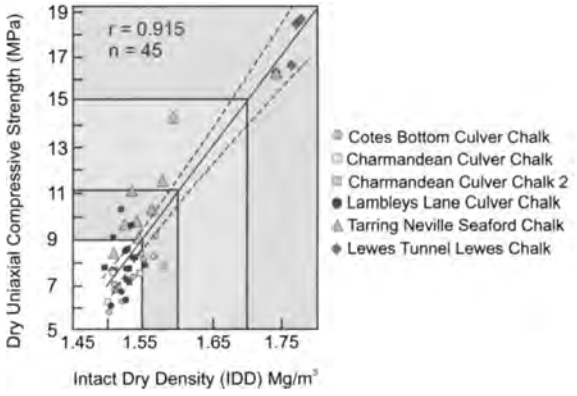

Fig. 8. Dry Uniaxial Compressive Strength compared with Intact Dry Density for intact chalks from Sussex.

Undrained Triaxial Test

Preparation of samples for the Undrained Triaxial Test proved as difficult as for UCS testing in terms of obtaining core of the required length and aspect ratio. The test requires the application of the major principal stress along the axis of the cylindrical core, and application of equal minor principal stresses to the diametrical surface of the core, through an impervious metal or rubber jacket by means of fluid confining pressure. Hence the need for careful sample preparation, particularly parallelness and flatness of ends to ensure uniform application of the stresses. Many samples were rejected for failing to meet the standard. The weaker, higher porosity chalks, tended to go out of true in the humidity of the laboratory. According to conventional Coulomb theory failure takes place in planes at $(45+\emptyset/2)$ to the major principal stress axis. Some test results support the theory but many do not, probably because the chalk is not a uniform homogeneous medium (Fig. 2). For all triaxial tests, tracing paper was wrapped around the core and details of the sample recorded prior to testing. After testing the failure planes were then recorded onto this tracing. It was found that failure planes frequently developed along pre-existing fabrics in the chalk such as wisps of marl, a vein fabric or a fossil.

Four stratigraphic levels in the Chalk were chosen for detailed analysis, covering the major units present in the cliffs. Sites for sampling were chosen where sufficient large blocks of chalk could be obtained to extract multiple cores. A summary of the results (Fig. 10) indicates a significant difference between dry and saturated samples. There is also a

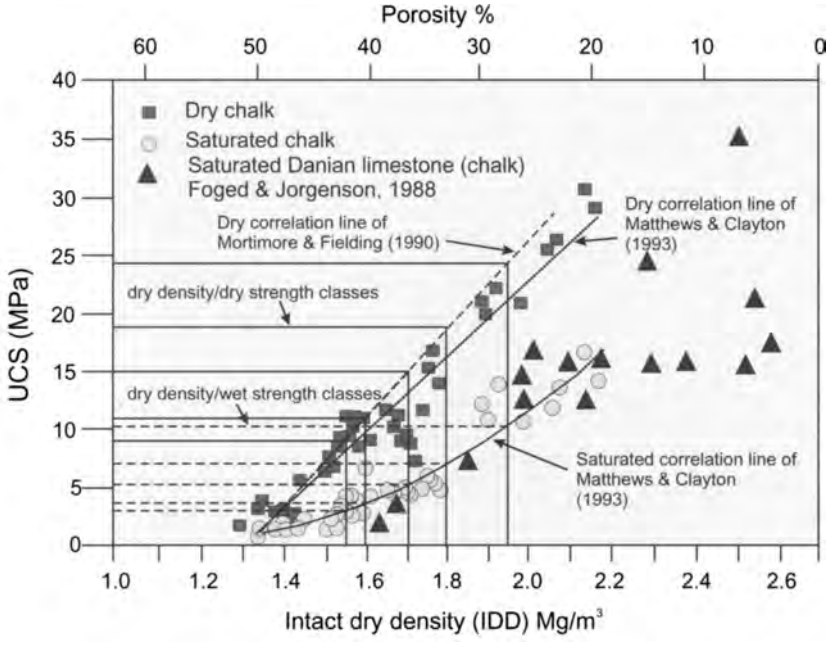

Fig. 9. Intact dry density and Uniaxial Compressive Strength (UCS) dry and saturated (modified from Matthews and Clayton 1993).

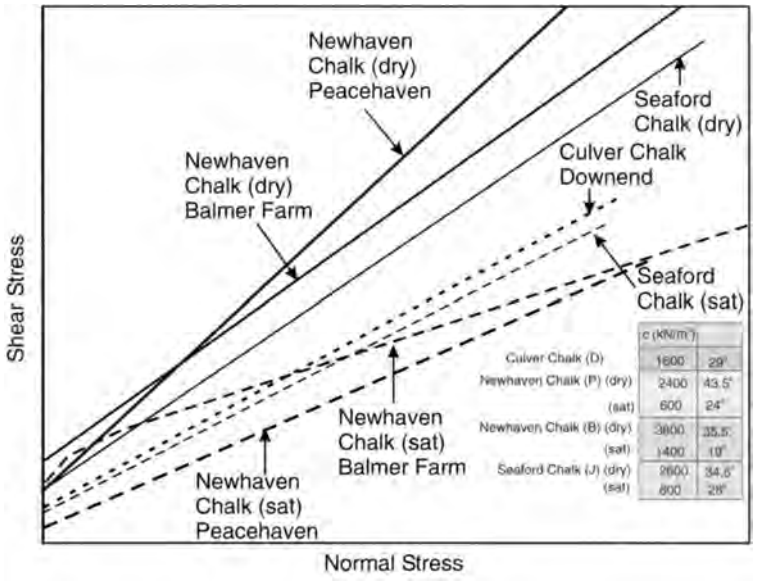

Fig. 10. Schematic overview of Mohr-Coulomb strength envelopes for different lithostratigraphic units in the Chalk.

significant correspondence within either dry or saturated strength results. Experimental error in the relatively small number of tests could be a cause of the variations. Nevertheless, it may be significant that some types of chalk (e.g. Newhaven Chalk from Peacehaven) show a greater range of variation between dry and saturated conditions than, for example, the Seaford Chalk.

During the triaxial tests variations in the brittle ductile behaviour of the different chalks and the style of failure planes was noted (Table 1).

Flint strength

Flints form an important part of much of the Chalk of the English Channel cliffs. Many modes of failure are seen to be controlled by the presence of flint bands whether as bedding layers or as fracture-fills. Flint strength may, therefore, be an important aspect of some cliff failures. Flint strength is variable and the method of measurement is crucial. Uniaxial compressive strengths vary from 100 to 800 MPa. However, impact strengths can be surprisingly low (Lautridou *et al.* 1986). Preparation of flints for point load or uniaxial compressive strength testing is exceedingly difficult and the ***K*** factor needs to be considered (Cumming 1999). There is very little information on the strength of flints. Lautridou *et al.* (1986) quote data from the Laboratoire Central des Ponts et Chaussées (Tourenq 1972) given in Table 2.

Lautridou *et al.* (1986) emphasize the importance on the mechanical properties of flint of the chemical state of the silica in a particular flint (chalcedony, quartz or opaline silica), and of porosity. Many of the flints in the highest beds of the Lewes Nodular Chalk have a carious, relatively high-porosity structure, which indicates that the flint strengths may be at the lower end of the scale.

Cumming (1999) has undertaken a number of point load strength ($I_{s\,50}$) and uniaxial compressive strength (UCS) tests on two types of flint, nodular and sheet flint. Her results are summarized in Table 3. On the basis of the limited UCS data, there does not appear to be a direct correlation between the measured point load and uniaxial compressive strengths of flint, normally expressed as a ***K*** factor. Thus the point load test does not seem to be a reliable strength indicator. The UCS tests on samples that could be prepared for such testing show remarkable consistency, with UCS about 600 to 700 MN/m^2 at laboratory temperature.

Application of physical properties test results to the cliff collapses

Few reported physical property or strength test results have been related precisely to stratigraphic position and to the lithological and textural character of individual beds and units of Chalk (e.g. Fig. 11). From studies of the rock mass character of the Chalk forming the cliffs of the English Channel it is evident that each Chalk formation has unique rock mass characters (Mortimore 2001; Mortimore *et al.* 2004; Duperret *et al.* 2002; Genter *et al.* 2002). These unique rock mass characters reflect physical properties and have a marked impact on the style and scale of chalk slope failures. As the cliffs range in height from a few metres to nearly

Table 1. *Behaviour of chalk tested in Undrained Triaxial conditions tested dry and saturated*

Chalk type	*Behaviour*
Culver Chalk, Downend, Portsdown	Ductile failure occurred at high confining pressure (4000kN/m^2). A specimen tested at 10000kN/m^2 failed at very low stress and showed an initial curve indicating that porosity collapse is a significant factor. 7 out of the 11 specimens tested had failure plane angles ranging between 50°–60°. Many failure planes followed pre-existing marly wisps and burrow structures.
Newhaven Chalk (top Old Nore, Peacehaven and Meeching Beds) Peacehaven	Only three saturated specimens were tested, hence the Mohr strength line needs to be treated cautiously. The three samples showed similar stress-strain curves, with pronounced initial curve indicating porosity collapse; all maintained constant strain after the peak stress In dry samples tested at 2000, 4000 and 6000kN/m^2 elastic properties were dominant. Those tested at 8000 and 10000kN/m^2 showed very slow initial stress increase, followed by a sudden increase in stress and then by ductile failure. Most specimens failed by formation of conjugate failure planes associated with some crushing.
Newhaven Chalk (Splash Point Beds) Balmer Farm	Stress strain curves for specimens tested at low confining pressure exhibited little ductility. Specimens tested at 2000 and 4000kN/m^2 had linear stress strain curves. Specimens tested at 6000, 8000 and 10000kN/m^2 showed an initial curve, suggesting porosity collapse. Where marl seams were present then failure planes followed these.
Seaford Chalk (Cuckmere Beds) Juggs Lane, Lewes	Specimens tested at 8000 and 10000kN/m^2 showed ductile behaviour before peak stress level was reached and failure occurred. Most specimens failed by formation of conjugate failure planes and in one case a horizontal plane also developed. Original chalk fabric controlled position of failure planes.

Table 2. *Strength of flints (from Lautridou et al. 1986)*

Compressive strength	391 MPa (3910 bars)
Brazilian strength	68 MPa (681 bars)
Impact toughness	13
Vickers Hardness	600–1200

Table 3. *Strength of flint (from Cumming 1999)*

	Point Load I_{s50} (kN)	*UCS (MPa)*
Number of samples	31	6
Mean (all samples)	11	679
Mean (nodular flints)	12	
Maximum (all samples)	25	748
Maximum (nodular flint)	25	
Minimum (all samples)	1	586
Minimum (nodular flint)	1	

200m, the chalk mass acting on any failure plane will also vary and the compressive and tensile strength of the chalk will also influence slope failures. Similarly, the weight of chalk will vary depending on degree of saturation and hence density/porosity. A combination of density and strength testing (Fig. 12) is used to develop a descriptive scheme for the chalk (Mortimore *et al.* 1990; Bowden *et al.* 2002; Lord *et al.* 2002). This descriptive scheme is used to provide a field method of identifying density and strength classes in chalk cliffs, reducing the need for great numbers of laboratory tests.

Density/porosity moisture contents and pore water chemistry

Each Chalk formation has a range of density/porosity (e.g. Mortimore & Pomerol 1998) and the density can also vary laterally depending on tectonic position in the basin or platform (Mortimore *et al.* 1990; 2001). It is not possible, therefore, to extrapolate physical property data directly from one locality to another in the same formation without knowing the geological setting. Nevertheless, the broad ranges of values shown (Figs 11 & 12) are applicable with care to the

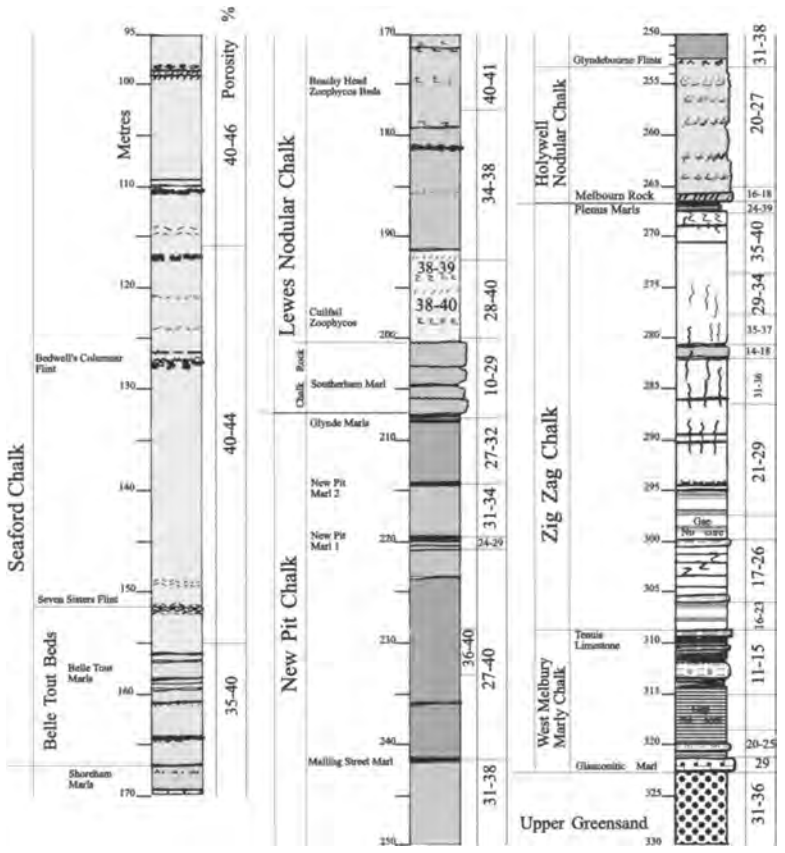

Fig. 11. Stratigraphy and porosity distribution in the Chalk based on the BGS Faircross Borehole, Berkshire. Compare this distribution of porosity with Bloomfield *et al.* 1995. Depth is in metres. Porosity measured by mercury intrusion (modified from Mortimore & Pomerol 1998).

cliffs in the main axis of the basin in Kent and Sussex and in the French Chalk cliffs north of Fécamp.

The impact of porosity/density differences on cliff instability are several. Firstly, high-porosity, low-density chalk such as occurs in the Seaford Chalk Formation loses and gains water readily. Cycles of wetting and drying related to weather will cause cyclic changes in bulk density and hence cyclic loading in the cliff. Combined with expansion and contraction (noticed on cores prepared for uniaxial testing which went out of true in the humidity of the laboratory), these cyclic changes will loosen the rock mass and progressively concentrate stresses at particular points. The uniaxial compressive strength of the chalk at these stress concentration points, in combination with the rock mass structure, will partly determine the modes and scales of failures.

Chalk is one of the most frost-susceptible materials and this aspect has been investigated for foundations to buildings and road construction (e.g. Croney 1977). Freezing leads to heave and the amount of heave depends partly on the porosity/IDD of the material and the duration of the freezing episode (Fig. 13). Soft, low-density, high-porosity chalks, such as occur in the Seaford Chalk Formation, are the most susceptible. Lautridou *et al.* (1986) also demonstrated that the degree of saturation was an important factor on the degradation of chalk during freeze–thaw cycles. A similar relationship has been observed in chalk earthworks (e.g. Greenwood 1990; Lord *et al.* 2002) where chalks which were >90% saturated degraded rapidly and were more likely to produce 'putty' chalk conditions. Thus, IDD/porosity and degree of saturation (moisture content) are important parameters for assessing cliff instability. The relationship between freezing episodes and cliff collapse is uncertain but field observations suggest that, following a night of freezing, the temperature rise in the morning is the time when a rain of debris is released from quarry faces and sea-cliffs. Melting, following a prolonged period of freezing, may lead to more extensive collapses as ice-heave has its effect. More climate data (e.g. Hutchinson 1971) and more data on the effects of freezing on different types of chalk is required to

Hardness	TI Average	IDD Av Mg/m³	IDD Mg/m³	T_d MPa	UCS_d MPa	UCS_w MPa	IDD Mg/m³	CIRIA divisions
Ex Soft	20	1.47	1.55	1.12	9	3	1.55	Low density
Very Soft	26	1.58	1.60	1.39	11	4		Medium density
Soft	33	1.63	1.70	1.88	15	5	1.70	
Medium Hard	47	1.73	1.80	2.38	19	7		High density
Hard	55	1.86	1.95	3.1	25	>10	1.95	
Very Hard	63	2.15	2.40	5.3	45			Very high density
Ex Hard*	73	>2.40						

*e.g. Ulster White Limestone Formation IDD > 2.6 Mg/m³ (Hancock, 1973, p.158)
TI = Texture Index of Mortimore & Fielding (1990)
T_d = Dry Brazilian Crushing Strength UCS_d = Dry Unconfined Compressive Strength
UCS_w = Saturated Unconfined Compressive Strength (based on Matthews & Clayton, 1993; see Figure 9)

Fig. 12. Summary table of physical properties and index strength tests used to classify chalk.

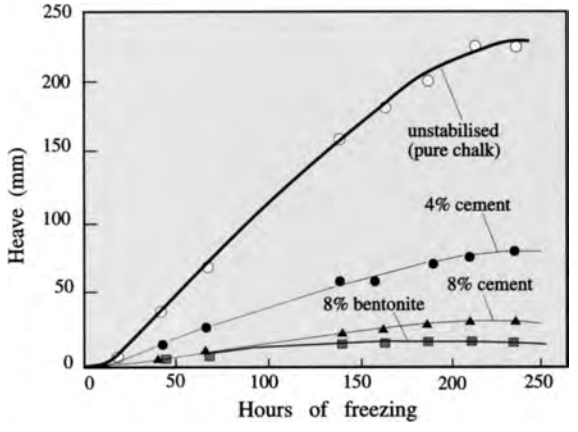

Fig. 13. Heave of low density soft chalk (SMC = 27%) IDD = 1.56Mg/m³) stabilized with cement and bentonite (From Croney, 1977, Fig. 9.29).

determine the relationship between frost episodes and cliff instability.

Pore water chemistry may also have an influence on chalk strength and cliff erosion rate. Overgrowths of salt in the very soft, high porosity Culver Chalk Formation sea cliffs at Newhaven (Fig. 14) produce 'skins' of chalk which progressively flake each year. Whether sea-saline water produces different strength results compared to meteoric groundwater is not known. However, the long-term exposure to salt spray and, in many cases, the inundation of cliffs by the sea during winter storms is likely to enhance 'weathering' by force of crystallization of salt in pore spaces (e.g. Benavente *et al.* 1999). Other minerals, such as gypsum, have also been recorded in chalk pore spaces in particular geological settings (e.g. beneath Palaeogene deposits at Newhaven and Seaford Head, Mortimore 1979). The influence of gypsum on the strength and weathering of chalk in the cliffs is uncertain. Cycles of wetting and drying, as well as cycles of precipitation of salt and gypsum in chalk pore spaces and joints, are likely to enhance weathering and rock mass loosening. A possible cause of sea-cliff sample deterioration in the laboratory prior to strength testing is the presence of salt or gypsum forming in the pores of test cores.

Distribution of chalk strength in coastal cliffs

Although there are broad strength classifications that can be applied to the chalk cliffs in terms of the main lithological units (formations), there are also individual smaller-scale units of weaker or stronger material. Chalk cliff failures are controlled primarily by a combination of the rock mass character and the strength of the material.

Data collected from site investigations for many engineering schemes in the Chalk of southern England illustrate the variation in physical properties within one Chalk formation (e.g. Fig. 15). The beds identified in road cuttings and tunnels can be extrapolated to the coast where, for example, the high-density (IDD $>1.85\,MN/m^3$), high P-wave velocity ($>2500\,ms^{-1}$), forms a hard rocky platform at Peacehaven, locally reducing marine erosion and changing the erosion characteristics along the cliff (Fig. 16).

The changes in the P-wave velocity profile (Fig. 15) are related to a combination of changes in density and changes in fracture style and tightness. The Old Nore Beds in particular, are characterized by inclined conjugate joints which are

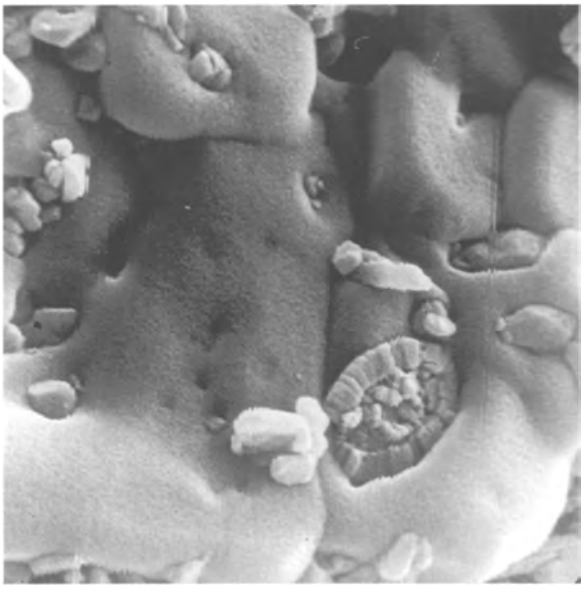

Fig. 14. Salt crystallizing in chalk pores and overgrowing coccolith matrix. Very soft, low density Culver Chalk Formation, Newhaven Cliffs (Sample no. 411/34; Mortimore, 1979).

generally tight and interlocking, potentially giving a very different velocity profile compared to chalks with closely spaced vertical joint sets.

Discussion

Determining physical properties and the strengths of different chalks is a key part of coastal chalk cliff instability investigations. Other key parts of the investigation are the rock mass character, local meteorological and marine wave climates and any temporal changes in these physical conditions. The very wet winter of 2000–2001 saw significant cliff collapses for the first time along supposedly protected lengths of coastline at Peacehaven and Brighton, and accelerated rates of collapse along unprotected cliffs such as Beachy Head and Holywell, Eastbourne (Mortimore *et al.* 2004). These observations suggest, as in other aspects of chalk engineering such as earthworks, that IDD/porosity and the degree of saturation, are critical factors in cliff instability. Further work, over a longer time-span than two years, is required to integrate the physical properties, rock mass character and climatic conditions to provide a detailed insight into mechanisms, scales and longer-term changes affecting rates of cliff collapses. However, there are some clues from the data obtained in this study.

Field observations have illustrated the different styles of fracturing in the different Chalk formations (e.g. Mortimore 2001). These observations have also shown the impact of marl seams as layers along which horizontal movements

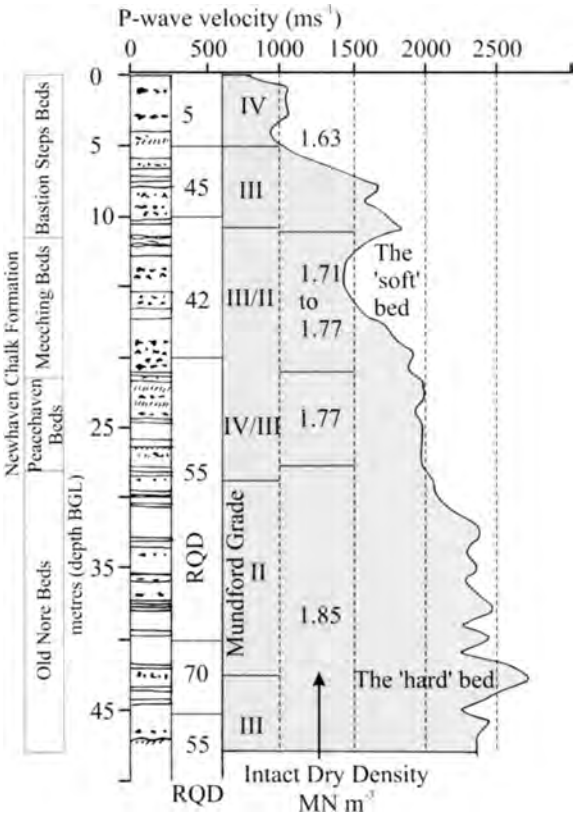

Fig. 15. The A27 Southwick Tunnel site investigation: P-wave velocity profile showing typical variation in physical properties within the Newhaven Chalk Formation, Mundford Grade based on Ward *et al.* 1968. (Data from L.G. Mouchel & Partners; modified from Mortimore 1993).

have taken place in chalks with predominantly conjugate joint sets. These observations were mimicked in the laboratory Undrained Triaxial test results (Table 1), where marls and original chalk fabric had a profound influence on the location of failure planes. The Undrained Triaxial tests for saturated and dry samples also indicate the potential for different angles of friction in the cliffs at reduced stress levels in saturated samples. Hence, the climatic conditions will have both short- and long-term impacts on cliff stability. Because of their differing physical properties and rock mass character each Chalk formation is likely to behave differently in terms of factors of safety against cliff collapse and modes and scales of failure. Pore collapse under relatively low stress levels indicated by the initial curve on the stress strain curves for Undrained Triaxial test results and the resulting powder-chalk is also seen in real cliff collapses. Remnant powder chalks are present on the stress concentration points where 'explosive' failures have occurred. Millar (2000), in a much more comprehensive study of the stress-strain behaviour of jointed chalk, also recognized the importance of pore

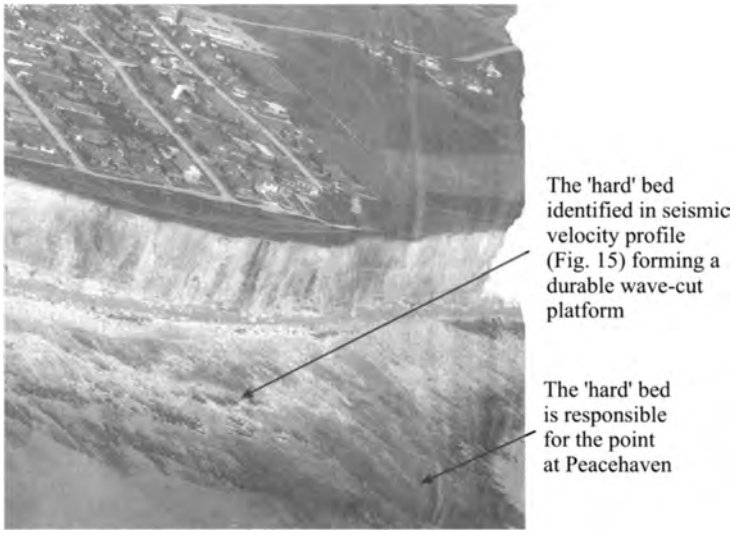

Fig. 16. The cliffs at Peacehaven photographed in 1976 prior to construction of the coast protection works.

collapse. He suggested from the results of his studies that jointed chalk could be adequately investigated in standard soil triaxial cells and that the behaviour of chalk could be described by Mohr-Coulomb or JCR-JCS parameters.

Bulking factors are an important part of estimating the volume of chalk involved in failures. Similarly, the percentage 'fines' resulting from breakdown of material during a cliff failure may influence mobility of the debris and the resulting volume estimations. In conventional chalk earthworks (e.g. Jenner & Burfitt 1975), the methods of compaction of fills and construction loss of material at fill sides results in shrinkage rather than bulking. Where chalk is taken to land fill or landscaping and where only light compaction is used, bulking in the order of 16% has been recorded (e.g. Lord *et al.* 2002). For the purposes of estimating volumes involved in cliff failures, the harder, higher density, more massive chalks (e.g. Lewes Nodular Chalk Formation at Beachy Head and Puys) are assumed to have higher bulking values of around 20% than the softer, lower density chalks (e.g. Seaford Chalk Formation), with bulking values around 16%.

Conclusions

The physical properties of different chalks have been investigated as part of the analysis of cliff collapse mechanisms.

Index properties of density, natural moisture content (degree of saturation), saturation moisture content and porosity suggest that chalks with densities below 1.70 Mg/m^3 can lose and gain water readily and are thereby likely to cause changes in the physical conditions in cliffs more readily than higher-density chalks. Exceptions to this trend, such as parts of the Newhaven Chalk, probably result from textural controls, particularly pore-throat diameters and degree of cementation in contrast to Seaford Chalk of the same density. IDD/porosity and degree of saturation are used as a measure of potential frost susceptibility, bulking/shrinkage calculations and mechanical behaviour in terms of strength and percentage of fines generated during cliff failures.

Index strength tests (Brazilian Crushing Strength and Uniaxial Compressive Strength) indicate that each Chalk formation contains material with particular strength characteristics, reinforcing the idea that there is no simple relationship between strength and density. Texture (e.g. degree and type of cementation) is probably an important factor controlling strength in chalks of the same density.

The Undrained Triaxial behaviour of chalk mimics the field observations on the style of fracturing and, in terms of the influence of fabric elements (marl seams, trace fossils, vein fabric), on the location of failure planes.

All chalk strength tests show a marked reduction with increased saturation. The angle of friction and cohesive strength is also reduced with increased saturation. These results emphasize the critical role of water, either meteoric or groundwater, contained in material pores or fissure pores, on chalk cliff instability. Water, in the context of degree of saturation, is also important in terms of the impact on stability of frost or freezing episodes.

A special outcome of the work is the recognition that each formation of the Chalk has unique physical properties and potentially unique mechanical behaviour, including slope failure mechanisms.

Acknowledgements. The collection of physical property data has taken many years and has been supported by several technicians and students in the Civil Engineering

Department at the University of Brighton, including Jon Holliday, Trevor Warman, John Lamont-Black, Gerry Mckinney, Mariani Mohammad, John Chapman and David Pearce. The work on the Chalk cliffs of the Channel has been a joint venture with colleagues from the Université du Havre (Anne Duperret) and BRGM (Albert Genter, Pierre Laville, Pierre Watremez) under The European funded INTERREG II Project ROCC.

References

BELL, F. G., CRIPPS, J. C., EDMONDS, C. N. & CULSHAW, M. G. 1990. Chalk fabric and its relation to certain geotechnical properties. *In*: BURLAND, J. B., MORTIMORE, R. N., ROBERTS, L. D., JONES, B. L. & CORBETT, B. O. (eds). *Chalk. Proceedings of the International Chalk Symposium, Brighton Polytechnic, 1989.* 187–194. Thomas Telford, London.

BENEVENTE, D., DEL CURA, M. A. G., FORT, R. & ORDONEZ, S. 1999. Thermodynamic modelling of changes induced by salt pressure crystallisation in porous media of stone. *Journal of Crystal Growth*, **204**, 168–178.

BLOOMFIELD, J. P. BREWERTON, L. J. & ALLEN, D. J. 1995. Regional trends in matrix porosity and bulk density of the Chalk of England. *Quarterly Journal of Engineering Geology*, **28**, 131–142.

BOWDEN, A. J., LAMONT-BLACK, J. & ULLYOT, S. 1998. Point load testing of weak rocks with particular reference to chalk. *Quarterly Journal of Engineering Geology*, **31**, 91–103.

BOWDEN, A. J., SPINK, T. W. & MORTIMORE, R. N. 2002. The engineering description of chalk: its strength, hardness and density. *Quarterly Journal of Engineering Geology and Hydrogeology*, **35**, 355–361.

BS 1377. 1990. British standard methods of test for soils for civil engineering purposes. Part 2. Classification tests. *British Standards Institution.*

BS 5930. 1981. Code of practice for Site investigations. *British Standards Institution.*

BS 5930. 1999. Code of practice for Site investigations. *British Standards Institution.*

CARTER, P. G. & MALLARD, D. J. 1974. A study of strength, compressibility and density trends within the chalk of southeast England. *Quarterly Journal of Engineering Geology*, **7**, 43–55

CLARKE, R. H. 1977. Earthworks in soft chalk: performance and prediction. *The Highway Engineer*, **1977 XXIV, (3)**, 18–21

CLAYTON, C. R. I. 1977. Chalk in Earthworks – Performance and Prediction. *The Highway Engineer*, **February 1977**, 14–20

CRONEY, D. 1977. *The design and performance of road pavements.* Transport and Road Research Laboratory. H.M.S.O. London.

CUMMINGS, F. C. 1999. *Machine Tunnelling Performance in Chalk with Flint with Particular Reference to the Mechanical Properties of Flint.* PhD Thesis, University of Brighton.

DOWNING, R. A., PRICE, M. & JONES, G. P. 1993. *The Hydrogeology of the Chalk of North-West Europe.* Oxford Science Publications.

DUPERRET, A., GENTER, A., MORTIMORE, R. N., DELACOURT, B. & DE POMERAI, M. 2002. Coastal rock cliff erosion by collapse at Puys, France: the role of impervious marl seams within the chalk of NW Europe. *Journal of Coastal Research*, **18**, 52–61

GENTER, A., DUPERRET, A., MARTINEZ, A., MORTIMORE, R. N., VILA, J-L. 2004. Multiscale fracture analysis along the French chalk coastline for investigating cliff collapse erosion. *In*: MORTIMORE, R. N. & DUPERRET, A. (eds) 2004. *Coastal Chalk Cliff Instability.* Geological Society London, Engineering Geology Special Publication, **20**, 57–74.

GREENWOOD, J. R. 1990. Specification of chalk for highway works. *In*: BURLAND, J. B., MORTIMORE, R. N., ROBERTS, L. D., JONES, B. L. & CORBETT, B. O. (eds), *Chalk. Proceedings of the International Chalk Symposium, Brighton Polytechnic, 1989.* 421–423. Thomas Telford, London.

HUTCHINSON, J. N. 1971. Field and laboratory studies of a fall in Upper Chalk cliffs at Joss Bay, Isle of Thanet. *Roscoe Memorial Symposium, Cambridge University, 29–31 March, 1971*, 1–12.

HUTCHINSON, J. N. 1988. General report: Morphological and geotechnical parameters of landslides in relation to geology and hydrogeology. *In*: Bonnard, C. (ed.) *Landslides*, Proceedings of the Fifth International Symposium on Landslides, Balkema, Rotterdam, 3–35

INGOLDBY, H. C. & PARSONS, A. W. 1977. *The Classification of Chalk for Use as a Fill Material.* TRL Laboratory Report 806.

JENNER, H. N. & BURFITT, R. H. 1975. *Chalk: an Engineering Material.* Unpublished paper presented to the ICE Southern Association Meeting, Brighton Polytechnic, 6th March, 1975. Southern Association of the Institution of Civil Engineers.

LAMONT-BLACK, J. & MORTIMORE, R. N. 1996. Determination of intact dry density of irregular chalk lumps: a new method. *Quarterly Journal of Engineering Geology*, **29**, 241–248.

LAMONT-BLACK, J. & MORTIMORE, R. N. 2000. Dissolution tubules: a new karst structure from the English Chalk. *Zeitschrift der Geomorphologie*, **44**, 469–489.

LAUTRIDOU, J. P., LETAVERNIER, G., LINDÉ, K., ETLICHER, B. & OZOUF, J. C. 1986. Porosity and frost susceptibility of flints and chalk: laboratory experiments, comparison of glacial and periglacial surface texture of flint materials, and field investigations. *In*: SIEVEKING, G. DE G. & HART, M. B. (eds.), *The Scientific Study of Flint and Chert.* Cambridge University Press, 269–282.

LEWIS, W. A. & CRONEY, D. 1966. The properties of chalk in relation to road foundations and pavements. *In*: Proceedings of a Symposium Chalk in earthworks and foundations. Institution of Civil Engineers, 1965, 27–42.

LORD, J. A. TWINE, D. & YEOW, H. 1994. *Foundations in Chalk.* Funders Report/CP/13 CIRIA Project Report 11.

LORD, J. A., CLAYTON, C. R. I. & MORTIMORE, R. N. 2001. *Engineering in Chalk.* Construction Industry Research and Information Association (CIRIA), **2002**.

MASSON, M. 1973. Pétrophysique de la craie. *In*: La Craie, *Bulletin de liaison des Laboratoires des Ponts et Chaussées*, **Spécial V**, 23–47.

MATTHEWS, M. C. & CLAYTON, C. R. I. 1993. Influence of intact porosity on the engineering properties of a weak rock. *In*: ANAGNOSTOPOULOS, A., SCLOSSER, F., KALTEZIOTIS, N. & FRANK, R. (eds). *Geotechnical Engineering of Hard Soils – Weak Rocks.* Balkema, Rotterdam, **1**, 693–702.

MEIGH, A. C. & EARLY, K. R. 1957. Some physical and engineering properties of chalk. *Proceedings of the 4th International Conference on Soil Mechanics and Foundation Engineering, 1957*, **1**, 68–73.

MILLAR, M. J. 2000. *The Stress-strain Behaviour of Jointed Chalk.* PhD Thesis, University of Brighton.

MIMRAN, Y. 1975. Fabric deformation induced in Cretaceous chalks by tectonic stresses. *Tectonophysics*, **26**, 309–316.

MORTIMORE, R. N. 1979. *The Relationship of Stratigraphy and Tectonofacies to the Physical Properties of the White Chalk of Sussex.* PhD Thesis, Brighton.

MORTIMORE, R. N. 1986. Stratigraphy of the Upper Cretaceous White Chalk of Sussex. *Proceedings of the Geologists' Association*, **97**, 97–131.

MORTIMORE, R. N. 1993. Chalk water and engineering geology. *In*: DOWNING, R. A., PRICE, M. & JONES, G. P. (eds). *The Hydrogeology of the Chalk of North-West Europe*. Oxford Science Publications, 67–92.

MORTIMORE, R. N. 2001. Chalk: a stratigraphy for all reasons. *Geoscience in South-west England*, **10**, 105–122.

MORTIMORE, R. N. & FIELDING, P. M. 1990. The relationship between texture, density and strength of chalk. *In*: BURLAND, J. B., MORTIMORE, R. N., ROBERTS, L. D., JONES, D. L & CORBETT, B. O. (eds.), *Chalk. Proceedings of the International Chalk Symposium, Brighton Polytechnic, 1989*. Thomas Telford, London, 109–132.

MORTIMORE, R. N. & POMEROL, B. 1998. Basin analysis in engineering geology: Chalk of the Anglo-Paris Basin. *8th International Congress International Association for Engineering Geology and the Environment, Vancouver*. Balkema, Rotterdam, 3249–3268.

MORTIMORE, R. N., POMEROL, B. & FOORD, R. 1990. Engineering stratigraphy and palaeogeography for the Chalk in the Anglo-Paris Basin. *In*: BURLAND, J. B., MORTIMORE, R. N., ROBERTS, L. D., JONES, D. L & CORBETT, B. O. (eds.), *Chalk. Proceedings of the International Chalk Symposium, Brighton Polytechnic, 1989*. Thomas Telford, London, 47–62.

MORTIMORE, R. N., POMEROL, B. & LAMONT-BLACK, J. 1996. Examples of structural and sedimentological controls on chalk engineering behaviour. *In*: HARRIS, S., HART, M. B., VARLEY, P. M. & WARREN, C. D. (eds.). *Engineering Geology of the Channel Tunnel*. Thomas Telford, London, 436–443.

MORTIMORE, R. N. WOOD, C. J. & GALLOIS, R. W. 2001. *British Upper Cretaceous Stratigraphy*. Geological Conservation Review Series No. 23, Joint Nature Conservation Committee, Peterborough.

MORTIMORE, R. N., LAWRENCE, J., POPE, D., DUPERRET, A. & GENTER, A. 2004. Coastal cliff geohazards in weak rock: the UK chalk cliffs of Sussex. *In*: MORTIMORE, R. N. & DUPERRET, A. (eds.), *Coastal Chalk Cliff Instability*. Geological Society, London, Engineering Geology Special Publications, **20**, 3–31

NORBURY, D. R. 1986. The Point Load Test. *In*: HAWKINS, A. B. (ed.). *Site Investigation Practice: Assessing BS 5930*. Geological Society, London, Engineering Geology Special Publication, **2**, 325–329.

WARD, W. H., BURLAND, J. B. & GALLOIS, R. W. 1968. Geotechnical assessment of a site at Mundford, Norfolk, for a large proton accelerator. *Géotechnique*, **18**, 399–431.

WARREN, C. D. & MORTIMORE, R. N. 2002. Chalk engineering geology – Channel Tunnel Rail Link and North Downs Tunnel. *Quarterly Journal of Engineering Geology and Hydrogeology*, **36**, 17–34.

Geological Society, London, Engineering Geology Special Publications

A Sturzstrom-like cliff fall on the Chalk coast of Sussex, UK

R. B. G. Williams, D. A. Robinson, U. Dornbusch, Y. L. M. Foote, C. A. Moses and P. R. Saddleton

Geological Society, London, Engineering Geology Special Publications 2004; v. 20; p. 89-97
doi:10.1144/GSL.ENG.2004.020.01.06

A Sturzstrom-like cliff fall on the Chalk coast of Sussex, UK

R. B. G. Williams, D. A. Robinson, U. Dornbusch, Y. L. M. Foote, C. A. Moses & P. R. Saddleton

Department of Geography, University of Sussex, Falmer, Brighton, BN1 9QN, UK

Abstract: In 1914 a notable cliff fall occurred on the chalk coast of the Seven Sisters in Sussex. Debris from the fall travelled outwards across the shore platform in front of the cliff for a distance of about 75 m, forming a narrow tongue-like projection. The reason why the debris exhibited such mobility is uncertain, but it may have flowed in a similar fashion to a sturzstrom, despite its modest volume (*c.* 12500 m^3) and the equally modest height of the cliff (44–45 m). If this suggestion is correct, the minimum volume of detached rock required to trigger sturzstrom-type flow is 1–2 orders of magnitude less than is commonly claimed.

Introduction

Chalk outcropping on the coast of southern and eastern England frequently forms vertical or near-vertical cliffs despite being quite a soft limestone. The steepness of the cliffs is due partly to their rapid rate of retreat. Waves repeatedly batter and undermine the base of the cliffs while weathering processes attack the rock faces above, detaching individual joint blocks and smaller pieces of chalk, which fall directly into the sea or onto the beach and shore platform, to be speedily swept away by the waves. Weathering losses are greatest in winter, particularly after heavy rains or a thaw following a hard frost (Hutchinson 1972; Robinson & Williams 1983). Losses in summer are quite minor and concentrated in periods of particularly stormy weather.

More substantial losses result from cliff falls in which sections of cliff fail *en masse*, collapsing onto the beach and shore platform, where they may come to rest as largely intact blocks but often disintegrate, forming a scree or talus cone. In many cases the failure extends over the entire cliff height, but some small falls are confined to just part of the cliff face, usually the top, though sometimes the middle or base. As noted by Hutchinson (1972), cliff failure is often preceded by the opening of a joint-controlled tension crack in the top of the cliff some distance behind the outer edge. The cracking tends to extend downwards as the cliff is undercut. Eventually, the lower part of the cliff fails in shear, causing the upper part of the cliff to collapse. The shear plane is often left grooved or slickensided.

Most chalk cliff falls are quite small, yielding less than 1000 m^3 of rock debris, but more substantial falls, yielding 20000 m^3 or more of debris occur occasionally. The sea often takes several years to remove the larger falls, but the smaller falls may linger for only a few weeks or months.

The screes or debris cones created by chalk cliff falls are usually quite steeply inclined, at angles of up to about 38°, which is the approximate angle of rest of loose, coarse chalk debris. They typically extend no more than about 30–40 m from the base of the cliff. Very occasionally, however, cliff falls occur with peculiarly long run-outs (Hutchinson 1980, 1983, 1988, 2002; Birch 1990). So far, the main reported British examples are from Kent, on the high chalk coast between Folkestone and just north of Dover (St Margaret's Bay). The cliffs in question vary between 80 and 150 m in height, which is higher than the average for English chalk. Many of the falls took place in the first quarter of the last century for reasons that are not entirely clear.

When describing mass movements it is useful to calculate the value of *H/L*, sometimes referred to as the 'fahrböschung' (Heim 1882, 1932; Hsü 1975, 1978) or 'mean drop gradient' (Kilburn & Sørensen 1998), where *H* is the difference in height and *L* is the horizontal distance between the top of the failure and the toe of the run-out. According to Hutchinson (1988), the *H/L* value for falls from chalk cliffs up to 50 m high is normally around 1.1 to 1.5. On the Sussex chalk coast, however, the debris from small falls commonly slumps downwards to rest immediately next to the toe of the cliff, yielding *H/L* values of 2.0 or more. A minimum value for *H/L* for scree-type accumulations can be calculated from the maximum angle of rest of coarse chalk debris, which, as already mentioned, is around 38°, giving a tangent of about 0.78. *H/L* will equal the tangent value in the theoretical limiting case of the debris extending to the cliff top but if, as is always observed, the debris reaches only part of the way up the cliff, the *H/L* value will exceed the minimum of 0.78. The peculiar long-run-out falls in Kent reported by Hutchinson (1988, 2002) and Birch (1990) have *H/L* values below 0.78, ranging downwards to 0.2, and imply a flow or momentum transfer mechanism rather than simple gravity-controlled accumulation.

This paper describes an interesting fall from the chalk cliffs of the Seven Sisters in Sussex that took place in 1914. A number of photographs survive that were taken soon after the fall, and these show that it had a much longer than

From: MORTIMORE, R. N. & DUPERRET, A. (eds) 2004. *Coastal Chalk Cliff Instability*. Geological Society, London, Engineering Geology Special Publications, **20**, 89–97. 0267-9914/04/$15.00

average runout. Contemporary newspaper accounts enable us to describe it in some detail, and to reconstruct some of the climatic and other environmental conditions that may have caused it.

The Seven Sisters coast

The near-vertical Seven Sisters cliffs trend WNW–ESE, more or less at right angles to the dip of the chalk strata (Fig. 1). They intersect a series of dry valleys descending the dip slope, which have been left hanging above the beach and shore platform because of the cessation of fluvial erosion and continuing marine erosion. The coast is very exposed to storm waves approaching up the English Channel from the southwest, which is the predominant wind direction and also the direction of maximum fetch (around 7200 km). Gales (wind speeds above 33 knots) occur on 15–20 days per year (Potts & Browne 1983) and wave heights of 1.5–2.0 m are exceeded for 10% of the year directly offshore (Dales & Gilbert 1998). The mean tidal range is about 4.9 m (6.0 m at Spring tides).

Comparison of the cliff top edge on Ordnance Survey 1:10560 maps of 1873 with the 1999 OS digital Land Line data suggests that the Seven Sisters cliffs are retreating at a long-term average rate of about $0.46\,m\,a^{-1}$ (Dornbusch 2001). The rate increases from west to east, probably because Seaford Head shelters the westernmost Sisters from the full force of Atlantic gales. Thus the mean for the Cuckmere Haven to Flat Hill section is about $0.36\,m\,a^{-1}$, whereas for the section from Flat Hill to Birling Gap it is $0.57\,m\,a^{-1}$. The retreat is most rapid at Birling Gap (around $0.71\,m\,a^{-1}$), seemingly because the cliff there is low and composed of badly weathered chalk and valley infill (May 1971; Cleeve & Williams 1987; South Downs Coastal Group 1996). The less exposed chalk cliffs of Kent to the east and Dorset to the southwest are eroding much less rapidly than the Sussex chalk cliffs such as the Seven Sisters (May & Heeps 1985).

The Seven Sisters cliffs are composed of Seaford Chalk of upper Coniacian–lower Santonian age, capped on the highest summits by Newhaven Chalk of upper Santonian age (Mortimore 1997). Well-defined vertical joints run almost parallel to the cliff face and at right angles to it, helping to define the geometry of the cliff falls (Duperret *et al.* 2001; Martinez *et al.* 2001). The chalk is fine-grained, soft to medium hard and relatively pure (Bristow *et al.* 1997). Numerous flint seams are present, which are concordant with the bedding. There are no conspicuous hard grounds or major marl seams, apart from the Belle Tout Marl, exposed at the base of the westernmost Seven Sisters.

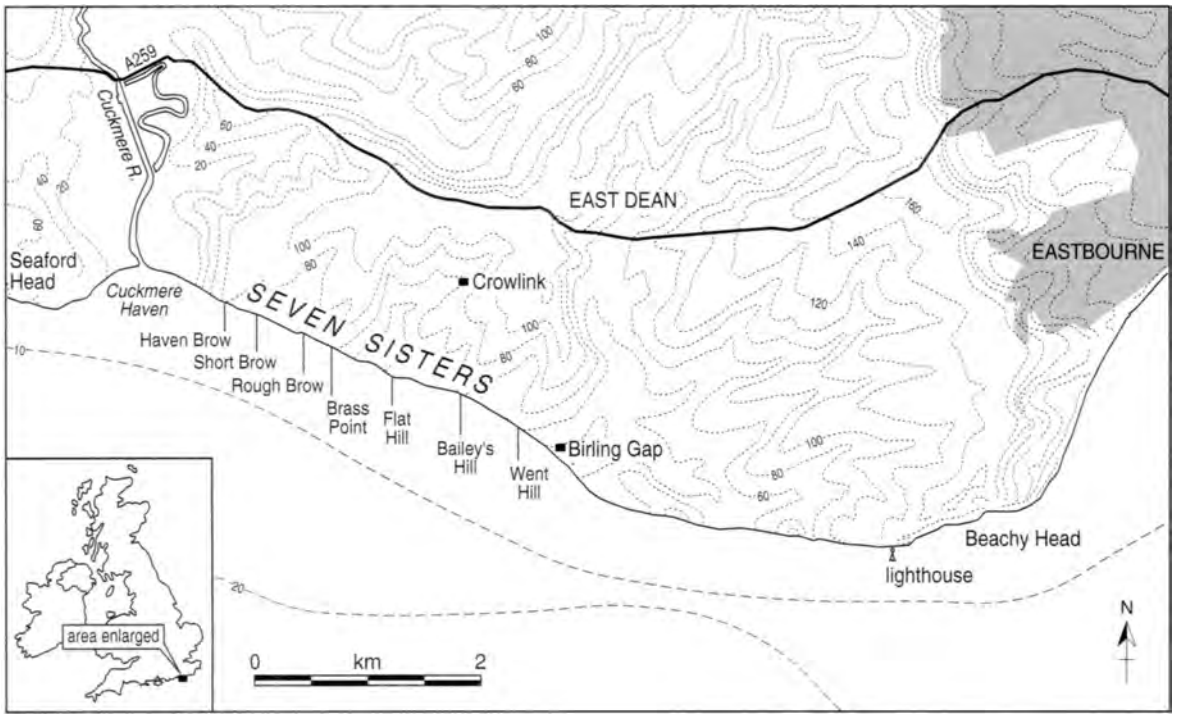

Fig. 1. Map of the East Sussex coast from Cuckmere Haven to Eastbourne, showing the location and names of the Seven Sisters.

The 'Great Fall' of 1914

Figure 2 reproduces an Edwardian picture postcard of the fall, found by Mr D. Puttick of Eastbourne. The photograph was taken from near Bailey's Brow, looking eastwards along the Severn Sisters. The fall evidently occurred at Went Hill, the easternmost Sister. The tongue-like form of the debris accumulation is immediately apparent, as is its gently sloping seaward profile, quite unlike the relatively steep profile that characterizes the debris normally produced by chalk cliff falls.

The photograph was the first in a set of at least four cards published by Wynter of Seaford. Number 2 has not been traced. Number 3, reproduced here as Figure 3 was a close-up photograph of the fallen debris on the shore. Number 4 (Fig. 4) showed four men and a dog standing on the debris. Another postcard publisher, who has not been identified, published a very similar card to Wynter's Number 3, labelled 'Fall of cliff near Birling Gap', and also a close-up of the seaward end of the tongue of debris.

The publishers did not include a date with the captions on their cards, but one example has been found that was posted in 1914, and there can be no doubt that the cards record a massive fall that occurred early on Easter Monday, 13 April 1914, which attracted much comment in the local papers as well as brief notice in the national press. A photograph of the fallen debris taken from the shore and published by the *Eastbourne Gazette* (22 April 1914) is too poorly preserved to be worth reproducing here, but it closely matches Wynter's card Number 3 and the corresponding card issued by the anonymous publisher.

According to the *Gazette*, the fall was the greatest that had 'taken place on this part of the coast within living memory'. It removed a 'huge slice of cliff from summit to base' (*Sussex Daily News*, 21 April) in the 'centre' of Went Hill (*Eastbourne Chronicle*, 25 April). The sea is said to have previously excavated a cave in the base of the cliff, in a reddish 'patch of earth and chalk rubble' (*Eastbourne Chronicle*, 25 April), which is likely to have been the infill of a fissure or solution pipe.

Contemporary estimates of the length of runout are contradictory. The *Sussex Daily News* reported that 'the fall extended from the base of the cliff sixty or seventy yards out to sea' (55–64 m), whilst the *Eastbourne Gazette* asserted that it 'extended about 150 feet towards low-water mark' (45 m). The Wynter photograph suggests that even the *Daily News* estimate was a little conservative, perhaps because the reporter did not visit the site until after the waves and tide had removed the seaward extremity of the fall. The length of run-out can be estimated from the Wynter photograph using as a scale either (1) the height of the cliff, (2) the size of the spectators or (3) the width of the shore platform:

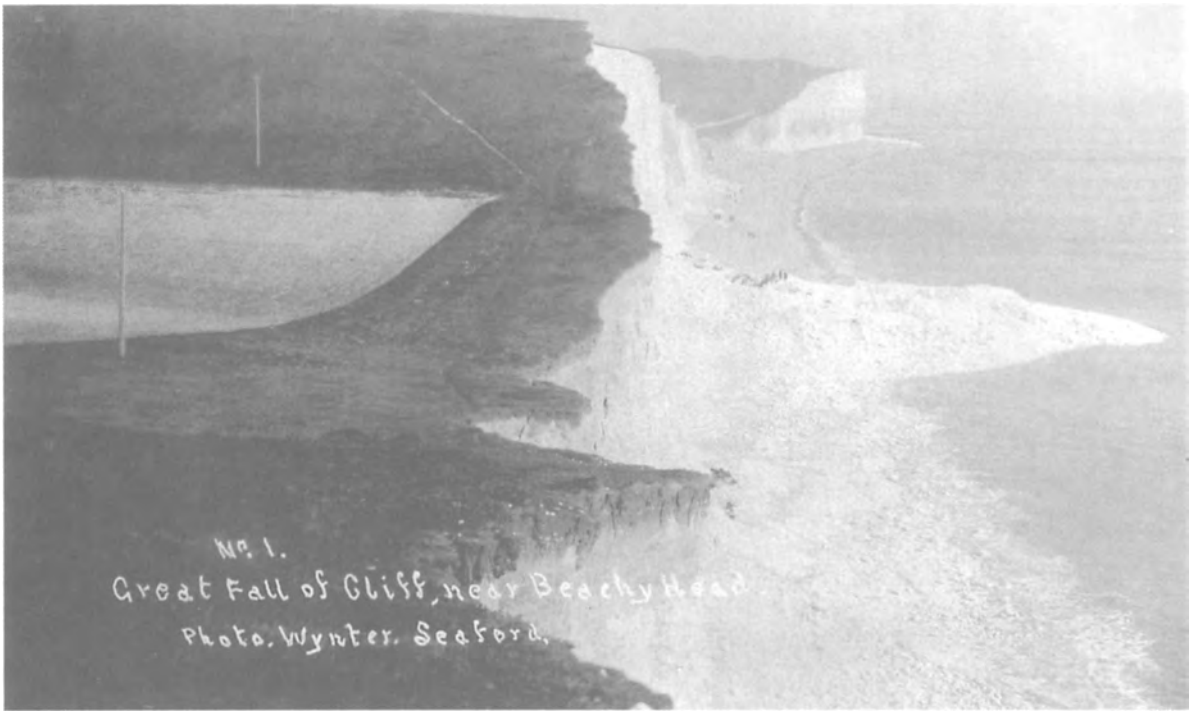

Fig. 2. Distant view of the 1914 cliff fall at Went Hill. The first in a series of at least four contemporary postcards published by Wynter of Seaford.

Fig. 3. The third of Wynter's postcards, showing the fall in close up.

(1) In 1914 the cliff top at Went Hill was, as today, about 44–45 m high (see the 1909 edition of the Ordnance Survey 1:2500 map, Sheet LXXXII.3). The run-out in Figure 2 appears to be about 1.8 times the height of the cliff or about 70–80 m. However, it is difficult to determine the true position of the base of the cliff because of the awkward perspective and masses of fallen debris. Also, the top of the cliff is ill defined in the photograph.
(2) A seemingly more reliable estimate can be prepared using Figure 3 and the spectators as a guide. Assuming that they were males and females of normal height (1.70 m and 1.66 m respectively), the length of run-out would appear to have been about 75 m.
(3) Figure 2 shows debris from the fall extending almost twice as far from the cliff base as the exposed portion of the shore platform. The 1909 Ordnance Survey map records that the inter-tidal width of the platform was about 75 m at Went Hill. The photograph was evidently taken within about two hours of low tide, when at least 35 m of the platform is likely to have been exposed, which suggests that the runout was 70 m or more.

Contemporary estimates of the size of the fall are even more problematic than the estimates of the run-out, varying from 'nearly 200000 tons' (*Sussex Daily News*) to '300000 tons or more' (*Eastbourne Gazette*). In arriving at these estimates, observers seem to have tried to calculate how much chalk was missing from the cliff rather than how much was piled up on the shore beneath. It was noted that the cliff-top path, which previously had lain 'some thirty feet or more' (9 m) from the edge, had disappeared in the fall, indicating the removal of a slice of chalk of at least this width.

The *Sussex Daily News* reported that the debris below the cliff varied from 'ten to fifty feet in height' (3–15 m). However, Figure 3, which includes spectators as a scale, suggests that the debris was probably around 13 or 14 m deep at the base of the cliff, and that its average depth (along its centre line) was about 6–7 m. Unfortunately, nobody seems to have recorded the width of the fall but, if it averaged about 25 m, the total volume of debris would have been of the order of 12500 m^3. Assuming that 1 m^3 of chalk debris weighed on average 1.35 metric tonnes (J. N. Hutchinson, pers. comm.) this suggests that the fall totalled nearly 17000 metric tonnes, far short of contemporary estimates, even allowing for the difference between Imperial tons and metric tonnes. If the fall was 30 m wide (it can hardly have been much wider given its elongated shape and *c.* 75 m length), the volume of debris would have been at the most about 15000 m^3, equivalent to

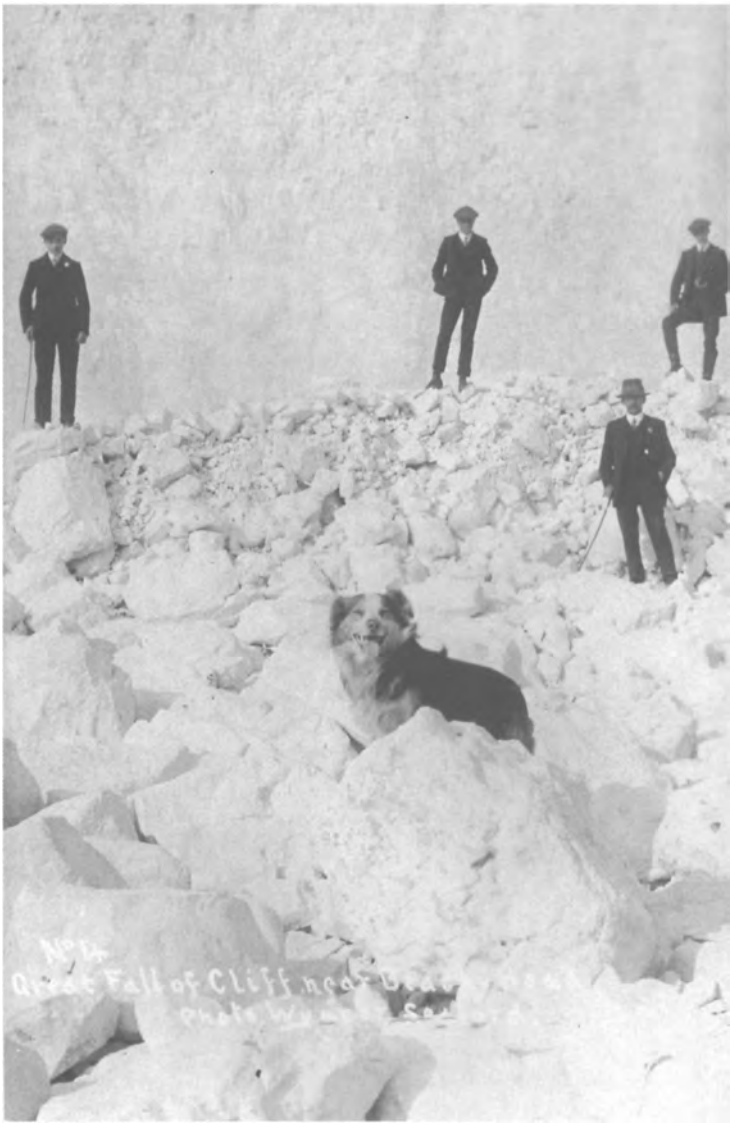

Fig. 4. The fourth Wynter postcard, providing a close-up view of the debris.

about 20000 tonnes of solid chalk. To justify an estimate of 200000 Imperial tons the fall would have needed to have been several hundred metres wide!

Predisposing factors

The factors that resulted in the unusually long run-out of the Went Hill fall are difficult to identify, partly because of the amount of time that has elapsed since the event. Almost certainly, however, the height of the cliff was important in determining the length of runout. Had the cliff been lower, the falling debris would have been less energized. If the top parts of the rock mass at Went Hill dropped 44–45 m in free fall, they could have reached a speed of 29–30 $m s^{-1}$ before hitting the shore. The impact doubtless shattered many of the descending joint blocks, creating quantities of chalk dust. Nevertheless, it is clear from the photographic evidence that the pulverization process was far from complete. Figure 4 shows four men standing close to the head of the fall amongst masses of broken chalk blocks. The largest blocks evidently have long dimensions of a metre or more. Big blocks are also

visible in Figure 3, mantling large areas of the fall including the toe. On the surface at least, the debris was seemingly no more pulverized than in ordinary cliff falls that do not exhibit long run-outs. Possibly the large blocks came from the top of the cliff and were carried seawards during the fall on a basal 'raft' of closely spaced, finer fragments, largely derived perhaps from the wreckage of the lower part of the cliff. A second factor determining the length of run-out is likely to have been the volume of the detached rock mass. In December 2000 there was a rock fall in almost the same place as the much larger 1914 fall. The debris formed a scree at the base of the cliff, extending seawards for only about 15 m. The volume of debris was 1000–1500 m^3, and the value of *H/L* about 2. It would appear that the fall had too small a mass to create a run-out, unlike its 1914 predecessor. Some other falls on the Went Hill stretch of coast in the 1930s and 1950s are recorded on picture postcards and they are also relatively small in volume and lacking in run-out.

The long run-out falls in Kent had estimated debris volumes of 25 000 to 1 million m^3 (Hutchinson 1988, 2002). The 1914 Went Hill fall with its estimated volume of 15 000 m^3 seems to have been significantly smaller than its Kentish counterparts and has a correspondingly shorter run-out.

The bedding, jointing and clay content of chalk greatly influences the character of cliff collapses (Pomerai 2000; Mortimore *et al.* 2001; Duperret *et al.* 2001). The Seaford Chalk exposed in the present-day cliff at Went Hill does not seem in any way exceptional, however. The fracture pattern and spacing is similar to that seen elsewhere along the Seven Sisters coast, as is the frequency of flint bands (averaging about one band per 1.4 m thickness of chalk). The clay content is very low. Falls frequently occur along this coast, some from an equivalent or greater height, but no others are known to have extended so far into the sea. The long run-out of the 1914 Went Hill fall cannot, therefore, be easily attributed to geological factors, though of course the rock removed by the fall may have had some special weakness that is now no longer visible.

Hutchinson (2002) has investigated the incidence of large cliff falls in chalk in Britain, France, Denmark and Germany, and argues that significant run-outs occur only where the porosity of the chalk exceeds about 40%. The porosity of the Seaford Chalk at the base of the Went Hill cliff is about 41%, close to Hutchinson's suggested threshold value. He notes that run-out falls are rare in Sussex compared with Kent, and attributes this to the generally lower porosity and greater strength of the Sussex chalk. Presumably, he considers that the porosity of most Sussex chalk is below 40%. This is perhaps questionable given the value for the chalk at the base of Went Hill. There is no evidence that this chalk is in any way anomalous.

Another factor contributing to the length of run-out may have been the cave recorded at the foot of the cliff. When the cliff fell into this basal cavity, the rock fragments may have gained more kinetic energy than if they had fallen or slid down the cliff face. The cavity may also have caused greater entrainment of air and thus more effective dispersal of the fragments. In addition, the collapsing chalk mass may have developed an unusually pronounced outward tilt, so that it fell like a collapsing canopy, trapping air (and possibly seawater) beneath it and imparting a seawards impetus to the falling debris. The vast majority of cliff falls on the Sussex chalk coast lack a significant toppling component and this may be why they fail to produce significant run-outs.

There is no evidence that freezing or thawing caused the 1914 cliff fall. The preceding winter was quite mild on the Sussex coast, with only occasional light frosts. However, the rains in February and March 1914 were heavier than normal, and this may well have helped trigger the cliff fall. At Eastbourne, about 6 km from Went Hill, the rainfall for these two months totalled 220 mm, about 28% of the average annual total. Records from other parts of Sussex tell the same story. At Hastings, for example, 232 mm of rain fell in February and March (D. Powell, pers. comm.), or about 32% of the average annual total. At Falmer, near Brighton, 259 mm fell in the same two months, or 29% of the expected annual total. The evidence suggests, therefore, that at the time of the fall the Went Hill cliff was more saturated than usual, which would have added to its weight and instability. The heavy rain doubtless also ensured that the joints in the rock were well lubricated. Whether it also promoted the run-out is more problematic, however. Winter 2000–2001, one of the wettest on record in Sussex, recorded an exceptional number of cliff falls, but none had long run-outs. Moreover, in 1914, even assuming 50 per cent pulverization on impact with the shore, it is difficult to envisage enough water being released from the void spaces in the rock to 'liquefy' the moving mass of debris on a such a scale that particle-to-fluid contacts predominated over particle-to-particle and particle-to-air contacts. Pockets of liquified material may have been created, particularly at its base, and this may have aided the flow of debris, but large-scale liquefaction seems most unlikely.

Another factor controlling the behaviour of the 1914 fall may have been the state of the tide. If the tide was covering the platform when the cliff fell, the expelled pore fluid could have been augmented with seawater, thus promoting greater than normal mobility. Also the sea surface could have assisted the debris to slide forwards. The first high tide on Easter Monday at Went Hill was around 0035 hours, the second at about 1255. Unfortunately, the precise time of the fall is unknown. The *Eastbourne Gazette* (22 April) reported that the occupants of the Birling Gap Hotel heard 'a sound like thunder' in the 'early hours of Easter Monday morning', whereas the *Chronicle* (25 April) described the fall as taking place 'during the night'. Despite the vagueness of these reports, it seems safe to conclude that at least part of the run-out from the fall was across water, but whether the sea covered the entire platform is less clear.

Process

It is evident that the fall from Went Hill on Easter Monday 1914 achieved a high degree of mobilization compared with other falls on the Seven Sisters coast. The best estimate that can be made of the length of the run-out would seem to be about 75 m. The drop can be estimated to have been 46–47 m (the height of the cliff above Ordnance Datum plus the difference in height between OD and the lowest point reached by the debris), giving an *H/L* value of around 0.62. This is substantially lower than the values generated by average-sized cliff falls on the Sussex chalk coast and below the threshold value of 0.78 suggested by the maximum angle of rest of coarse chalk debris. However, it lies within the range of values recorded by Hutchinson (1988) and Birch (1990) for cliff falls in Kent that exhibit run-out.

Hutchinson (1988) referred to the Kentish falls as 'flow slides', a term that he also used for the wet, slurry-like flows that have occurred in mining waste at Aberfan, South Wales, and elsewhere. He now (2002) refers to them as 'chalk flows' or 'flow slides'. Birch (1990) likened the falls to sturzstroms, as described by Heim (1882) and later writers. Sturzstroms are most common in high mountains where the volumes of failed rock can be huge and the run-outs several kilometres in length.

In his classic study of the massive sturzstrom at Elm in Switzerland, Heim (1882) suggested that the debris travelled forwards at high speed as a cohesionless stream of highly energized colliding blocks. In contrast, Shreve (1968*a*, *b*) suggested that the spectacular Blackhawk Landslide, and other historic, long-run-out flows in North America and elsewhere, moved long distances because they flowed on a basal cushion of trapped air. Kent (1966) also invoked the entrainment of air to explain long-run-outs and Goguel (1978) suggested that the vaporization of pore water was important.

It has since been shown that these alternative theories do not explain all cases (Howard 1973; Melosh 1987; Campbell 1989), notably lunar sturzstroms, and some refinement of Heim's original theory based on fragment dynamics still seems to be the most likely mechanism (Hsü 1975, 1978; Eisbacher 1979; Melosh 1987; Campbell 1989; Campbell *et al.* 1995; Kilburn & Sørensen 1998). Thus it would appear that in a sturzstrom, friction is reduced or eliminated because the break-up of the original rock mass on impact, and subsequent high-energy collisions within the moving debris, efficiently transmit motion from one fragment to another with little loss of energy. The 'flow' is non-viscous, highly turbulent and sufficiently dense to generate frequent collisions. A basal layer of pulverized rock dust may decrease basal friction, increase buoyancy and help facilitate very rapid movement of the colliding blocks (Kilburn & Sørensen 1998).

Although Hutchinson (1988) notes that the long run-out Kentish cliff falls bear some resemblance to sturzstroms, he goes on to argue that they are in fact entirely separate phenomena. In his view, sturzstroms are extremely rapid flows of very large volumes of relatively dry debris. The chalk cliff falls, by contrast, create relatively small amounts of much wetter debris. Impact collapse generates high pore-water pressures within the debris, leading to a high degree of fragmentation, and flow of the water-saturated fines.

The present authors agree with Hutchinson that excess fluid pressures may be produced in the pore water when chalk cliffs collapse, but whether long run-outs result from a wet flow mechanism or a dry flow remains questionable. There is no evidence from the photographs to show that any of the debris at Went Hill formed a wet slurry as required by Hutchinson's flow slide mechanism. A dry flow mechanism as envisaged for sturzstroms seems preferable. An intermediate condition of moisture is unlikely, as it would have created a sticky, pasty mass that would have tended to inhibit movement.

Melosh (1987) and Kilburn & Sørensen (1998) suggest that sturzstroms develop only when the volume of failed rock exceeds about a million m^3. This volume is thought to be required to release enough energy to separate the fragments during collapse so that collisions can play a major part in momentum transfer. That there is a threshold volume for sturzstroms seems highly likely, but the present authors are unaware of any theoretical grounds for supposing that it is as large as a million m^3 and not, say, 12 500 m^3. In any case, the energy generated during a cliff collapse is dependent not just on the volume of failed rock but also on the drop height, *H*. It is to be noted that the *H/L* value for sturzstroms is typically about 0.5 for failures of around million m^3, reducing to as little as 0.1 for massive failures of a cubic kilometre or more (Kilburn & Sørensen 1998). On this basis the 1914 fall at Went Hill comes very close to qualifying as a sturzstrom, and clearly does so if its relatively small size is taken into account.

Conclusion

Although there can be no certainty about the precise nature of the 1914 cliff fall, the evidence suggests that it resembled a sturzstrom event: a small-scale version of the spectacular failures normally associated with high mountain terrain. That it and other historic long run-outs in Kent (Hutchinson 1988, 2002; Birch 1990) have been generated by relatively modest sized falls of chalk from sea cliffs in areas of otherwise quite gentle relief poses an interesting geotechnical anomaly.

If the identification of the Went Hill fall as a sturzstrom-type failure is correct, the minimum volume of detached rock required to trigger this type of mass movement is 1–2 orders of magnitude less than is claimed by Melosh (1987) and Kilburn & Sørensen (1998).

The Went Hill fall invites comparison with the much discussed January 1999 fall at Beachy Head, which yielded significantly more chalk debris than its 1914 counterpart. The British Geological Survey (1999) estimate that 50 000–100 000 tons of chalk debris descended on the shore, but Duperret *et al.* (2001) suggest that the volume was around 150 000 m^3 (which presumably equates to about

180000 tons). The debris did not quite reach the lighthouse, contrary to the impression fostered by some newspaper photographs. The length of run-out (between 70 and 90 m) was about the same as at Went Hill, or a little greater, but the drop (about 120 m) was three times as large, giving a *H/L* value well in excess of 1.0, far outside the range for sturzstroms. The debris exhibited a longer than average run-out with a relatively low gradient surface and there may have been some sturzstrom-type collisions between the moving debris. However, the run-out was relatively modest given the height of the cliff and the amount of energy that would have been released. The Went Hill fall was a much more mobile event as measured by its *H/L* value.

According to Eastbourne residents (and an undated magazine clipping) there was a fall of about 20000 tons of chalk from Beachy Head in the 1960s that had an appreciably longer runout than the 1999 fall. The debris actually reached the lighthouse, leaving chalky impact marks on the walls of the lighthouse and filling the rooms with dust. It would be interesting to learn more about this poorly recorded event, and in particular to determine the *H/L* value.

The precise conditions necessary for a fall of chalk to develop a long run-out remain uncertain, but they evidently occur only very infrequently, generally after a period of heavy rainfall. Possibly, a low tide and a wide shore platform are important. Impacting with seawater may check many potential long-run-out falls, and may indeed have checked the Went Hill fall. Like many of the Kent falls the Went Hill fall occurred in the first quarter of the 20th century. Presumably, there were specific climatic triggers, but they have not yet been identified. Unlike many of the Kentish falls, the fall at Went Hill was generated by a cliff of relatively modest height. The volume of debris was also much smaller than in the case of the Kentish falls.

Fortunately for the many holidaymakers who frequent chalk coasts, cliff falls normally have quite restricted runouts. By not walking or sitting close to the cliffs one can greatly reduce the risk of being hit by falling debris. The Went Hill event, however, demonstrates that even 75 m from the cliff base there is a possibility of death or injury.

Acknowledgements. The authors are very grateful to D. Puttick and J. Puttick for the loan of several of the postcards and for invaluable information on cliff erosion in the Eastbourne area. They also wish to thank R. Mortimore, M. de Pomeroi and A. Duperret for much helpful advice. In addition they are indebted to J. N. Hutchinson for valuable comments and a preview of his 2002 paper on chalk cliff falls in Europe.

References

BIRCH, G. P. 1990. Engineering geomorphological mapping for cliff stability. *In*: *Chalk: Proceedings of the International Chalk Symposium, Brighton, 1989*. Thomas Telford, London, 545–549.

BRISTOW, C. R., MORTIMORE, R. N. & WOOD, C. J. 1997. Lithostratigraphy for mapping the Chalk of southern England. *Proceedings of the Geologists' Association*, **108**, 293–315.

BRITISH GEOLOGICAL SURVEY 1999. Rockfall at Beachy Head, south coast of Britain. World Wide Web Address: *www.bgs.ac.uk/bgs/w3/beachy/beachy.htm*.

CAMPBELL, C. S. 1989. Self lubrication for runout landslides. *Journal of Geology*, **97**, 653–665.

CAMPBELL, C. S., CLEARY, P. W. & HOPKINS, M. 1995. Large-scale landslide simulations, global deformation, velocities and basal friction. *Journal of Geophysical Research*, **100**, 8267–8283.

CLEEVE, J. & WILLIAMS, R. B. G. 1987. *Cliff erosion in East Sussex*. GEMS, University of Sussex, Brighton.

DALES, D. & GILBERT, K. 1998. Wind and water. *In*: BARNE, J. H., ROBSON, C. F., KAZNOWSKA, S. S., DOODY, J. P., DAVIDSON, N. C. & BUCK, A. L. (eds.). *Coasts and Seas of the United Kingdom, Region 8 Sussex, Rye Bay to Chichester Harbour*. Joint Nature Conservation Committee, Peterborough, 25–27.

DORNBUSCH, U. 2001. Mean annual retreat rates of the undefended chalk cliffs of East Sussex, 1873 to 1999. *In: Beach Sustainability in East Sussex*. Interim report of the English Partner, BERM project. University of Sussex, Brighton.

DUPERRET, A., GENTER, A., MORTIMORE, R. N., LAWRENCE, J. A. & MARTINEZ, A. 2001. A classification of chalk cliff failures, based on recent cliff collapses along the Channel coasts of England and France. Abstract, *International Conference on Coastal Rock Slope Instability: Geohazard and Risk Analysis*. Le Havre, France, 18–19.

EISBACHER, G. H. 1979. Cliff collapse and rock avalanches (sturzstroms) in the Mackenzie Mountains, northwestern Canada. *Canadian Geotechnical Journal* **16**, 309–334.

GOGUEL, J. 1978. Scale-dependent rockslide mechanisms, with emphasis on the role of pore fluid vaporization. *In*: VOIGHT, B. (ed.) *Rockslides and Avalanches, 1: Natural Phenomena*. Elsevier, Amsterdam, 693–708.

HEIM, A. 1882. Der Bergsturz von Elm. *Zeitschrift der Deutschen geologischen Gesellschaft*.

HEIM, A. 1932. Bergsturz und Menschenleben. Fretz und Wasmuth: Zurich (English translation by Skermer, N.A. 1989. *Landslides and Human Lives*. BiTech Publishers, Vancouver, BC.)

HOWARD, K. E. 1973. Avalanche mode of motion, implication from lunar examples, *Science*, **180**, 1052–1055.

HSÜ, K. J. 1975. On sturzstroms – catastrophic debris streams generated by rockfalls. *Geological Society of America Bulletin*, **86**, 129–140

HSÜ, K. J. 1978. Albert Heim: observations on landslides and relevance to modern interpretations. *In*: VOIGHT, B. (ed.) *Rockslides and Avalanches, 1: Natural Phenomena*. Elsevier, Amsterdam, 69–93.

HUTCHINSON, J. N. 1972. Field and laboratory studies of a fall in Upper Chalk cliffs at Joss Bay, Isle of Thanet. *In:* PARRY, R. H. G. (ed.). *Stress Strain Behaviour of Soils*. Foulis, Henley on Thames, 692–706.

HUTCHINSON, J. N. 1980. Various forms of cliff instability arising from coast erosion in the UK. *Fjellsprengningsteknikk – Bergmekanikk – Gesteknikk* 1979, 19.1–19.32. Trondheim; Tapir for Norsk Jord-og Fjelltekmisk Forbund tilknyttet NIF.

HUTCHINSON, J. N. 1983. *Engineering in a Landscape*. Inaugural Lecture, 9 October 1979. Imperial College of Science and Technology, University of London.

HUTCHINSON, J. N. 1988. General report: morphological and geotechnical parameters of landslides in relation to geology and

hydrology. *Proceedings of the 5th International Symposium on Landslides, Lausanne*. Balkema, Rotterdam, **1**, 3–35.

HUTCHINSON, J. N. (2002). Chalk flows from the coastal cliffs of northwest Europe. *In*: EVANS, S. G. & DEGRAFF, J. V. (eds) Catastrophic landslides: effects, occurrence, and mechanisms. *Geological Society of America Reviews in Engineering Geology*, **15**, 257–302.

KENT, P. E. 1966. The transport mechanism in catastrophic rockfalls. *Journal of Geology*, **74**, 79–83.

KILBURN, C. R. J. & SØRENSEN, S-K. 1998. Runout lengths of sturtzstroms: The control of initial conditions and of fragment dynamics. *Journal of Geophysical Research*, **103**, B8, 17877–17844.

MARTINEZ, A., DUPERRET, A., GENTER, A., MORTIMORE, R. N., DE POMERAI, M. R., PIFFARD, E. & DELACOURT, B. 2001. Pre-existing fracture pattern along the chalk cliff coast in East Sussex (UK), Upper Normandy and Picardy (France) regions. Abstract, *International Conference on Coastal Rock Slope Instability: Geohazard and Risk Analysis, Le Havre, France*, 13–14.

MAY, V. J. 1971. The retreat of chalk cliffs. *Geographical Journal* **137**, 203–206.

MAY, V. J. & HEEPS, C. 1985. The nature and rates of change on chalk coastlines. *Zeitschrift für Geomorphologie, Supplementband*, **57**, 81–94.

MELOSH, H. J. 1987. The mechanics of large rock avalanches. *Review of Engineering Geology VII*, 41–49.

MORTIMORE, R. N. 1997. *The Chalk of Sussex and Kent*. Geologists' Association, London.

MORTIMORE, R. N., DUPERRET, A., WATREMEZ, P., LAWRENCE, J. A. & MARTINEZ, A. 2001. Risk of chalk cliff collapse on the Channel coast. Abstract, *International Conference on Coastal Rock Slope Instability: Geohazard and Risk Analysis. Le Havre, France*, 9–10.

POTTS, A. S. & BROWNE, T. J. 1983. The climate of Sussex. *In*: *Geography Editorial Committee. Environment, Landscape and Society*. Sutton, Gloucester, 88–108.

POMERAI, M. R. de. 2000. Risk of cliff collapse (ROCC). World Wide Web Address: *www.bton.ac.uk/environment/ROCC*.

ROBINSON, D. A. & WILLIAMS, R. B. G. 1983. The Sussex coast past and present. *In: Geography Editorial Committee. Environment, Landscape and Society*. Sutton, Gloucester, 50–66.

SHREVE, R. L. 1968*a*. The Blackhawk Landslide. *Geological Society of America Special Paper* **108**.

SHREVE, R. L. 1968*b*. Leakage and fluidisation in air-layer lubricated avalanches. *Geological Society of America Bulletin* **79**, 653–658.

SOUTH DOWNS COASTAL GROUP 1996. *South Downs Shoreline Management Plan – Selsey Bill to Beachy Head*. Gifford and Partners.

Geological Society, London, Engineering Geology Special Publications

Prediction of nearshore wave energy distribution by analysis of numerical wave model output, East Sussex coastline, UK

S. B. Mitchell and D. J. Pope

Geological Society, London, Engineering Geology Special Publications 2004; v. 20; p. 99-107
doi:10.1144/GSL.ENG.2004.020.01.07

Prediction of nearshore wave energy distribution by analysis of numerical wave model output, East Sussex coastline, UK

S. B. Mitchell & D. J. Pope

Hydraulic Engineering Research Unit, School of the Environment, University of Brighton, Lewes Road, Brighton, BN2 4GJ, UK

Abstract: Prediction of wave energy distribution in coastal areas is necessary if an assessment of the likelihood of cliff collapse is to be undertaken. Use has been made of numerical modelling to predict relative wave heights along the chalk cliff coastline of East Sussex between Brighton and Eastbourne, UK. In this study, wave modelling has been undertaken using the University of Delaware REFDIF-1 software with a 100 m mesh size to predict nearshore wave heights for boundary unit wave height conditions from a range of different incident directions. The results from this wave modelling have been combined with the frequency distribution of incident waves obtained from analysis of time series of 12 years of hindcast wave data in the English Channel, obtained from the UK Meteorological Office. The resulting distribution of nearshore wave heights is presented as a surrogate for the distribution of wave energy over the 12-year period. Some concern exists about the quality of the output data, in particular of the effect of the relatively coarse bathymetry grid used for the model. Some wave focusing is evident from the model output, caused by the presence of local shoals in the model grid, leading to a 'banding' effect in the model output. Some suggestions are made for the improvement of the modelling scheme, including the use of finer mesh size, bathymetric smoothing and the use of a spectral model such as REFDIF-S.

Introduction

There is a pressing need for coastal scientists and engineers to be able to access good quality data concerning the distribution of wave energy along coasts that are exposed to wave attack. With the threat of changing weather patterns and rising sea levels, an assessment is required of the likely impact of storms on these sections of coast in terms of their effects on the integrity of natural and artificial coastal defences. One of the principal aims of the ROCC (EU-INTERREG II funded Risk of Cliff Collapse) project was to assess these risks in terms of a hazard map showing the risk to existing cliffs along the stretch of East Sussex coast between Brighton and Eastbourne in southern England, UK. The distribution of wave energy along this coastline would appear to be of key relevance in producing such a hazard map, and could be combined with other geophysical and hydrological data concerning cliff stability, in order to provide data on the risk of cliff failure. The use of numerical mathematical models in this analysis would seem to be of paramount importance in assessing the cumulative impact of offshore wave energy. This is generated by successive storm events on the shoreline. This model output may be combined with the frequency distribution of wave height and direction data to provide an overall representation of the likely distribution of wave energy over a long time period.

Recent concern about the effects of increased storminess and sea-level rise have led to a perceived need to study the interaction between wave energy and coastal erosion rates in more detail. Recent work by Hall *et al.* (2000), for example, has suggested a probabilistic approach to assessing the risk associated with cliff recession. In this way, cost-benefit analyses may be undertaken in a more rigorous way, whenever new coastal development is planned. An important case study for a section of the East Anglia coast (Burgess *et al.* 2000) demonstrated the need for an integrated approach using different numerical hydrodynamic and sediment transport models to predict net sediment movements in the cross-shore and long-shore directions. Some consideration of the impact of wave energy was given in a recent study of cliff recession rates in Italy (Budetta *et al.* 2000), which additionally considered the relative importance of some of the likely geophysical cliff failure mechanisms. In these and similar analyses, relatively little attention has been paid to the nearshore wave transformation processes occurring as a result of refraction and bottom friction. Likewise, the effect of these waves on the shoreline in relation to their relative frequency of occurrence needs closer investigation. Several numerical models have been described (e.g. Berkhoff *et al.* 1982; Kirby & Dalrymple 1983; Li 1994; Monbaliu *et al.* 2000). These or other similar models may be used to investigate the impact of waves from different incident directions relative to the shoreline. Many models of this type have been successfully calibrated and are in use by coastal engineers and researchers worldwide.

The results from a numerical wave modelling study are used here to predict a wave energy impact factor along an important stretch of coast in Southern UK. This approach may be used as a surrogate for the likely distribution of wave energy caused by waves approaching from a given direction. If the frequency of occurrence of waves from this direction is also known, this will provide a measure of the likely wave

From: MORTIMORE, R. N. & DUPERRET, A. (eds) 2004. *Coastal Chalk Cliff Instability*. Geological Society, London, Engineering Geology Special Publications, **20**, 99–107. 0267-9914/04/$15.00

energy caused by this particular wave condition. If this exercise is repeated for all incident wave directions and offshore wave heights, a preliminary estimate of the total nearshore wave energy may be obtained. However, in order to reduce computation and data processing time for this preliminary study, only a small selection of input wave heights was considered for this preliminary analysis.

It is recognized that the key mechanisms relating nearshore wave height to cliff collapse are highly complex. These are related to the structure and geology of the cliff, the degree of saturation of the cliff material and the degree of abrasion by sediment at the base of the cliff. These factors have been the subject of other investigations (Brossard 2001; Budetta *et al.* 2000; Benumof *et al.* 2000). Nevertheless, it is suggested both here and elsewhere (Andrade *et al.* 2001) that the predicted data yielded by such an exercise is a useful measure of the likelihood of different wave energies impacting on a particular stretch of coast. This information may then be used, in conjunction with other data on cliff recession rates, hydrological data and rock structure, to begin to develop an improved overall understanding of the risk of a particular stretch of cliff collapsing.

In order to assess the relative risk of cliff collapse due to wave attack in a particular coastal zone, it was decided to carry out a preliminary study using statistical analysis of wave data and numerical wave modelling, based on a short stretch of coast between Brighton and Eastbourne, Southern UK.

Methodology

Wave data from 11 sites in the English Channel/Manche were obtained from the UK Meteorological Office (UKMO). Data were provided at three-hourly intervals of spectral energy density (S) and direction for a range of different principal frequencies over the period of available data (15 June 1988 to 22 March 2000). These data had been derived by the UKMO through an advanced wave hindcasting model (*http://www.met-office.gov.uk/research/ocean/climate/development.html*), using observed wind speed and direction data for the area. The location of each of the sites is shown in Figure 1. A detailed map showing locations along the coast referred to in this paper is given in Figure 2.

Processing of the raw wave data was carried out in the following sequence:

- calculation of representative time series of wave parameter data in terms of significant wave height (H_s), zero-upcrossing period (T_z) and predominant direction;
- classification of resultant time series to provide a 'wave rose' at each reference position.

By calculating the spectral moments of these wave frequency data using a method outlined in Chadwick & Morfett (1998), a time series of H_s, T_z and wave direction at three-hourly intervals was obtained for each of the sites. It was assumed that:

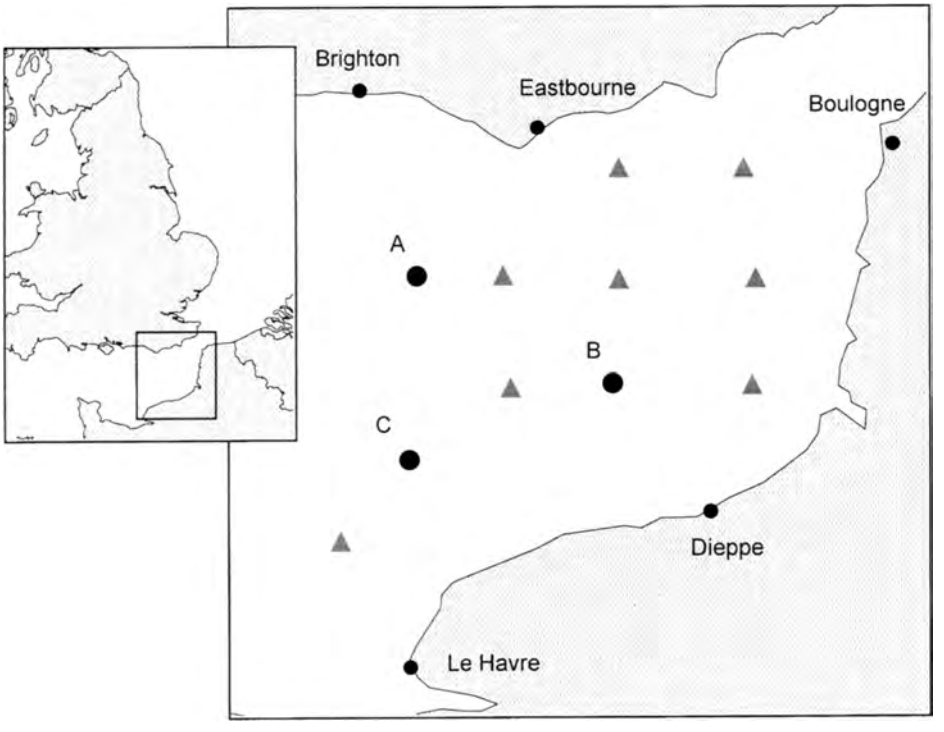

Fig. 1. Location of UKMO data points. Triangles are points not referred to in the text.

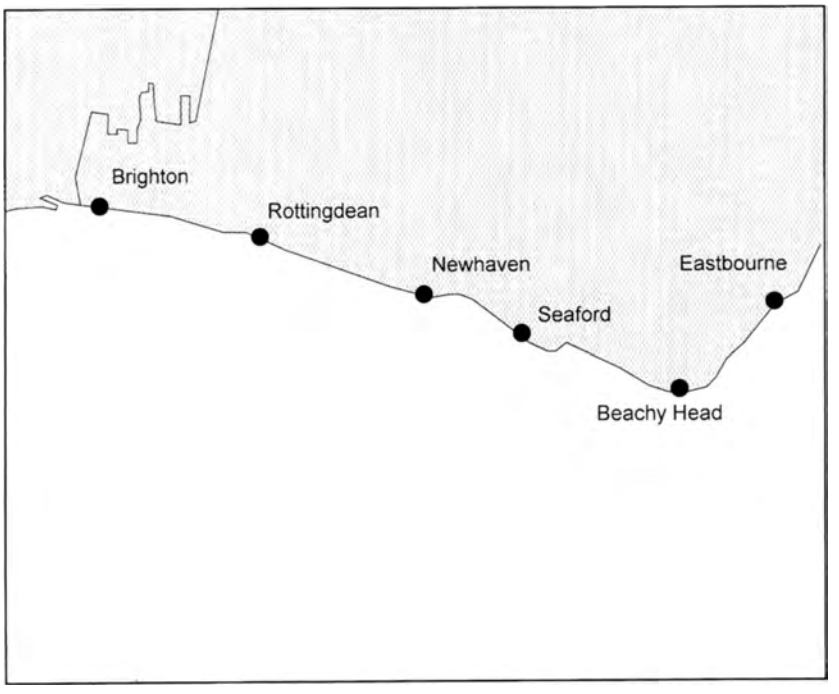

Fig. 2. East Sussex Coast: Brighton to Eastbourne.

$$H_s = 4(m_0)^{0.5}$$

$$T_z = \left(\frac{m_0}{m_2}\right)^{0.5}$$

where m_n is the nth spectral moment, calculated from the k different wave frequencies given at each time interval, i.e.

$$m_n = \sum_{i=1}^{k} S(f_i) f_i^n$$

The wave direction at each time interval was taken as being coincident with the direction of the wave frequency having the greatest energy density.

An example of a time series of wave data obtained using this method is shown in Figure 3, for location *A*.

The time series obtained in this way was analysed in order to obtain the relative frequency of waves of different heights and directions, by separating the data into classes depending on wave height and direction (a 'wave rose'). The wave rose diagrams obtained for the three points *A*, *B* and *C* are shown in Figure 4. These show that at all three sites, the predominant wave condition is from the southwest or west. For the case of the point *A*, off the English coast, the predominant wave direction is within the sector 240°N ± 15°, and for locations *B* and *C*, off the French coast, the predominant wave direction was in the sector 270°N ± 15°.

Wave modelling

Although several commercially available regional wave models exist and have been reviewed in Li (1997), wave modelling was carried out for this study using a numerical model (REF-DIF 1) designed by the University of Delaware (Kirby & Dalrymple 1983, and see website reference below). This is a monochromatic wave model, which takes into account the effects of bed friction, wave refraction and wave breaking in calculating wave height and direction on a user-defined grid covering the area of interest.

For this study, it was decided to obtain data predicted by the model of nearshore wave heights for a range of input wave conditions. Although a larger number of input conditions would be required for a more comprehensive study of this type, it was decided to select only a few representative cases for this preliminary analysis. Due to the time required to set up each model run, it was possible only to carry out a limited number of model runs using representative boundary conditions. Waves approaching from directions greater than 240°N, or less than 120°N, were not modelled, as these would probably have only limited impact on the UK shoreline. Only one wave period (7 s) was chosen, this representing an approximate median wave period for the offshore conditions described above (see Table 1). A unit wave height was used at the model boundary throughout for simplicity, and as a means for investigating generic wave transformation processed in the modelled area.

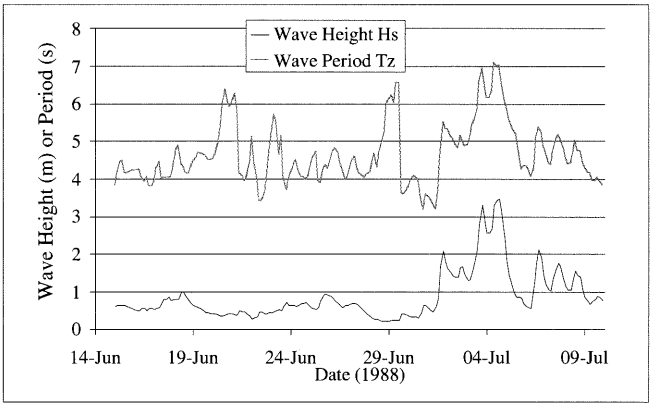

Fig. 3. Example wave data for location *A* on figure 1.

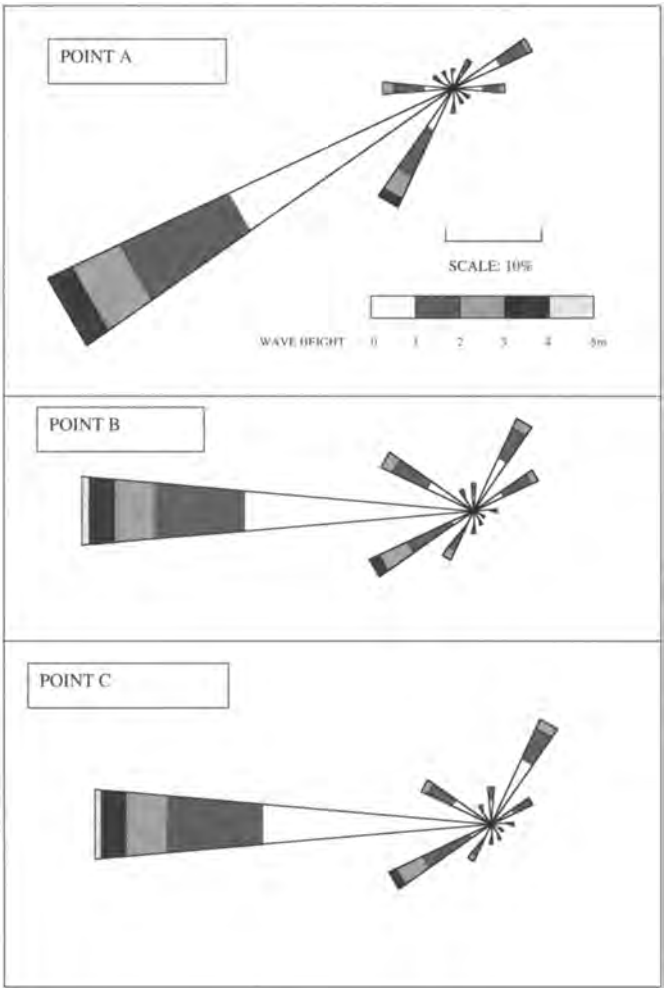

Fig. 4. Wave rose showing distribution of wave frequency. See Fig. 1 for locations.

Bathymetric data for the area were obtained by digitizing water depths from Admiralty Chart SC 1652 (2000) and Admiralty Chart SC 0536 (2000). A rectangular grid was obtained by application of a surface-fitting program to the data. The principal grid used for the study was 361×316 nodes, covering a rectangular area bounded by the grid lines 530000E–566000E, and 73500N–105000N (Fig. 5). The grid spacing was maintained constant throughout the different bathymetric configurations used, at 100m. The grid therefore covered an area including the entire coastline between Brighton and Eastbourne. For model runs using input wave data from directions other than 180°N, the grid was rotated such that the wave direction was parallel to the wave-generating boundary. For simplicity a constant water level was used throughout of 3.5m above chart datum, which was approximate mean sea level. Computer runs were carried out on a stand-alone PC with a processor speed of 500 MHz and 64 MB RAM.

Analysis of wave energy distribution at coastline

An example of typical wave model output produced is shown in Figure 6. From this data set, nearshore wave height data was obtained by identifying the wave heights in known depths of water (approximately 5m throughout for the mean sea level selected) at specified locations along the coastline. These wave heights are listed in Table 2, and shown graphically in Figure 7.

The wave heights obtained from the modelling in this way represent the relative wave energy reaching the coastline caused by a unit wave height from each of the five wave directions tested. It was not possible to obtain data for some of the sites nearest the Brighton end of the model area for all the wave directions; this was due to insufficient coverage of the grid after rotation parallel to the wave generating boundary. These nearshore wave heights may be considered as wave height multiplication factors (*WHF*). Hence, a 2.0m wave approaching from the 120° direction at Rottingdean (see Fig. 2), for example, would be predicted as having a wave height of (2×0.79)=1.58m. It must be emphasized that the wave transformations affecting waves of 2.0m wave height may not be linearly related to those affecting a 1.0m wave, but for simplicity this assumption is made. Similar procedures could be followed for any incident wave height from any direction.

Table 1. *Input wave conditions selected for REF-DIF 1 model*

Wave Height (m)	*Wave direction (°N)*	*Wave Period (s)*
1	120	7
1	150	7
1	180	7
1	210	7
1	240	7

Thus by combining the wave rose data with the model output for nearshore wave heights, an overall picture of the distribution of nearshore wave energy may be obtained using:

$$\text{Wave Energy Risk Factor} = \Sigma(WHF \times H \times P(H))$$

where H is the modelled wave height and $P(H)$ is the probability of that wave height from that direction occurring, obtained from the wave rose analysis described earlier.

The distribution of wave height factors along the stretch of coastline under investigation is shown in Figure 8. Sensitivity tests using different grid mesh sizes, as outlined below, suggest that an accuracy of ±10% is appropriate. These lines are also shown on Figure 8.

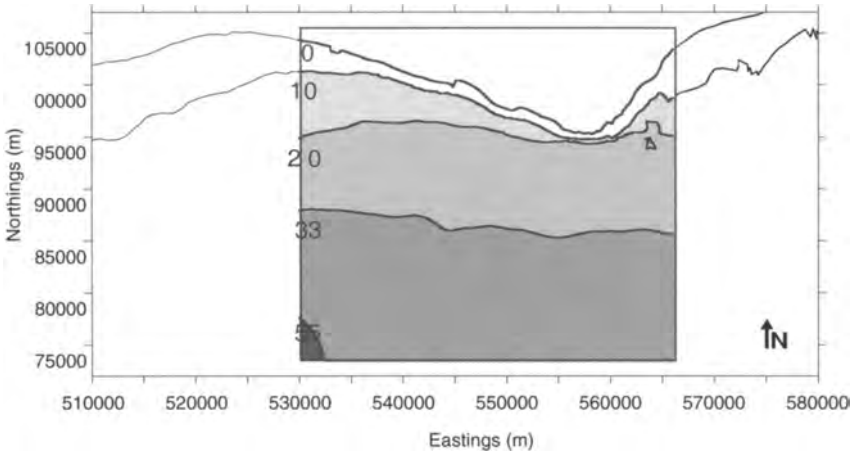

Fig. 5. Model grid bathymetry (Wave Direction 180°N Only). Contour depths are in m below Admiralty Chart datum.

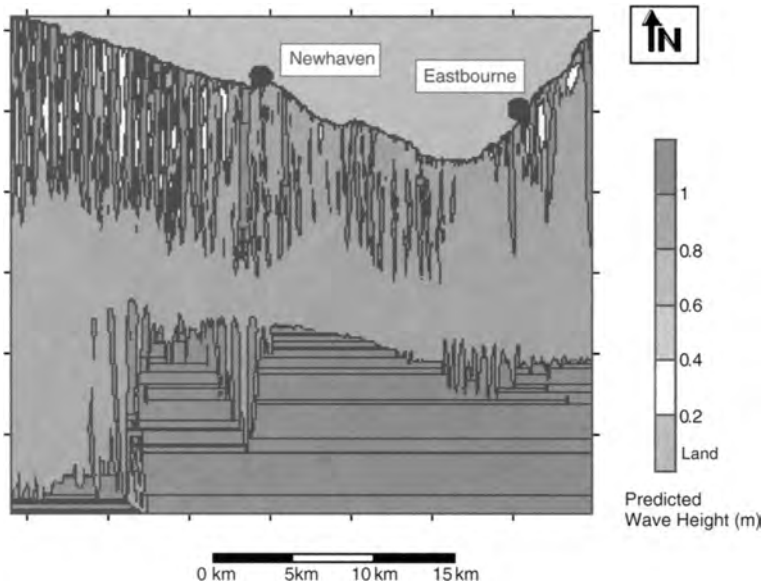

Fig. 6. Predicted wave height for waves approaching from 180 degree direction using REFDIF 1 model. Boundary wave height 1.0m, period = 7 sec.

Table 2. *Wave Height Factors obtained from numerical modelling. For locations see Fig. 2*

Point No.	*Location*	*Direction (°N)*					
		chainage (km)	*120*	*150*	*180*	*210*	*240*
1	Brighton (Palace Pier)	0.00			0.84		
2	Brighton marina	2.66		0.97	0.87		1.02
3		4.31	1.08	0.98	1.13	0.99	1.02
4	Rottingdean	5.89	0.79	1.07	0.77	0.87	0.99
5	Portobello, Telscoombe Cliffs	8.42	1	0.87	0.94	0.93	1.11
6	Peacehaven (meridian)	10.13	1.02	0.88	0.95	0.86	0.66
7		12.31	0.71	0.95	0.8	0.99	0.79
8	Newhaven (mouth of harbour)	14.41	1.35	0.95	0.82	1.06	0.67
9		16.31	0.46	1.12	1.14	0.7	0.78
10	Seaford (start of cliffs)	18.79	1.05	1.05	0.94	0.77	0.9
11		20.24	1.31	0.99	0.97	1.03	1.07
12	Cuckmere Haven (mouth of river)	21.75	0.82	0.92	0.79	1.15	0.85
13		23.81	0.99	0.92	0.94	0.9	0.93
14	Birling Gap (steps)	26.00	0.98	0.91	1.04	0.98	0.81
15	Beachy Head	28.82	0.99	0.91	0.86	1.02	1.09
16		30.83	0.87	0.79	0.98	1.14	0.87
17	Eastbourne (Pier)	33.52	0.87	0.76	0.69	0.95	0.26

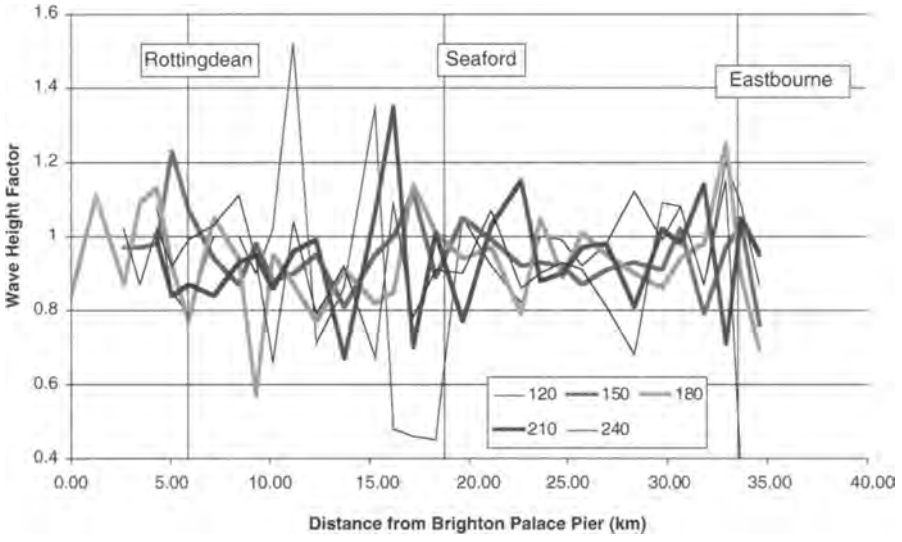

Fig. 7. Distribution of predicted nearshore wave heights for different boundary incident wave directions.

Discussion of results

Whilst these results form a useful starting point on which to base a risk analysis for the impact of wave action along the shoreline, it is clear that there are some shortcomings in the model setup that need to be addressed in the future. The model results shown in Figure 6 suggest that considerable variations in nearshore wave height existed for a given input wave condition. The reasons for this, and suggested remedies, are outlined below.

Grid size

Due to the complexities involved in setting up a model of this type, a grid was selected having a relatively coarse mesh size, which needed to be sufficiently large to enable complete coverage of the area under investigation. Furthermore, the maximum number of nodes allowed in the model area was 400×400, thus limiting the minimum mesh size for complete coverage of the area in one model run. The grid size used in the numerical model was 100 m. A sensitivity analysis was carried out using a finer mesh size, to investigate the degree to which the mesh size affected the model results. The two grids used for this analysis used a mesh size of 50 m and 20 m. A comparison of the output at two nearshore points from model runs using the three different grid sizes is given in Table 3. This sensitivity testing to different model features suggests that reducing the grid size can affect model output. Further work would be needed to investigate this feature more fully, and in the light of other factors such as those outlined in the following sections.

Bed Roughness

It was evident from the modelling results that sudden changes in the bathymetry in the nearshore region has caused focusing of the wave energy, so that abnormally high waves are predicted at the shore line. This occurs when wave fronts are refracted around a local shallow area in the model bathymetry, causing superposition of waves in the region downstream of the shallow point. Although this phenomenon has been demonstrated both in physical and numerical models on many occasions (Berkhoff *et al.* 1982; Li 1994), in this exercise, wave focusing leads to over-prediction of wave height in many locations in 'bands' perpendicular to the shoreline (Fig. 6). In order to remedy this, more careful consideration would need to be given to the modelling methodology. A number of issues should be addressed, as outlined below:

- It may be necessary to 'smooth out' the bathymetry using an averaging process. In this way, the impact of local 'shoals' of shallower bathymetry on model results could be reduced. Careful consideration would then have to be given to the effect of this on the accuracy of the area altered. The orientation of the model grid will also effect the accuracy implications of this.
- Some use could be made of the spectral model (e.g. REFDIF-S (University of Delaware)). This model utilizes a range of different input wave directions and periods, centred on the single boundary condition selected. The final output is calculated by taking a mean of different wave model outputs from the spread of different wave directions and period selected. In this way the wave focusing effect of

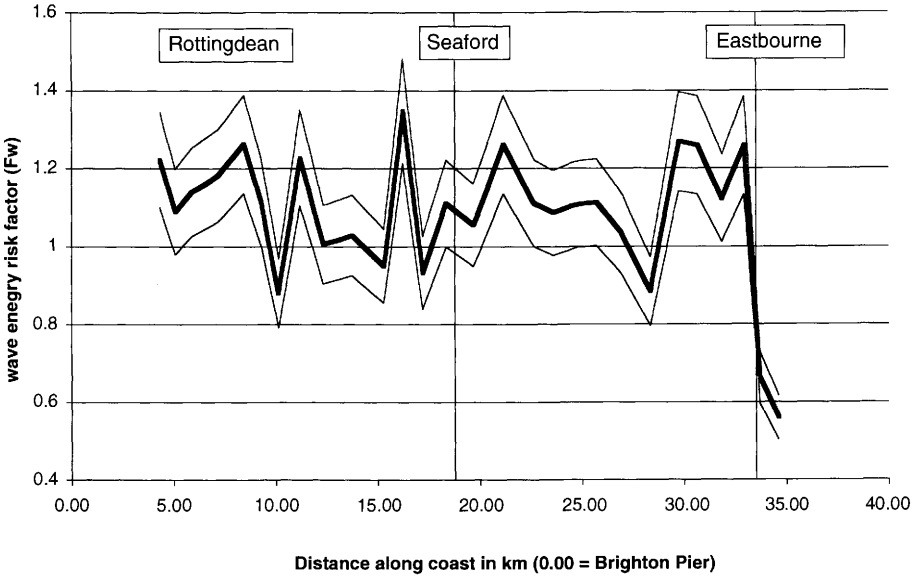

Fig. 8. Distribution of combined rish factors including +/−10% Lines.

Table 3. *Wave Height Factors using different mesh sizes*

Point No.	*Location*	*Grid size (m)*			
		chainage (km)	*100*	*50*	*20*
10	Seaford (start of cliffs)	18.79	0.94	1.04	
11		20.24	0.97	1.08	
12	Cuckmere Haven (mouth of river)	21.75	0.79	0.65	
13		23.81	0.94	0.92	
14	Birling Gap (steps)	26.00	1.04	0.97	0.89
15	Beachy Head (behind lighthouse)	28.82	0.86	0.87	0.86

local shoaling described above may be reduced and a more realistic distribution of predicted wave heights could be obtained (Li *et al.* 1993).

- Use of a smaller grid size, as discussed in the previous section, although it is recognized that this will not remove the wave focusing effect.

Any further work carried out using one or more of the above approaches should also take into consideration the inter-relationships between the different approaches. There is also a need to implement either or both of two strategies. Either it is necessary to increase the time and computational resources available to the problem (i.e. by reducing the grid size) and/or by the introduction of some sort of averaging process (i.e. by smoothing the bathymetry or using a spectral version of the model). This continues to be the case despite recent advances in modelling techniques and data processing technology.

Input Data

For the scheme used, only a limited number of input parameters were considered for the model. Thus a single water level, representing mean sea level (only) was used. At deeper water levels, it is likely that the degree of wave attenuation predicted by the model in the nearshore region by wave breaking would be reduced. In addition, only one wave period was considered. In future work, it is therefore strongly recommended that a wider range of input parameters be used in the model.

Conclusions

A preliminary study has been undertaken to predict the risk of cliff collapse due to wave attack. The coast between Brighton and Eastbourne, Southern UK, is used as a case study. A number of conclusions result from the study.

1. Using hindcast wave data obtained from the UK Meteorological Office, a frequency distribution, in the form of a wave rose, has been produced for a particular location off the English coast, and two points off the French coast. Off the English coast, the predominant wave direction was in the sector 240°N ± 15°; Off the French coast, the direction was in the sector 270°N ± 15°.

2. The monochromatic wave transformation model (REFDIF-1) has been used to predict the nearshore wave heights for unit boundary wave heights from a range of offshore directions, using a fixed wave period.
3. The results of the wave modelling have been combined with a frequency analysis to produce a risk diagram showing the relative risk factors along the stretch of coastline under investigation.
4. This study could form the basis of future investigations to refine the predicted risk factors for the study area, and other similar areas. In particular, it is suggested that one or more of the following approaches is adopted:
   - use of finer mesh size;
   - use of spectral model (REFDIF-S);
   - adoption of bathymetric smoothing;
   - modelling using a wider range of input wave heights, periods and water levels.

Furthermore, it is anticipated that future studies will also investigate the long-term impact of patterns of wave energy distribution along stretches of coastline. For example, data on observed, long-term cliff recession rates could be correlated with the model output described above, in order to provide an initial estimate of the significance of wave attack to historical patterns of shoreline erosion. Such an investigation could also provide highly significant data on the effectiveness of sea defences.

Despite the limitations of the results obtained, it is believed that this method for assessing wave energy distribution shows considerable promise in delivering useful data to coastal managers, and could be replicated at other coastal sites.

Acknowledgements. This project was part funded by the EU under the INTERREG-II 'ROCC' project. The authors would like to thank Brighton and Hove council and Lewes District Council for their additional support in purchasing wave data. The assistance of the REF-DIF developers at the University of Delaware, and Pierre Watremez and his colleagues at BRGM, Brest, France for their help in developing the methodology described in the paper, is also gratefully acknowledged.

References

ANDRADE, C., BARATA, A., HENAFF, A. & VILLANUEVA, G. 2001. Possible causes of regional variations in shore platform morphology and rates of downwearing on European coasts: oceanographic factors. *European Rock Coasts, 17–18 December 2001, Brighton, UK.*

BENUMOF, B. T., STORLAZZI, C. D. & GRIGGS, G. B. 2000. The relationship between incident wave energy and seacliff erosion rates: San Diego County, California. *Journal of Coastal Research* **16** (4), 1162–1179.

BERKHOFF, J. C. W., BOOY, N. & RADDER, A. C. 1982. Verification of numerical wave propagation models for simple harmonic linear water waves. *Coastal Engineering* **6**, 255–279.

BROSSARD, J. 2001. Marine factors of cliff erosion along upper Normandy coastline. *International Conference on Coastal Rock Slope Instability: Geohazard and Risk Analysis, 30–31 May 2001, Le Havre, France.*

BUDETTA, P., GALIETTA, G. & SANTO, A. 2000. A methodology for the study of the relation between coastal cliff erosion and the mechanical strength of soils and rock masses. *Engineering Geology*, **56**, 243–256.

BURGESS, K. A., PARSONS, A. P., JAY, H., BURCHETT, S. M. & MITCHELL, S. B. 2000. Development and application of a geomorphic model for analysing (shoreline change and) the impacts of coastal protection. *In*: EDGE, B. L. (ed.), Coastal Engineering 2000 Conference Proceedings, 2794–2807.

CHADWICK, A. J. & MORFETT, J. C. 1998. *Hydraulics in Civil and Environmental Engineering*, 3rd Edn. Spon, London.

HALL, J. W., LEE, E. M. & MEADOWCROFT, I. C. 2000. Risk-based benefit assessment of coastal cliff protection. *Proceedings of the Institution of Civil Engineers Water and Maritime Engineering* **142**(3), 127–139.

KIRBY, J. T. & DALRYMPLE, R. A., 1983. A parabolic equation for the combined refraction-diffraction of Stokes waves by mildly-varying topography. *Journal of Fluid Mechanics*, **136**, 453–466.

LI, B. 1994. An evolution equation for water waves. *Coastal Engineering* **23**, 227–242.

LI, B. 1997. Parabolic model for water waves. *Journal of Waterway, Port, Coastal and Ocean Engineering*, **123** (4), 192–199.

LI, B., REEVE, D. E. & FLEMING, C. A. 1993. Numerical solution of the elliptic mild-slope equation for irregular wave propagation. *Coastal Engineering* **20**, 85–100.

MONBALIU, J., PADILLA-HERNANDEZ, R., HARGREAVES, J. C., ALBIACH, J. C. C., LUO, W., SCLAVO, M. & GUNTHER, H. 2000. The spectral wave model, WAM, adapted for applications with high spatial resolution. *Coastal Engineering* **41**, 41–62.

For a more comprehensive list of references relating to REFDIF see: *http://chinacat.coastal.udel.edu/~kirby/programs/refdif/refdif_pubs.html*

For details of the UK Met Office Wave Hindcast Model see: *http://www.met-office.gov.uk/research/ocean/climate/development.html*

Geological Society, London, Engineering Geology Special Publications

Coastal chalk cliff erosion: experimental investigation on the role of marine factors

J. Brossard and A. Duperret

Geological Society, London, Engineering Geology Special Publications 2004; v. 20; p. 109-120
doi:10.1144/GSL.ENG.2004.020.01.08

Coastal chalk cliff erosion: experimental investigation on the role of marine factors

J. Brossard & A. Duperret

Laboratoire de Mécanique, Physique et Géosciences, Université du Havre, 25 rue Philippe Lebon, BP 540, 76058 Le Havre cedex, France

Abstract: In this paper the marine factors of erosion contributing to the chalk cliffs located on either side of the English Channel are examined. From an analysis of the literature, the main physical phenomena determining the marine erosion of the shore platform and the foot of the cliff are considered. Field observations of the coastal chalk cliff show that the vertical erosion of the shore platform does not appear to be the main cause of cliff erosion, which is mainly governed by cliff collapse processes. To estimate the impact of waves on the base of the cliff, experiments were carried out in a wave flume. The pressure due to the waves and the dissipation of waves were measured for three simple configurations of the boundary conditions between the cliff and the sea. The pressure never exceeded the compressive strength of chalk rock. Nevertheless, pressure fluctuations due to periodic waves can induce a fatigue process within the fracture structures.

The experimental results showed that the shingle by itself has a low effect on wave energy dissipation. The main effect of shingle is to reduce the water depth at the toe of the cliff. Furthermore, it is demonstrated that a lower water depth leads to a lower impact of the waves on the cliff.

Introduction

The French and English chalk cliff coastline located on either side of the English Channel retreats with a mean recession rate varying between 0 and 0.7 m/year (May 1971; Costa 2000). However, the erosion is not uniform with time, but occurs by sudden collapse that may induce a cliff retreat of 10–20 m in one event. A European scientific project named ROCC (Risk Of Cliff Collapse) has therefore been launched involving the coastlines of Upper-Normandy and Picardy in France (120 km long) and East Sussex in the UK (40 km long), in order to identify the critical parameters leading to coastal cliff collapses in chalk rock (Fig. 1).

The stability of coastal chalk cliffs is governed simultaneously by both subaerial and marine processes, as well as the mechanical characteristics of the rock (lithology, fracture pattern). The evolution of the cliff, from stability towards failure, depends on changes occurring within the rock mass, such as the development and opening of fractures (resulting from stress relief, fatigue, wetting and drying, freeze–thaw action) and the deterioration of the rock material as a result of the infiltration of water (resulting in solution, chemical alteration, physical breakdown through freeze–thaw or salt crystallization). These internal changes in the rock mass are brought about through external agencies of meteorological origin (including rain, wind, frost, drought), removal of stress constraints at the cliff face and of marine origin (including wave action, tidal conditions, the presence or absence of deposits at the cliff toe, vertical erosion of the shore platform) (Duperret *et al.* 2002).

Some authors have suggested that rock material strength subjected to subaerial processes is the main mechanism of sea cliff erosion, such as the Californian calcareous coast (Benumof *et al.* 2000) or along the English Channel chalky coast (Duperret *et al.* 2002). The marine parameters, such as wave impact factors appear as a secondary mechanism of sea cliff erosion. Nevertheless Benumof *et al.* (2000) suggest that wave energy distribution may be important in determining the timing of cliff collapse events. The role of marine parameters needs to be specified more closely in such geological contexts. The aim of this paper is to study the contribution of marine factors on coastal chalk cliffs erosion, using experimental investigations focus on pressure wave measurements on a wall/cliff and wave attenuation through sediments located at the toe of the wall/cliff.

Chalk cliffs geomorphology

Coastal chalk cliff exposures along each part of the English Channel are composed of nearly vertical cliffs ranging from 20 to 200 m high and the foreshore area is often a chalky seaward beach platform with a low slope. The foreshore area exposes a flat beach platform made of eroded chalk or hardground levels with a higher material strength than chalk. In some places, the beach platform is partially covered by a thin veneer of sand and by shingle accumulation composed of smooth flints, whose distribution is somewhat discontinuous along the coastline. The shingle accumulations are always located in the upper part of the foreshore area at the toe of the cliff (Fig. 2), whereas sand cover may extend seaward to low tide level. Such sand cover is transitory, readily resuspended and may be absent under storm conditions (D. J. Pope, pers. comm.).

From: MORTIMORE, R. N. & DUPERRET, A. (eds) 2004. *Coastal Chalk Cliff Instability*. Geological Society, London, Engineering Geology Special Publications, **20**, 109–120. 0267-9914/04/$15.00

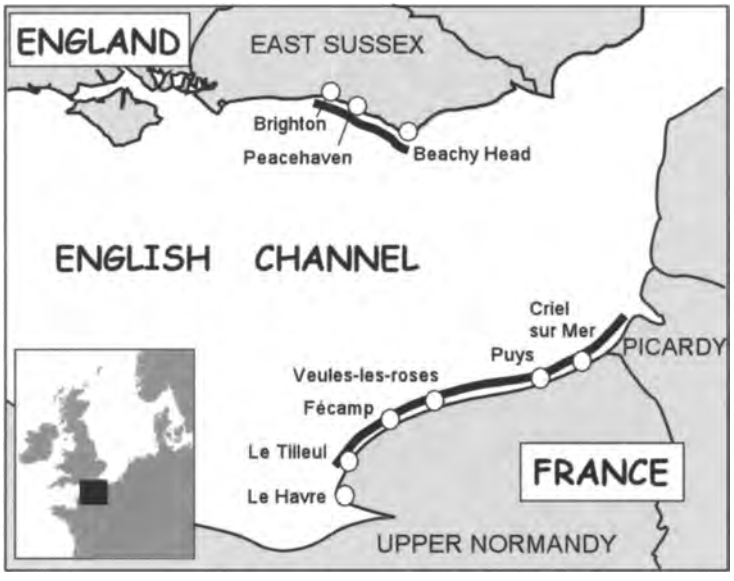

Fig. 1. Location of the study area along the coasts of the English Channel. Continuous black line represents portion of coasts made of chalk cliffs, used for the study. All reported sites are cited in the text.

Chalk cliff geomorphology is a type of foreshore often referred to as a wave cut platform (e.g. Sunamura 1977, 1992; Robinson 1977) . Marine parameters of chalk cliff erosion may act on the shore platform, by vertical erosion and on the cliff face, by horizontal recession.

Marine parameters on the shore platform

The shore platform erosion results from subaerial weathering and wave action. The two main weathering processes are salt weathering and water layer weathering (Stephenson & Kirk 2000, part II). The salt effects refer to the expansion in volume due to the growth of salt crystals and their subsequent hydration, which can induce high pressure in the cracks of the platform (Cooke & Smalley 1968). The water layer weathering is associated with the wetting and drying process during the tidal cycle and can induce a superficial disintegration of the rock (Trenhaile 1987). Stephenson & Kirk (2000, part II) have evidenced that the highest rate of shore platform erosion occurs between 0.6 and 0.9 m above mean sea level which, they argue, suggests that shore platform erosion results mainly from weathering caused by repeated wetting and drying. Weathering processes may be accentuated by living organisms such as micro-organisms, boring organisms and grazing organisms (Trenhaile 1987; Spencer 1988; Sunamura 1992), which can play a double role firstly by building some specific morphologies and secondly by enhancing morphological denudation rates due to other geomorphological processes (Fornos *et al.* 2001).

According to Sunamura (1977, 1992) and Trenhaile (1987), the primary agent of shore platform development is deduced from the relative intensity of two forces: the erosive force of waves and the lithology-related resistance. The erosive force of waves is due to the bed shear stress and the dynamic pressure. Sanders (1968) proposed that breaking wave shock, water hammer and air compression in joints are the main causes of erosion on the shore platform. Stephenson & Kirk (2000, part I) suggested that erosion by waves can only occur when waves break on the shore platform, and the depth of water in front of platforms therefore appears to be an important control on wave energy arriving on platforms. But, generally, the erosion induced by the bed shear stress and the pressure is very much lower than the erosion induced by the abrasion phenomenon. The abrasion is due to the sand, rock fragments or shingle produced by the erosion itself. Sunamura (1977) has developed a model of temporal evolution of erosion taking account of this phenomenon. Nevertheless, vertical erosion is of greatest concern for soft cohesive sediments and soft rocks (Davidson-Arnott & Ollerhead 1995; Skafel & Bishop 1994).

Along the cliffed coastlines, the ratio between the mechanical resistance and the marine stresses for the platform is, everywhere, very large. Along chalk coasts of the Channel, the vertical erosion of the shore platform does not appear to be the main cause of cliff recession, which is mainly governed by cliff collapse processes. After a collapse, a lobate deposit made of large pieces of chalk coming from the cliff expands on the shore platform. In this case, waves have an effect on the alteration of chalk blocks which result from cliff collapses.

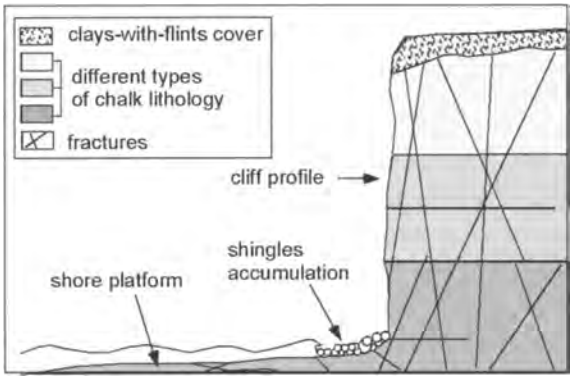

Fig. 2. Schematic sketch of a chalk cliff profile of the channel coasts.

Marine parameters at the cliff base

Marine processes acting at the base of the cliff are also closely linked to the water depth and therefore vary significantly in macro-tidal contexts. A large number of authors have argued that wave action is the main parameter of coastal cliff erosion, by wave-attack processes at the toe of the cliff (e.g. Sanders 1968; Sunamura 1977; Robinson 1977; Hoek & Bray 1977; Mc Greal 1979; Sunamura 1982). Wave action consists of: (1) hydraulic action such as compression, tension, cavitation and wear; (2) abrasive action due to pebbles and boulders in motion by wave action; (3) wedge action due to the air compressed in fissures by waves. Erosion occurs when the assailing forces from waves are higher than the resisting force of the rocks. Even if the resisting force of the rocks is controlled by their mechanical properties and their structure (such as joints and stratification), the deterioration of the resisting force is brought about by weathering and fatigue due to the repeated stresses generated by wave action (Sunamura 1977).

Along the coastline, three main cases of wave impact may occur: (a) wave breaking on the shore platform; (b) wave reflection at the cliff face without breaking; (c) wave breaking impact directly on the cliff face.

(a) When waves break on the shore platform, initially a rapid flow occurs and a large part of the potential energy is transformed into kinetic energy. If the flow reaches the foot of the cliff and if some pebbles, shingle or sand are available on the beach, the abrasion induced by the removal of sediments during the swash may produce a slight basal notching at the cliff base. In the case where no sediments are available, weathering by salt and by repeated drying and wetting processes during the tidal cycle may also induce slight peeling of the chalk surface. Field observations along the Channel chalk coastline have found basal notching in only a few places, with a maximum undercutting of about 0.5–1 m (Fig. 3a).

(b) When waves are reflected at the cliff face without breaking, the maximum variation of the wave pressure on the cliff is very low, in the order of $2\rho gH$ where H is the wave height. For example, for a wave of $H=5$ m the variation of pressure is of the order of 1.1 MPa and, in most cases, it never exceeds the compressive strength of wet chalk rock (1 to 20 Mpa, for chalks dated from Turonian to Senonian) (pers. comm. CETE 1980). The highest impact pressures were recorded by De Rouville (1938) on a prototype sea wall at Dieppe in France, with a magnitude of 610 kPa (Wolters & Müller 2004), which is always lower than the compressive strength of wet chalk rock.

The occurrence of storm surges increases the absolute pressure, because the increasing of the still water level, but has a limited effect on the variation of the pressure. Nevertheless, the repeated cycles of wave pressure may generate processes of fatigue within the cracks of the rock. In the case of large cracks, Peregrine & Kalliadasis (1996) have demonstrated that the filling flow may induce an especially large pressure in cracks, leading to a large tensile stress in the rock itself and higher susceptibility to fatigue processes. Such processes may occur on a chalk cliff coastline, within caves of several metres in height and 1–2 m in depth, which may develop at the base of the cliff along large-scale fracture structures (Fig. 3b).

(c) The last type of wave-impact occurs when waves break directly on the cliff face. It is the so-called 'perfect breaking' (Kirkgöz 1991, 1995). Perfect breaking appears when the breaker has a perfect vertical face and strikes a vertical wall. In only this case is the greatest wave impact pressure produced. The pressure is greater by one or two orders of magnitude than the wave pressure without perfect breaking (i.e. 1 to 20 Mpa) on the cliff face and the pressure values may reach the compressive strength of the weakest wet chalk rock. The pressure profile on the wall shows a large peak but with a very short duration of a few milliseconds.

From experimental studies in a wave flume, the highest impact pressures occur with a foreshore slope of 1/10 in front of the cliff (Kirkgöz 1982). The maximum impact pressure probability in a flume follows a log-normal distribution. The maximum pressures are reached for a wall with a slope angle varying between 10° and 30° and occur most frequently just below the still water level. For any given wave condition there is a critical value of the water depth at the wall, d_{wm}, for which perfect breaking occurs (Kirkgöz 1991). To analyse the effect of wave breaking on a cliff it is necessary to know the water depth at the foot of the cliff. The empirical relation

$$d_{wm} = \frac{H_0}{0.78}[(1 - 0.3\tanh(20H_0/L_0)]$$

where H_0 is the wave height and L_0 the wavelength in the offshore zone gives the height of the waves which could just break on the front of the cliff (Kirkgöz 1995). As noted by Kirkgöz (1995), perfect breaking obtained during laboratory experiments shows variations in the magnitude of impact on which the unevenness of waves in the natural environment must be added. Consequently a wave height band can be defined for which perfect breaking can occur, in a probabilistic sense, and this band is determined by the water depth at the foot of the cliff.

Fig. 3. (a) Basal notching at the toe of the chalk cliff, which is clearly evidenced by the retreat of the cliff and the white colour of the washed chalk. Noted the shingle occurrence. The person gives an approximate scale. Veules-les-Roses, Upper-Normandy, France. (b) Large-scale fracture (Normal fault in-filled by clays) expanding all over the cliff height, ending by an open cave at the toe of the cliff. Note the associate excavation of the cliff face. The person gives an approximate scale. Veules-les-Roses, Upper-Normandy, France. (c) Horizontal and vertical cracks at the base of the cliff. The horizontal fissure is located at the top of a hardground level and the vertical crack is an open joint. Note that the base of the cliff is more white, due to washing by sea-water during high tide. Fécamp, Upper-Normandy, France.

The Channel coastlines are subjected to macro tidal effects, with variations of 0.1 to 10m in water height. Observations in the field have shown that sea water level at high tide does not always reach the base of the cliffs. For these reasons, the frequency of violent wave impacts with perfect breaking seems to be low along the cliffs of the Channel, even if this frequency may increase during periods of both storms and spring tides.

Where cracks occur at the base of the cliff, they can be filled by sea water during the high tide. The propagation into cracks of impact pressures due to wave breaking may occur when cracks are filled by water. From experimental modelling on water filled cracks, Müller (1997, 1998), demonstrated that the magnitude of the pressure peak decreases during the propagation into the crack and that the propagation velocity is finite. In fact, the celerity is very dependent on the dissolved air. Additional experimental work on cracks has shown that partially submerged cracks show a faster propagation of wave impact pressure (300 m/s) than fully submerged cracks (50–100 m/s) and without significant attenuation (Wolters & Müller 2004).

The short duration of the peak pressure and the finite celerity induces a phase difference between the peak pressure at the crack entrance and the end of the crack, and this may lead to dislodgement of a piece of rock at the front of the cliff (Müller 1997).

The base of the chalk cliffs of the Channel shows numerous types of vertical fracture pattern, with various apertures and persistence, such as open master joints with a persistence all over the cliff height and open isolated joints with a persistence of several metres from the base of the cliff. Normal and strike-slip faults may also extend over the full cliff height, but they are often filled by clays and are consequently closed, except in the case where a cave develops at the base of the fault (Fig. 3b) (Genter *et al.* 2001). Open fissures may also develop horizontally along hardground levels or marl seams within the chalk cliff (Fig. 3c).

The presence or the absence of shingle on the beach platform has an effect on the dissipation of waves and therefore on cliff erosion. The dissipation of energy is related to the roughness of the shingle beach and to the momentum transfer from flow to the cobbles. However, another effect of shingle is to decrease the water depth at the base of the cliff and, as suggested by Kirkgöz (1995) and Stephenson & Kirk (2000, part I), the water depth above the platform is the main parameter controlling erosion.

To investigate this assumption and to further understand the role of marine factors on chalk cliff erosion, experiments were carried out in a wave flume. To take into account the large diversity of morphological conditions observed along the Channel, three simple configurations of the boundary conditions between the cliff and the sea have been tested. They have been selected from the natural configurations of the chalk cliffs observed on each side of the Channel. Their behaviour was compared through measurements of the pressure on a wall modelling the cliff, the wave reflection characteristics and the dissipation of wave energy.

In such experimental work it is necessary to measure, with high accuracy, the wave characteristics; period T or angular frequency $\omega = 2\pi/T$, wavelength λ or wave number $k = 2\pi/\lambda$, direction of propagation or the sign of the celerity $C = \lambda/T = \omega/k$ and amplitude A or wave height $H = 2A$.

Method of wave measurement in the flume

The method of wave measurements (Brossard *et al.* 2000) allows an accurate measurement of all regular modes propagating in the wave flume. Each mode has its own celerity. If the level of the free surface is recorded by a moving probe (Fig. 4) with a fixed speed V, the signal is shifted by the Doppler effect (Brossard *et al.* 2000). In the spectrum of the signal, for any mode, the frequency is different from that obtained with a fixed probe. The Doppler shift has a negative value if the probe is moving towards the direction of propagation of the mode and has a positive value if the probe is moving against the direction of propagation. Nevertheless the Doppler shift method is applicable to conditions where the wave celerity maintains a constant value. Consequently the measurements must be carried out upstream or offshore of the sand accumulation where the water depth is constant.

This method enables measurement of the amplitudes of the fundamental incident and reflected modes and subsequently the reflection coefficient. Concerning the higher harmonics; there are two kinds of harmonics travelling in a wave flume. Non-linear modelling of the free surface provides a description of this by the sum of sinusoidal components (Stokes model components), so-called 'phase locked modes' because these modes have the same celerity as the fundamental mode. Furthermore, even if the wave generator produces a regular wave (only one angular frequency corresponding to

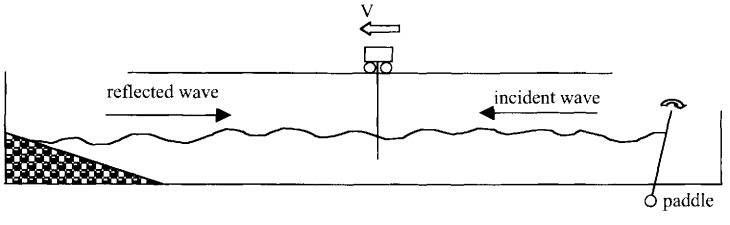

Fig. 4. Experimental set-up for wave measurements.

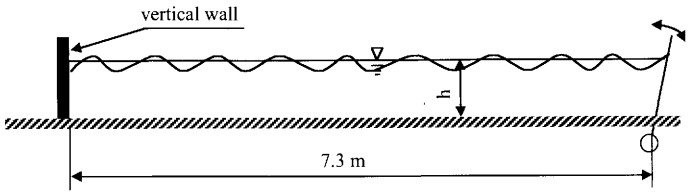

Case 1 :horizontal smooth foreshore

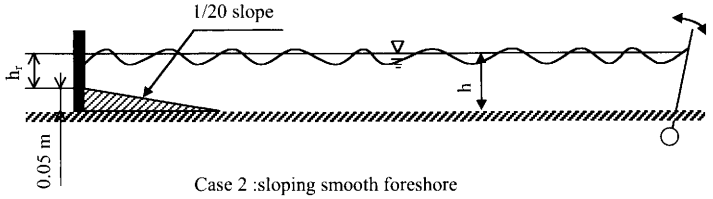

Case 2 :sloping smooth foreshore

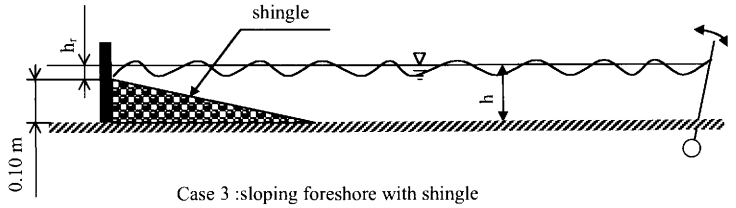

Case 3 :sloping foreshore with shingle

Fig. 5. Modelled beach morphologies.

the fundamental mode), the non-linear interaction between the gravity waves and a beach, a breakwater or a wall, produces higher harmonics (free modes) by transference of energy from the fundamental mode to higher harmonics. However, for the free modes the harmonic celerity is not dependent on the fundamental mode celerity; their angular frequencies are a multiple of the fundamental one but their wave numbers are not multiples of the fundamental mode. The wave numbers of the free harmonics follow the dispersion relationship of the fundamental mode. Consequently the Doppler shift is different to that of the phase locked modes although they have the same angular frequencies. The frequency peaks are separated in the spectrum and the discrimination of the phase locked modes and the free modes allows the generation of harmonics to be quantified and non-linear interactions between the waves and sediment accumulation to be analysed.

Experimental set-up

The cliff was modelled by a vertical, impermeable wall and the beach platform by an impermeable surface with various gradients. Three configurations were modelled:

(1) a flat smooth foreshore area, without shingle or fresh deposits of debris;
(2) a sloping smooth foreshore area with 1/20 slope, without shingle cover;
(3) a sloping (1/20) foreshore area with shingle cover (Fig. 5).

Each configuration was subjected to various levels of water, which represented the tidal effect. The experiments were carried out in a regular wave flume 0.3 m wide. The wave generator was an oscillating paddle driven by an electrical

motor. The generated waves were regular with a second free harmonic amplitude less than 4% of the fundamental amplitude. At the downstream end, the vertical wall was located at 7.3 m from the paddle (Fig. 5).

The shingle was modelled by sand in these experiments. The sand had a narrow particle size distribution with a mean grain size of 0.4 mm. At a geometric model scale of 1/60, the Froude scaling law indicates a corresponding *in situ* shingle size of 24 mm. This size average is closely representative of the natural shingle of the Channel coastline. The Froude similarity law is well adapted for sea hydrodynamic problems because it represents the scaled ratio between the gravitational force and the inertial force. Nevertheless, this similarity law leads to a lower porosity effect at model scale than *in situ*. The sediment thickness above the slope bed was 0.05 m (Fig. 5), corresponding to a 3 m high natural beach. As sediment accumulation extended over a length of 1.2 m in the flume, the remaining length for wave measurements, at constant depth, was 6.2 m long.

The tidal effects were modelled by varying the water depth in the range 0.07 m–0.15 m in the off-shore horizontal section corresponding to 4.2 m–9 m *in situ*. For all experimental runs the wave period was 0.79 s, corresponding to a wave period of 6.12 s, *in situ*. The dispersion characteristics in the flume resulted in a wavelength varying in the range 0.6 m for a water depth of $h = 0.07$ m to 0.8 m for a water depth of $h = 0.15$ m. The wave amplitudes were adjusted to avoid wave breaking within the offshore section and to limit the non-linear effects associated with the closed geometry of the flume. In all experiments, wave breaking occurred above the sediment accumulation.

Pressure measurement at the vertical wall

The intention was to estimate the stresses induced by non-breaking waves on the cliff face. The pressure profile at the front of the vertical wall was measured, using six pressure transducers. The measuring range of these sensors was $0–10^4$ Pa with an active sensor area of 12 mm diameter. The variation of the pressure at the front of the vertical wall in the flume was small in comparison to the pressure range of the sensors used, but to achieve a significant increase in sensitivity would have required a sensor too large in relation to the spatial resolution required. The experimental conditions were not that of perfect breaking ones, consequently there were not transitory effects like rapid peak pressures. The frequency of the signal was the wave frequency (1.27 Hz) and this value was very low in relation to the ability of the sensors. To improve the accuracy of the measurements, all transducers were calibrated frequently using a parabolic calibration relationship. Such measurements enabled the response of the cliff to be followed to stresses induced by the repeated pressure variation during tidal cycles.

The pressure measurements have been carried out at two water depths ($h = 0.150$ m and $h = 0.120$ m), which correspond to high tide and low tide. At each of these two water depths the three cases of shore platform morphology have been examined. In the next sections the results obtained are compared with the Sainflou model (Sainflou 1928) that predicts the pressure field on a vertical wall. Table 1 gives the amplitude of the incident waves for each experiment.

Table 1. *Amplitudes of the incident waves for the test cases*

water depth	*h = 0.150 (m)*	*h = 0.120 (m)*
Case 1: horizontal smooth platform	$6.6\ 10^{-3}$ (m)	$4.2\ 10^{-3}$ (m)
Case 2: sloping smooth platform	$6.9\ 10^{-3}$ (m)	$4.2\ 10^{-3}$ (m)
Case 3: sloping platform covered by shingle	$6.7\ 10^{-3}$ (m)	$4.4\ 10^{-3}$ (m)
Sainflou model for horizontal smooth platform	$6.6\ 10^{-3}$ (m)	$4.2\ 10^{-3}$ (m)

Two sets of values have been extracted from the pressure measurements: the maximum value of the pressure and the amplitude of the pressure oscillations due to the periodic waves. Information about the maximum pressure is useful for studying the behaviour of the cliff by comparison with the resisting force of the chalk rock. The amplitude of the pressure oscillations is an important parameter to enable analysis of the fatigue stress phenomenon at the front of the cliff or directly on the shore platform.

Maximum pressure

In Figures 6 and 7 plots of the relative (in relation to the hydrostatic pressure) maximum pressure along the wall are presented. At high tide, $h = 0.150$ m in the flume, the relative water depth, defined as the distance between the mean sea level and the bed at the cliff toe, is large. The pressure plots are similar for all three cases and agree well with that of Sainflou model (Fig. 6). When the water reaches the cliff face during high tide level, the pressure induced by the waves on the cliff are similar for each geomorphological situation. In fact, the occurrence of sediment accumulation at the toe of

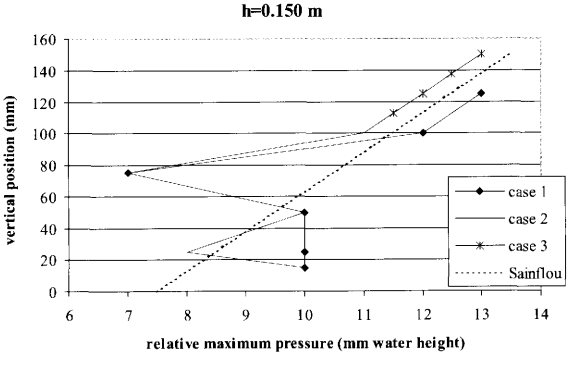

Fig. 6. Maximum pressure distributions along the vertical wall for 0.150 m water depth. Case 1: horizontal smooth platform. Case 2: sloping smooth platform. Case 3: sloping platform covered by shingle. Sainflou: Sainflou model for horizontal platform.

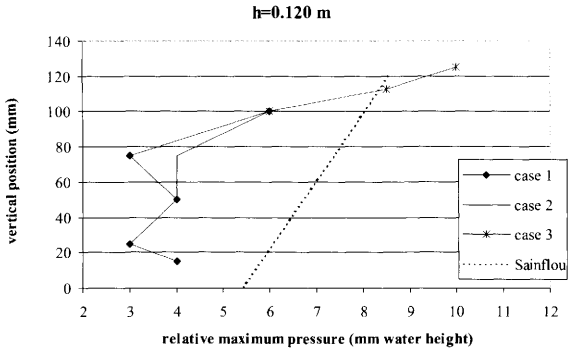

Fig. 7. Maximum pressure distributions along the vertical wall for 0.120m water depth. Same cases as Figure 6.

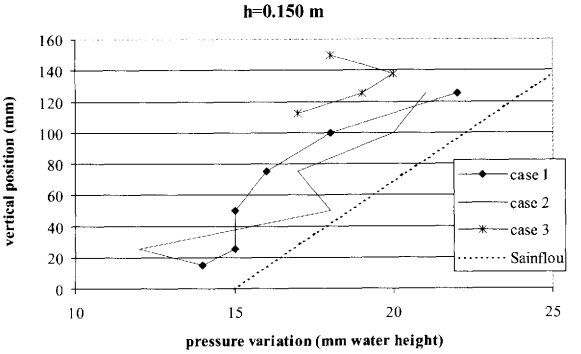

Fig. 8. Pressure variation distributions along the vertical wall for 0.150m water depth. Same cases as Figure 6.

the cliff does not induce perturbation of the wave impact on the cliff, if the sediment accumulation is well covered during high tide.

At low tide, $h = 0.120$m in the flume and for case 1 and 2 (horizontal and sloping smooth beds) the pressure distributions are similar and only differ slightly from the Sainflou model although there is probably some drift of the zero pressure reading of the sensors (Fig. 7). For case 3 (sloping shingle beach) the pressures are higher than both the previous ones. In this case the relative water depth is small but the sea level can reach the vertical wall with a rise of the mean sea level due to the occurrence of sediment accumulation. This rise therefore induces an increase in pressure at the toe of the cliff. Nevertheless, the measured pressure values at low tide (28–100 Pa) are lower than pressure values measured during high tide (70–130 Pa).

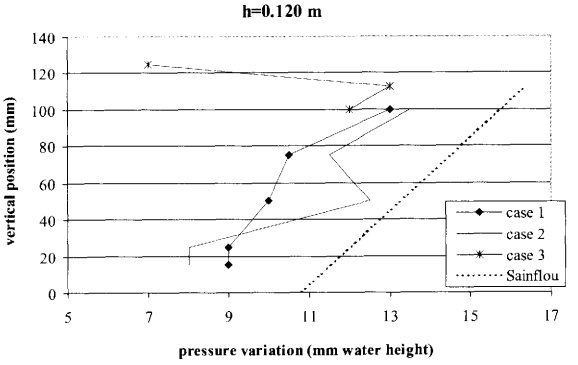

Fig. 9. Pressure variation distributions along the vertical wall for 0.120m water depth. Same cases as Figure 6.

Pressure fluctuations

The amplitude of the pressure variations recorded on the wall for each case are compared with each other and with the Sainflou model at both high tide (Fig. 8) and low tide (Fig. 9). For each case, the amplitude of the pressure variations are lower than for the Sainflou model. This result cannot be related to a zero drift of the sensors because the amplitudes of pressure oscillations are calculated by difference between the maximum pressure and the minimum pressure. It can be explained by a dissipation effect because the Sainflou model assumes the fluid as inviscid. Nevertheless, for the two tide conditions, the pressure variations are higher for the sloping bed (case 2) than for the horizontal bed (case1). For an equivalent vertical position of the sensor, pressure variations for the sloping bed with sediment (case 3) are lower than for the sloping bed without sediment (case 2); this result can be explained by a larger dissipation with shingle present. The last recorded value for case 3 in Figure 9 is drastically lower than the previous one at low tide (Fig. 8); this lower value is due to the fact that the sensor is not covered with water throughout all of the wave period.

Comparisons between the three cases do not indicate large-amplitude variations in pressure on the vertical wall. A gently sloping shore platform favours higher pressure variations on the cliff face than a flat shore platform because of a shoaling effect, whilst sediment accumulation on a gently sloping shore platform seems to decrease the pressure variations on the cliff face. For this last case, the dissipation effects due to the bottom shear stress and the breaking of waves are more important than the shoaling effect.

Morphology of the beach profile (case 3)

Waves were generated in the flume for the equivalent of half a tide (about six hours *in situ*) to analyse the behaviour of the shingle beach. The evolution of the sand modelling the shingle was recorded by means of a video camera.

At a tidal time scale, the mean section of sediment accumulation is stable, with a slope of about 1/20, which is significantly below the accepted equilibrium value of 1/10 (Dean 1977), under such conditions. As experiments were

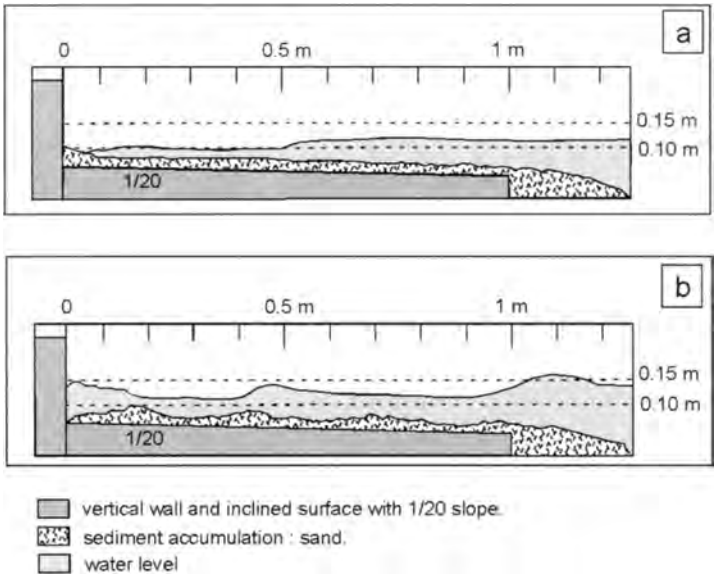

Fig. 10. Modifications of the beach profile during a half a tide.

performed in a wave flume and not in a basin, only the cross-shore sediment transport was observed. At smaller scale, the sediment accumulation shows several morphological characteristics, such as bars, ripples and scouring.

At higher water depths, during high tide, when the water reaches the vertical wall, the reflected waves interfere with the incident waves and lead to the formation of a set of nodes and anti-nodes within the water oscillations at sea bed level. This induces sediment transport and the formation of transverse bars whose wavelength is about half that of the free surface propagating waves. These bars have a beneficial effect on cliff erosion by increasing wave reflection and, consequently, by decreasing wave energy arriving at the cliff front.

The second effect is the development of superficial ripples with a wavelength of about 30 mm. This wavelength is related to water depth and is a classical phenomenon with bed sediments and an oscillating flow (Fredsoe & Deigaard 1992). But *in situ* this phenomenon has not been observed with shingle. Such differences may be due to the model sediment density and size, which are not ideally suitable for simulating shingle transport at this scale.

At high tide the wave impact on the vertical wall produces a very high vertical velocity, inducing scour of the sediment at the toe of the vertical wall. At mid-level of the ebb tide during the following tidal cycle, the scour hole is re-filled as the wave-breaking zone migrates seaward across the sediment, thus inducing significant sediment transport (Fig. 10 a,b). At the end of the ebb tide, a bank or berm is formed at the top of the sediment.

The experimental investigation shows that shingle berms located at the cliff toe are temporarily removed seaward at high tide. This fact may be increased under storm conditions, so exposing the toe of the cliff/wall to subsequent wave impact.

Wave energy and sediment accumulation

Reflection of waves

Measurement of incident and reflected waves allow us to quantify the dissipation of the wave energy through the sediment accumulation of the foreshore area. The reflection coefficient is defined as the ratio of the amplitude of the reflected fundamental wave to the amplitude of the incident fundamental wave. However, the energy of the various waves is related to the square of the respective amplitudes. The experimental results concerning the change in reflection coefficient with water depth in the offshore zone are reported in Figure 11 for all three cases of shore platform morphology.

Case 1: Wave reflection is greatest in the case of the flat smooth shore platform. For this case there is no energy transfer to higher harmonics. Reflection coefficient values less than 1 can be interpreted as a dissipation process at the wall. Decreasing values of reflection coefficient in relation to the decreasing water depth reinforce this assumption because the flow velocities under gravity waves increase when the water depth decreases. Consequently, case 1 can be used as a reference state for the other experiments.

Case 2: This behaviour can also be observed for the sloping smooth shore platform in the range 0.1 m–0.15 m of water depth because the water depth above the smooth slope is lower than in case 1 and dissipation by viscous drag at the

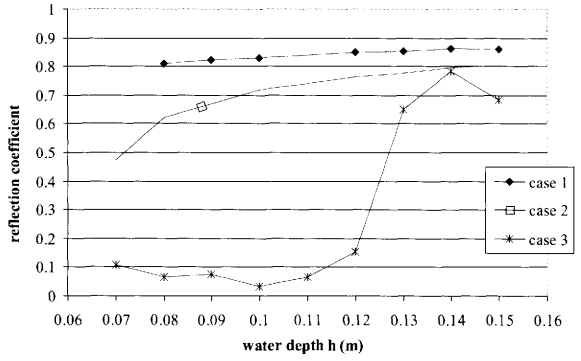

Fig. 11. Relationship between the reflection coefficient and the water depth. Same cases as Figure 6.

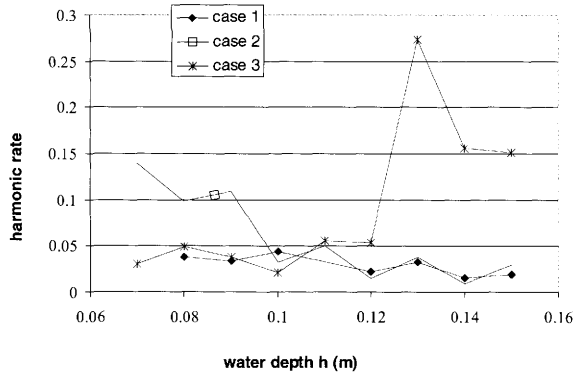

Fig. 12. Evolution of the harmonic rate with the water depth h at the offshore area. Same cases as Figure 6.

floor increases in a similar way to that for case 1 at the lowest values of water depth. For the range 0.07–0.1 m in case 2, the decrease in reflection coefficient is linked both to the dissipation process and to an energy transfer from fundamental mode to higher harmonic (Fig. 12), where the second free harmonic rate (ratio of the amplitude of the second free harmonic mode to the amplitude of the fundamental mode) increases with a fall in water depth. This last effect is related to the non-linear behaviour of the wave propagation in the shoaling zone due to the low water depth. Nevertheless, the reflection coefficient is always lower than that for the case 1, with a reduction of about 0.1 unit.

Case 3: For the sediment shore platform case, the variation in reflection coefficient exhibits two quite different behaviours. For water depths greater than 0.12 m within the offshore area, i.e. during the tidal cycle from low tide to high tide (flood tide), the reflection coefficient is similar to that for the case 2, with a reduction of about 0.1 unit due to energy dissipation by viscous drag and a transfer of energy from fundamental mode to the higher harmonics (Fig. 12). For water depths lower than 0.11 m, the reflection coefficient is very

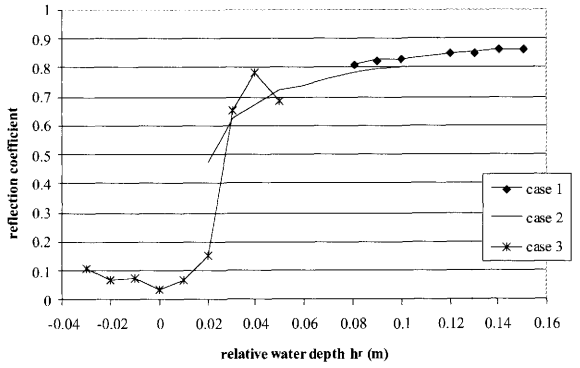

Fig. 13. Evolution of the reflection coefficient with the relative water depth h_r at the toe of vertical wall. Same cases as Figure 6.

low (between 0 and 0.1). Because the water level does not reach the wall, the wave impact conditions are very different. As shown in Figure 12 the energy transfer to higher harmonics is very low; in this case, all the energy is dissipated by the beach sediment.

Effectively we can consider the relative water depth above the sediment, which is the water depth at the top of the sediment located at the toe of the wall and expressed by h_r in Figure 5. The variation in reflection coefficient with water level above the shingle has been compared for all three cases (Fig.13). For each case, this change is continuous. Thus, if the foreshore zone is completely covered by sea water, the presence of a slope and shingle cover reduces the water depth above the beach and wave attack conditions become similar to an horizontal smooth slope (case 1) with a lower water depth. If the sea level does not reach the top of the foreshore the main phenomenon is a dissipation process and the effect of the waves on the cliff is very small.

Dissipation of waves

The wave energy dissipation in the foreshore zone can be represented by the coefficient $D = 1 - E_r/E_i$ where E_r is the incident energy flux and E_r the reflected energy flux. For this calculation both the fundamental mode and the second harmonics (free and phase locked modes) are taken into account. Wave energy dissipation versus relative water depth above the foreshore zone are plotted in Figure 14 for all three cases. Dissipation is therefore mainly a function of the relative water depth h_r. For case 3, the dissipation effect of the sediment cannot be distinguished from that of a simple non porous sloped beach. Nevertheless, in these laboratory conditions, the ratio between the permeability of the sediment and the viscosity of the fluid was lower than in prototype conditions.

The dissipation rate gives an indication of wave impact on the cliff toe and shows that the type of material covering the foreshore area is not the main parameter for wave dissipation. The water depth above the foreshore area seems to be the predominant parameter for wave dissipation.

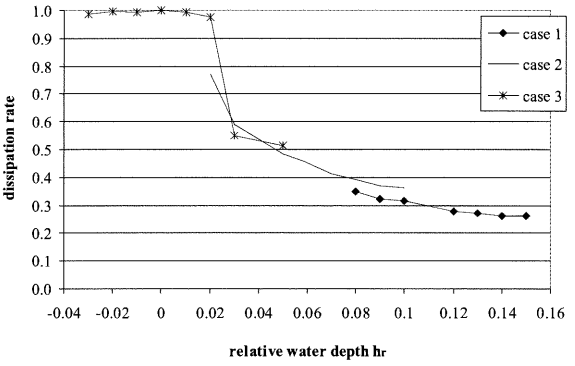

Fig. 14. Evolution of the dissipation rate with the relative water depth h_r at the toe of vertical wall. Same cases as Figure 6.

Discussion

Field observations along the French and English coastline have indicated local erosion of the chalk cliff, by rock-fall events over the various coastal configurations. These beach and cliff forms include a shore platform with shingle (rock-fall at Le Tilleul, Upper-Normandy, France, in November 1998), a shore platform without shingle (rock-fall at Criel sur mer, Upper-Normandy, France, in December 1997), a shore platform with sea wall at the toe of the cliff (rock-fall at Peacehaven, East Sussex, UK, in January 2001), poorly fractured coastal chalk cliffs (rock-fall at Puys, Upper-Normandy, France, in May 2000) and highly fractured coastal chalk cliffs (rock-fall at Beachy Head, East Sussex, UK, January 1999, May 2001) (Fig. 1). The problem is to determine if rock-falls and the subsequent cliff erosion along the Channel coastline are mainly governed by subaerial or marine parameters. On the one hand, Le Tilleul and Peacehaven rock-falls are clearly not linked to marine action at the toe of the cliff, because even at high tide, the sea-level never reaches the base of the cliff; at Le Tilleul, the shingle thickness is very high and at Peacehaven the base of the cliff is protected by a continuous sea-wall. On the other hand, the Criel s/mer rock-fall may be linked to marine action at the toe of the cliff, because the water level reaches the toe of the cliff at high tide and the cliff face presents large open fractures extending the full cliff height and ending in caves at the base of the cliff.

The link between marine attack of the toe of the cliff and the initiation of a rock-fall also needs to be specified. One of the proposed solutions is to determine the volume involved for each observed rock-fall. Field observations of recent rock-falls have indicated different volumes of cliff collapse: either collapse occurs on the lower part of the cliff with small volumes of material involved or, with the largest events, the collapse involves the whole cliff height. Marine factors can only be implicated in the triggering of a collapse where the collapse is located in the lower part of the cliff, i.e. for cliff falls involving volumes below ten thousand cubic metres for one event (Duperret *et al.* 2001*a*, *b*).

Repeated pressure fluctuations may favour fatigue phenomena at the base of the cliff face and the pressure changes can propagate within the chalk rock if an open network of fractures transversely oriented to the cliff face is located at the base of the cliff. Very little is known about the minimum pressure change needed to initiate rupture along a pre-existing fracture within chalk and hence trigger a rock-fall. The initiation of the rupture, which may lead to a collapse by pressure propagation through fractures, can only occur along a previous horizontal or vertical fracture network transversely oriented to the cliff face, with open cracks at the base of the cliff.

The other mode of marine attack is wetting and drying processes and salt weathering, which may favour the superficial disintegration of the chalk rock at the toe of the cliff. Such processes only lead to a slight basal notching of the cliff.

Finally, marine action is also responsible for removal of cliff fall material by abrasion and chalk dissolution. Littoral drift characteristics would be informative to know cliff fall material and shingles displacements on the foreshore area.

Conclusion

One of the frequently asked questions regarding Channel coastline erosion is: What is the role of shingle in the cliff recession? The common idea is that shingle dissipates the wave energy and that this dissipation of energy is the main factor which protects the chalk cliff from erosion. The implied reasons are the roughness of the shingle beaches, the dissipation by infiltration into the porous medium and the momentum transfer from the water to the cobbles. The experiments conducted in the wave flume show that the dissipation of wave energy by beach sediments and particularly through shingle accumulation is too poor to protect a cliff when the foreshore area is completely covered by the sea. The main effect of shingle accumulation is to decrease the water depth at the base of the cliff. From the literature and the experiments conducted in the wave flume it can be deduced that the lower the water depth, the less the wave impact energy. But, in fact, if the water level covers the shingle, the wave attack at the base of the cliff presents the same conditions as that of a shore platform devoid of sediment.

The experiments show that, for non-breaking waves on the front of cliff, the simple Sainflou model is appropriate for predicting the pressure field at the front of cliff. Along the Channel coastline, the water depth at the cliff toe is low in most of the cases and the intensity of compression stress due to the impacts of waves on the front of the cliff is too low and is not sufficient to trigger a large rock fall.

Among the marine factors of erosion, the abrasion phenomenon of the base of cliff can be retained to explain any slight rock falls, restrained to the lower part of the cliff. In this case, the collapse is limited upward by horizontal hard-

grounds levels, marl seams or flint bands. This phenomenon is favoured by a slight sloping shore platform by comparison to a horizontal bare shore platform.

The literature on the pressure propagation into cracks and the observations of open fracture networks *in situ* suggest that the fatigue phenomenon due to pressure oscillations could be a sensitive parameter of erosion. Further work would be very useful to obtain more exhaustive knowledge on cliff erosion.

Acknowledgements. The ROCC project is funded by the European community through the INTERREG II Rives Manche initiative (contract I99059). This research work has also been funded by the Centre National de la Recherche Scientifique in the framework of Programme National des Risques Naturels, through the contract PNRN 99-35-AS. We thank David J. Pope for his critical and helpful review of the first version of this manuscript.

References

BENUMOF, B. T., STORLAZZI, C. D., SEYMOUR, R. J. & GRIGGS, G. B. 2000. The relationship between incident wave energy and sea-cliff erosion rates: San Diego County, California. *Journal of Coastal Research*, **16**(4), 1162–1178.

BROSSARD, J., HÉMON, A. & RIVOALEN, E. 2000. Improved analysis of regular gravity waves and coefficient of reflection using one or two moving probes. *Coastal Engineering*, **39**(2–4), 193–212.

COOKE, R. U. & SMALLEY, I. J. 1968. Salt weathering in deserts. *Nature*, **220**, 1226–1227.

COSTA, S. 2000. Le recul des falaises du pays de Caux. *Bulletin d'Information des Géologues du Bassin de Paris*, **37**(1), 31–34.

DAVIDSON-ARNOTT, R. G. D. & OLLERHEAD, J. 1995. Nearshore erosion on a cohesive shoreline. *Marine Geology*, **122**, 349–365.

DEAN, R. G. 1977. *Equilibrium beach profiles: US Atlantic and Gulf Coasts*. **Ocean Eng. Report No 12,** University. of Delaware, Newark.

DE ROUVILLE, A. 1938. Etat actuel des études internationales sur les efforts dus aux lames, Annales des Ponts et Chaussées, **108 (II)**, Paris, 5–113.

DUPERRET, A. GENTER, A., MORTIMORE, R. N., DELACOURT, B. & DE POMERAI, M. R. 2002, Coastal rock cliff erosion by collapse at Puys, France: the role of impervious marl seams within chalk of NW Europe. *Journal of Coastal Research*, **18**(1), 52–61.

DUPERRET, A., MARTINEZ, A., GENTER, A., MORTIMORE, R. N. & WATREMEZ, P. 2001*a*. Subaerial chalk cliff failures on the English channel coast, based on field data from recent collapses. trans. *AGU Fall Meeting (San Fransisco, USA)*.

DUPERRET, A., MARTINEZ, A., GENTER, A., MORTIMORE, R. N. & LAWRENCE, J. 2001*b*. Recent collapses along the coastal chalk cliffs of the English channel: the role of lithology and fracturation on the rupture type. *European Rock Coasts 2001 Conference, Brighton, UK, 17–18 December 2001*, 56–57.

FORNOS, J. J., SOUSA-DIAS, A., PONS, G., MELO, R. 2001. Possible causes of regional variations in platform morphology and rates of downwearing on European coasts: Biological variations. *European Rock Coasts 2001 Conference, Brighton, UK, 17–18 December 2001*, p.17.

FREDSOE, J. & DEIGAARD, R. 1992. Mechanics of coastal sediment transport. *Advanced Series on Ocean Engineering, World Scientific*, **3**, 290–309.

GENTER, A., DUPERRET, A., MARTINEZ, A. & VILA, J-L. 2001. Fracture evaluation along the french chalk coast. Structural guidelines for building a GIS application for the ROCC project. International Conference on coastal Rock Slope Instability: Geohazard and Risk Analysis (Le Havre, France), 16–17.

HOEK, E. & BRAY, J. 1977. *Rock Slope Engineering*. IMM, London.

KIRKGÖZ, M. S. 1982. Shock pressure of breaking waves on vertical walls. *Journal of Waterway, Port, Coastal, and Ocean Engineering*, **108**, 81–95.

KIRKGÖZ, M. S. 1991. Impact pressure of breaking waves on vertical and sloping walls. *Ocean Engineering*, **18**(1/2), 45–59.

KIRKGÖZ, M. S. 1995. Breaking wave impact on vertical and sloping coastal structures. *Ocean Engineering*, **22**(1), 35–48.

MAY, V. J. 1971. The retreat of chalk cliffs. *Geographical Journal*, **137**, 203–206.

MC GREAL, W. S. 1979. Marine erosion of glacial sediments from a low-energy cliffline environment near Kilkeel, northern Ireland. *Marine Geology*, **32**, 89–103.

MÜLLER, G. 1997. Propagation of wave impact pressures into water filled cracks. *Institution of Civil Engineers, Water, Maritime and Energy*, **124**(2), 79–85

MÜLLER, G. 1998. Time scale effects in pressure propagation into cracks. *Minutes of 1st BLOCS workshop, HR Wallingford.*

PEREGRINE, D. H. & KALLIADASIS, S. 1996. Filling flows, cliff erosion and cleaning flows. *Journal of Fluid Mechanics*, **310**, 365–374.

ROBINSON, L. A. 1977. Marine erosive processes at the cliff foot. *Marine Geology*, **23**, 257–271.

SAINFLOU, S. 1928. Essai sur les digues maritimes verticales. *Annales Ponts et Chaussées*, **98**, No. 4.

SANDERS, N. K. 1968. Wave tank experiments on the erosion of rocky coasts. *Royal Society of Tasmania Papers and Proceedings*, **72**, 106.

SKAFEL, M. G. & BISHOP, C. T. 1994. Flume experiments on the erosion of till shores by waves. *Coastal Engineering*, **23**, 329–348.

SPENCER, T., 1988. Coastal biogeomorphology. *In*: VILES, H. A. (ed.) *Biogeomorphology*, Basil Blackwell, Oxford, 255–318.

STEPHENSON, W. J. & KIRK, R. M. 2000. Development of shore platforms on Kaikoura Peninsula, South Island, New Zeland, part I: the role of waves, p. 21–41, part II: the role of subaerial weathering, *Geomorphology*, **32**, 43–56

SUNAMURA, T. 1977. A relationship between wave-induced cliff erosion and erosive force of waves. *Journal of Geology*, **85**, 613–618.

SUNAMURA, T. 1982. A predictive model for wave-induced cliff erosion, with application to Pacific coasts of Japan. *Journal of Geology*, **90**, 167–178.

SUNAMURA, T. 1992. *Geomorphology of Rocky Coasts*. Wiley, New York.

TRENHAILE, A. S. 1987. *The Geomorphology of Rock Coasts*. Oxford University Press, 338 p.

WOLTERS, G. & MÜLLER, G. 2004. The propagation of wave impact induced pressures into cracks and fissures. *In*: MORTIMORE, R. N. & DUPERRET, A. (eds.) *Coastal Chalk Cliff Instability*, Geological Society, London, Engineering Geology Special Publication, **20**, 121–130.

Geological Society, London, Engineering Geology Special Publications

The propagation of wave impact induced pressures into cracks and fissures

G. Wolters and G. Müller

Geological Society, London, Engineering Geology Special Publications 2004; v. 20; p. 121-130
doi:10.1144/GSL.ENG.2004.020.01.09

The propagation of wave impact induced pressures into cracks and fissures

G. Wolters & G. Müller

Queen's University Belfast, Civil Engineering Department, David Keir Building, Stranmillis Road, Belfast BT7 5AD, UK

Abstract: Rock cliffs and blockwork coastal structures often suffer a peculiar type of damage, whereby individual blocks are removed out of their location towards the sea. The location of damage suggests that breaking wave action is the main cause. It has been suggested that wave impact pressures travel into the water or air filled cracks and fissures of the structures, leading to large pressures acting inside of the structure or cliff and to the removal of blocks. This assumption was only recently confirmed for water filled cracks with a series of model tests at Queen's University Belfast. Real cracks in rock cliffs are, however, often only partially filled with water. A new experimental study, also conducted at Queen's University Belfast, revealed that wave impact generated pressures can travel into both fully or partially water filled cracks or joints. In partially submerged cracks the pressure pulse was found to travel in the air, propagating fast and with little attenuation deep into the structure, signifying that partially filled cracks are potentially more dangerous for the integrity of the structure than completely water filled cracks. These pressure pulses may be the main cause for the *seaward* removal of blockwork in coastal engineering structures or of rock cliff material.

Introduction

Many man-made or natural coastal structures such as breakwaters or rock cliffs contain cracks or fissures which extend above and below the mean water line, and which are exposed to wave attack. During storms, the effect of wave action on the cracks and the 'structure' becomes much more violent when waves start to break against the crack entrance, generating high but short pressure peaks. The effect of storms on rock cliffs and the houses on top of the cliff are described as (e.g. in Benumof & Griggs 1999): 'Waves ... were extremely powerful, often "shaking" and "rattling" the cliffs'. Later it is said that 'Cliffs with many open joints, where water can compress air and cause recoil, are more subject to erosion than those which are relatively free from such openings'. In the context of damages to rocks and blockwork coastal structures, Shield (1895) states: 'Wherever joints occur, either in rock or in artificial structures, both mechanical and chemical action proceeds the fastest. Apart from the inherent weakness of joints, the air or water confined within them, when struck by a wave, is converted into a very destructive agent'. These facts were repeated again, in a more modern language, in a more recent textbook. 'One practical indication of shock forces against concrete sea walls is the manner in which ill-designed or badly constructed lift joints become rapidly exploited by the sea' (Muir Wood & Fleming 1981).

Cliff erosion can have many causes: increased ground water level, salt weathering, water-table fluctuations, biogenic activity, piezometric pressure changes, freeze–thaw action, just to name a few. The action of waves is, however, mostly held not directly responsible or even important for cliff failure. Carter (1991) states that there are numerous studies of coastal cliff morphology that never mention waves at all. The importance of wave action has, however, been acknowledged in the context of toe erosion (undercutting of cliffs), which initiates mass movements like blockfalls and landslips, and the removal of detritus products from the toe of the cliff.

In the field of coastal engineering, the damage caused by wave action on coastal structures, dams, ships or offshore platforms is, however, well known. The action of breaking waves against such structures is considered to constitute the major cause of the damage. Although modern structures are built as monolithic blocks wherever possible, older coastal structures in particular were built from blockwork and contain cracks or joints, which are exploited during storms. Typical damage mechanisms of blockwork structures and rock cliffs include the seaward removal of individual blocks in breakwaters or, in the case of rock cliffs, the breaking off of large blocks around mean water level, undercutting the cliff. This type of damage leads to the suspicion that wave impact induced pressures are acting not only from the outside, but also in the inside of the structure or rock cliff.

Although in the last 20 years considerable research effort has been directed towards the investigation of wave impact pressures, very little was known until recently about impact pressure propagation and the pulse characteristics. Müller (1997) was the first to demonstrate that these impact pressures can actually enter water filled cracks or fissures and that they have the characteristics of a compression wave. Following his work, further studies were carried out to analyze pressure pulse propagation in completely submerged cracks (e.g. Müller *et al.* 2002). In a very different context, namely the erosion of rock underneath plunge pools, it was

From: MORTIMORE, R. N. & DUPERRET, A. (eds) 2004. *Coastal Chalk Cliff Instability*. Geological Society, London, Engineering Geology Special Publications, **20**, 121–130. 0267-9914/04/$15.00

recently shown that compression waves entering water filled cracks in rocks can erode the rock severely (Bollaert & Schleiss 2001). In rock cliffs, however, completely filled cracks are not typical; crack networks with both partially and fully submerged cracks are found more often. Such partially filled cracks are the topic of this study.

Literature review

Comparison of rock cliffs and breakwaters made from blockwork

The authors' field of research originally centered on blockwork breakwaters with rubble filling which were built during the 19th century. Figure 1 (a) shows a typical cross section (Admiralty Breakwater, Alderney/Channel Islands, see Crawford 1999), and Figure 1 (b) a view (Le Havre Breakwater) of such structures. Damage is often caused by the seaward removal of individual blocks during storms, with a subsequent loss of integrity of the blockwork and removal of further blocks.

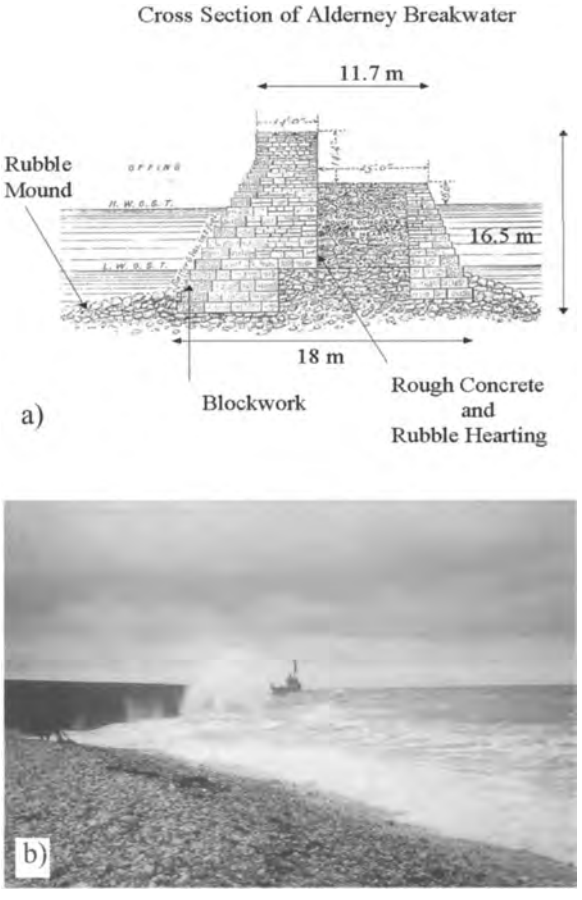

Fig. 1. Cross section and side view of blockwork breakwaters: (a) Admiralty Breakwater (Crawford 1999); (b) Le Havre Breakwater.

Although blockwork breakwaters are not representative for all coastal structures, they share common features with rock cliffs and other old engineering structures: they all contain joints and are often composed of brittle materials with high compressive but low tensile strength. All are exposed to breaking wave action. The implication is that similar damage mechanisms, as observed in coastal structures, may occur in rock cliffs, although the compressive/tensile strength of the rock material may be higher.

Erosion by wave action

One of the reasons why wave action has not attracted much attention in geological circles is illustrated in the following statement, in Carter (1991): 'Many rock types are immensely strong, so that wave forces may have little effect. Many cliffed coastlines have a primary tectonic control through jointing and faulting and are little altered by wave action.'

Figure 2 (a) shows the tensile rock strength plotted against the compressive strength. It can be seen that the compressive strength of rock is generally ten times higher than its tensile strength. The tensile strength, which varies between 0.01 and 10 MPa is, however, well within the range of wave impact pressures. Pressures recorded from five field measurements range from 50 to 690 kPa. The pressure rise times were measured as 0.005–0.3 seconds; the highest pressures coinciding with the shortest rise times (e.g. Blackmore & Hewson 1984). The actual compressive forces of a breaking wave acting against a rock face can thus be expected not to do any damage, except when stones are hurled by the wave against the rock. This damage mechanism would, however, be expected to leave mostly ground down rock – sand, and not large blocks, as a residue. In Benumof & Griggs (1999), the sea cliff erosion rates at various sites in California (given as cm/year) are given as a function of rock strength, 'structural discontinuities', weathering and fatigue, groundwater seepage and offshore wave energy flux. Figure 2 (b) shows the cliff erosion rate plotted against joint spacing (a measure of crack distance or structural discontinuity). It can be seen that erosion rates increase for decreasing joint spacing, indicating some relationship between these two parameters. Benumof & Griggs (1999) conclude that 'waves are one of the leading forcing mechanisms of seacliff erosion', secondary only to the material properties of the rock itself.

The photos in Figure 3 were taken at the Normandy coastline in France, near Le Havre (Etretat). Figure 3 (a) shows chalk cliffs exposed to marine erosion leaving in its wake arches and spikes (cliff retreat), and Figure 3 (b) a cliff undercutting. The cliffs are about 100 m high, composed of chalk layers with flint or without flint inlay and sometimes separated by darker and much harder layers of dolomite chalk. Between the chalk layers several metre-wide cracks can be seen (b), which extend a couple of metres into the cliff, showing that the layer boundaries are very susceptible to

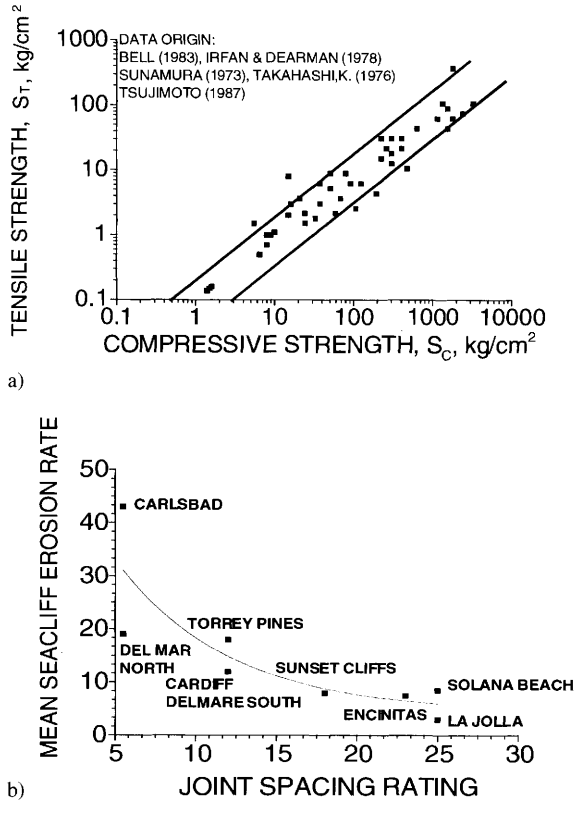

Fig. 2. Rock parameters: (a) relationship between tensile strength and unconfined compressive strength for saturated rock samples (Sunamura 1992; 1 kg/cm^2 = 100 kPa); (b) erosion versus joint spacing (Benumof & Griggs 1999).

wave attack. Figure 3 (c), taken at St Pierre en Port, shows a house on top of an eroding cliff, illustrating the current implications of cliff erosion.

Breaker types and wave impact pressures

From the previous discussion and the pictures in Figure 3 it can be seen that wave action, and in particular breaking wave impacts, can be expected to be a contributing factor to cliff erosion. There appears, however, to be some uncertainty about the conditions under which the most severe wave action occurs. Carter (1991) mentions briefly that the wave loadings depend on the ratio of breaker height to water depth at the cliff toe; ratios of 0.8 giving plunging breakers and the highest loading. Benumof & Griggs (1999) show a graph relating offshore wave energy to erosion rate; in this graph, however, no definite relationship between these two parameters can be seen. In the engineering literature it is widely recognized that the type of breaker is a function of the wave steepness and, more importantly, the sea bed slope. Violent or plunging breakers, which generate the highest impact loadings, can

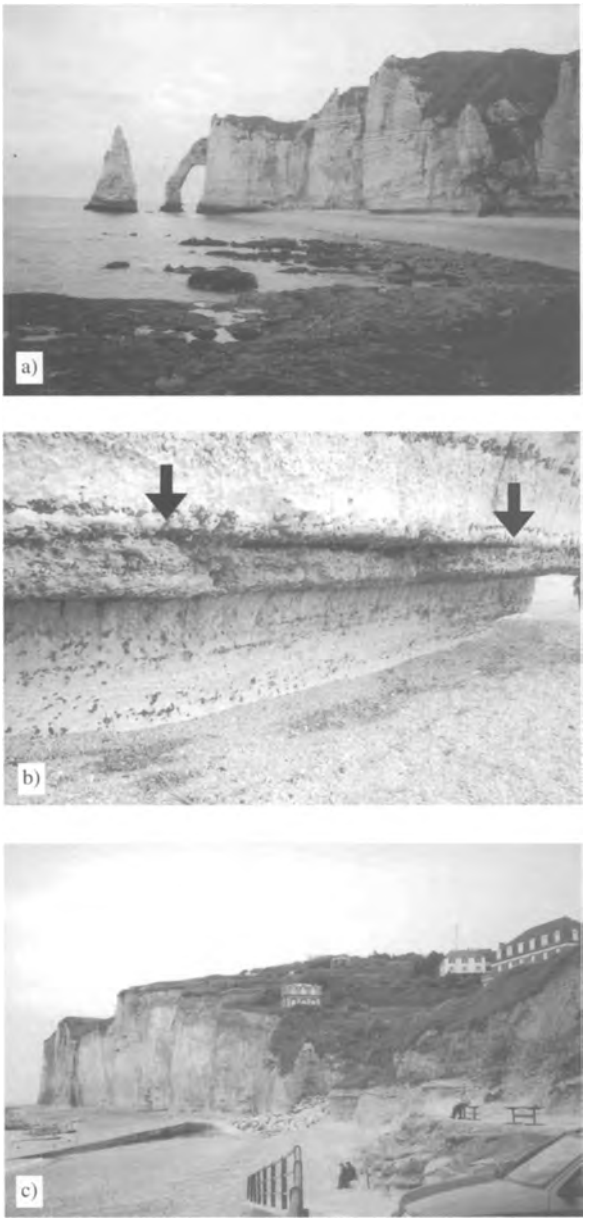

Fig. 3. Cliff erosion: (a) marine erosion; (b) cliff undercutting; (c) cliff collapse.

only exist for seabed slopes of 1:5 to 1:30; at steeper slopes the breaker can not develop any more, at shallower slopes it curls over long before reaching the coastline. The breaker type is usually determined by calculating the surf similarity parameter or *Iribarren number* (e.g. Battjes 1968). If wave action constitutes a major contribution to cliff erosion, it can be expected that there should be some relationship between wave climate, surf similarity parameter and erosion rate.

When slamming against an obstacle, a plunging breaker generates a so-called wave impact pressure. These pressures are characterized by a very short but high pressure peak which is followed by a significantly smaller hydrodynamic pressure. Rise times of 0.005 s and pressure magnitudes of up to 690 kPa were reported by Rouville (1938). Recent measurements on Alderney breakwater recorded pressures of up to 435 kPa (Bullock *et al.* 1999). The dynamic force of moving water masses acting on blocks in the coastline can be very considerable too. A block which was separated from the structure or rock cliff can very often be easily moved by the waves. During the breakwater failure at Sines, Portugal, in 1978, concrete blocks protecting the sea wall, each weighing 42t, were displaced and moved by wave action.

It is important to notice that the pressure magnitude is not related to the wave height. In Rouville's measurements, e.g. wave heights of up to 4.50m were recorded. The highest impact pressure of 690 kPa was, however, generated by a rather small wave of 2.5m height. Recent research confirmed the fact that it is not wave height or length but rather the breaker type which determines the magnitude and the duration of these pressures, with plunging breakers generating the most severe impacts (Hull & Müller 2002).

Conclusions from literature review

From the facts reported so far, the following conclusions can be drawn:

- Breaking waves generate impact pressure pulses of high magnitude and short duration.
- The breaker type, and thus the impact pressure magnitude, depends on the surf similarity parameter (a function of incident wave steepness and sea bed slope), and is not directly governed by the incident wave energy or the wave height.
- Wave impact pressures can travel as compression pulses into water filled cracks.
- Blockwork coastal structures as well as cliffs appear to be susceptible to damages created by wave impact pressures entering water filled cracks.
- The erosion rate of rock cliffs depends on the joint width and spacing.

The action of breaking waves on structures with water filled cracks or joints therefore appears to cause erosion. Many cracks in rocks are, however, partially filled with air and partially with water. The effect of wave impact pressures on such cracks has, to the authors' knowledge, not been investigated so far.

Hydraulic model tests at Queen's University Belfast

Aims of model tests

Wave impact pressures propagating into cracks are suspected to erode rock cliffs; very little is however known about this effect. Model tests were conducted to address the following main questions:

- Can pressures propagate into partially water filled cracks?
- What are the characteristics of the pressure pulses?
- Can the pressure pulse propagation through partially filled cracks be modelled?

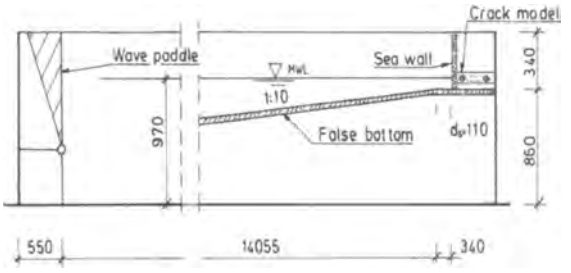

Fig. 4. Wave tank with sea wall model (all dimensions in mm).

Experimental set-up

A series of experiments was conducted in the Hydraulics Laboratory at Queen's University Belfast (QUB) Civil Engineering Department, in a wave tank of 17m length, 350mm width and with a water depth of 1m (Fig. 4). An inserted false bottom made of fibreglass brought the water depth from 1m to 110mm with a slope of 1:10. At the shallow end, a vertical wall was installed. Waves were generated with a flap-type wave paddle in the deep water section of the tank. A single breaker, with a deep water wave height of 71mm, was generated every 82 seconds by generating a small wave group consisting of three waves of 1 second period. The first smaller wave was reflected by the sea wall, the second wave developed into a plunging breaker, and the third wave, which again was smaller, did not break. Since the first breaker was relatively unaffected by previous waves, the impact pressures were repeatable within acceptable limits.

Two brackets were manufactured which were inserted into the vertical sea wall alternately. The first bracket was used to record the wave impact pressures on the sea wall (Fig. 5a). The second bracket allowed any of the crack configurations to be securely inserted into the wall, whereby the crack centre was located 72mm above the sea bed. The cracks studied were 0.5, 1 and 3mm in width, 115 and 600mm long, while the height was constant at 25mm. Cracks were examined while being totally submerged as well as partially submerged. In order to investigate partially filled cracks, the water depth at the sea bed was reduced. Submergence varied between 0.1 h, 0.5 h, and 0.9 h (where h is the crack height), corresponding to water depths of 62, 72 and 82mm at the sea wall. The fully submerged case corresponded to the original water depth of 110mm, which was later increased to 150mm to guarantee an air free crack. Figure 5(b) shows the positioning of the bracket in the model wall. All the apparatus was made of stiff Perspex. Pressures were measured with

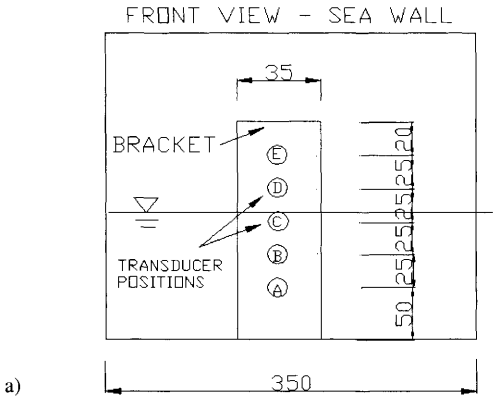

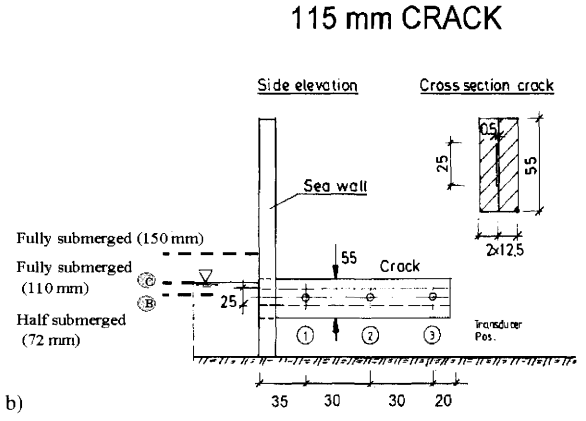

Fig. 5. Model sea wall with transducers and crack unit: (a) front view with bracket; (b) crack model (all dimensions in mm).

ENTRAN 8510B pressure transducers with a load capacity of 34.5 kPa. The pressures were recorded using in-house written data acquisition software based on LabView. Data was acquired with a sampling frequency of 10 kHz.

Experimental results

Wave impact pressures

Initially, the impact pressures created by the breaking wave on the vertical wall were recorded. Figure 6 shows a typical impact pressure record for the transducer positions A–D as indicated in Figure 5(a). Figure 7 shows the maximum pressures for two series of 15 measurements. From Figures 6 and 7 it can be seen that the impact pressures are of comparatively short duration and that, despite the single breaker technique, a considerable variability of peak pressures exists. The pressure magnitude ranges from approximately 5 to 40 kPa. The highest pressures are encountered at Mean Water Level (MWL, position C).

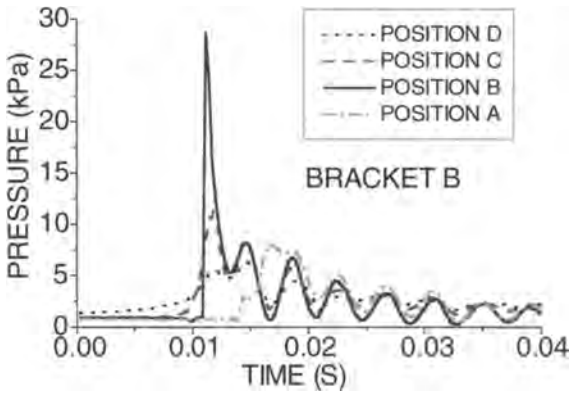

Fig. 6. Typical impact pressure records for positions A–D.

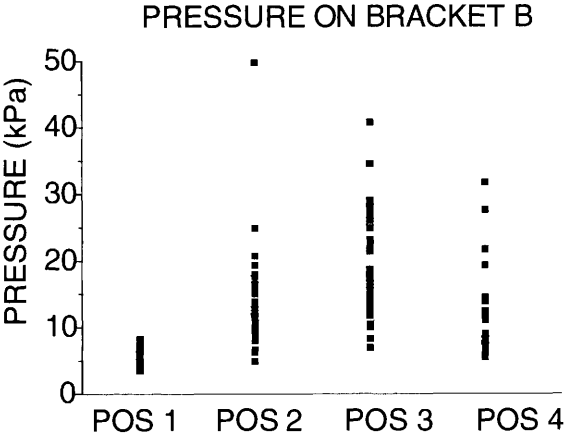

Fig. 7. Maximum peak pressures for each position and 30 waves.

Pressure propagation

Fully submerged 115mm crack

In Figure 8 the pressures measured inside of the crack model, measured at positions 1–3, are shown for cracks of 115 mm length and 0.5, 1.0 and 3 mm width. The measurements in fully submerged cracks are shown in Figure 8(a), (c), (e) and for later comparison, the results for partially submerged cracks in (b), (d) and (f). The pressure–time trace in Figure 8 (a) and (c) shows that the pulse travels at a speed of around 90 m/s (measured between positions 1 at the entrance, and 3 at the end of the crack). Propagation speeds were determined by measuring the distance between the points where 10% of the maximum pressure at each location was reached. This value was chosen for two reasons:

(i) The pressure signal changes; damping occurs and the signal becomes longer so that the peak distances do not give a clear indication of the speed of propagation.

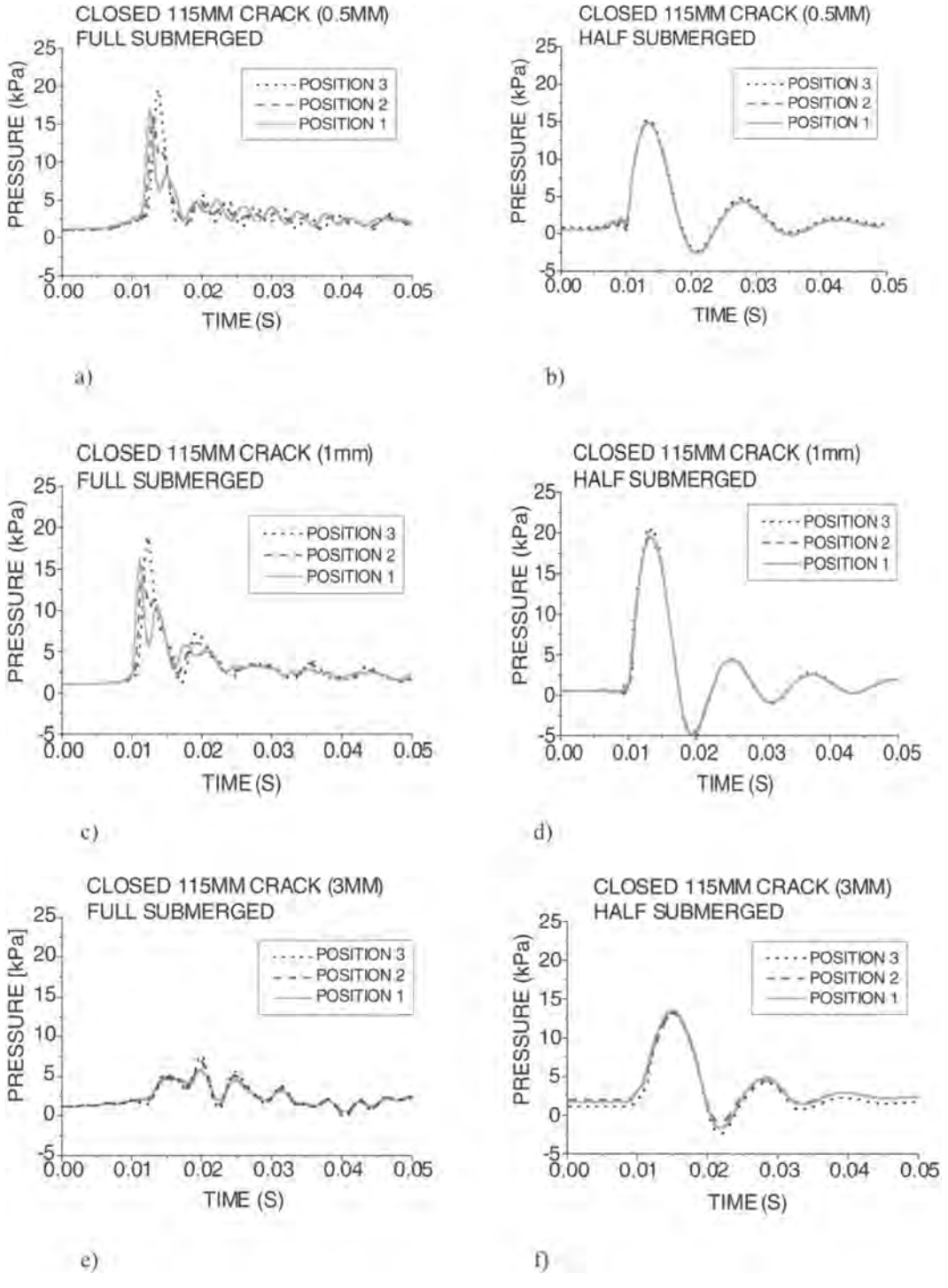

Fig. 8. Pressure–time traces from experiments with 115 mm crack: (a) fully submerged crack, 0.5 mm width; (b) partially submerged crack, 0.5 mm width; (c) fully submerged crack, 1.0 mm width; (d) partially submerged crack, 1.0 mm width; (e) fully submerged crack, 3.0 mm width; (f) partially submerged crack, 3.0 mm width.

(ii) The reflected wave starts to influence the incoming wave after a very short time, increasing the pressure signal and thus changing its shape.

The velocity can then be determined as: $v = 0.06\,\text{m}/0.0007\,\text{s} = 86\,\text{m/s}$. This surprisingly low speed of propagation is attributed to the water containing a small amount of air (approximately 1.2%), which dramatically reduces the speed of sound in water. For a more detailed discussion of this topic, see Müller *et al.* (2002). Positions 1 and 2 (entrance and centre of crack) show a double-peak signal, indicating that the pressure pulse was reflected at the end of the crack, subsequently traveling out again. The speed of propagation in Figure 8 (e) appears to be higher; this effect was also observed in other experiments and attributed to wall effects; it is the subject of another investigation. The pressure–time trace also looks more ragged, with somewhat smaller pressure magnitude, than that for the narrow cracks. This is thought to be caused by the fact that, just before the wave hits the crack entrance, the water table lowers below the top surface of the crack and water can flow out. It appears therefore that during the impact the crack is also partially filled with air.

Partially submerged 115 mm crack

In Figure 8 (b), (d) and (f), practically no time lapse between the different transducer positions can be identified. From the pressure record, the speed of propagation was found to be around 300 m/s, with very low attenuation. The speed of propagation and the shape of the pressure time trace implies that the air enclosed in the crack responds dynamically to the excitation from the wave impact pressure. The pressure signal oscillates with a frequency of approximately 85 Hz.

600 mm crack

An additional series of experiments was conducted with a similar crack as described previously with 0.5 mm width, but of 600 mm length. Figure 9 shows the pressure–time traces measured at locations 50 mm (Position 1), 150 mm (Position 2), 350 mm (Position 4) and 550 mm (Position 6) into the crack. The fully submerged crack (Fig. 9 a) shows a pressure pulse propagating with similar speed to that in Figure 8 (a); again reflection and superposition can be identified. The pressures in the partially submerged crack in Figure 9 (b) are also propagating at 300 m/s, as in the 115 mm crack. The shape of the pressure pulse does, however, show a damped oscillation with a rather long frequency of around 18 Hz.

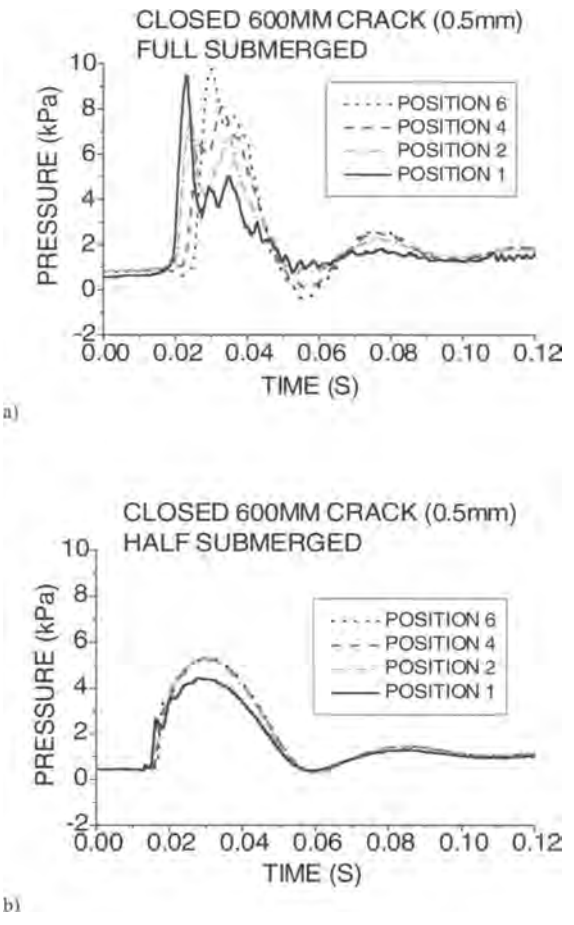

Fig. 9. Pressure propagation through 0.5×600 mm crack: (a) submerged crack; (b) partially submerged crack.

Analysis of partially submerged cracks

Speed of propagation

Figure 10 (a) shows the comparison of the velocities for partially and completely submerged cracks. The data acquisition rate of 10000 Hz did not give sufficient data points to evaluate velocities above 300 m/s accurately, resulting in some spread of values around this value. It can be seen that in partially filled cracks the pressure signal travels significantly faster than in fully submerged cracks. In Figure 10 (b), the influence of crack width is shown. Whereas the pulses travel through the 0.5 and 1.0 mm wide cracks with a speed of around 90 m/s, the speed in the 3 mm crack increases to up to 200 m/s. No clear reason for this effect has been confirmed as yet; currently it is thought that surface tension effects retain more small air bubbles in the very narrow cracks. In Figure 10 (c) finally the effect of crack length is shown. It can be seen that the crack length does not affect the speed of propagation of the pressure pulse.

Propagation mechanism in partially submerged crack

Originally it was thought that the air–water medium is less stiff than the air, since its speed of sound is considerably smaller than 300 m/s, so that it would compress more easily and thus dominate the behavior of the system. The experiments, however, showed otherwise: low velocities were found for the full submerged crack whereas high velocities

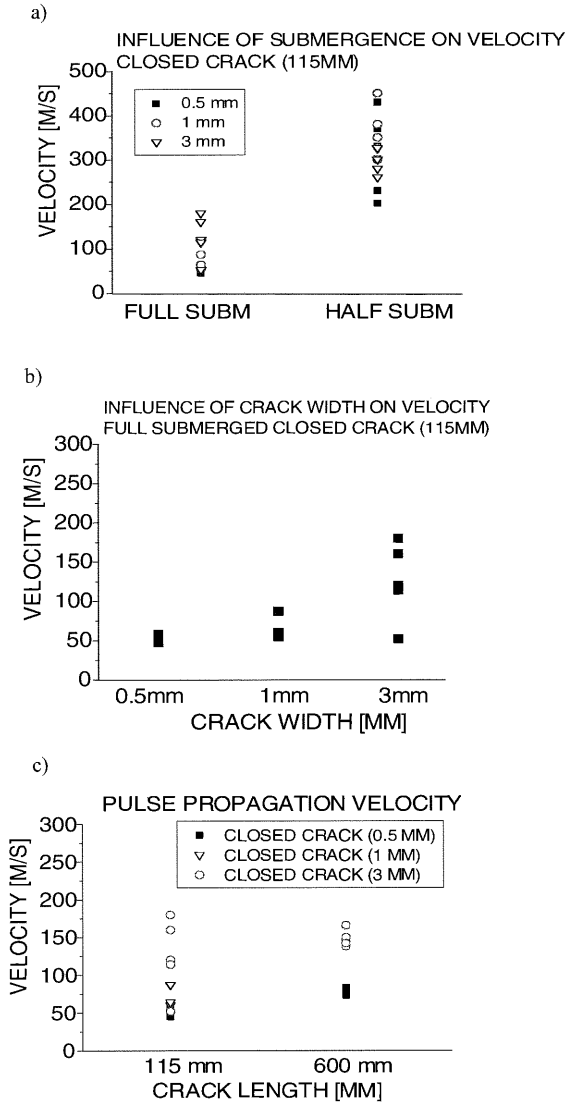

Fig. 10. Speed of propagation for fully and partially submerged crack: (a) effect of submergence; (b) effect of crack width; (c) effect of crack length.

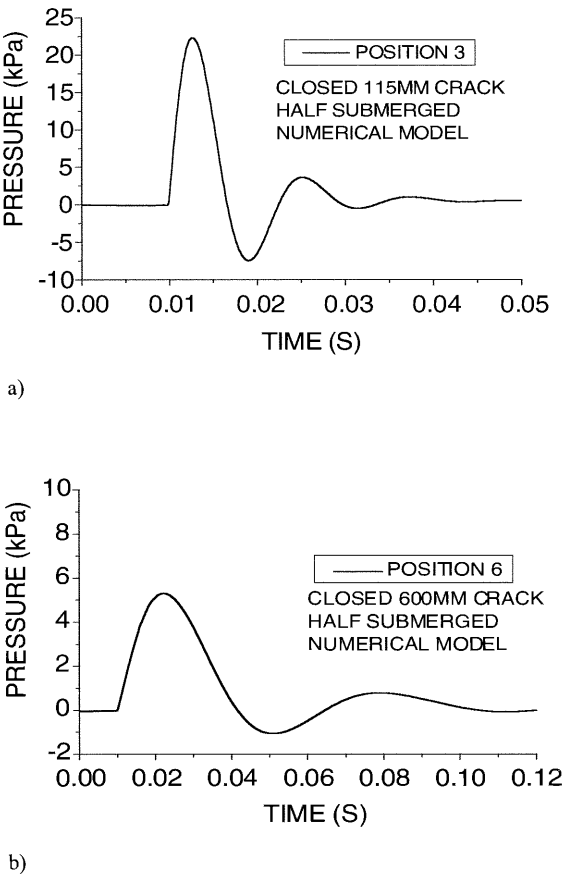

Fig. 11. Numerical simulation of pressure propagation into partially water filled crack: (a) 115mm crack; (b) 600mm crack.

were found for the partially submerged case. A comparison between the pressure propagation in the 115mm and the 600mm long crack shows that although the speed of propagation appears to be similar, the frequency of the pressure signal's oscillation is different: around 85 Hz for the 115 mm crack, and 18 Hz for the 600 mm long crack. The frequencies thus have a ratio of 85/17 = 5.0, similar to the length ratio of 600/115 = 5.2. A Single-Degree-Of-Freedom (SDOF) dynamic model consisting of the enclosed air (spring) and an added mass of water was used to analyze the results. The 'added mass' is considered to be that part of the impacting water mass which enters the crack during wave impact. A frequency analysis showed that the added mass has a length of 2.5% (115 mm) and 2.1% (600 mm) of the crack length, resulting in frequencies of 87.5 and 18.3 Hz. A numerical model was written in order to simulate the response of the SDOF to the forcing function given by the pressure record at the crack entrance as shown in Figure 6, Position C. It should be noted that when the wave hits the air filled upper part of the crack, the water particles of the 'added mass' already are in motion so that as an initial condition the added mass was given a velocity of 0.1 m/s. The SDOF model contained viscous damping at 30–45% of the critical damping in order to match the experimentally observed pressure magnitudes. Figure 11 shows the numerical simulations.

From Figures 8 (b), (f) and 11 (a) and (b) it can be seen that the SDOF model simulates the measurements reasonably well, indicating that the physical assumptions underlying the model are valid. It can therefore be said that the air contained in the crack acts as a spring; a small part of the impacting

water mass (approximately 2.3% of the crack length) enters the crack and becomes an 'added mass' and also takes part in the response of the system. With an average damping ratio of 37.5% the damping is quite high and very probably generated by the moving fluid inside of the crack. The numerical model still has to be further verified; it can however already be used to assess the effect of wave impacts of air filled cracks.

This gave rise to the following conclusions:

- the pressure pulse can be identified as an elastic wave travelling in the air rather than in the water at the speed of sound;
- partially filled cracks transport wave impact pressures fast and deep into the inside of the structure and behind the protective blockwork;
- the pressure inside of a partially air filled crack can be modeled with a SDOF system, whereby the air enclosed in the crack becomes the spring.

The high propagation velocity and the low attenuation within partially filled cracks indicates that partially filled cracks could lead to structural failure much earlier than completely water filled ones.

Impact induced stress in the rock material

The propagation of impact pressures into water or air filled cracks generates a pressure inside of the crack. In order to assess whether or not this can cause a growth of the crack, which would initiate rock erosion, a Finite Element model of a simple pressurized crack was analysed. It was found that the pressure acting inside of the crack generates very high tensile stresses at the crack tip. Figure 12 shows the stress magnitude normalized with the pressure magnitude inside of the crack plotted against the ratio of distance from the crack tip and crack length. It can be seen that the stress at the crack tip reaches ten times the stress magnitude acting inside of the crack. Wave impact pressures can reach 500–700 kPa, and the tensile strength of soft rock is in the range of 100–1000 kPa. This, in combination with the fact that rock is a very brittle material, implies that pressure pulses propagating into cracks can indeed cause the rock at the crack tip to fail, the crack to grow and thus lead to a progressive deterioration of the integrity of the rock itself.

Discussion

A review of the engineering literature showed that the exposure risk of a coastal structure to breaking wave action is a function of wave steepness and sea bed slope; only plunging breakers generate the high impact pressures held responsible for damage to such structures. Due to the high compressive strength of rock when compared with recorded wave impact pressures, direct wave action against rock faces appears not to constitute a significant erosive force. Model tests indicated

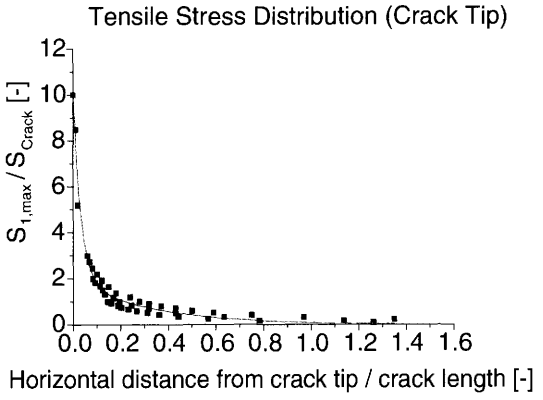

Fig. 12. Normalized tensile stresses at the tip of a pressurized crack.

that wave impact pressures can travel into partially water filled cracks with the speed of sound in air, generating seaward pressures in blockwork structures and splitting forces in fissured rock. This mechanism can be assumed to contribute significantly to damages to coastal structures as well as to the undercutting of rock cliffs. One peculiar aspect of wave impact driven undercutting seems to be that, since breaking waves only occur in storm events, the erosion (and subsequent failure) of rock cliffs occurs not continuously but possibly only within a few days in every year. Further research in this field is required in order to assess exposure condition and erosion rate, to investigate the propagation of impact pressures into water or air filled crack systems and to relate rock undercutting to these influences. In particular, the following topics seem to promise to give further information on the mechanism and probability of cliff erosion:

(i) the relationship between breaker type, cliff properties and rock erosion;
(ii) the effect of pressurized cracks on the rock material itself (crack growth);
(iii) the change of shape of a rock cliff created by wave induced erosion (e.g. undercutting), and the effect this has on stresses inside of the cliff;
(iv) cliff instability;

At Queen's University Belfast, a more detailed numerical study focusing on the effect of wave induced erosion on the stability of idealized rock cliffs is currently under way.

Conclusions

Wave action on rock cliffs is not usually regarded as one of the main erosive forces on rock cliffs. If wave action is considered, the forces generated are assumed to be a function of the incident wave energy and subsequently the wave height. The erosion mechanism usually assumed is wave pressure induced abrasion of the rock front. In coastal engineering, it has long been established that the exposure risk of a coastal

structure to breaking waves is a function of sea bed slope and incident wave steepness, with sea bed slopes of 1:5 to 1:30 generating the maximum exposure. Within a study of wave induced damages of blockwork coastal structures it was found that wave impact generated pressures can travel into water filled cracks or joints, thus damaging or destroying the structure from within. A similar damage mechanism may apply to rock cliffs, generating splitting pressures inside of the rock thus straining the material where it is weakest, in tension. In rock cliffs, cracks are however continuous systems and may well be only partially filled with water. A series of experiments was conducted in Queen's University of Belfast's wave channel to assess the characteristics of breaking wave impact induced pressure pulse propagation through fully and partially water filled cracks and thus to determine the possibility of this erosion mechanism for rock cliffs. In completely submerged cracks the pressure pulses generally travel at very low velocities of 70–100 m/s corresponding to an air content of 1–3%. This slow speed of propagation for completely submerged cracks was attributed to the fact that the water constitutes a two-phase-medium with very different properties than pure water (air content of approximately 1.0%). Velocities in partially submerged cracks were found to be around 300 m/s; significantly higher than in water filled cracks and in the range of the speed of sound in air. It was also found that pulses attenuate fast inside the fully submerged crack, and slowly in partially submerged ones. The impact of waves on partially filled cracks or crack systems would thus allow the propagation of high and short pressure pulses deep into the system with little attenuation of the pulse. Pressures applied within a crack will enforce an opening of the crack and lead to very high tensile stresses at the crack tip, causing the brittle rock material to fail at this location and leading to crack growth. It is hypothesized that partially water filled cracks which are exposed to breaking waves are possibly even more dangerous for the integrity of blockwork structures and rock cliffs than water filled cracks.

Acknowlegements. The authors would like to gratefully acknowledge the financial support for this research from the German Academic Exchange Board (*Deutscher Akademischer Austauschdienst*, DAAD) and from the UK's Engineering and Physical Science Research Council EPSRC under Grant GR/ R 30600.

References

BATTJES, J. A. 1968. Refraction of water waves. *Journal of Waterways and Harbour Division,* American Society of Civil Engineers (ASCE), **WW4**, 437–457.

BENUMOF, B. T. & GRIGGS, G. B. 1999. The Dependence of Seacliff Erosion Rates on Cliff Material Properties and Physical Processes: San Diego County, California. *Shore & Beach*, **67**, No.4, pp. 29–41.

BLACKMORE, P. A. & HEWSON, P. 1984. Experiments on full scale impact pressures. *Coastal Engineering*, **8**, 331–346.

BOLLAERT, E. & SCHLEISS, A. 2001. A new approach for better assessment of rock scouring due to high velocity jets at dam spillways. *Proceedings 5th International comission on Large Dams (ICOLD) Symposium*, Geiranger, Norway.

BULLOCK, G. N., HEWSON, P., CRAWFORD, A. R. & BIRD, P. A. D. 1999. Field and laboratory measurements of wave loads on vertical breakwaters. *Proceedings Coastal Structures,* **99**, Santander, Spain, 613–622.

CARTER, R. W. G. 1991. *Coastal Environments: An Introduction to the Physical, Ecological and Cultural Systems of Coastlines*. Academic, London.

CRAWFORD, A. R. 1999. *Measurement and Analysis of Wave Loading on a Full Scale Coastal Structure*. PhD thesis, University of Plymouth.

HULL, P. & MÜLLER, G. 2002. Breaker shape and impact pressures. *Ocean Engineering,* **29**, 59–79.

MUIR WOOD, A. M. & FLEMING, C. A. 1981. *Coastal Hydraulics,* 2nd edition. MacMillan, London.

MÜLLER, G. 1997. Propagation of wave impact pressures into water filled cracks. *Proceedings Institution of Civil Engineers, Water, Maritime and Energy*, **124**(2), 79–85.

MÜLLER, G., COOKER, M. J., ALLSOP, W., BRUCE, T. & FRANCO, L. 2002. Wave effects on blockwork structures, part 1: field observations and model tests. *Journal of Hydraulic Research*, **40**, 117–124.

ROUVILLE, M. A. 1938. Etudes internationales des efforts dus aux lames. *Annales des Ponts et Chaussees*, **VII**, Paris, 2–113.

SHIELD, W. 1895. Principles and Practice of Harbour Construction. Longmans, London.

SUNAMURA, T. 1973. Coastal cliff erosion due to waves – field investigations and laboratory experiments, *Journal of the Faculty of Engineering, University of Tokyo*, **32**, 1–86

SUNAMURA, T. 1992. *Geomorphology of Rocky Coasts*, Wiley, Chichester.

Geological Society, London, Engineering Geology Special Publications

Laboratory abrasion tests on beach flint shingle

U. Dornbusch, C. A. Moses, D. A. Robinson and R. B. G. Williams

Geological Society, London, Engineering Geology Special Publications 2004; v. 20; p. 131-138
doi:10.1144/GSL.ENG.2004.020.01.10

Laboratory abrasion tests on beach flint shingle

U. Dornbusch, C. A. Moses, D. A. Robinson & R. B. G. Williams

Centre for Environmental Research, School of Chemistry, Physics and Environmental Science, University of Sussex, Falmer, Brighton, BN1 9QJ, UK

Abstract: Laboratory tumbling experiments demonstrate that rounded flint beach shingle is less durable than commonly supposed. The mean rate of abrasion for dark grey Sussex flints (Senonian) in the first few hours of tumbling increases with weight whereas that of white Normandy flints (Turonian and Coniacian) does not. Depending on pebble weight, the Sussex flints abrade at up to six times the rate of the Normandy flints. Abrasion rates also vary according to tumbler load, the water:shingle ratio, and tumbling period. The abrasion rate of Sussex flints decreases with time at a much greater rate than could be expected from the reduction in size. The abrasion debris is mostly silt sized, but small quantities of sand are produced from samples containing larger pebbles. *In situ* abrasion of flint shingle is estimated to be significant, reducing the protection shingle beaches afford to cliffs thus exacerbating Chalk cliff instability.

Introduction

The Cretaceous chalk outcrop gives rise to impressive sea cliffs and shore platforms on the Channel coast of Sussex and Normandy (the Rives Manche). Weathering of the cliff faces and wave erosion release flints that contribute to beach shingle that rests on the shore platform in front of the cliffs. Erosion of Quaternary and Tertiary gravels that overlie the chalk also supplies flints to the beaches, though in much smaller quantities. The shore platforms and the beaches combine to reduce the energy of waves striking the cliffs, and can so be assumed to reduce the rate of cliff retreat. The flint shingle beaches are also important because they help to protect low-lying stretches of coast from flooding, forming shingle bars across valley mouths and former marine embayments.

In both Sussex and Normandy, movement of shingle along the beaches is generally in an easterly direction under the influence of the prevailing southwest winds. In addition to this 'longshore drift' there are frequent movements of shingle up and down the shore. This repeated disturbance must cause abrasion of the shingle. However, the rate of any reduction in beach volume resulting from such abrasion is not known. The traditional assumption, based on very little research, is that flint shingle is highly resistant to wave action, and that abrasion losses are not a significant coastal management issue within the 50 year time scale of most engineering projects. The experiments described here are designed to estimate the susceptibility of flint shingle to abrasion under controlled laboratory conditions and are the basis for estimating flint shingle abrasion in the surf zone (Dornbusch *et al.* 2002); the results challenge the traditional view that flint shingle is highly durable.

Previous studies

Laboratory investigations of rock abrasion have a long history from early tumbling experiments using stone and iron jars (Daubrée 1879), wood lined drums (Wentworth 1919; Krumbein 1941) and rocking troughs (Kuenen 1964) to more recent experiments using rubber lined metal drums (Bigelow 1984; Latham *et al.* 1998; Lewin & Brewer 2002; Loveday & Naidoo 1997). Interpreting the results of these experiments is made difficult by the variety of rock types, sizes and shapes that have been tested, as well as the lack of standardization of container size, shape and revolution velocity. Many of the experiments have been concerned to study shape changes rather than measure abrasion rates, and have used materials such as angular limestone or sandstone clasts that become rapidly rounded when subjected to artificial abrasion. Flint, and its pale coloured variant chert, abrade less quickly and so have been relatively neglected, though flint has been used as an abrasive for tumbling with softer rock materials (e.g. Latham *et al.* 1998). The result is that views on the abrasion rate of flint are, at best, semi-quantitative. For example, Kuenen (1964, pp. 29 and 42) reports from experiments that 'rounded chert is ten times as resistant as quartzite', and estimates that it would take 'a thousand years for chert to form an ellipsoid'. Bray (1997, p. 1041) suggests from laboratory and field experiments that freshly supplied angular flint gravel 'suffers an approximate 10% loss within the first year on the beach, whilst well rounded pebbles are abraded very slowly'. Using flint from Reculver in Kent as an abrasive for other lithologies, Latham *et al.* (1998) reported negligible abrasion rates for the flint.

From: MORTIMORE, R. N. & DUPERRET, A. (eds) 2004. *Coastal Chalk Cliff Instability*. Geological Society, London, Engineering Geology Special Publications, **20**, 131–138. 0267-9914/04/$15.00

Method

All the laboratory experiments described here were conducted by tumbling flint shingle collected from beaches in Sussex and Normandy in rubber lined hexagonal barrels, rotating at 28 rpm (fixed rotation speed of the equipment). The smallest diameter of the barrels was 200 mm, the largest diameter 225 mm and the length 205 mm, giving a volume of 7000 cm^3. Individual pebbles varied from 20 g to 500 g in weight with grain size (*b*-axis) varying from 15 to 70 mm. The pebbles were tumbled in reconstituted seawater with a salinity of 3.6%, which was prepared by mixing additive-free, culinary sea salt from France with deionized water. The tumbling was stopped at intervals to allow the pebbles to be weighed. Any loss of weight was assumed to be due to abrasion. Before tumbling was resumed, the sea water in the barrels was changed and any abrasion debris was removed.

In order to establish a standard test procedure preliminary experiments were carried out using a variety of flint loads, water to flint ratios, tumbling periods and water types.

Preliminary experiments

Experiment 1

This was designed to compare the abrasion rates of well rounded beach flint and freshly broken flint. Eight weighed flints between 56 and 211 g were tumbled in a barrel for a total of 130 hours (Fig. 1). One was a freshly broken angular fragment of flint from a recent rockfall at Friars Bay, Peacehaven, Sussex [TQ40700020] and the other nine were well-rounded flint pebbles from the beach next to the fall. The flints were tumbled in the reconstituted seawater, except between 90 and 107 hours of the experiment when deionized water was temporarily substituted to estimate the influence of the water's chemical composition in accordance with experiments by Bigelow (1988).

Five minutes after the start of the experiment, the tumbling was stopped and the flints were removed from the barrel, surface dried using paper towels and re-weighed. They were then returned to the barrel for further tumbling. The tumbling was interrupted for re-weighing many more times, at intervals varying from 10 minutes to 16 hours until, after 76 hours of tumbling, the interval was standardized at 2.5 hours (accommodating three tumbling intervals into one working day). During the first few hours of tumbling the angular flint fragment lost ~3% weight from breakage of its edges and corners, producing fragments up to 0.18 g. After this it wore down much more slowly with no visible fragments, except at 93 hours when a small piece of 0.1 g detached (Fig. 1). The rounded flint pebbles initially suffered less wear than the angular fragment, but as the experiment continued the total amounts of wear increased. By the end one of the pebbles had suffered a greater percentage weight loss than the angular fragment. The abrasion rates were quite variable, and not obviously correlated with the size of pebble.

Changing to deionized water during the experiment did not appear to affect the abrasion rate, although Bigelow (1988) found that distilled water induced more wear than seawater. In the interests of standardization it was decided to use reconstituted seawater in all subsequent experiments. The change of the tumbling interval to 2.5 hours at 72 hours marks a break in all curves, indicating that in this experiment the tumbling interval influences the abrasion rate.

A subsidiary experiment confirmed that the relatively rapid abrasion shown by the angular flint was a real effect and not chance sampling. Figure 2 records the progressive rounding of the edges and corners of ten freshly broken tabular flint fragments, totalling 640 g, from the rockfall at Friars Bay. Eleven grams, or nearly 2% by weight, of small broken fragments were produced during the first 15 minute

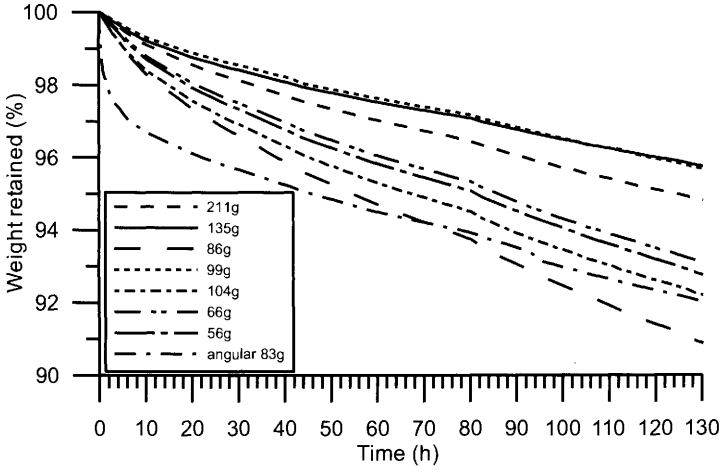

Fig. 1. Individual wear for one angular and seven rounded flints in relation to tumbling time and tumbling interval.

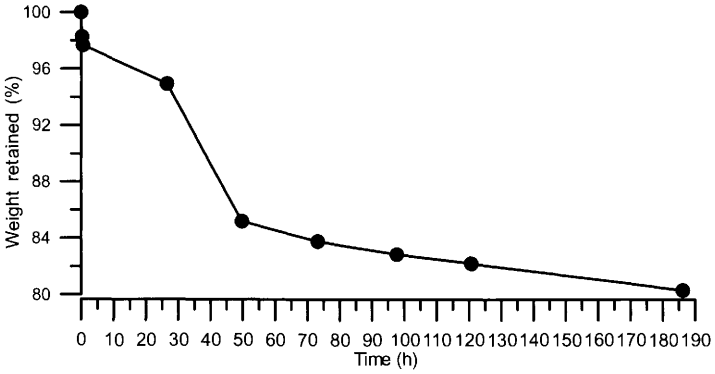

Fig. 2. Combined wear of ten freshly broken flints over 186.15 hours of tumbling showing phases of breakage and abrasion.

tumbling interval and rapid wear occurred until 50 hours after which major breakages ceased. These two experiments support previous findings (Bray 1997; Loveday & Naido 1997) and confirm field observations that freshly broken angular fragments from rockfalls lose several per cent of their weight in a short period of time to become subangular.

Experiment 2

The aim of this experiment was to assess the influence of barrel load on abrasion rates. One barrel was filled with well rounded, near-spherical flint pebbles of similar size (*b*-axis = 32–48.5 mm, mean weight 104 g), collected on Newhaven beach [TV54460999]. Reconstituted seawater was added to fill the voids and cover the pebbles. The pebbles were then decanted and randomly assigned to three barrels to create 50%, 35% and 15% flint loads. The interstitial water was divided amongst the barrels according to the same percentages so as to maintain a constant shingle:water ratio. Prior to weighing, the pebbles were surface dried using a paper towel. Each barrel was then tumbled for three successive tumbling intervals of 2.5 hours. The average weight loss of the pebbles over 7.5 hours was 0.4%.

As shown in Figure 3, the abrasion rate (as percentage weight loss per hour) in all three barrels decreased from one tumbling interval to the next. The rate also decreased with increasing barrel load. As more and more pebbles are placed in a barrel, their freedom of movement becomes increasingly restricted, thus reducing the number of impacts and hence the abrasion. The decrease of abrasion rate with time, which was also observed in subsequent experiments, seems to indicate that the pebble surface texture also changes during tumbling.

Experiment 3

This was designed to establish whether the shingle:water ratio is an important determinant of flint abrasion rates. The experimental design is based on the observation that the abrasion rate decreases over time (experiment 2). Three barrels were each one-third filled with flints (mean weight 80 g) from Newhaven Beach, tumbled for four successive 2.5 hour intervals and re-weighed each time. For the first and last tumbling

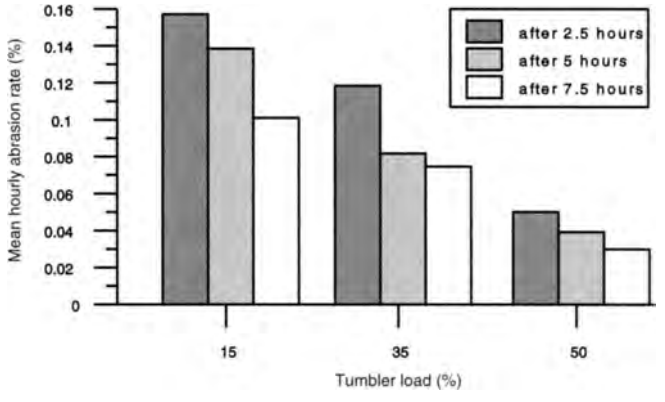

Fig. 3. Mean hourly abrasion rates expressed as percentage weight loss for three different barrel loads and three successive tumbling intervals each of 2.5 hours duration.

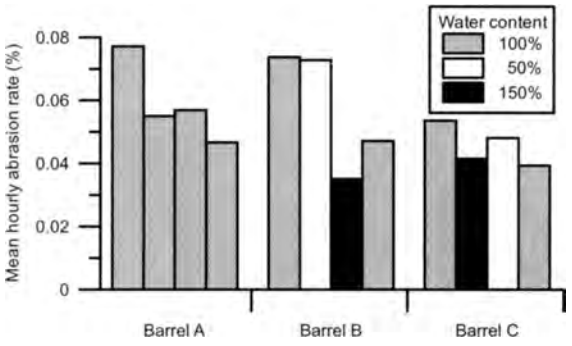

Fig. 4. Mean hourly abrasion rate for a random beach flint sample from Telscombe. Barrels were filled to 33% with pebbles, water content varied between 50 and 150%.

intervals, seawater was added to each barrel until it filled the voids and just covered the flints when the barrel was placed in an upright position. For the second and third tumbling intervals one barrel (A) was recharged with the same amount of water as before, a second (B) was recharged with only 50% as much water for the second interval and with 150% for the third interval, while the third barrel (C) was recharged first with 150% and then with 50% in mirror image of B.

The mean hourly abrasion rates for the three barrels are shown in Figure 4. Barrel A with the unchanged shingle:water ratio should have shown a gradual decrease in the abrasion rate like the one seen in Figure 2. However, during the second tumbling interval the abrasion rate was lower than expected. Barrel B shows a similar abrasion rate for the second interval to the first, indicating that the reduced amount of water increases abrasion. With an increased water amount the abrasion rate drops during the third interval and increases again when the water amount is decreased to 100%. Barrel C shows: a mirror image with a decreased abrasion rate during the second interval, coinciding with an increased amount of water; an increased abrasion rate during the third interval, coinciding with a decreased amount of water; and a decreased abrasion rate during the fourth interval, coinciding with an increased water amount. The experiment therefore seems to indicate that with an increased water:shingle ratio the abrasion rate decreases.

The three preliminary experiments indicate that, in order to ensure comparability between tumbling experiments, tumbling interval, barrel load and water:shingle ratio should be kept constant.

Main experiment

The aim was to assess the influence of shingle size and origin on abrasion rates. In light of the preliminary experiments, a standardized procedure was adopted. Sufficient pebbles of a chosen size were collected to fill one barrel. The barrel was then filled with water to determine the interstitial void space and the pebbles left to soak for 24 hours. The number of pebbles was then halved randomly to obtain two samples to be tumbled separately. All pebbles were then dried for 24 hours at 50°C after which individual pebble weights were recorded (sample Sussex A was weighed as bulk). The two samples were then placed into one barrel, which was filled with half the amount of water using reconstituted seawater. After being left to soak for 21.5 hours, the pebbles were tumbled for 2.5 hours; they were then removed, cleaned with water to wash off any abrasion material, again dried for 24 hours, and re-weighed. This procedure was repeated twice more, giving a total tumbling period of 7.5 hours. As before, abrasion rates were recorded as percentage weight loss per hour (Fig. 5).

The pebbles tested were from East Sussex beaches at Newhaven (samples Sussex A–B in Figures 4 and 5) and Telscombe [TQ53921014], samples Sussex C-H), and from Normandy beaches at Fécamp (~3110/55158, samples Normandy A and C) and Étretat (~2980/55098, samples Normandy B, and D to G). The number of pebbles used ranged from 12 (Sussex H) to 232 (Sussex A) per barrel.

In the case of the Sussex flint samples, the abrasion rate increased quite markedly (and linearly) with increasing pebble weight. Figure 5 and Table 1 summarize the results for the first 2.5 hours of tumbling. A similar increase in rate with size has been reported for other lithologies (e.g. Daubrée 1879; Krumbein 1941; Loveday & Naido 1997). Unexpectedly, however, the flints from the Normandy coast showed no increase in rate with size, and were much more resistant than the English flints.

The abrasion products were predominantly silt sized (Fig. 6), though the samples Sussex D–F each produced between 0.7 to 0.15% of fine sand grains in the range 300 to 500 μm. With the exception of Normandy C, the abrasion products of the Normandy flints were finer than those from Sussex. The mean size of the abrasion products appeared to be unrelated to shingle pebble size.

Figure 7 shows the change in the abrasion rate with time over the three successive 2.5 hour tumbling intervals averaged over all samples from Sussex and Normandy. The abrasion rate of the Sussex samples decreased with time, supporting the trend observed in preliminary experiments 2 and 3. The behaviour of the Normandy samples was quite different: the rate of abrasion dropped after the first 2.5 hours, but then rose after five hours to exceed the initial value.

Movement of the flint pebbles in the tumblers was observed by replacing the metal lids with Perspex. This showed that abrasion is caused by low impact collisions and by the pebbles rolling and sliding over each other. High-energy collisions do not occur because the tumblers are small, preventing the pebbles from gaining much kinetic energy. The seawater in the barrels also helps to cushion impacts.

Discussion

Several researchers (e.g. Krumbein 1941; Bigelow 1984; Sunamura *et al.* 1985) have observed decreases in abrasion

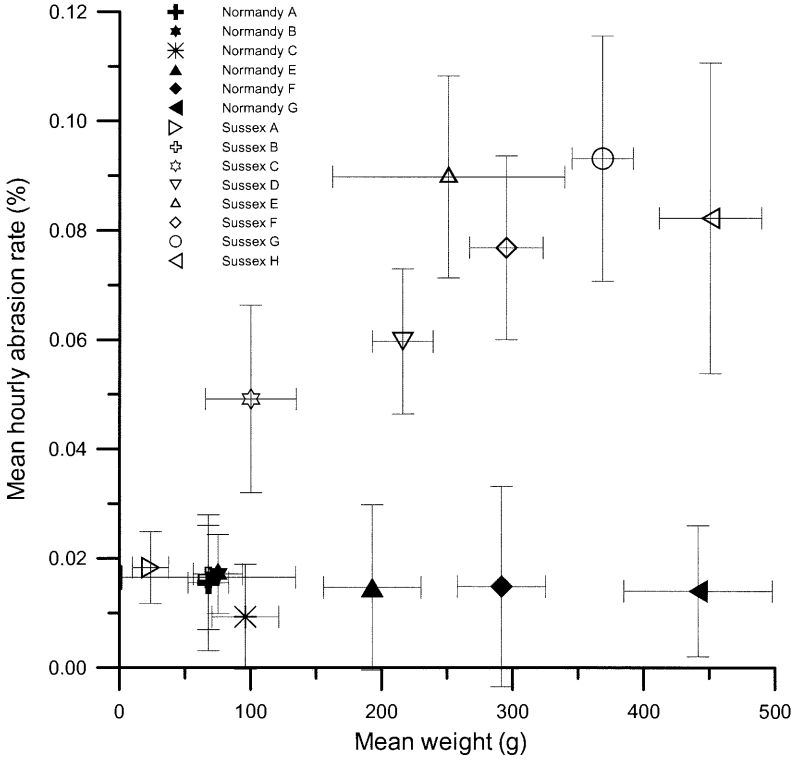

Fig. 5. Comparison of abrasion rates between flints from East Sussex and Normandy in relation to mean pebble size (weight). Error bars are one standard deviation.

Table 1. *Summary of shingle parameters and abrasion rates*

	Weight (g)						*Abrasion rates as loss per hour (%)*				
	N	$\bar{X}$	σ	*maximum*	*minimum*	*median*	$\bar{X}$	σ	*maximum*	*minimum*	*median*
Normandy A	156	67.798	15.532	108.515	31.787	65.839	0.0174	0.0114	0.0731	0.0009	0.0151
Normandy B	138	75.172	18.847	131.086	31.142	73.287	0.0176	0.0061	0.0397	0.0057	0.0168
Normandy C	118	96.050	25.530	188.328	47.443	89.906	0.0093	0.0096	0.0846	0.0038	0.0097
Normandy D	64	148.932	45.806	276.430	69.996	144.231	0.0216	0.0134	0.0792	0.0046	0.0210
Normandy E	50	192.946	37.135	259.423	123.088	194.787	0.0184	0.0151	0.0501	0.0009	0.0174
Normandy F	34	291.647	33.724	362.963	238.029	292.255	0.0200	0.0108	0.0454	0.0021	0.0170
Normandy G	24	441.480	56.489	556.760	349.670	428.750	0.0156	0.0079	0.0296	0.0010	0.0155
Sussex A	464	23.721	13.907	69.391	2.775	21.544	0.0183	0.0066	not calculated for individuals†		
Sussex B	278	40.145	66.638	148.724	11.768	34.566	0.0171	0.0087	0.0793	0.0001	0.0157
Sussex C	48*	100.315	34.687	213.527	53.185	92.784	0.0492	0.0172	0.0830	0.0044	0.0528
Sussex D	48	216.305	23.184	249.585	173.342	220.205	0.0597	0.0133	0.0886	0.0266	0.0580
Sussex E	40	251.323	88.626	474.820	107.265	216.855	0.0898	0.0185	0.1282	0.0546	0.0943
Sussex F	34	295.404	28.035	351.308	250.042	291.475	0.0768	0.0168	0.3695	0.1401	0.1853
Sussex G	28	368.845	23.386	400.446	304.994	375.243	0.0931	0.0224	0.1317	0.0467	0.0946
Sussex H	24	451.004	38.970	545.82	404.910	439.110	0.0823	0.0284	0.1337	0.0267	0.0815
Reculver I	249	42.797	14.715	85.980	14.053	41.751	0.0195	0.0158	0.2393	0.0057	0.0181
Reculver II	98	96.912	47.057	346.816	28.387	86.879	0.0264	0.0120	0.1076	0.0051	0.0243
Le Criel	92	122.469	38.646	232.489	57.597	110.233	0.0524	0.0142	0.1064	0.0228	0.0514

* only one barrel used.
† weight loss was calculated from bulk material and not individual pebbles.

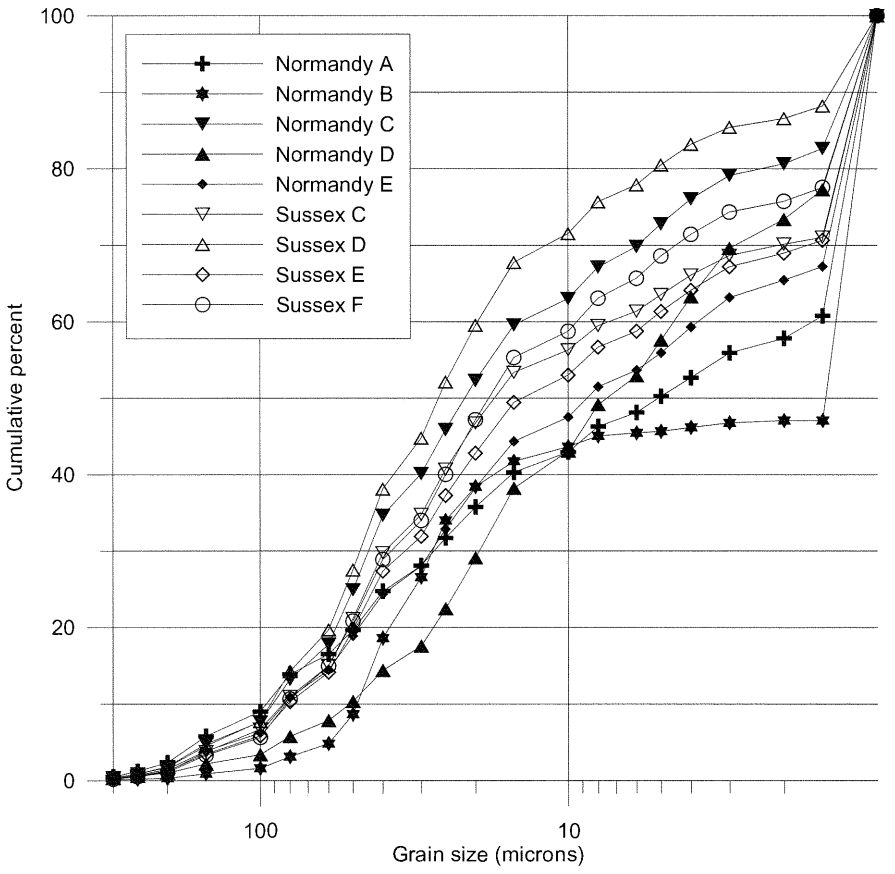

Fig. 6. Comparison of grain size of the abrasion products after the first 2.5 hours tumbling interval.

rates over time but only from initially angular fragments to more rounded pebbles and have attributed this to changes in shape or weight. Sunamura *et al.* (1985), investigating sliding rock cubes, claim that the reduction is merely a function of decreasing pebble size. However, neither shape nor weight changes of the Sussex flints over a few hours are large enough to explain the observed decrease in the abrasion rate. In the tumbling experiments described here, the abrasion rate drops 15% between the first two tumbling intervals even though weight loss is of the order of 0.2% for a mean pebble size of 300 g. Only a small fraction of the decrease in abrasion rate can thus be attributed to weight loss. With such small weight changes, appreciable changes in shape or roundness do not occur. Most of the reduction must be due to other factors, the most important of which may be changes in pebble surface texture.

Minute crescentic fractures develop on the surfaces of flint pebbles on Sussex beaches causing the initial black surface to appear grey. These 'chatter-marks' are believed to develop during storms when the pebbles make high-energy impacts with each other (Williams & Roberts 1995). When the pebbles are tumbled in the laboratory, where most of the movement is rolling and sliding, the chatter marks are likely to be slowly worn away so that the pebbles become smoother. Impacts between the pebbles are evidently too gentle and too few to create new, or sustain existing, chatter marks.

The failure of the tumbling to renew chatter-marked surfaces may well explain why the rate of wear of the pebbles decreased with time. It may also mean that the experiments underestimate the abrasion rate of flint pebbles in the high-energy beach environment. Differences in the extent to which the surface of individual pebbles in the field are chatter-marked may result from differences in exposure to waves and could explain the large variability of abrasion rates indicated by the error bars in Figure 5.

Further experiments are planned to quantify the degree of surface microfracturing and brittleness, and to investigate its influence on abrasion rates. These experiments will also examine the question of why the samples of flint shingle from the Normandy beaches proved much more resistant to abrasion than the samples of Sussex shingle. All the flint pebbles tested are thought to have originated from erosion of

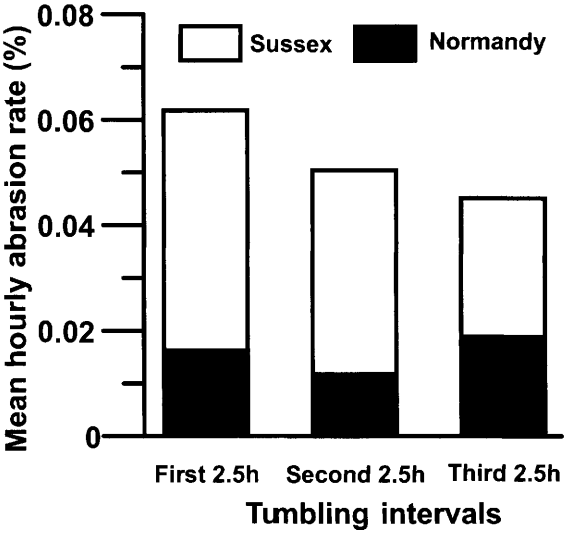

Fig. 7. Abrasion rates for three successive tumbling intervals of 2.5 hours each, averaged over all samples from Normandy and Sussex included in the main experiment.

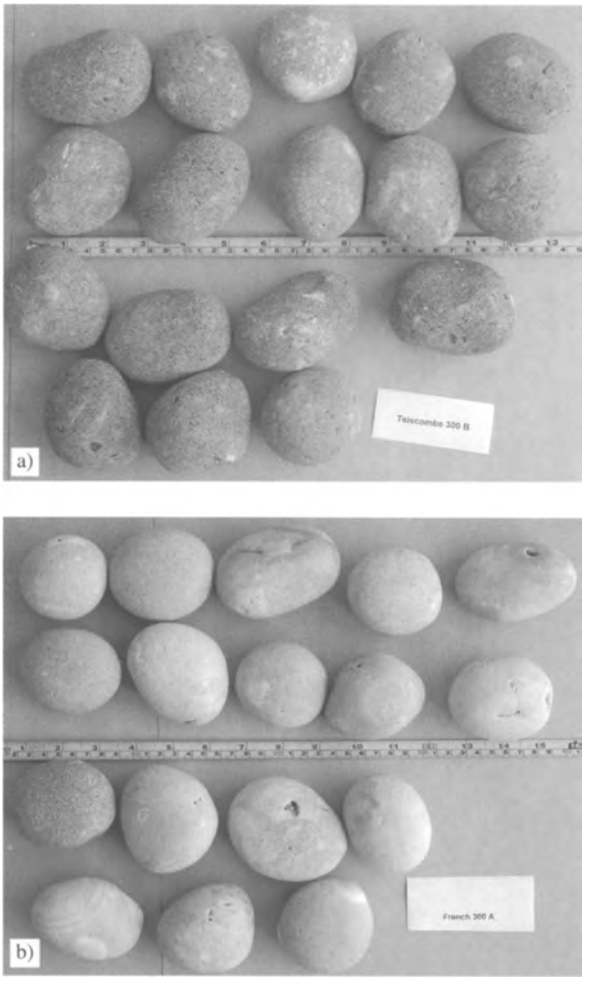

Fig. 8. Visual comparison between the samples (a) Sussex E and (b) Normandy E.

the Chalk strata exposed in the cliffs and shore platforms immediately adjacent to or just west of the sampling sites, and not from Quaternary gravels or other secondary sources. The dark grey to black Telscombe and Newhaven flint pebbles (Fig. 8) were almost certainly derived from the High Santonian–Lower Campanian Newhaven and Culver chalks, which form the local cliffs and shore platforms. Likewise, the flint pebbles from Étretat and Fécamp can be assumed to have originated from the older Turonian and Coniacian chalk, which forms the local cliffs and platforms. They are pale grey to white and sometimes banded, unlike flints from equivalent strata in Sussex which are dark grey or black. Despite their different age and colour, the flints from both the Sussex and Normandy locations have a density of 2.5–2.6 g cm^{-3} and Schmidt Hammer hardness tests conducted on samples Normandy E ($\bar{x}=60.47$, $\sigma=3.2$) and Sussex E ($\bar{x}=60.4$, $\sigma=2.8$) showed no appreciable differences (N for each sample = 17).

Although the Normandy coast is more sheltered from the prevailing southwest gales than its Sussex counterpart, significant wave heights are on average only slightly lower than for the Sussex coast (BODC 1998). Significant wave heights for extreme conditions, however, are ~0.5 m lower on the French than on the Sussex coast (Posford Duvivier 1993; Allen & Delannoy 1990). Thus, the wave environment on the two coasts does not appear to be sufficiently different to explain the significantly different abrasion behaviours of the flint pebbles. Nevertheless preliminary examination suggests that the Normandy pebbles may be smoother and less intensely chatter-marked than the Sussex pebbles. Further tests are planned to examine the influence of different surface texture characteristics. That the flints from Étretat and Fécamp are likely to be much different from other Normandy flints is indicated by the tumbling of two barrels filled with dark grey and black flints from Criel-sur-Mer (it is difficult to give the petrographic provenance to these flints due to longshore drift). Criel-sur-Mer flints with a mean size of 122 g abraded at 0.052% per hour (Table 1) and fit well into the abrasion curve of the Sussex flints. Two samples of dark grey flint from Reculver (Table 1) produced abrasion rates closer to the range for the Sussex flints than for the Normandy flints but the limited grain size of the samples does not produce conclusive results. However, these abrasion rates show that the flints abrade measurably and that the differing results obtained by Latham *et al.* (1998) are likely to be caused by differences in tumbler and general experimental design.

As Figure 5 shows, the abrasion rate in the first 2.5 hours roughly doubles (abrasion rate = 0.0002mean weight + 0.0183 with $R^2 = 0.828$) with increasing pebble weight from 100 to 500 g for the Sussex flints. It is difficult to explain why abrasion rates increase with pebble size for Sussex but not for Normandy flints. Because large pebbles are heavier than smaller pebbles they could be expected to generate greater impact pressures. This explanation ought to apply equally to the Normandy pebbles but clearly it does not, perhaps because they are much more resistant to the relatively weak abrasion forces of the tumbler. However, this is not supported by the Schmidt hammer values.

Conclusion

The tumbling experiments, using flint pebbles from the Sussex and Normandy beaches, have shown that the Normandy flints are much more resistant to abrasion than those from Sussex. In the first 2.5 hours of tumbling, Sussex flints lose on average about 0.06% of their weight per hour whilst the Normandy flints lose 0.018% (averaged over all grain sizes). Impacts in the tumbler are frequent but of much lower energy than those on the actual beaches, which could suggest that abrasion losses on the beaches are by no means negligible. If flint shingle volumes on Sussex beaches are being appreciably reduced by abrasion, the beaches may provide less effective protection from flooding and cliff erosion than is commonly supposed. The implications for coastal zone management are considerable, and further research will combine field experiments with laboratory tests to estimate rates of flint pebble abrasion on actual beaches.

Acknowledgements. The research was part of the project 'Beach Erosion in the Rives Manche (BERM)', funded by the EU, European Regional Development Fund, Interreg II Programme. The authors would like to thank S. Costa, J. Pagny and P. Gabriel for helping with the collection of pebbles from Normandy and David Pope and Steve Mitchell for helpful comments on the draft.

References

ALLEN, H. & DELANNOY, B. 1990. *Mesure de Houle en Differents Sites du Littoral Français.* Rapport EDF-LNH HE-45/88.03.532.

BIGELOW, G. E. 1984. Simulation of pebble abrasion on coastal benches by transgressive waves. *Earth Surface Processes and Landforms*, **9**, 383–390.

BIGELOW, G. E. 1988: Laboratory study of the role of seawater in basalt pebble abrasion. *Journal of Coastal Research* **4(1)**, 103–113.

BRAY, M. J. 1997. Episodic shingle supply and the modified development of Chesil Beach, England. *Journal of Coastal Research*, **13(4)**, 1035–1049.

BODC (British Oceanographic Data Centre) 1998: United Kingdom Digital Marine Atlas.

DAUBRÉE, A. 1879. Études synthétiques de Géologie Expérimentale. Paris. Dunod.

DORNBUSCH, U., WILLIAMS, R. B. G., MOSES, C. & ROBINSON, D. A. 2002. Life expectancy of shingle beaches: measuring in situ abrasion. *Journal of Coastal Research, Special Issue*, **36**, 249–255.

KRUMBEIN, W. C. 1941. The effects of abrasion on the size, shape and roundness of rock fragments. *Journal of Geology*, **49**, 482–520.

KUENEN, P. H. 1964. Experimental Abrasion: 6. Surf action. *Sedimentology*, **3**, 29–43.

LATHAM, J.-P., HOAD, J. P. & NEWTON, M. 1998. Abrasion of a series of tracer materials on a gravel beach, Slapton Sands, Devon, UK. *In*: LATHAM, J.-P. (ed.) Advances in Aggregates and Armourstone Evaluation. Geological Society, London, Engineering Geology Special Publications, **13**, 121–135.

LEWIN, J. & BREWER, P. A. 2002: Laboratory simulation of clast abrasion. *Earth Surface Processes and Landforms*, **27**, 145–164

LOVEDAY, B. K. & NAIDOO, D. 1997. Rock abrasion in autogenous milling. *Minerals Engineering*, **10(6)**, 603–612.

POSFORD DUVIVIER, 1993. Eastbourne Borough Council, Coastal Strategy Study Stage 2A, Appendices.

SUNAMURA, T., MATSUKURA, Y. & TSUJIMOTO, H. 1985. A laboratory test of tractive abrasion on rocks in water. *Transactions of the Japanese Geomorphological Union*, **6(1)**, 65–68.

WENTWORTH, C. K. 1919. A laboratory and field study of cobble abrasion. *Journal of Geology*, **27**, 505–521.

WILLIAMS, A. T. & ROBERTS, G. T. 1995. The measurement of pebble impact and wave action on shore platforms and beaches: the swash force transducer (swashometer). *Marine Geology* **129**, 137–143.

Geological Society, London, Engineering Geology Special Publications

Quantification of the Normandy and Picardy chalk cliff retreat by photogrammetric analysis

S. Costa, D. Delahaye, S. Freiré-Diaz, L. Di Nocera, R. Davidson and E. Plessis

Geological Society, London, Engineering Geology Special Publications 2004; v. 20; p. 139-148
doi:10.1144/GSL.ENG.2004.020.01.11

Quantification of the Normandy and Picardy chalk cliff retreat by photogrammetric analysis

S. Costa[1], D. Delahaye[2], S. Freiré-Diaz[2], L. Di Nocera[2], R. Davidson[1] & E. Plessis[3]

[1] Université de Caen Basse-Normandie, Département de Géographie, Laboratoire Géophen, UMR-CNRS-LETG 6554, Esplanade de la Paix, BP 5186, 14032 Caen cedex, France

[2] Université de Rouen, Département de Géographie, Laboratoire MTG, UPRESA 6063 Idées, 76821 Mont-Saint-Aignan cedex, France

[3] Université de Nantes, Département de Géographie, Laboratoire Géolittomer-Nantes, UMR-CNRS-LETG 6554, BP 81227, 44 312 Nantes cedex 3, France

Abstract: The chalk cliffs of Normandy and Picardy are retreating rapidly and approaching the built-up areas located near the shore. Previous studies of cliff retreat in this area suffer from a large margin of error (absolute error in cliff position is ±7 m) due to the techniques and methods used. This paper presents a recent study which aims to quantify the chalk cliff retreat between 1966 and 1995 by means of photogrammetric analysis. In addition to the very high accuracy of the results (absolute error in cliff position is ±0.3 m), this technique gives geo-referenced numeric data allowing the creation of a geographical databank intended to become a tool for hazard management in coastal zones. Three scales of analysis have been used: a retreat value per hydro-sedimentary cell, per sub-cell and one every 50 m. These scales show that this regressive dynamic is spatially very variable. However, three zones of distinct retreat rates are apparent. These appear to be linked with the lithological characteristics of the chalk. Furthermore, the quantification associated with the flint content of the cliff allows an assessment of the flint shingle provision from the cliff to the shore.

Introduction

The coast of Haute-Normandy and Picardy is of special interest for the analysis of hazards in coastal erosion. This is due to its specific lithological characteristics (Upper Cretaceous flinty chalk), to its facing Atlantic storms and also to its urbanization close to the shore. This threat to the local population and its activities is very important, especially as the weakness of the chalk cliff leads to vigorous retreat. Even if this evolution is well understood, quantification of the rates and of the processes involved remains a problem. These difficulties are due to a lack of accurate, reliable and comparable documents over long time periods and to the discontinuous of the cliff erosion rhythm. Even if the erosion is continuous, the retreat occurs discontinuously, at various rates, according to different agents and processes in time and space. The coastal erosion management in Haute-Normandy and Picardy has been performed through construction of rigid defences in times of crisis which have a limited lifetime, a localized effect, and are often disruptive for the pebble longshore drift.

This review prompted territorial institutions from two regions to consider an interregional partnership dealing with coastal erosion. This was initiated within the framework of the 'Contract de Plan Interrégional du Bassin Parisien (CPIBP)' and continued by an Interreg II programme: 'Beach Erosion of the Rives-Manche'.

The first step in this interregional cooperation is the establishment of a reliable long-term follow-up method. The chosen method is the analysis of numerical photogrammetric surveys, which have been performed in 1966 and 1995 by the French National Geographic Institute (IGN) from the Cap d'Antifer to the Baie d'Authie. This method gives very accurate geo-referenced planimetric and altimetric values, providing information on the shoreline mobility. After a presentation of the first results and their limits, we will show the various advantages of this technique for developing a more accurate knowledge of the shoreline evolution and for improving its management. In addition to its high degree of accuracy, this study enables a determination of the future of hazard zones, and also an assessment of the flint supply due to cliff erosion. This flint feeds the shingle beach protecting the cliff foot and the urbanized valley mouth against the action of stormy swells. This last result is an important element in the understanding of the sediment budget of the Normandy and Picardy shore.

From: MORTIMORE, R. N. & DUPERRET, A. (eds) 2004. *Coastal Chalk Cliff Instability*. Geological Society, London, Engineering Geology Special Publications, **20**, 139–148. 0267-9914/04/$15.00

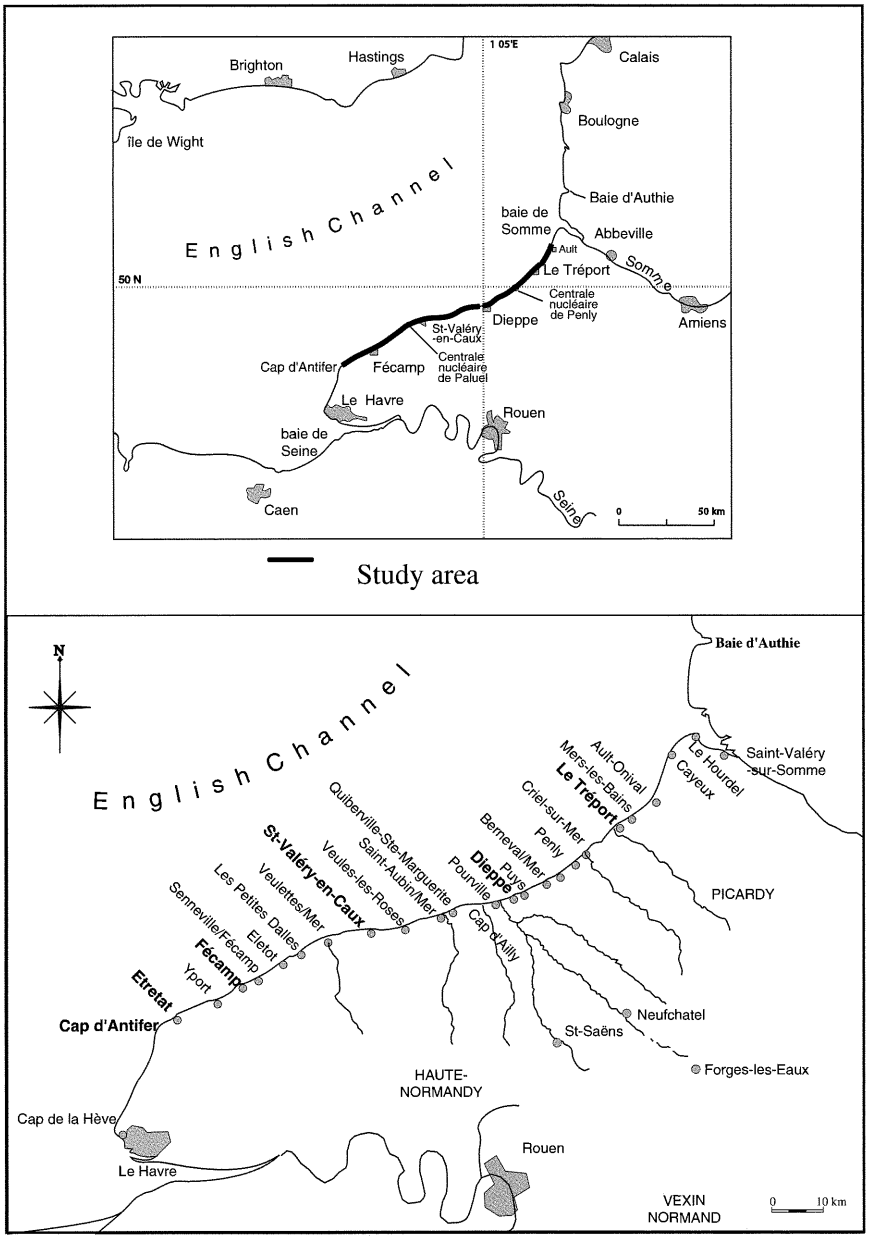

Fig. 1. Location maps of the study area.

Characteristics of the study area

The cliffs of the study area extend over 130 km of shoreline between the Cap d'Antifer (Haute-Normandy) and Ault-Onival (Picardy) (Fig. 1). The cliffs have an average height of 70 m. A wide shore platform (150–300 m) develops at their feet, covered on its landward margin by a thin shingle beach. These cliffs are cut by numerous dry and drained valleys perpendicular to the shoreline, and protected by a shingle beach that is often thick and between 30 and 100 m wide. These valleys represent the lowest points on the cliffs. Their altitude is no higher than the highest High Tide Level, which makes these zones very fragile.

Geologically, this area corresponds to the North-West

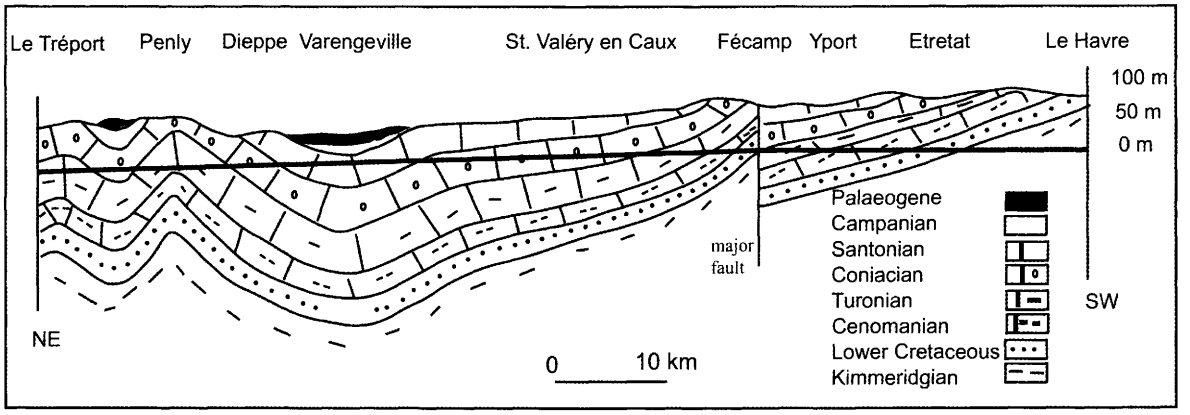

Fig. 2. Schematic geological section of the Haute-Normandy coast.

termination of the Parisian Basin. The plateau of Haute-Normandy and Picardy, and consequently its cliff, is formed of Upper Cretaceous chalk (Cenomanian to Campanian) more or less rich in flints (Cavelier *et al.* 1979; Mégnien *et al.* 1980 ; Pomerol *et al.* 1987). Residual formations with flint and Quaternary loess are also deposited on this karstified chalk.

Major tectonic deformations in NW–SE directions result in the outcrop of various layers from the Upper Cretaceous (Fig. 2). It is well known that the majority of cliffs are formed by Senonian white chalk rich in flint (Coniacian, Santonian and locally Campanian). Nevertheless, this apparent homogeneity hides more complex details (Juignet 1974; Kennedy & Juignet 1974; Bromley & Ekdale 1986 ; Pomerol *et al.* 1987; Mortimore & Pomerol 1987; 1990 ; Juignet & Breton 1994; Laignel 1997). Coniacian chalk is present between Antifer and Saint-Valéry-en-Caux, and also between Dieppe and Le Tréport. Santonian chalk is found continuously only in the central part of the shore from Saint-Valéry-en-Caux to Puys. Campanian is present locally from Quiberville to Pourville. Turonian, chalk comprising clayish, greyish to whitish, with little or no flint, protrudes from Antifer to Etretat, from Fécamp to Eletot, and from Puys to Tréport where it reaches its maximum extension at Penly. Locally, at the Antifer and Etretat cliff feet, and at the east of Fécamp, Cenomanian chalk protrudes. These are heterogeneous, sometimes rich in detrital componants (clay and quartz) and can be glauconitic or nodular. A cover approximately 10 m thick of sandy, clayish sediment of palaeogene origin can be found at the cliff top at cap d'Ailly, Sotteville and at Bois de Cise (Bignot 1962, 1983). For this paper, we used the chronostratigraphic stages. Nevertheless, for a good understanding of the cliff retreat, it is necessary to analyse in more detail the physical characteristics of the chalk that determine its strength. This requires the adoption of the established litho-stratigraphic classification used in the south of England by Mortimore (1983, 1986).

Because of their different structural characteristics favourable to weathering, the various ages of chalk layers correspond to different types of cliff morphology with contrasting rates of evolution. So, one of the aims of this paper is to bring out possible relations between cliff morphologies, the spatial distribution of the outcrop and the retreat rates of the cliff.

Methodology

The quantification of coastal evolution, especially cliff retreat, is not new. Numerous historical sources from the XVIII and XIX centuries mention the catastrophic disappearance of buildings or entire urban areas (De Lamblardie 1789, Guilmeth 1851). Because of the threat due to cliff erosion, its quantification is of significant interest and numerous studies have been undertaken (Briquet 1930; Dallery 1955; Prêcheur 1960; Bialek 1969; Regrain 1992; LCHF 1972; LCHF-BRGM 1987; Costa 1997, 2000; Dolique 1998; SOGREAH 1999). Nevertheless, as indicated in Table 1, results from various authors working on the same stretch of coastline can differ considerably. The high disparity of the results is due to the techniques and documents used, but also due to the time period where the study focused. As a result, it is difficult to compare these data.

The first documents used to assess the retreat of the shoreline are vertical aerial photographs from the French National Geographic Institute taken between 1947 and 1990. Routinely used, photo-interpretation contains various sources of error

Table 1. *Annual average retreat of the chalk cliff at Ault-Onival according to several authors*

Origin of the results	*Annual average cliff*
Dallery (1955)	0.5m
Hascoet (1987)	0.3–0.6m
Dolique (1992)	0.4m
Costa (1997)	0.35–0.7m
SOGREAH (1999)	0.43m

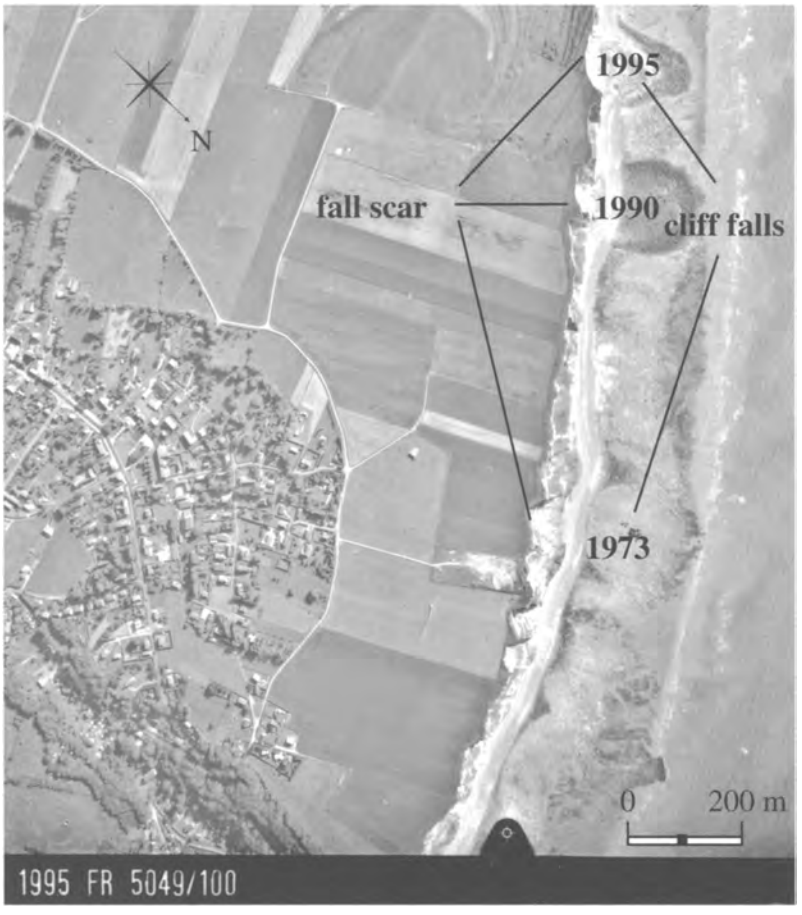

Fig. 3. Aerial view of the National Geographic Institute showing the cliff falls left on the shore platform (Berneval-sur-Mer, Haute-Normandy, 1995; scale 1:10 000).

(Stafford 1971; Dolan *et al.* 1980; Leatherman 1983; Thieler & Danforth 1994; Moore 2000). Indeed, investigations are limited by the photograph scale (between 1:20000 and 1:30000), parallax between the plane and the geographical object, the scale distortion of the pictures from centre to periphery, as well as the quality of the photographs. Because of these limits, it is not possible to map the entire shoreline, to compare them, and to quantify detailed modifications (Costa 1997; Costa *et al.* 2001). On the other hand, to limit the margin of error of the retreat results, it is possible to use marks left by rockfalls on the shore platforms which can remain for several decades (Costa 1997). The localization of these whitish masses on the shore platform enables observations to be focused on the departure zone at the cliff top (Fig. 3). With this reduction in area, the main problem inherent in the use of aerial photographs (scale distortion) is limited. The absolute error in cliff position is ± 7 m, i.e. an error margin of ±20% in the rate of cliff retreat. Moreover, the scale of the aerial photographs limits the accuracy and does not enable the localization of small rock falls, by photo-interpretation, which, on the Sussex chalk cliffs, represent 68% of the total number of events and 11% of the total lost land (May 1971; May & Heeps 1985). Despite the large margin of error, this method gives useful information on the exact location and the spatial and temporal evolution of the frequency of cliff falls.

To quantify accurately the rates of the Normano-Picard chalk cliff retreat, a photogrammetric analysis has been performed. The 1966 (Mission FR-1191/100) and 1995 (Mission FR-5049/100) vertical aerial photographic surveys from the French National Geographic Institute have been used (1:10000). These surveys have been chosen because of their large scale and above all because they have been especially collected for photogrammetric treatment. Indeed, the flight path followed the shoreline during low tide, and georeferenced markers (linked via planimetry and altimetry to the Lambert I projection system) were also placed along the flight path to improve the accuracy of the analysis. Then, a stereo-preparation and an aero-triangulation of the shots

were undertaken, allowing a paper and numerical reconstruction to a scale of 1:2000. Consequently, the cliff top from 1966 to 1995 is perfectly reproduced in planimetry in the Lambert I projection system. Moreover, altimetric points have been collected on the cliff-top and on shingle beaches (80 points per hectare) and on the shore platform (5 points per hectare).

The advantages of the photogrammetric technique are twofold. First, it provides highly accurate results. While the studies previously listed have a plurimetric margin of error (±7 m for the absolute error in cliff position), according to the French National Geographic Institute, this technique provides a decimetric accuracy (±0.30 m). The second advantage of this technique is based on the fact that data are numerical and geo-referenced. Consequently, the methodology can be performed again later on the same stretch of coast and on the fragile areas. This will give superimposable information allowing a diachronic analysis of the evolution.

The retreat value calculated is equivalent to the area of the lost land on the cliff top over the distance of studied shoreline. This measurement was performed at three scales:

(1) for each hydro-sedimentary cell delimited by harbour jetties;
(2) inside these cells, for each hydro-sedimentary sub-cell delimited by major groynes;
(3) every 50 metres.

The flint content of the cliff was assessed for each chalk stratum by a section survey and by photographic analysis. For the first method, flint content was calculated by measuring flintless chalk layers according the method of Ehrmann (1990). Photographic analysis consists first of perpendicular shots of the cliff by means of a digital camera. Then, this picture is processed with software to calculate a surface percentage of pixels equivalent to the flint quantity (Laignel 1997). Finally, these two methods are validated by granulometric analysis (Laignel 1997; Laignel *et al.* 1999).

Results

The photo-interpretation analysis of oblique aerial photography from the French National Geographic Institute between 1947 and 1990 (7 missions; National Geographic Institute) provided information on the cliff retreat, the location of rockfalls and the mean volume of rockfalls. Moreover, we have observed zones which have been retreating several times at the exact same spot. Consequently, it is possible to give information on the length of time per area between these events.

This study shows that we can distinguish two sectors having a distinctive regressive evolution (Fig. 4). One of these sectors, comprising two intervals between Etretat and Saint-Valéry-en-Caux, then between Berneval and Le Tréport, is affected by a smaller retreat rate (0.14 to 0.17 m a^{-1}), and is characterized by rare but massive rockfalls (mean return period over 25 years; mean retreat per event typically over 8 m). On the other hand, the area between Saint-Valéry-en-Caux and Berneval is affected by a more rapid rate of retreat of 0.20 to 0.51 m a^{-1}, and is characterized by more frequent but less massive rockfalls (mean return period of about 15 years; mean retreat per event about 6 m) (Costa 1997). Furthermore, this method allows the location and determination of the rockfall frequency evolution

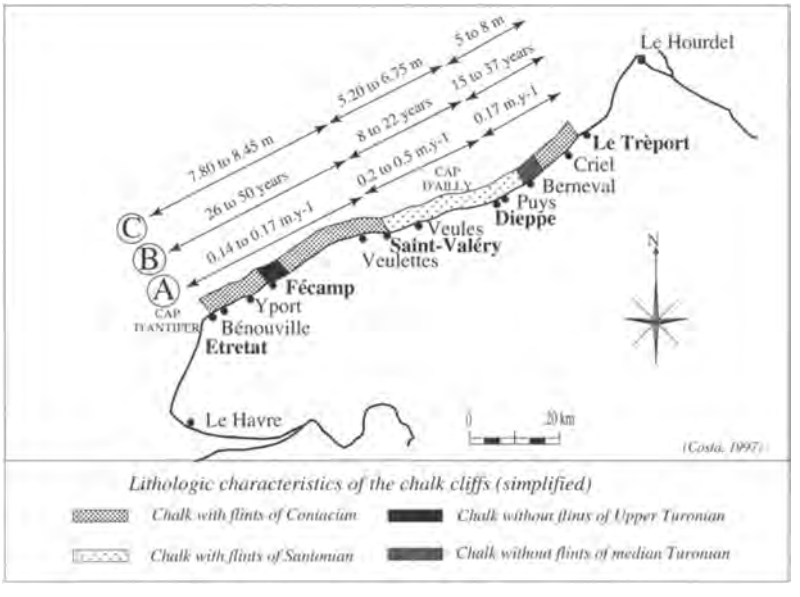

Fig. 4. Spatial location of the average cliff retreat rate (A), the average repeat period of cliff falls (B), and the average retreat per fall, in relation to the cliff toe stratigraphy (C), per area between 1947 and 1995 (Costa 1997).

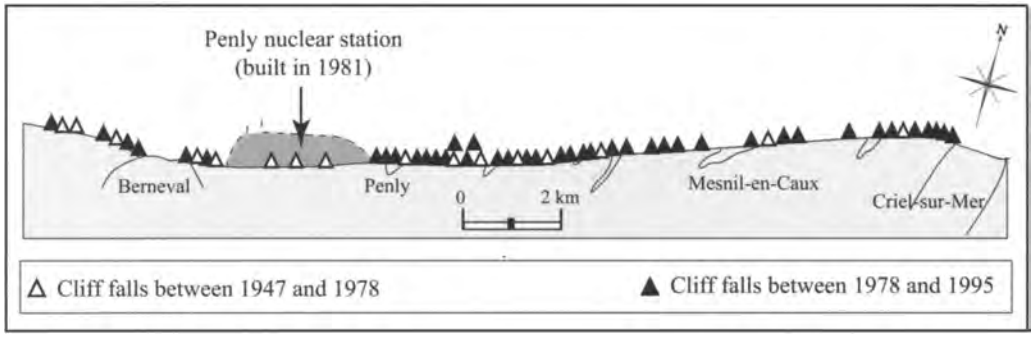

Fig. 5. Cliff falls location and frequency in the Berneval/Criel-sur-Mer area from the vertical views study of the National Geographic Institute (IGN) (Costa 1997).

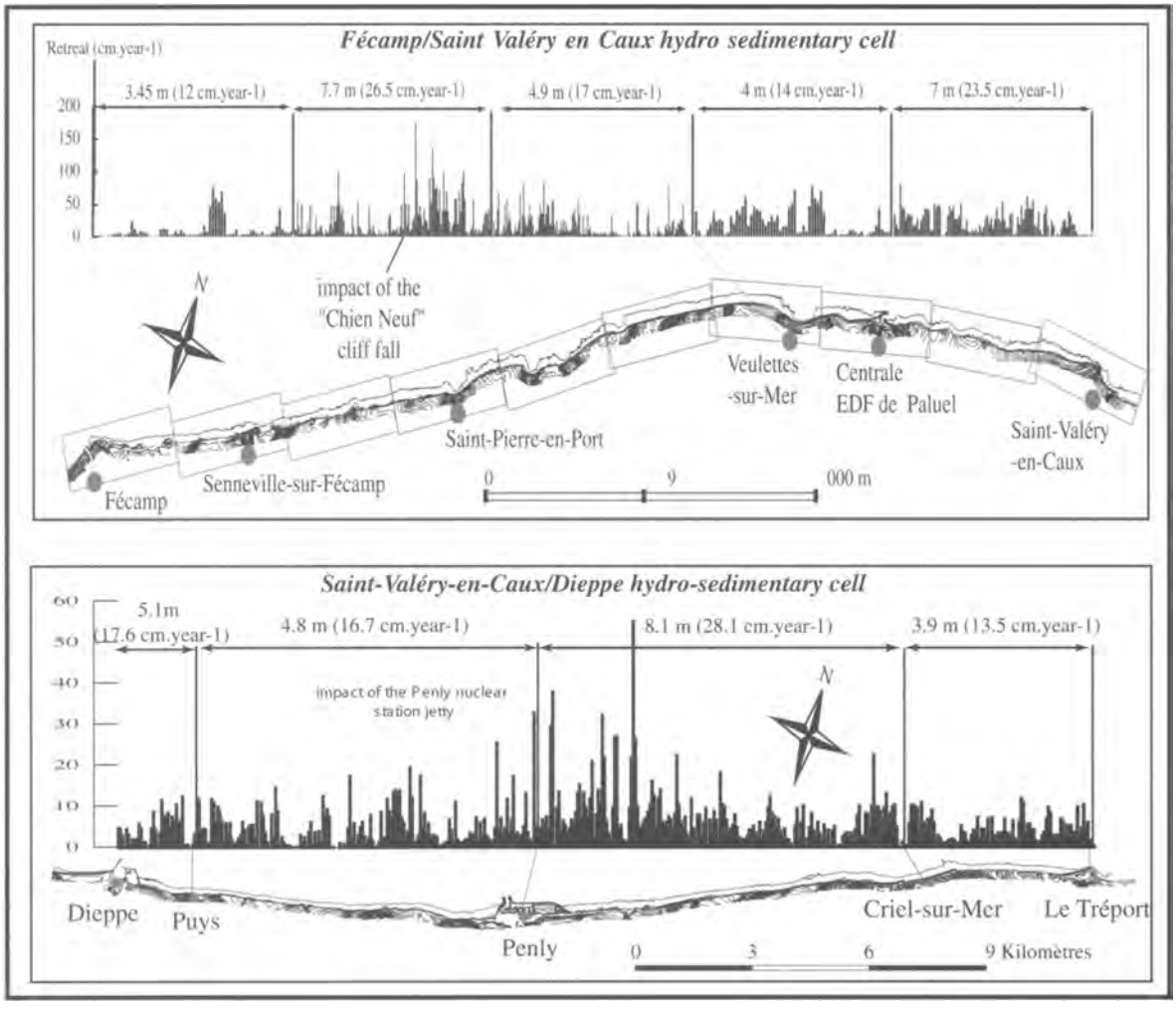

Fig. 6. Chalk cliff retreat for every 50 metres on the Haute-Normandy coast between 1966 and 1995 (Costa 2000).

Table 2. *Annual flint pebble provision from cliff erosion on the Haute–Normandy coast.*

Name of the hydro-sedimentary cells and sub-cells	*Volume of the chalk fall between 1966 and 1995 (m^3)*	*The flint content in the cliff (%)*	*Length of the coast (meter)*	*Annual flint pebble provision from the cliff erosion (m^3)*	*Annual flint pebble provision per km (m^3)*
Cap d'Antifer/Etretat	674,941	14	4,123	1,955	474
Etretat/Fécamp	3,992,919	11.2	14,424	8,944	620
Eretat/Vaucottes	2,602,448	12.2	7,937	6,569	828
Vaucottes/Yport	267,049	10.7	1,294	591	457
Yport/Fécamp	1,103,402	10	5,194	2,283	440
Fécamp/Saint-Valéry-en-Caux	9,274,008	10.1	27,615	19,379	702
Fécamp/Senneville-sur-Fécamp	890,435	9.4	3,323	1,732	521
Senneville-sur-Fécamp/St-Pierre-en-Port	4,174,969	8.7	6,970	7,515	1,078
St-Pierre-en-Port/Veulettes-sur-Mer	2,868,060	9	8,831	5,341	605
Veulettes-sur-Mer/Centrale EDF de Paluel	680,547	10.5	2,868	1,478	516
Centrale EDF de Paluel/St-Valéry-en-Caux	2,922,691	10.9	5,623	6,591	1,172
Saint-Valéry-en-Caux/Dieppe	10,743,201	9.2	28,060	20,449	729
Saint-Valéry-en-Caux/Veules-les-Roses	2,337,869	11.6	6,696	5,611	838
Veules-les-Roses/Quiberville	3,429,919	8.8	9,144	6,245	683
Quiberville/Pourville	3,346,063	8	8,450	5,538	655
Pourville/Dieppe	2,242,387	8.3	3,769	3,851	1,022
Dieppe/Le Trépot	9,470,987	6.1	24,046	11,953	497
Dieppe/Puys	242,972	8.6	1,361	432	318
Puys/Penly	3,361,818	6.2	9,592	4,312	450
Penly/Criel-sur-Mer	4,829,854	5	7,663	4,996	652
Criel-sur-Mer/Le Tréport	1,375,652	5.2	5,430	1,480	273
Antifer/Le Tréport	34,156,055		98,268	62,680	638

of the entire cliff face. As indicated in Figure 5, an increase of the rockfall frequency appears at the immediate down of transversal sea defences, showing the impact of these obstacles on the pebble longshore drift. This sediment budget modification produces an increase of the hydrodynamic conditions which are favourable to the cliff retreat.

The photogrammetric analysis confirms and quantifies the observations obtained by photo-interpretation. The mean retreat rate of the entire shoreline under study is about 6 m between 1966 and 1995, that is to say $0.21\,m\,a^{-1}$. Nevertheless, this figure is somewhat meaningless because of the very high spatial variability of cliff retreat in Normandy and Picardy. The analysis of the retreat per hydro-sedimentary cell and sub-cell enables three distinctive areas to be distinguished: (1) an area of low retreat rate (0.8 to $0.13\,m\,a^{-1}$) between Antifer and Fécamp; (2) an area of moderate retreat rate (about $0.19\,m\,a^{-1}$) between Fécamp and Saint-Valéry-en-Caux, and between Dieppe and Le Tréport; (3) an area with fast retreat (0.21 to $0.28\,m\,a^{-1}$) between Saint-Valéry-en-Caux and Dieppe. This division into sectors is identical to the division found through photo-interpretation.

Nevertheless, important variations may exist within a sector. These sharp variations are linked with the influence of cliff falls or anthropic obstacles (harbour jetties or major groynes) that disrupt the shingle transit (from the southwest to the northeast). These observations are confirmed by the analysis of the retreat at 50 m intervals (Fig. 6). The results are obtained by the quantification of the top cliff surface eroded, divided by the length of the coast studied (here, 50 metres). This scale of analysis brings out the influence of numerous rockfalls at the cliff toe and near the transversal sea defences.

The accuracy and reliability of the results on cliff retreat coupled with the information about the flint content enables the potential shingle production to be established. These supplies influence the sedimentary balance of beaches and their capacity to resist wave attack. The flint content of the chalk cliffs in Haute-Normandy ranges from 4.5 to 15.7% (Laignel 1997). These values are quite homogeneous within a particular geological layer but change from one layer to another. In the case of the Cenomanian, the flint contents are about 15–18% but can change vertically (16–17% for the lower Cenomanian, 17–20% mid-upper Cenomanian, and between 0.5 and 2% for the upper-terminal Cenomanian). Flint content in the Turonian layer is low; between 0 and 1% for the mid-lower Turonian and between 3–5% for the Upper Turonian. Regarding the Coniacian, the proportions are about 10%, and reach 10–15% for the Santonian and the Campanian. Regarding the entire shore under study, a progressive decrease of the flint content from the southwest to northeast is observed. Important variations, especially some decreases, are linked to intervals of flintless Turonian outcrops.

The potential production of shingle due to cliff retreat, calculated from fallen chalk volume and the flint content of the chalk, is 62500 $m^3\,a^{-1}$ for the entire shoreline under study during the period 1966–1995 (i.e. an average of 638 $m^3\,a^{-1}$ per linear kilometre) (Table 2). This result considers that flint loses

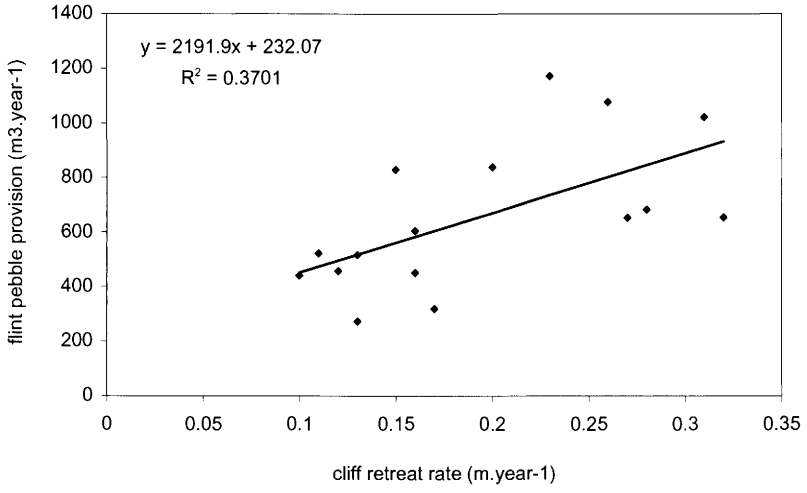

Fig. 7. Relation between the cliff retreat rates and the flint pebble provision.

40% of this volume in becoming shingle (Bialek 1960; LCHF 1972). For the sectors of Fécamp/Saint-Valéry-en-Caux and Saint-Valéry-en-Caux/Dieppe the volume of shingle produced is 700 to 730 $m^3 a^{-1}$ per linear kilometre. The lowest values are obtained for the sectors Antifer/Etretat, Dieppe/Le Tréport, Etretat/Fécamp (respectively 475, 500 and 620 $m^3 a^{-1}$ per linear kilometre). Regarding these last sectors, the reasons for the low shingle production are different. The cliffs in the Antifer/Fécamp sector contain relatively large quantities of flint but the retreat is very slow, whereas the more intense retreat rates of the Dieppe/Le Tréport sector are compensated by the low flint content of the cliffs due to significant Turonian outcrops (Fig. 7).

Discussion

As interesting as these results are, the photogrammetric analysis represents only a snapshot between two dates (1966–1995). It provides a reference database, a reliable and homogeneous baseline, but does not elucidate the rhythms of the cliffs retreat.

The identification, using two different methods, of three sectors with distinctive retreat rates poses questions about the causes of this spatial distribution of the cliff retreat rates, and especially, its relations with the chalk outcrops. If the influence of major obstacles is excluded, the sectors with 'low' and 'moderate' retreat still affected by rare but voluminous rockfalls correspond to cliff toe Turonian, Cenomanian, and even Coniacian outcrops (Antifer/Etretat; Etretat/Fécamp; Fécamp/Saint-Valéry-en-Caux; Dieppe/Le Tréport) (Fig. 8). On the other hand, the rapidly retreating sectors, affected by frequent but less voluminous rockfalls, correspond to Santonian and Campanien outcrops (Saint-Valéry-en-Caux/Dieppe). This spatial distribution of retreat rates seems to be confirmed by the shape of the general shoreline of Haute-Normandy, marked by a concave form between Saint-Valéry-en-Caux and Dieppe, that is to say in the zone where the retreat is the most significant. Nevertheless, new studies must show if the shoreline geometry due to differential erosion, is determined by the lithology and/or spatial evolution of the erosion process efficacy.

To confirm and to clarify the general and simplified lithological influence on the rate cliff retreat distribution found by the research programme, it is necessary to analyse in more detail the physical characteristics of the chalk that determine its strength. This requires the adoption of the established litho-stratigraphic classification used in the south of England by Mortimore (1983, 1986). The reconnaissance of these chalk facies, established by means of bio-stratigraphic indicators of marly layers and specific flint beds, seems to be well suited to the understanding of the mechanical behaviour of chalk. This classification, which is applicable to the entire anglo-parisian basin (Mortimore & Pomerol 1987) is currently underway within the framework of the European Risk of Cliff Collapse (ROCC) programme on the coast of Haute-Normandy and East Sussex. Also, this work will determine whether the lithological influence on the chalk cliff retreat rates found in Haute-Normandy is comparable in East Sussex.

The knowledge of chalk cliff retreat rates and flint content enables an estimate of the potential shingle supply due to erosion. This information is required to establish the sedimentary budget (shingle) of the shore under study, and to determine the ability of the shingle beach to protect less elevated built-up coasts from sea flooding. Due to shingle removal by the extraction industry (approximately 3 000 000 m^3 extracted during the twentieth century) (LCHF 1972), the shingle production due to cliff retreat cannot by itself compensate for the beach sedimentary crisis in the foreseeable future.

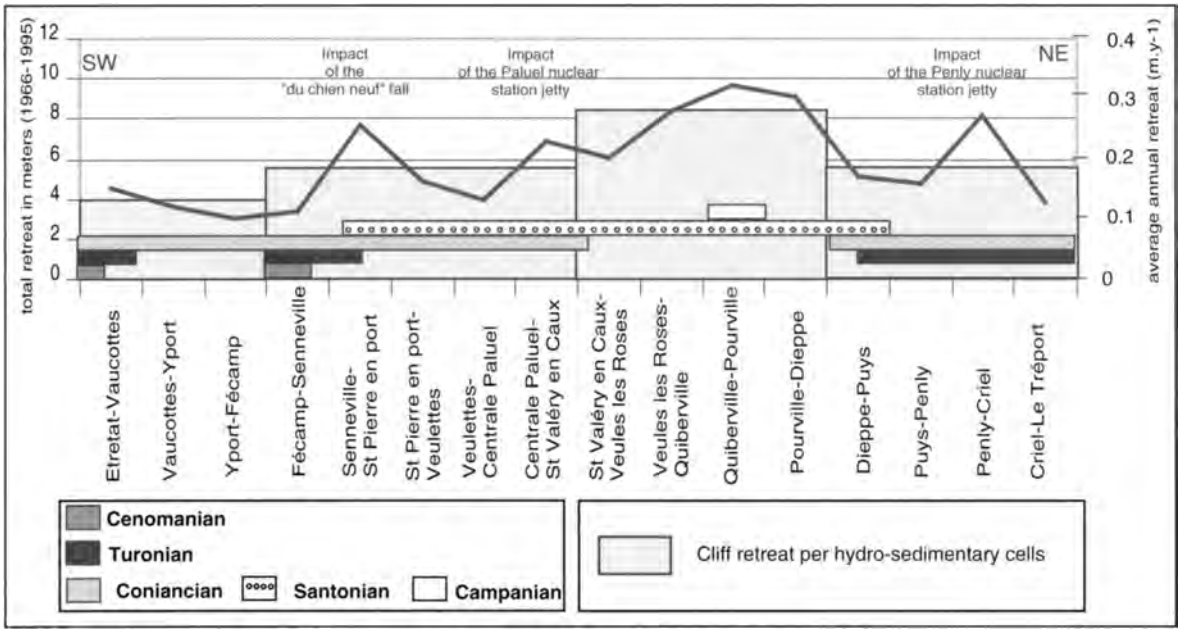

Fig. 8. Relation between the cliff retreat rates and the chalk stratigraphy.

Conclusion

By definition, chalk cliffs are erosional features and thus only retreat. This erosion is all the more rapid given that rock present on the shores of Haute-Normandy and Picardy are of low resistance. This fact seems to have been forgotten or at least neglected by decision-makers as cliff retreat is currently threatening many built-up areas. Before giving any advice on political choices for future management, cliff retreat rates must be evaluated. Photogrammetric analysis provides accurate, reliable and homogeneous numerical data that enables the establishment of a geographical databank.

This study shows firstly that cliff retreat is very spatially variable. Second, it shows that the retreat rates, and the frequency and intensity of rockfalls, seem dependent on lithology. Indeed, cliffs comprising Cenomanian, Turonian, and Coniacian chalk are retreating less rapidly than those comprising Santonian and Campanian chalk. Moreover, the latter are subjected to frequent but less voluminous rockfalls which are quickly cleared away by marine erosion.

This study provides only a snapshot of happenings between 1966 and 1995. It does not provide any information on the rhythms of chalk cliff retreat. On the other hand, this research is a first layer of information which is necessary to build upon. Diachronic analysis of the shoreline (through photogrammetry, airborne laser or field survey) is one of the methods enabling a better knowledge of the rate and modality of shore evolution.

This research has been initiated within the 'Contrat de Plan Interrégional du Bassin de Paris (CPIBP)' framework in which the Haute-Normandy and Picardy regions wish to investigate coastal erosion at the scale of the natural phenomena that generate the damage. This work forms the early stage of a follow-up policy of the coastal dynamics essential for a coherent management.

References

BIALEK, J. 1969. Le recul des falaises du cap d'Antifer au Tréport, entre 1830 et 1966. *Direction Départementale de l'Equipement de Seine-Maritime, Arrondissement de Dieppe*, 63.

BIGNOT, G. 1962. Etude sédimentologique et micropaléontologique de l'Eocène du Cap d'Ailly (près de Dieppe-Seine-Maritime). *Thèse 3ième cycle, Faculté des. Sciences., Paris.*

BIGNOT, G. 1983. Le gisement paléogène de Criel-sur-Mer (76-Haute-Normandie). *Bulletin d'Information des Géologues du Bassin de Paris*, **20**, 2, 25–33.

BRIQUET, A. 1930. Le littoral du Nord de la France et son évolution morphologique. *Thèse de Lettres, Paris*, 439.

BROMLEY, R. G. & EKDALE, A. A. 1986. Flint and fabric in the European chalk. *In*: SIEVEKING, G. & HART, M. B. (eds.) *The Scientific Study of Fint and Chert*. Cambridge University Press, 71–82.

CAVELIER, C., MÉGNIEN, C., POMEROL, C. & RAT, P. 1979. Le Bassin de Paris. *Bulletin d'Information des Géologues du. Bassin de Paris*, **16**, 4, 2–52.

COSTA, S. 1997. *Dynamique littorale et risques naturels: L'impact des aménagements, des variations du niveau marin et des*

modifications climatiques entre la Baie de Seine et la Baie de Somme. Thèse de doctorat, Université de Paris I.

COSTA, S. 2000. *Réactualisation des connaissances et mise en place d'une méthode de suivi de la dynamique du littoral haut-normand et picard*. Rapport final. Préfecture de Picardie. Contrat de Plan Interrégional du Bassin de Paris (CPIBP). 103.

COSTA, S., FREIRÉ-DIAZ, S. & DI-NOCERA, L. 2001. Le littoral haut-normand et picard: une gestion concertée. *Annales de Géographie,* **618**, 117–135.

DALLERY, F. 1955. Les rivages de la Somme, autrefois, aujourd'hui et demain. *In*: PICARD, A., PICARD, J. & PARIS, C. (eds). *Mémoires de la Société d'Émulation Historique et Littéraire d'Abbeville*, 307.

DOLAN, R., HAYDEN, B. P., MAY, P. & MAY, S. 1980. The reliability of shoreline change measurements from aerial photographs. *Shore and Beach*, **48**(4), 22–29.

DOLIQUE, F. 1998. *Dynamique morpho-sédimentaire et aménagements induits au sud de la Baie de Somme*. Thèse de doctorat, Université du Littoral, Dunkerque.

EHRMANN, W. U. 1990. Upper cretaceous flints in central North-West Europe, paleoproductivity and Milankovitch cycles. In Colloque International sur le silex. *Cahier du Quaternaire*. Edition CNRS, Bordeaux, **17**, 77–83.

GUILMETH, 1851. *In*: MONBORGNE, J. *Histoire du bourg d'Ault*. Luneray, Imprimerie. Berthout, 433.

INSTITUT GÉOGRAPHIQUE NATIONAL. MISSIONS ETRETAT-NEUFCHÂTEL (1947); Etretat-Poix (1952); Etretat-Doudeville (1957); 2889 (1973); 1809–2109 (1978); IFN 85 06 (1985); FR 8265 (1990).

JUIGNET, P. 1974. La transgression crétacée sur la bordure orientale du Massif armoricain. *Thèse de Doctorat, Université de Caen.*

JUIGNET, P. & BRETON, G. 1994. Stratigraphie, rythmes sédimentaires et eustatisme dans les craies turoniennes de la région de Fécamp (Seine-Maritime, France). Expression et signification des rythmes de la craie. *Bulletin trimestriel de la Société Géologique de Normandie et Amis du Muséum du Havre*. **81**, 2, 55–81.

KENNEDY, W. J. & JUIGNET, P. 1974. Carbonate banks and slump beds in the Upper Cretaceous (Upper Turonian-Santonian) of Haute-Normandy, France. *Sedimentology*, **21**, 1–42.

LABORATOIRE CENTRAL D'HYDRAULIQUE DE FRANCE (LCHF) 1972. Etude de la production des galets sur le littoral haut-normand, **63**.

LABORATOIRE CENTRAL D'HYDRAULIQUE DE FRANCE (LCHF) & BUREAU DE RECHERCHES GÉOLOGIQUES ET MINIÈRES (BRGM) 1987. Etude du littoral haut-normand entre le Havre et le Tréport. Rapport général, **98**.

LAIGNEL, B. 1997. Les altérites à silex de l'ouest du Bassin de Paris: caractérisation lithologique, genèse et utilisation potentielle comme granulat. *Thèse, Université de Rouen*, Edition BRGM, 264, Orléans.

LAIGNEL, B., QUESNEL, F., MEYER, R. & BOURDILLON, C. 1999. Reconstitution of the Upper Cretaceous chalks removed by dissolution during the Cenozoic in the western Paris Basin. *Geologische Rundschau*, **88**, 467–474.

LAMBLARDIE (De), E. 1789. Mémoire sur les côtes de la Haute-Normandie comprises entre l'embouchure de la Seine et celle de la Somme, considérées relativement au galet qui remplit les ports situés dans cette partie du la Manche. Imprimerie. P.J.D.G. Faure, Le Havre. *Bulletin de la Société Géologique de Normandie*, 1908, 55–93.

LEATHERMAN, S. P. 1983. Shoreline mapping: A comparison of techniques. *Shore and Beach*, **51**, 28–33.

MAY, V. J. 1971. The retreat of chalk cliffs. *Geography Journal*, **137**, 203–206.

MAY, V. J. & HEEPS, C. 1985. The nature and rates of change on chalk coastlines. *Zeitschrift für Geomorphologie*. Supplementband **57**, 81–94.

MÉGNIEN, C. F. 1980. Synthèse géologique du Bassin de Paris. *Mémoire du Bureau de Recherches Géologiques et Minière*, 3 volumes, n° 101, 102, 103.

MOORE, L. J. 2000. Shoreline mapping techniques. *Journal of Coastal Research*, **16**(1), 11–124.

MORTIMORE, R. N. 1983. The stratigraphy and sedimentation of the Turonian-Campanian in the southern province of England. *Zittelania*, **10**, 27–41.

MORTIMORE, R. N. 1986. Stratigraphy of the Upper Cretaceous white chalk of Sussex. *Proceedings of the Geologists' Association*, **97**, 97–139.

MORTIMORE, R. N. & POMEROL, B. 1987. Correlation of the Upper Cretaceous (Upper Cenomanian to Campanian) white chalk in the Anglo-Paris Basin. *Proceedings of the Geologists' Association*, **98**, 97–143.

MORTIMORE, R. N. & POMEROL, B. 1990. Les silex du Turonien: niveaux repères et corrélation de part et d'autre de la Manche. In Colloque International sur le silex, *Cahiers du Quaternaire*, Edition du CNRS, Bordeaux, **17**, 85–94.

POMEROL, B., BAILEY, H. W., MONCIARDINI, C. & MORTIMORE, R. N. 1987. Lithostratigraphy and biostratigraphy of the Lewes and Seaford chalks: a link across the Anglo-Paris basin at the Turonian-Senonian boundary. *Cretaceous Research*, **8**, 289–304.

PRÊCHEUR, C. 1960. Le littoral de la Manche: de Saint-Adresse à Ault. *Etude morphologique*. Norois, volume spécial.

REGRAIN, R. 1992. Protéger le littoral ouest des Bas-Champs de Cayeux. *In*: *Les littoraux en France: risques et aménagement. Centre Régional de Documentation Pédagogique.*

SOCIÉTÉ GRENOBLOISE D'AMÉNAGEMENT HYDRAULIQUE (SOGREAH) 1999. Station littorale d'Ault-Onival ; Etude de la restauration des plages et du littoral. Rapport général, 74.

STAFFORD, B. D. 1971. An Aerial Photographic Technique for Beach Erosion Surveys in North Carolina. Washington DC: U.S. Army Corps of Engineers, Coastal Engineering Research Center, Technical Memorandum, n° 36.

THIELER, E. R. & DANFORTH, W. W. 1994. Historical shoreline mapping: Improving techniques and reducing positioning errors. *Journal of Coastal Research*, **10**(3), 600–620.

Coastal cliff erosion vulnerability on the Canadian east coast (Baie des Chaleurs area): a multi-parameter visualization tool

M. Daigneault, J-L. Bouchardon & B. Guy

Département Géochimie, Environnement, Ecoulement, Réacteurs industriels et Cristallisation (GENERIC), Centre Sciences des Processus industriels et Naturels (SPIN), École des Mines de Saint-Etienne, 158 cours Fauriel, Saint-Etienne, Cedex 2, 42023, France

Abstract: In order to assess a cliff's vulnerability to erosion, researchers must consider a number of parameters that collectively account for all possible erosional processes. The authors have developed a radial diagram that allows the most active processes of erosion to be visualized (e.g. hydrodynamic, gravity-driven or atmospheric), and when such diagrams are presented on a map, they can be used to rapidly identify the contributing erosional processes at a given location. The diagram, developed for the Baie des Chaleurs region (eastern coast of Canada), displays numerical values that represent the relative importance of various weakening parameters for a set of cliffs. In addition, a colour code represents the dominant lithology, and the diagram diameter is a function of the erosion rate. The data for each diagram are based on field observations, experimental work and results of mineralogical and petrophysical analyses. Ten fundamental parameters were used to assess the structural, petrophysical and environmental processes of erosion: porosity, percentage of matrix or cement, homogeneity of the stratification, presence of schistosity, fracture density, number of fracture sets, presence of faults, dip of the strata, effect of waves, and the presence of groundwater. Coastal managers can use these diagrams in conjunction with natural risk maps to estimate the vulnerability of a cliff and decide whether engineering structures are required for preservation.

Introduction

Waves that crash against coastal cliffs wear them down by pressure and abrasion (Trenhaile 1987; Sunamura 1992; Belov *et al.* 1999). In addition to these hydrodynamic erosional forces are processes of chemical or mechanical origin that depend largely on geographic location as well as the mineralogical, chemical, textural and structural nature of the exposed rock (e.g. Selby 1980; Emery & Kuhn 1982). Recent work in the Baie des Chaleurs on the eastern coast of Canada (Fig. 1), allowed us to document erosional processes and demonstrate their relative contributions to cliff retreat according to various combinations of lithology and structure (Daigneault 2001). Until now, few studies have addressed the problem of cliff erosion in the Gaspésie region. Reid *et al.* (1990) described the vulnerability of cliffs in the Baie des Chaleurs area, but did not provide a sufficiently precise estimate or method by which they measure the retreat. More recently, the Quebec Ministry of Transport became interested in the region's cliff retreat due to the risk it poses to their road system, and consequently conducted an overview of the area's geomorphology (Morneau *et al.* 2001).

The Baie des Chaleurs lies along the eastern coast of Canada within a cold temperate zone (Fig. 1). The coast of the bay extends for approximately 150 km and is dominated by cliffs with an average height of 10 m. The average annual temperature at Baie des Chaleurs is 3.1°C (Environment Canada 1998). Winters are cold, with a mean daily temperature in January of −12.5°C, but summers are hot with a mean daily temperature of 16.6 °C in August. The average annual precipitation is 1052.2 mm (Environment Canada 1998). Summer water temperatures vary between 10 and 20°C (Lacroix & Filteau 1969). During winter, the ice floe forms in mid-January and disappears at the end of March (Cardinal 1967). The tides are semi-diurnal and of small amplitude, averaging only 2 m (Cardinal 1967). Wave heights are minimal in the bay, and only 5 to 15% of waves exceed two metres, except during the last three months of the year when the proportion rises to 30% (Environment Canada 1994). The small wave size is due to a gentle intertidal slope of only 2 to 10°, and consequently the water depth rarely exceeds 4 m in the first 500 m of the intertidal zone. The maximum water depth in the bay is approximately 40 m.

Few studies have been conducted on cliff erosion in northern environments. Dionne (1970, 1974) demonstrated the devastating effects of sea ice on coastal cliffs but did not quantify the process, and a study by Moign (1966) related specifically to the role of sea ice at Spitsberg, Norway. More recently, studies have demonstrated the effectiveness of the freeze–thaw cycle in cliff disintegration, but not necessarily in a coastal environment (e.g. Prick 1996, 1999), whereas numerous other studies have emphasized the general importance of a wide variety of terrestrial and marine parameters in cliff erosion (e.g. Suzuki 1982; Trenhaile 1987; Tsujimoto 1987; Sunamura 1992; Benumof & Griggs 1999; Belov *et al.* 1999). Benumof & Griggs (1999) established the role of

From: MORTIMORE, R. N. & DUPERRET, A. (eds) 2004. *Coastal Chalk Cliff Instability*. Geological Society, London, Engineering Geology Special Publications, **20**, 149–167. 0267-9914/04/$15.00

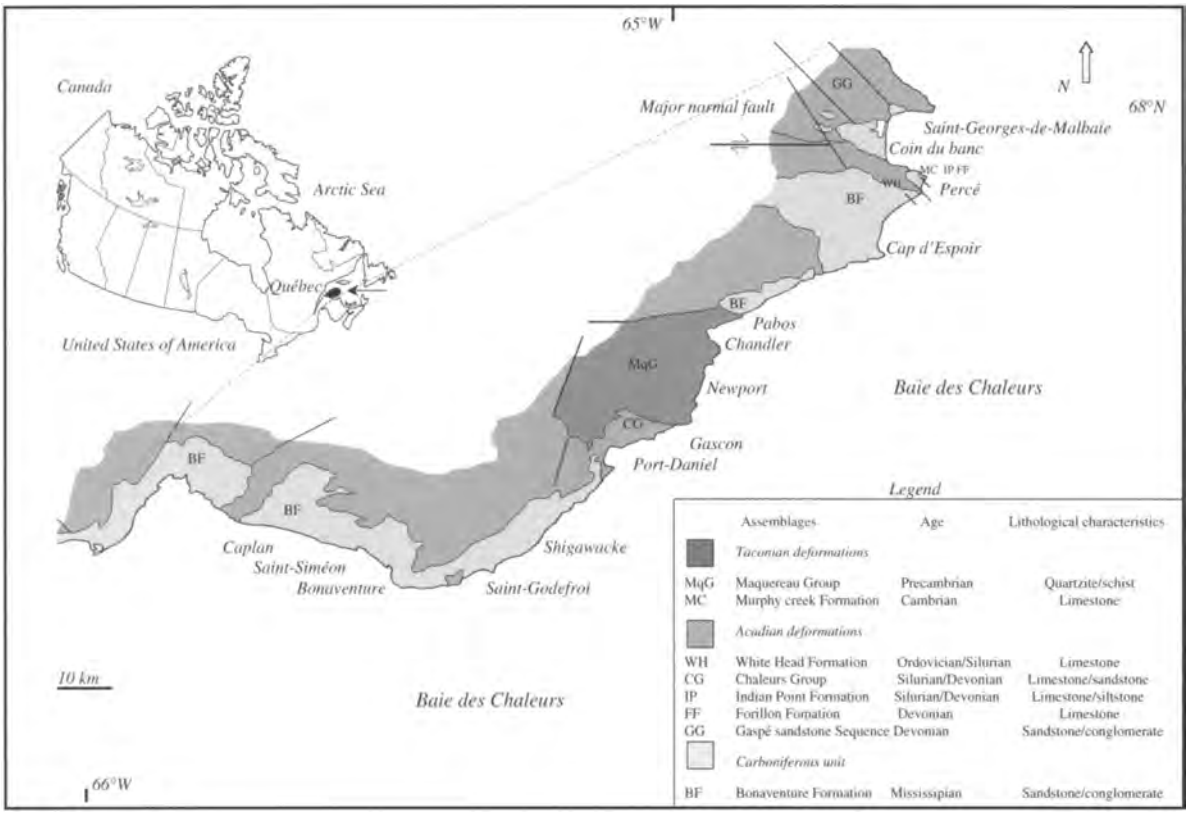

Fig. 1. Location and geological setting of the Baie des Chaleurs region, eastern Canadian coast. The Baie des Chaleurs study area is part of the Gaspesian Peninsula and is indicated by the black arrow.

seven parameters (intact rock strength, structural discontinuities, cliff height, porosity, wave climate, beach profile, offshore profile), but in a region where the freeze–thaw cycles and sea ice are absent and the geological context is considerably different to that of the Gaspésie. Some researchers have concluded that the mechanical resistance of rocks (e.g. Budetta *et al.* 2000) or the presence and distribution of rock joints (Selby 1980; Allison 1989) are the major factors in cliff vulnerability.

In this article, the authors have characterized and quantified the most important parameters for cliff retreat at Baie des Chaleurs, Quebec. Our method includes field-based characterization (number of fractures, presence of faults, presence of groundwater, influence of waves), as well as laboratory analysis (porosity and mineralogy) coupled with experiments to determine rock durability (freeze–thaw, salt weathering and wetting–drying). A value was assigned to each parameter in order to visualize their importance on a radial diagram. Furthermore, since the rate of cliff retreat is not well known in the Baie des Chaleurs area, present-day rates were established using information from earlier studies and new measurements made in the field.

Geological setting

The Gaspesian Peninsula is part of the Appalachian Mountains and consists of three distinct chronological units (Malo 1994; Table 1): (1) the Taconian unit, which includes rocks from Precambrian to Cambro-Ordovician age, deformed and metamorphosed during the Taconian orogeny (Middle to Late Ordovician); (2) the Acadian unit, which includes sedimentary rocks of Siluro-Devonian age, deformed during the Acadian orogeny (Middle Devonian); (3) a sedimentary unit of Carboniferous age (sandstone – conglomerate)

The northern part of the peninsula is strongly deformed, including a southward-dipping E–W thrusting event that placed the metamorphosed units of the Taconian orogeny over the deformed but unmetamorphosed sequences of the Acadian orogeny (Fig. 1 and Table 1). In contrast, in the Baie des Chaleurs region in the southern part of the peninsula, a late system of NE–SW and NW–SE Acadian-age normal faults separate blocks of deformed or undeformed sedimentary and metamorphic sequences.

Metamorphic rocks (quartzites and schists) within the Taconian unit dip steeply in the study zone (Table 2;

Table 1. *Lithological characteristics of the main geological assemblages in the Baie des Chaleurs region*

Assemblages		*Age*	*Lithological characteristics*	*Coastline (%)*
I (Taconian deformations)				
Precambrian/Cambro–ordovician				
Maquereau Group (Chandler/Gascon)	MqG	Precambrian–Lower Cambrian	Quartzite-shist	14
Murphy Creek Formation (Percé)	MC	Middle–Superior Cambrian	Limestone	<1
II (Acadian deformations)				
Middle Ordovician–Superior Devonian				
White Head Formation (Percé)	WH	Middle Ordovician-Silurian	Limestone	<1
Chaleurs Group (Port-Daniel/Gascon)	CG	Silurian–Lower Devonian	Limestone-sandstone	9
Indian Point Formation (Percé)	IP	Silurian–Devonian	Limestone-silstone	<1
Forillon Formation (Percé)	FF	Lower Devonian	Limestone	<1
Gaspé sandstone Sequence (North of Percé)	GG	Lower–Middle Devonian	Sandstone-conglomerate	6
II Carboniferous				
Bonaventure Formation	BF	Mississipian	Sandstone-conglomerate	70

Williams 1979; St-Julien *et al.* 1983). While they constitute the main rock type in the northern part of the peninsula, only two Taconian series are exposed along the coast of Baie des Chaleurs, and in several isolated places. The stratified limestone of the Murphy Creek Formation crops out at Percé Point, whereas the quartzite and schist units of the Maquereau Group are irregularly exposed between Gascon and Chandler (Fig. 1; Tremblay & Bourque 1991; Brisebois *et al.* 1991; Brisebois & Brun 1994; Marquis 1994).

Acadian rocks (Table 1) consist of deformed but unmetamorphosed lithified continental shelf sediments, including fine- and coarse-grained sandstone and stratified limestone alternating with calcareous silts. These high dip formations are autochthonous and discordantly overlie the younger sequences (Tremblay & Bourque 1991).

The Carboniferous unit is represented by rocks of the Bonaventure Formation that discordantly overlie the other assemblages. Although these rocks are volumetrically minor in the Gaspé region, this formation covers almost 70% of the coastline in the Baie des Chaleurs area (Table 1; Malo 1994). The Bonaventure Formation presents a low dip and is characterized by alternating sandstone and conglomerate layers, the latter of which bears a calcareous and ferruginous matrix (McGerrigle 1968). The conglomerate unit is mostly polygenic, containing fragments inherited from the erosion of younger, generally calcareous sequences. These rocks (Table 1) are well exposed in the supratidal zone of the study region and typically form cliffs 10 to 15 m high, although they may exceed 70 m in height along the northern part of Percé Point.

After the last period of geological activity in the Gaspesian Peninsula during Permian time, a significant portion the Appalachian Mountain Range had been levelled and deposited elsewhere. Continental icecaps during the Quaternary Period further sculpted the topography by eroding, transporting and depositing an enormous quantity of material (Hocq & Martineau 1994). In the Gaspé region, the last icecap began to recede around 14 ka, and although its complete retreat is estimated to have occurred around 9.8 ka, isostatic uplift continues at a rate of 1 mm/year in the Baie des Chaleurs area (Lebuis & David 1977; Dyke & Prest 1987).

Measure of cliff retreat and macroscopic erosional processes

Two main types of processes are responsible for macroscopic (large-scale) episodic erosion along the Baie des Chaleurs coast: mass movements (including toppling, sliding and collapse), and dislocation due to sea ice action. Both of these instantaneous processes are governed by gravity, but small-scale continuous processes, such as abrasion, water circulation, salt weathering, freeze–thaw and wet-dry cycles, initially weaken the material and make it more susceptible to the larger-scale processes. The authors quantify the macroscopic mechanisms causing cliff retreat along the Baie des Chaleurs using field observations and comparative analyses with the few available earlier documents (Reid *et al.* 1990; Gouvernement du Québec 2001; various public photos and private documents). The rate of retreat was calculated by comparing measurements of cliff edge position taken by Daigneault in 2000 (Daigneault 2001) with those of Reid *et al.* (1990) taken between the cliff edge and nearby infrastructures a decade earlier (Table 2). For the Bonaventure Formation, it was thus determined that sandstone cliffs are receding at a rate of 0.10 to 0.30 m/year, but that the conglomerates are retreating more slowly at only 0.05 m/year. A rate of 0.10 m/year was calculated for the steeply dipping Acadian and Taconian limestone units.

The two sets of aerial photos available for the area of interest span the last 30-year period and were taken at a scale of 1:15000, which is unfortunately inadequate to estimate a retreat of only a few metres. Results were consequently completed by conducting a survey of property owners along the coast. Based on direct and indirect measurements made during the construction of protective structures (a total of 50) and information from dated photographs (e.g. archived photographs), it was estimated that the retreat during the last

Table 2. *Typical field characteristics of the various lithologies and estimation of erosion rates in the Baie des Chaleurs area*

Description (assemblage)	*Age/Gr-Fm*	*Dip of strata*	*Number of fractures (m^3)*	*Number of fractures networks (m^3)*	*Presence of fault*	*Wave and sea ice influence*	*Groundwater*	*Homogeneity of the strata*	*Erosion rates measured (m/yr)*	*Erosion rates estimated (m/yr)*
Taconian										
Quartzite	Precambrian/MqG	60°	5 at 10	1 at 2	no	low and high tide	no	high	no data	~0.1
Schist	Precambrian/MqG	60°	10	2	no	high tide	no	high	0.20	>0.1
Limestone	Camb.–Ordo./MC	80°	>25	2 at 3	yes (rarely)	high tide	no	high	no data	~30.1
Acadian										
Limestone	Camb.Ordo./WH	80°	>25	2 at 3	yes (rarely)	high tide	no	high	no data	~0.1
Limestone	Silurian–Devonian/CG, FF	70°–80°	10 at 20	2	yes	high tide	yes (rarely)	low	no data	~0.1
Siltstone	Silurian–Devonian/IP	80°	>20	2	yes (rarely)	high tide	no	low	0.1–0.125	~0.1
Conglomerate	Devonian/GG	70°	2	2	no	high tide	no	low	no data	no data
Conglomerate	Devonian/GG	50°–70°	10 at 20	2 at 3	no	low and high tide	no	high	0.05	~0.05
Sandstone	Devonian/GG	50°–70°	10 at 20	2	no	low and high tide	no	high	no data	~0.1
Carboniferous										
Conglomerate	Carboniferous/BF	10°	up to 5	<1	no	high tide	no	low	0.05	~0.03–0.05
Sandstone	Carboniferous/BF	10°	10 at 20	2	yes (rarely)	low and high tide	yes	very low	0.25–0.3	~0.3
Cong./sandstone	Carboniferous/BF	10°	10 at 20	2	yes (rarely)	low and high tide	yes	very low	0.25–0.3	~0.3

decade was 0.15 m/year for the inclined limestone units of the Acadian and Taconian assemblages (0.15 m/year to 0.2 m/year at Percé/MC and 0.1 m/year at Port-Daniel/CG; several ancient photographs show retreats of more than 0.10 m/year in Percé area/MC-IP-FF), 0.19 m/year for the schist of the Maquereau Group (Newport/MqG), and 0.24 m/year for the Bonaventure Formation/BF. For this Formation, from West of Saint-Georges-de-Malbaie to Caplan, loss estimates vary between 0.1 and 0.45 m/year (over 20 data). These estimates reach 0.25, 0.2, 0.08, 0.1, 0.1, 0.2, 0.3, 0.13 m/year between Saint-Georges-de-Malbaie and West Percé, and 0.4, 0.4, 0.45, 0.3, 0.3, 0.25, 0.1, 0.3, 0.1, 0.2, 0.25, 0.3 m/year from West Percé to Pabos (the oldest photographs show retreats superior to 0.2 m/year). From South Port-Daniel to Caplan, the loss estimate is 0.3 m/yr (3 data).

For the Gaspé Sandstone Sequence, it was estimated that the retreat during the last decade was 0.8 m/year (0.05 to 0.1 m/year for Saint-Georges-de-Malbaie).

The mass movements that govern episodic erosion by toppling, sliding and collapse are inherited from existing instabilities (e.g. fractures or faults). Collective observations along the coast revealed that cliff overhangs, mainly present in the Bonaventure Formation, are particularly well developed when the cliff base consists of sandstone overlain by conglomerate (40% of the cases). The maximum depth of the overhangs (3 m) coincides with the spacing of the orthogonal vertical joints in the conglomerate horizons (E–W and N–S orientations). Furthermore, the volume of talus from recent toppling events also appears to correlate with the 3 m joint spacing. On the other hand, where the cliff is composed entirely of conglomerate (5% of the cases), erosion is slow or absent, and where the cliff is dominated by Bonaventure sandstone (55% of the cases), the depth of the overhangs rarely exceeds 1 m, which corresponds to a much denser joint spacing compared to that of the conglomerate units. For the Carboniferous Sequence, the volume of material produced during toppling is small ($<$10 m of retreat; $\leq$100 m^3 in volume), but the events are frequent (1 to 2 per 100 m of shoreline each year).

The cliffs along the coastline that are dominated by steeply inclined rock layers (i.e., Maquereau Group, White Head Formation, Chaleurs Group and Gaspé Sandstone Sequence) show evidence of abrasion by the sea along the rock base. The volume of cliff material that can be affected by this process is determined by the orientation of the layers relative to the coastline, and by the thickness of the layers (decimetres to metres). The largest mass of fallen rocks was encountered at Coin du Banc, which collapsed in 1998. It measures 30 m high, 50 m long and is approximately 30 m wide. The lithology at this site is conglomerate with metre-scale, subvertical layering parallel to the coastline. The base of the beds is hidden behind talus, which makes it difficult to determine the process responsible for the collapse. Where the base of the unit is accessible, the amount of retreat can be estimated by measuring the thickness of the beds, the depth of the overhangs, and the volume of recent slides (Table 2). With the exception of the collapse at Coin du Banc, the observed thickness of these apparently unstable rock layers ranges between 0.5 and 1 m, and the linear extent and volume of the slides are 5–10 m and 50–100 m^3, respectively. These collective observations indicate a critical overhang depth of approximately 1 m for steeply dipping rocks with decimetre- to metre-scale layering, such as those of the White Head Formation, Chaleurs Group and Gaspé Sandstone Sequence. The Maquereau Group is dominated by very homogenous and relatively unfractured quartzite with layers that range in thickness from several decimetres to several metres. The quartzite beds alternate with schist layers that rarely reach several decimetres in thickness. This formation generally lies perpendicular to the coastline and is primarily affected by rockfalls in which the unstable blocks, on the order of a cubic metre each, are defined by a combination of bedding planes and two orthogonal fracture systems. Such rockfalls typically affect only a few metres of cliff face at a time, and their frequency is less than 1 per 100 m of coastline.

It is often a simple matter in the Baie des Chaleurs area to determine how recently small-scale mass movements have occurred (e.g. other than Coin du Banc). Each spring, the sea ice clears away the debris of the previous year, and small collapses produced during the spring thaw are easily measured as they sit perched on the snow banks or any remaining intact ice. The authors therefore conducted a systematic inventory of iced-up zones over the winter months (December to March/April; 1998, 1999 and 2000), in order to assess the effects of freezing. Three main processes were identified (Fig. 2):

(1) the collapse of ice blocks produced by frozen seawater causes rocks to become dislocated at the base of the cliff (Fig. 2a);
(2) the break-up of the ice floe forms blocks that travel and abrade the cliff base (Fig. 2b, 2c and 2d);
(3) the collapse of ice walls, formed from frozen stream and meltwater run-off along the cliff face, contributes to the dislocation of material from the upper reaches of the cliff (Fig. 2e).

The collapse of ice blocks along the cliff causes local rockfalls that are limited in size to several metres and a volume of 0.5–2 m^3 (Fig. 2a). Abrasion of the cliff base and of the subtidal-intertidal platform by ice floes is generally minor due to the light and fragile nature of the thin ice sheets ($\sim$50 cm thick). However, ice floes appear to play an important role by clearing away the debris of earlier falls. The effect of collapsing ice walls is variable. During the present study, a semi-continuous zone of collapsed cliff face was observed throughout the Bonaventure Formation. The zone measured 10 cm wide and always occurred within the uppermost metre of the cliff walls (Fig. 2e). The most steeply inclined cliffs of the Gaspé Sandstone Sequence, however, remain unaffected by this phenomenon. It is possible that the steep inclination causes ice accumulations to slip, and that the depth of the groundwater flow is too deep to allow water to freeze, even during the winter. Also, the calcareous and quartzitic lithologies may not be as weakened as those of the Bonaventure

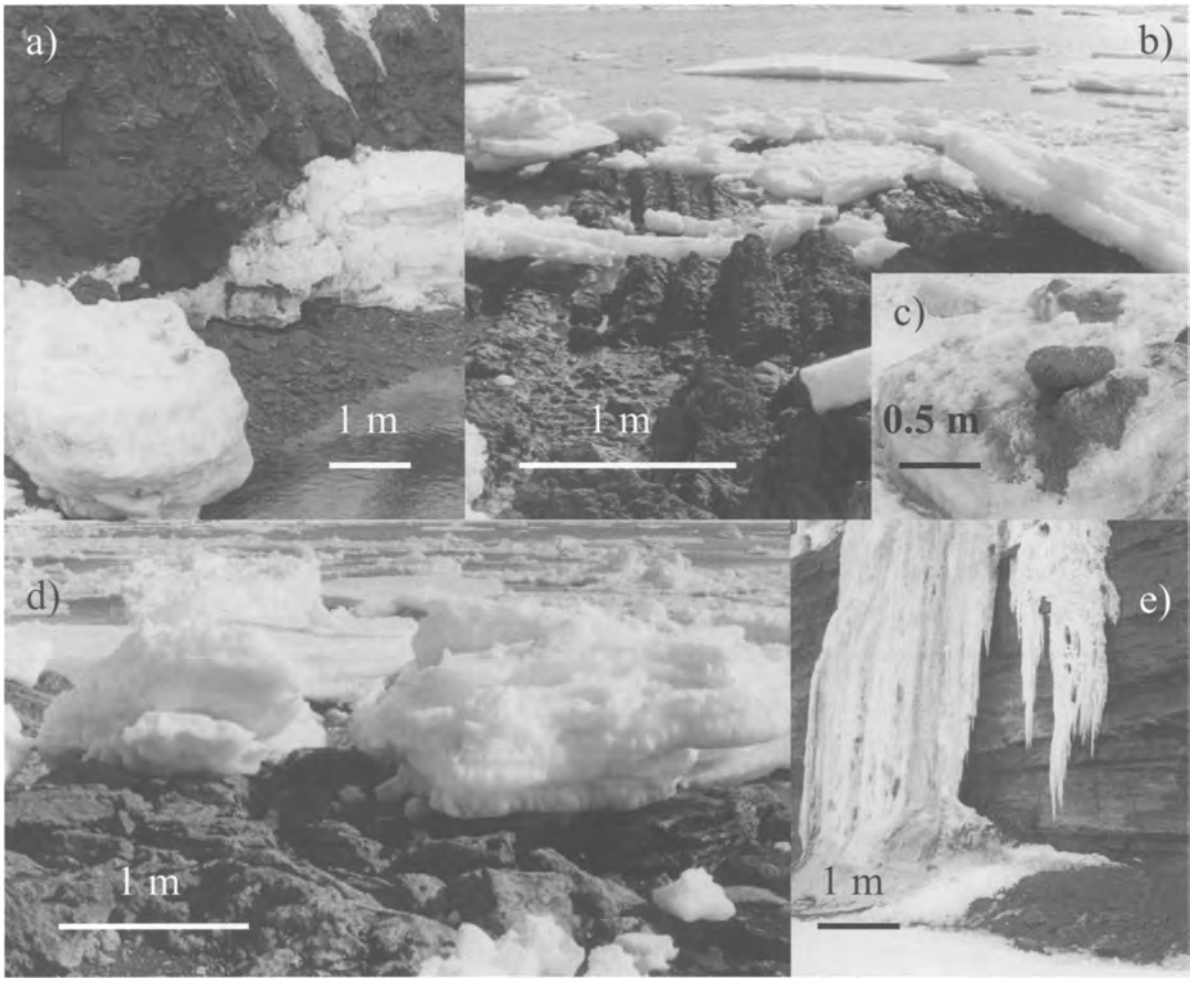

Fig. 2. (a) Dislocation of ice blocks and collapse of material along the cliff base; (b) to (d) Abrasion in the intertidal zone and dispersion of blocks accumulated along the cliff base; (e) Removal of the uppermost part of the cliff face during the break up of ice walls.

Formation due to their poor permeability. This issue needs to be examined further.

Overall, the mechanism of overhang collapse appears to be directly related to fracture patterns in the cliffs. These patterns, easy to observe and measure, reflect not only the mechanical resistance of the individual rock types but of entire rock assemblages and lithological combinations within the cliffs. The actions of sea ice are generally of minor importance and affect only small areas by dislocating ice blocks from the cliff face or by weakly abrading the cliff base or shore platform. On the other hand, the removal of debris from the cliff area by ice movement is very important in that it exposes the area to subsequent wave erosion. Finally, if the collapse of ice walls along the cliff face is related to structural dip or lithology, then the overall processes are largely pre-determined by the vulnerability of the rock type to disintegration.

Rock disintegration

Field study was made of all continuous and semi-continuous erosional phenomena by observing and measuring the various factors related to the alteration-erosion processes. Some of the processes, however, are not easy to observe directly and require an experimental approach, either in the laboratory or in the field. This was the case for freeze–thaw processes, salt weathering, wetting–drying, and dissolution related to the physiological activity of algae (Table 3). The change in chemical composition of acidic freshwater flowing

Table 3. *Typical characteristics of various lithologies and their vulnerability to the various erosional processes*

Description/ assemblage	*Age/Gr-Fm*	*Mineralogy*	*Matrix (%)*	*Porosity*	*Schistosity*	*L W/D (%)*	*L S/W (%)*	*L F/T (%)*
Taconian								
Quartzite	Precambrian/MqG	Qtz, fd, micas	40	10	no	0.07	1.39	0.46
Schist	Precambrian/MqG	Qtz, fd, calcite	60	15 at 20	High	6.88	17.12	14.8
Limestone	Camb.–Ordo./MC	Calcite	>90	2.5	no	0.08	0.8	0.1–0.3
Acadian								
Limestone	Silurian–Devonian/CG, FF	Calcite	>90	2.1–2.7	no	0.13–0.21	0–0.76	0.1–0.28
Limestone	Camb.–Ordo./WH	Calcite	>90	2.5	no	0.08	0.8	0.1–0.3
Siltstone	Silurian-Devonian/IP	Qtz, calcite	>80	2.2	low	0.07	0.52	17.47
Conglomerate	Devonian/GG	Qtz, calcite	25	5.3	no	3	5.6	100
Conglomerate	Devonian/GG	Qtz, calcite	70	9.1	no	1.28	1.83	1.57
Sandstone	Devonian/GG	Qtz, calcite	20	5	no	0.39	1.68	no data
Carboniferous								
Conglomerate	Carboniferous/BF	Qtz, calcite	30–35	5 at 10	no	0.01–2.3	0.03–6.66	5.2
Sandstone	Carboniferous/BF	Qtz, calcite	30–45	5 at 10	no	5.4	0.5–2.72	1.21–100

Notes: L_{WD}, weight loss (%) after wetting–drying experiment using fresh water; L_{SW}, weight loss (%) after wetting–drying experiment using seawater (salt weathering); L_{F-T}, weight loss (%) after freeze–thaw experiment.

through sandstone was also examined and factored into the results of the other experiments (Daigneault 2001).

According to the results of our field experiments, dissolution related to the physiological activity of algae appears to be a very limited phenomenon and is not considered further as a contributing factor to cliff erosion (see Daigneault 2001 for details). On the other hand, freeze–thaw, salt weathering and wetting–drying processes clearly have a significant impact by reinforcing the effect of water in conjunction with porosity, percentage of matrix/cement, schistosity and fracturing (Tables 2 and 3).

The freeze–thaw experiments were designed to simulate three years of exposure in a natural environment. Each trial consisted of 200 freeze–thaw cycles under water-immersed conditions (at 1 atm, not under vacuum conditions) at −5°C for 6 hrs, +10°C for 12.5 hrs, and +15°C for 5 hrs (temperature transitions accounted for the remaining 1.5 hours per day). In order to calculate a first approximation of the loss by freeze–thaw, we selected representative samples (natural cubes delimited by fractures to keep the natural cohesion of the rock). Those included two sandstone and three conglomerate samples, from the post-tectonic (Bonaventure Formation; Carboniferous) and Acadian domains (Gaspé Sandstone Sequence; Devonian), one sample each of massive limestone, schistose limestone and siltstone from the Acadian domain (Indian Point Formation, White Head Formation, Forillon Formation; Cambrian to Devonian Chaleurs Group), and one sample each of schist and quartzite from the weakly metamorphosed Taconian unit (Maquereau Group, Precambrian). Two of the samples, sandstone from the Bonaventure Formation and conglomerate from the Gaspé Sandstone Sequence, were completely disintegrated by the process (Fig. 3). The calcareous siltstone (Fig. 3a) lost 17.5% of its original mass, whereas the mass loss for the conglomerate (Fig. 3b) and massive limestone samples was small or negligible (0.1% to 1.6%). Although it is difficult to apply the results directly to the natural environment, these experiments clearly demonstrate the significance of two fundamental parameters: effective porosity and rock texture/structure (e.g. Prick 1996).

Salt weathering and wetting–drying experiments were performed on the same sample population. The first experiment involved immersing the samples (four for each rock type) in fresh water for 2 hours per day (1 hr in the morning and 1 hr in the evening) in order to simulate the natural meteoric cycle. The duration of the experiment was three months, which equals the number of days of rain and melting snow in the Gaspésie region (average of 96). A second experiment using seawater involved two hours of wetting followed by ten hours of drying, repeated twice per day, in order to reproduce the tidal cycle in the upper intertidal zone.

In both experiments, the disintegration of the samples began during the very first week. Once established, however, the mass loss initially exhibited by some samples progressed slowly and remained minor despite an enlargement of the planes of weakness in the rock (Fig. 4). The results of the salt-water experiments were much more significant than those for the freshwater experiments, including significant mass losses for the conglomerate, sandstone and schist samples (up to 17.1%; Table 3), as well as exposure of conglomerate pebbles (Fig. 4b), and production of debris during disintegration of the sandstone (mainly quartz grains and minor amounts of matrix). The limestone samples remained essentially unaffected by the experimental process, producing no debris or water discoloration and exhibiting only minor mass loss (0.1–0.8%; Table 3). Those results are in agreement with most of the observations made by several authors (e.g. Prick 1999).

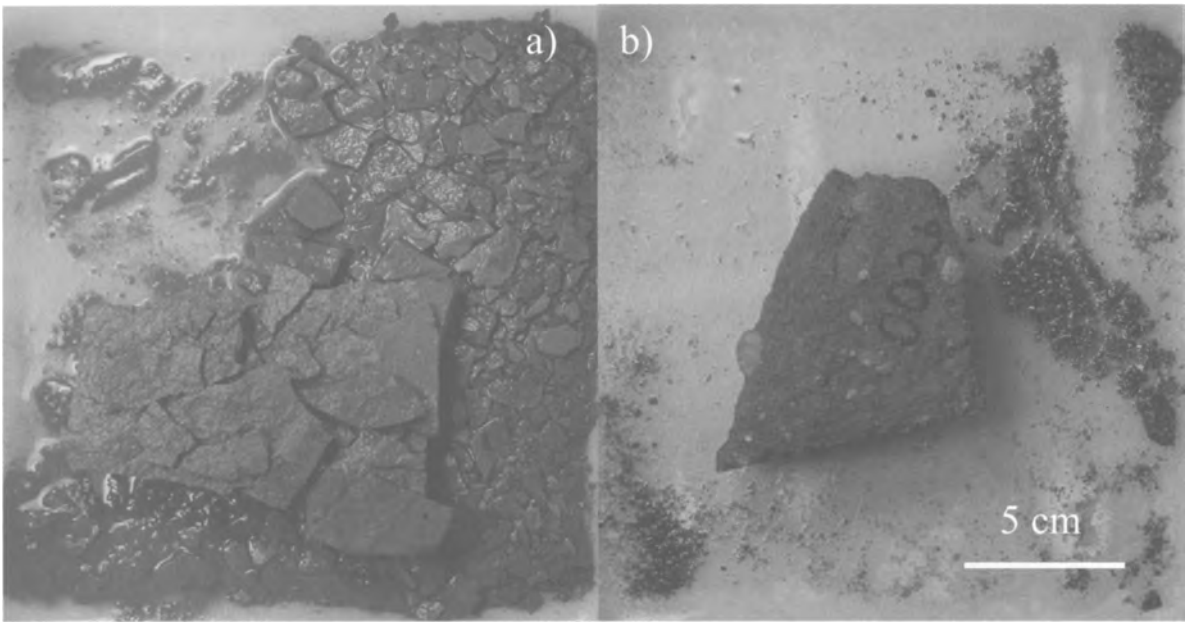

Fig. 3. Disintegration of (a) sandstone and (b) conglomerate from the Bonaventure Formation after 200 freeze–thaw cycles.

In summary, the presence of water alone is not a primary factor controlling rock integrity, as demonstrated by the fresh water wet–dry experiments in which mass losses were minor for all rock types. It appears that porosity changes induced by freeze–thaw cycles and salt crystallization in the marine environment during wet–dry cycles play the more essential roles. In the case of terrigenous samples, disintegration was primarily along matrix-grain or at matrix-clast boundaries. In the case of massive samples, disintegration took place mainly along planes of weakness, such as fractures or schistosity. The vulnerability of rocks that are subjected to small-scale erosional processes in the Gaspé region is therefore directly dependent on lithology and, more importantly, its textural and structural characteristics. Nevertheless, extrapolation of experimental data to the natural environment is always critical, because saturation is actually very difficult to attain in the field, even in the intertidal zone (Trenhaile & Mercan 1984).

Fundamental parameters and vulnerability diagram

Observations of Gaspesian cliff retreat during this study revealed ten fundamental and easily observed parameters that characterize the erosional processes. Two of them, both hydrodynamic in nature, are external parameters that appear to be essential in a coastal environment: (1) waves at high or low tide or any intertidal height (ranging from constant action to absent) are responsible for ordinary abrasion during summer and ice crashing during spring, in addition to their ability to clear debris from the intertidal zone; and (2) the presence or absence of ice floes along the cliff face governs the freeze–thaw process. Three other petrophysical parameters control the primary vulnerability of the rocks exposed to coastal erosion: porosity, percentage of matrix or cement, and homogeneity of stratification. Finally, five structural parameters that strongly affect cliff erosion have also been added to the list: dip of the strata, nature of the schistosity (open or closed), joint density, number of joint systems, and the presence of fault zones.

These ten parameters were used to construct a radial diagram called a 'vulnerability diagram', which is divided into three zones that each represent a possible cause of erosion (Fig. 5). Zone 1 groups the structural characteristics of the outcrop, zone 2 represents the physical characteristics of the rock, and zone 3 reflects the external parameters of the site. Each parameter is normalized by assigning a numerical value between 0 (negligible influence for the site in question) and 3 (maximum influence; Table 4). The sum of the numerical values (from 0 to 30) is called the 'erosion vulnerability index' and provides a first approximation of susceptibility without specifying the causes. The parameters incorporated into the radial diagram (Fig. 6) are colour-coded according to the lithology of the site, and the size of the diagram is determined by a dimensional code (erosional intensity), as in seismic risk cartography (e.g. Anglin *et al.* 1993). Displayed on a map, radial vulnerability diagrams allow for comparison with natural risk maps.

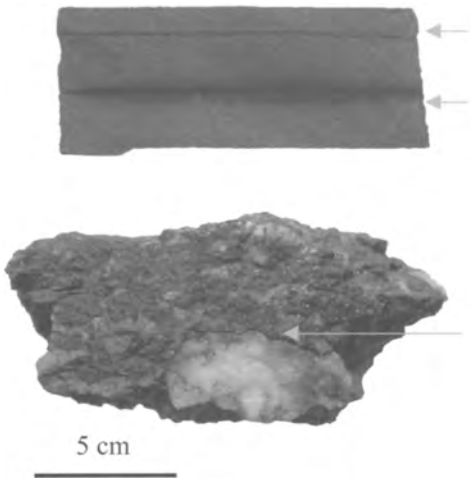

Fig. 4. State of (a) sandstone and (b) conglomerate from the Bonaventure Formation after 90 cycles of wetting/drying using seawater (salt weathering).

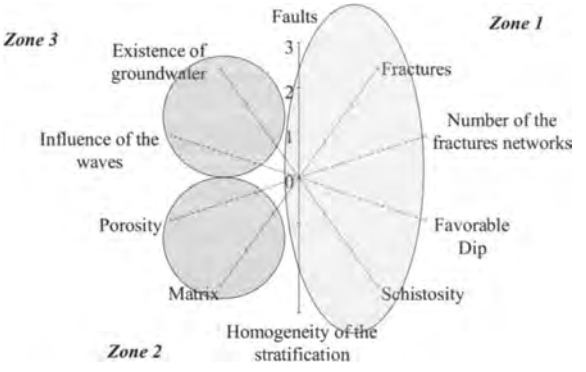

Fig. 5. Erosion vulnerability diagram. Zone 1: Structural characteristics of the cliff. Zone 2: Physical characteristics of the rocks. Zone 3: Environmental characteristics.

Many researchers (e.g. Hayashi 1966; Selby 1980; Benumof & Griggs 1999; Budetta *et al.* 2000) considered rock strength to be among the most important erosional parameters, however it will be demonstrated below that fracturing dominates over rock resistance in determining erosional vulnerability for the Baie des Chaleurs region. Other authors consider cliff height to be a significant factor in some circumstances (e.g. Trenhaile 1987), yet cliff height varies very little around the Baie des Chaleurs, even from one dominant lithology to another.

Effect of wave action

In order to determine the influence of wave action on cliff erosion, several zones were selected to represent the various degrees of cliff-wave contact (Table 2): continuous contact at both high and low tides; permanent contact in which there is considerably less influence at low tide (<1 m at the base of the cliff is hit by waves); contact at high tide only; and no contact at all between the cliff and the sea (unless during storms that were not observed). Outcrops that were continuously subjected to wave action in the study area generally exhibit deep basal notches (Fig. 9d). Wave power is variable and is clearly stronger at high tide. Moreover, wave action and the slower action of swells act indirectly by reinforcing the impact of sea ice (e.g. abrasion and dislocation; Carter & Drouin 1973*a*,*b*). This study demonstrates that where rocks are in permanent contact with the sea, the depth of the basal notches is determined in large part by the rock type. The sandstone of the Bonaventure Formation, is particularly vulnerable in this respect, with basal notches ranging from 0.5–3 m deep. Ice blocks detached from the cliff face or from

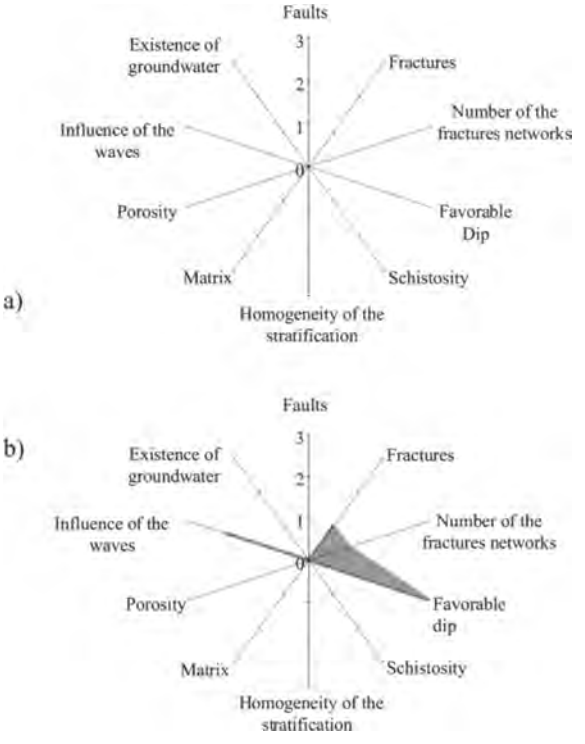

Fig. 6. Erosion vulnerability diagram: *Y* axes correspond to the most significant parameters in the retreat evaluation. Once assigned values, the parameters are linked and coloured in order to underline the most vulnerable zones.

an ice floe have considerable effect in eroding these notches. Where the contact with the sea is almost exclusively at high tide (e.g. Chaleurs Group, Indian Formation, Murphy Creek Formation and White Head Formation), the main role of

Table 4. *Numerical values assigned to parameters as a function of their influence on erosion*

Parameter	*Value*			
Porosity	20% and more	20–10%	10–5%	5% and less
Value	3	2	1	0
Matrix (%)	50% and	50–70%	70–90%	90% and more
Value	3	2	1	0
Schistosity state	Open (more than 20%)	Open (more than 10%)	Closed	Absent
Value	3	2	1	0
Density of the fractures (m^3)	20% and more	20–10%	5–10%	0–5%
Value	3	2	1	0
Density of the fractures networks (m^3)	2 and more	2	1	0
Value	3	2	1	0
Stratification dipping	45° and more	30–45°	15–30°	15° and less
Value	3	2	1	0
Presence of faults	In contact	at 1 to 5 m	at 5 to 20 m	at 20 m and more
Value	3	2	1	0
Influence of the waves	permanent contact	low tide	high tide	never
Value	3	2	1	0
Existence of flows	permanent	low wetting	after rain	never
Value	3	2	1	0
Homogeneity of the stratification	70 and less	70–90%	90–100%	100%
Value	3	2	1	0

waves and sea ice is to clear away debris from the cliff base, thus allowing new mass movements to occur. On the basis of these observations, the following values were assigned to the wave action parameter: 0 if there is no contact with the sea; 1 if the contact is only at high tide; 2 if the contact is at both high and low tide but with considerably less effect at low tide; and 3 if the cliff-sea contact is permanent (Table 4).

Presence of groundwater

Groundwater circulating inside the weaker planes of a cliff is a potential agent of chemical dissolution and, even more importantly, a potential agent of mechanical transport for a mixture of water and solid particles that can act as either a lubricant or abrasive (cf. Trenhaile 1987; Benumof & Griggs 1999). In temperate-cold regions, like Baie des Chaleurs, the freeze–thaw of underground water weakens the cliffs, and the most severely affected areas are those where the flow is permanent, like the sandstone of the Bonavcnture Formation at Percé Point. In fact, sandstone is the dominant groundwater-bearing lithology, especially in the Bonaventure Formation (Table 2). Whether intermittently or permanently wet, such zones appear restricted to thin layers (several decimetres thick) that are commonly fractured and do not extend laterally for more than a dozen metres. In zones of permanent flow, differential erosion of 10 to 15 cm was observed and collapse of material above the groundwater flow horizon was not uncommon (e.g. Percé, Cap d'Espoir and Anse-à-Beaufils; 1 to 2 m^3 in volume), suggesting that the water-saturated zones act as lubricating surfaces. Based on field observations, a value of 0 was assigned where groundwater is absent, 1 where flow occurs following rainfall (e.g. Shigawake), 2 where the rocks are continuously wet, and 3 for zones where groundwater flow is permanent (Table 4).

Porosity

Open porosity (n) is one of the most important weakening parameters associated with a number of erosional processes related to water, including groundwater circulation, frost fracturing, salt weathering and wetting–drying (Bradley *et al.* 1978; Pissart & Lautridou 1983; Hames *et al.* 1987; Ozouf 1987; Prick 1996; Benumof & Griggs 1999). A conventional Micrometric™ poresizer was used to determine porosity, and a scanning electron microscope (JEOL JSM-840™) was used to characterize the morphology of grains and pores, as well as the microstructural grain arrangement (Fig. 7). Use of the JEOL JSM-840™ allowed for observation by secondary electrons and X-rays. On the basis of previous experimental work (see Rock Disintegration), it was determined that the effects of open porosity are minor when values are less than 5% (e.g. massive calcareous rocks; see Table 3), but freeze–thaw and salt weathering become particularly efficient at 5 to 10% porosity (e.g., Gaspé sandstones, see Table 3). Between 10 and 20% porosity, water circulation

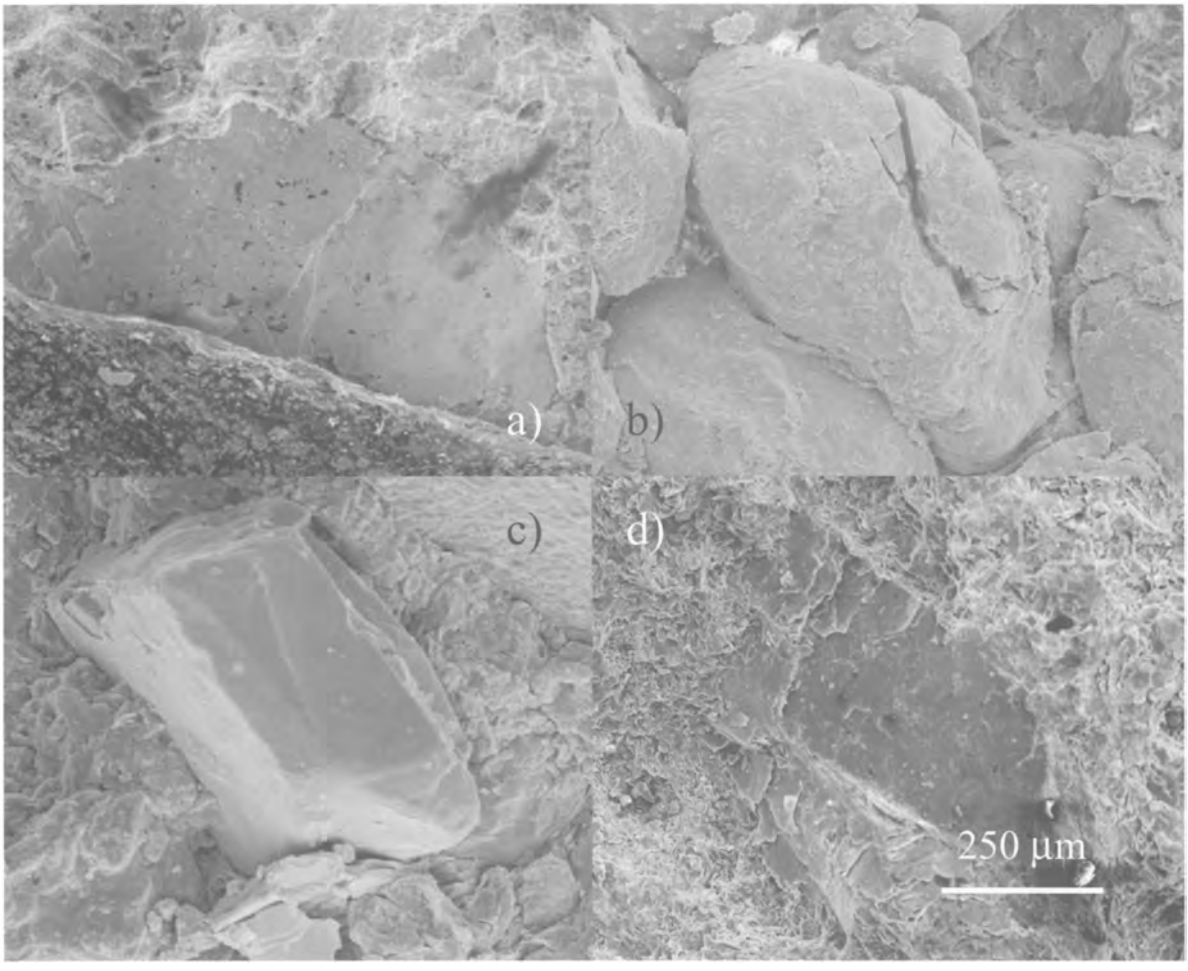

Fig. 7. Scanning electron photomicrographs: (a) Fossil debris in limestone from the White Head Formation; (b) Sandstone of the Bonaventure Formation (quartz grains and minor amount of matrix); (c) Matrix in a conglomerate from the Bonaventure Formation (quartz grain surrounded by calcite matrix); (d) Quartzite of the Maquereau Group (quartz grain surrounded by a silica matrix).

favours dissolution and leaching, and beyond 20%, cohesion is lowered as the rock becomes weak and significant disintegration occurs (Remy 1993; e.g., Bonaventure sandstones, see Table 3). A value of 0 was attributed to rock types with less than 5% porosity, a value of 1 for 5 to 10% porosity, a value of 2 if porosity is between 10 and 20%, and finally a value of 3 for rocks with >20% porosity (Table 4). The latter represent the most vulnerable rocks of the Baie des Chaleurs coast, which account for only 3% of the study area.

Percentage of matrix/cement

Results of laboratory experiments (freeze–thaw, wetting–drying and salt weathering) on the relationship between matrix or cement content (measured by optical microscopy) and erosional vulnerability revealed that an abundance of matrix or cement (>90%) significantly increases a rock's resistance to disintegration. For example, one hand, limestone samples suffered little or no mass loss. On the other hand, when the percentage of matrix or cement falls below 50%, disintegration is almost always considerable (e.g., sandstone of the Bonaventure Formation and conglomerate of the Gaspé Sandstone Sequence, Table 3; Figs 7 & 8). Consequently, a value of 0 was assigned to rocks with >90% matrix or cement (all limestone), a value of 1 if the percentage ranges from 70 to 90 (conglomerate of the Gaspé Sandstone Sequence), a value of 2 for 50 to 70%, and a value of 3 for rocks with less than 50% (some sandstone of the Bonaventure Formation; Table 4).

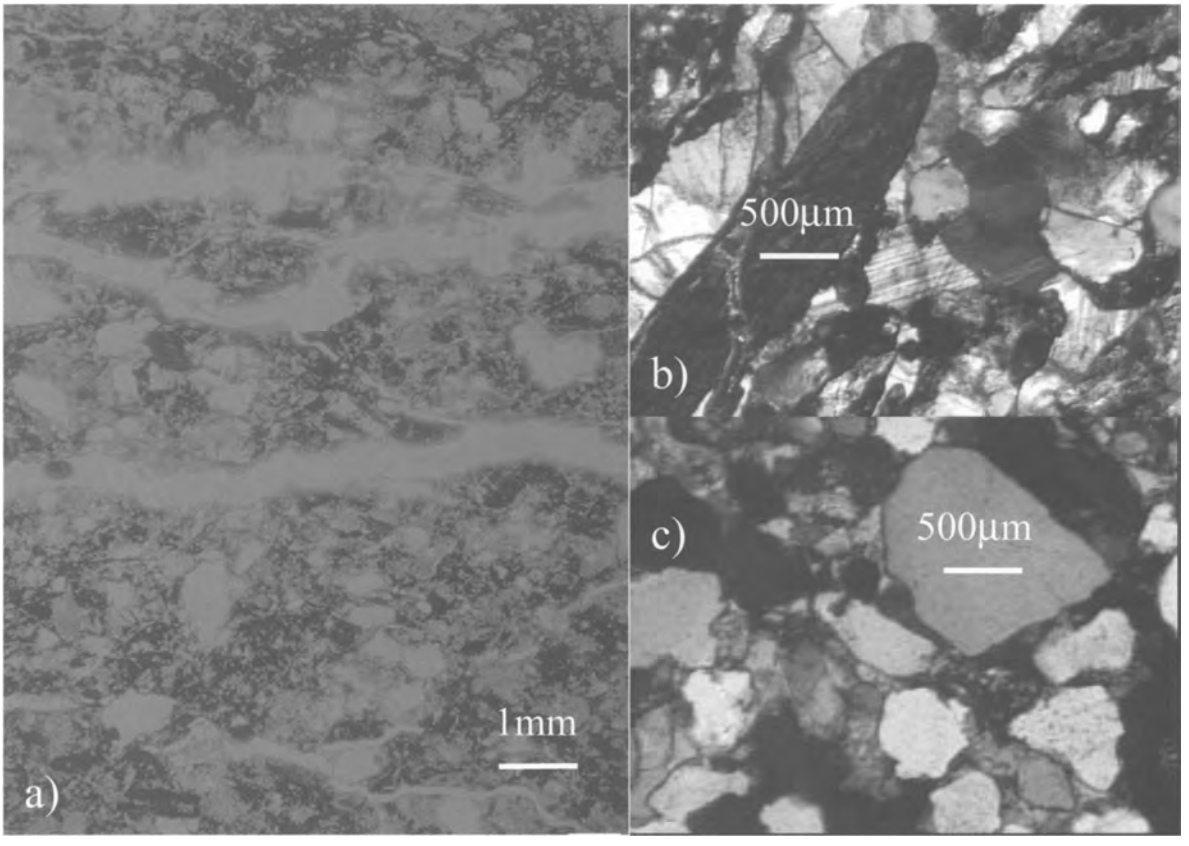

Fig. 8. Optical photomicrographs: (a) Schistosity in quartzitic schists of the Maquereau Group; (b) Conglomerate matrix in the Bonaventure Formation (limestone debris and quartz grains surrounded by a calcite matrix); (c) Sandstone from the Bonaventure Formation (quartz grains and minor amounts of matrix composed of calcite, iron oxides and organic mud).

Schistosity

Open schistosity strongly favours water circulation in zones with strata that dip downhill. In the Baie des Chaleurs area, the schist of the Maquereau Group has the most pronounced schistosity (Fig. 8a). The schistosity is displayed as deep (5 to 15 m) eroded grooves a few metres wide that are protected by a quartzite cap. Schistosity has also been observed in the calcareous siltstone units of the Indian Point Formation (Table 3), but cliff retreat is not as strong because layering is closed and the siltstone is interstratified with massive (non-schistose) calcareous horizons. In either case, samples with any type of schistosity react to freeze–thaw experiments (Table 3). Results of the experiments combined with field and microscopic study led to the following classification for this parameter: a value of 0 was assigned for rocks in which schistosity is absent (Table 3); a value of 1 for rocks with closed schistosity (accounts for $<10\%$ of open spaces in the rock; e.g. siltstone of Indian Formation), a value of 2 when open schistosity accounted for 10% to 20% by volume (e.g. most of schist units in the Maquereau Group); and a value of 3 when the open schistosity accounted for more than 20% (e.g., about 10% of the schists in the Maquereau Group).

Homogeneity of stratification

Field observations show that erosion rates are related to lithological differences. In the case of the gently dipping Bonaventure Formation, rapid erosion of the sandstone resulted in an erosional profile 20 to 50 cm deeper than that for the conglomerate causing the latter layers to project outward. As a consequence, interstratification between the two lithologies (10–40 cm spacing) causes instability in the conglomerate horizons that manifests itself as minor collapses ($\sim 0.5\,m^3$). Above the notches near the base of the cliff, water is held as ice under the overhangs during the winter, and ice walls preferentially form in these locations. Both the alternating beds of sandstone and conglomerate in the Bonaventure Formation, and the alternating beds of fine-

to coarse-grained calcareous siltstones at the Indian Point Formation (Percé region), are affected by this erosional process. The preferential erosion of the steeply dipping (>70°) calcareous siltstone of the Indian Formation favours rock slides of up to 1 m (field measurement). The homogeneity parameter is assigned a value of 0 if the cliff consists entirely of one rock type, a value of 1 if the dominant rock type represents >90% of the lithostratigraphy, a value of 2 if it represents only 70 to 90%, and 3 if the dominant lithology constitutes less than 70% of the cliff (Table 4).

Dip of strata

The influence of dip on rock face stability has been widely demonstrated. According to Bouchard (1991), a dip of <15° generally results in relative stability in the outcrop, whereas a dip steeper than 15° results in an increased tendency for landslides (see also Daigneault 2001). Where stratification slopes downhill, which is common in the Baie des Chaleurs region, the instability of the rock face increases rapidly with increasing dip. In fact, long-term sliding events that affect 10 to 15 m of a cliff face (volume of <30 m^3) have been observed in dipping conglomerate and sandstone units of the Gaspé Sandstone Sequence. The slow movement of the layers can be observed over several years. Sliding becomes particularly significant for dips between 30° and 45°, and rapid larger-scale events may occur (~100 m^3) where the dip exceeds 45° (e.g., in the limestone sequences of the Chaleurs Group, Indian Formation and White Head Formation; Fig. 9a, b and c). In the case of permeable rocks, sliding is never the sole cause of cliff retreat. The flow of water and the resulting fragmentation and transport of solid material considerably increase the vulnerability of steeply dipping sequences (e.g., the large collapse at Coin du Banc). Table 4 summarizes the values attributed to various sites according to the following criteria: a value of 0 is applied where the dip is <15° (negligible effect on erosion; e.g., Bonaventure Formation); a value of 1 if the dip is between 15 and 30° (slow sliding action); a value of 2 if the dip is between 30 and 45° (recurrent sliding associated with rockfalls); and a value of 3 where dips exceed 45° (e.g., pre-Carboniferous sequences have some segments with steeply dipping layers).

Fracture number per cubic metre

By increasing the connected porosity, the number of fractures directly influences the effects of frost, salt and wetting–drying during experiments (cf. Coutard 1995; Table 2). On a small scale, field records show that the contribution of rock disintegration to cliff retreat during the freeze–thaw period can be locally important, being greater than 6 cm/year for some carboniferous sandstones and 4 cm/year for limestone. Block decoupling effects are very limited in zones where the number of apparent fractures is less than 5 per cubic metre (e.g. the conglomerate of the Bonaventure Formation and the Gaspé Sandstone Sequence), but rockfalls appear to be a much more significant erosional event where the cliff contains 5 to 10 apparent fractures/m^3 (e.g., quartzite cliffs of the Maquereau Group), and particularly at frequencies greater than 10 apparent fractures/m^3. The sandstone/conglomerate strata of the Bonaventure Formation provide a natural demonstration of the effect of contrasting fracture densities: sandstone beds (20 apparent fractures/m^3) are undergoing preferential retreat, whereas the conglomerate horizons (0 to 5 apparent fractures/m^3) form relatively resistant overhangs (Fig. 9d). Values of 0 to 3 are assigned to lithologies with <5, 5–10, 10–20 and >20 apparent fractures/m^3, respectively (Table 4).

Number of fracture systems

The shape and volume of most of the rock fragments at the cliff base is determined by the fracture pattern. From a mechanical point of view, the number and orientation of the fractures constitutes an essential parameter for most mass movements (e.g. Selby 1980; Benumof & Griggs 1999). In accordance with Whalley (1984), erosion by rockfall (blockfall) is observed where more than two fracture sets coincide (Fig. 9b). An increase in the number of fracture sets will increase the number of blocks, decrease the average block size, and facilitate groundwater movement. As the number of fracture sets equals or drops below 1/m^3, rockfalls are not observed and the effect of freeze–thaw cycles is small. As the number of fracture systems exceeds 2/m^3 (e.g. Bonaventure Formation conglomerate, some conglomerate units of the Gaspé Sandstone Sequence, Chaleurs Group, Indian Formation, and White Head Formation) unstable blocks appear along the cliff face and the vulnerability to frost damage increases. The main mechanism for cliff retreat in these cases is rockfall, and volumes can attain 100 m^3 per event. As the number of fracture systems exceeds 3/m^3, fracturing becomes intense and all other related parameters are affected, resulting in a weak rock that is easily broken by sea ice. On the basis of field observations, a value of 0 was assigned to unfractured cliffs (0 fracture systems), and values of 1, 2 and 3 to cliffs that are crosscut by 1 to 3 fracture systems per cubic metre, respectively (Table 4).

Presence of faults

Fault zones are generally marked by weakened rock of various types (e.g., rock flour, highly fractured zones, weakly or non-lithified sediments; Fig. 9c), thus enhancing erosional vulnerability. However, the fault zones recognized in the area are of limited extent and their influence on the surrounding rock rapidly fades with distance from the fault (influence rarely extends beyond 20 m; Fig. 9c). The rocks in the fault zone are pulverized and display a powdery texture that is a favourable medium for water circulation and frost–thaw processes. Fractures are abundant proximal to the fault zone (e.g., 100 fractures/m^3 in the first 5 m from the margin). This zone is particularly vulnerable to small mass movements, like rockfalls of approximately 1 m^3. The fracture density

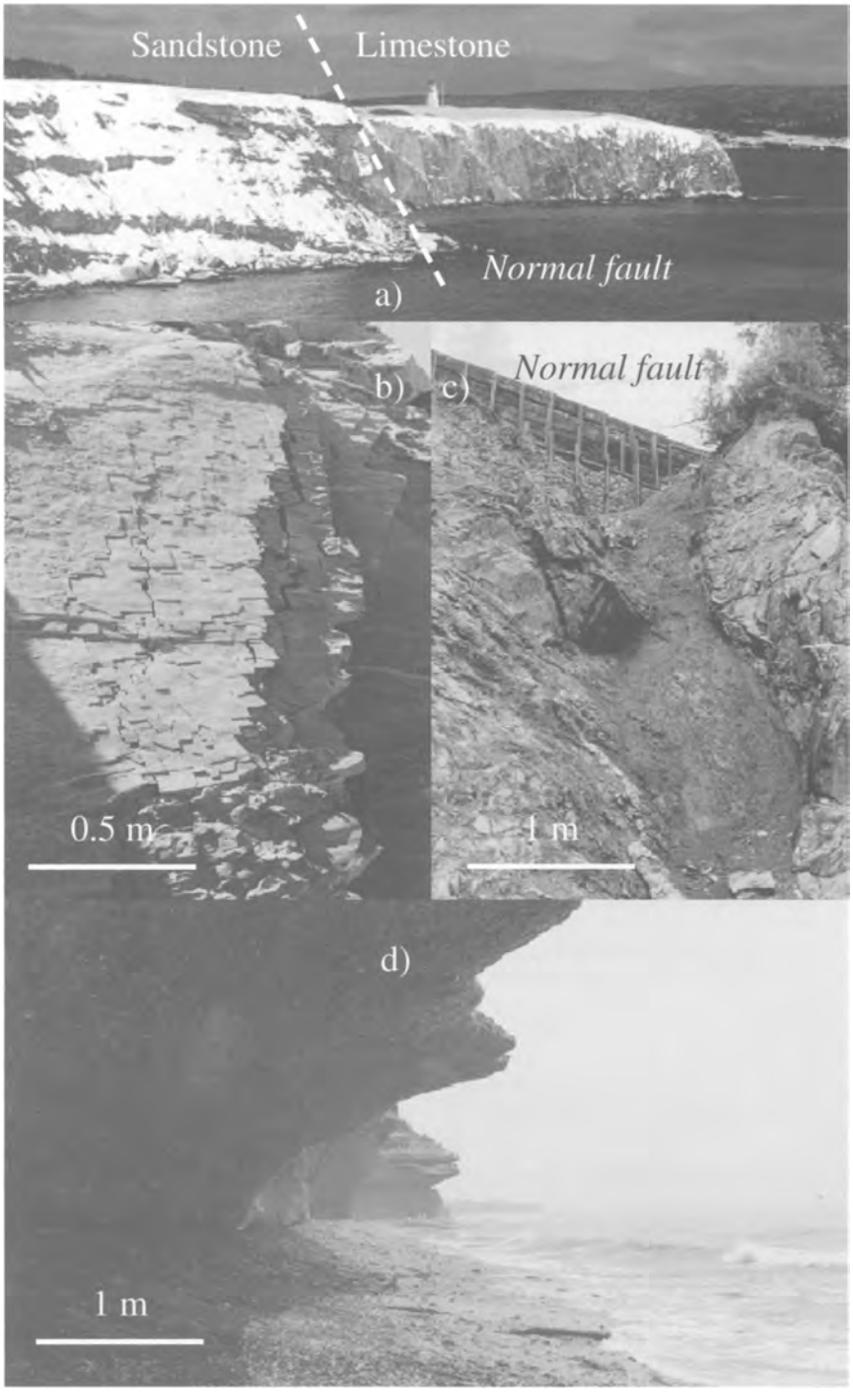

Fig. 9. (a) Unconformable contact between the Bonaventure Formation and the limestone of the White Head Formation (Percé area); (b) Fracture style in calcareous siltstone of the Indian Point Formation (dip: 70° towards the sea); (c) Normal faults in the limestone of the Chaleurs Group; (d) Erosional notch along the cliff base in the Bonaventure Formation (entire cliff is composed of conglomerate).

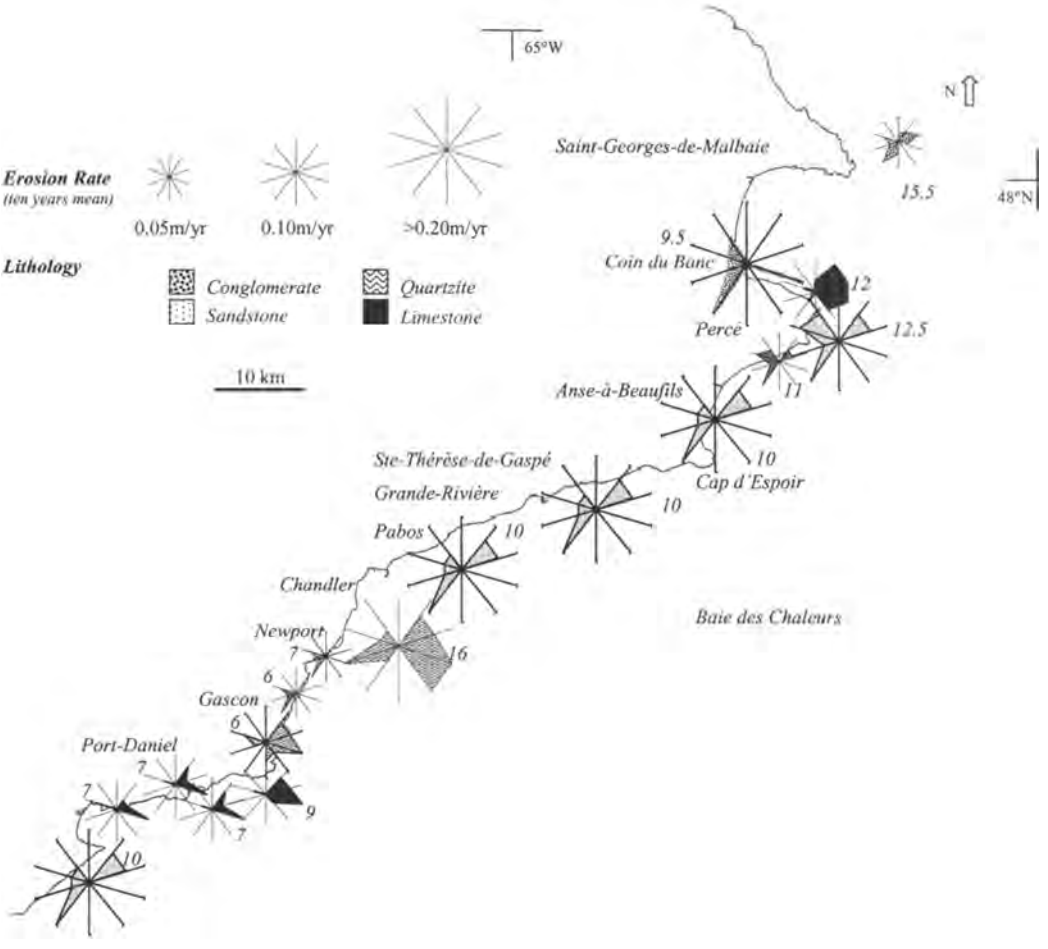

Fig. 10. Examples of erosion vulnerability diagrams for the Baie des Chaleurs.

remains significant 5 to 20 m away from the fault zone, but drops below 100 fractures/m^3. At distances greater than 20 m, the influence of the fault zone is negligible. In places where faults spatially coincide (e.g., the numerous normal faults of Acadian age in the Chaleurs Group), the landscape is noticeably affected and notches 1.5 to 3 m deep form along the cliff face due to differential weathering (Fig. 9c). North–south normal faults that dip to the west were observed in the Port-Daniel and Gascon areas (Chaleurs Group), and in the vicinity of Percé Point (Indian, Murphy Creek and White Head formations). Faults are particularly common in the Port-Daniel and Gascon regions where they occur every 200–300 m over a distance of twenty kilometres. This results in weak zones averaging 1.5 m wide, with a maximum of 5 m. Approximately 10 faults in the Percé region have similar effects on the country rock over a distance of 5 km. Three other faults spaced 250 m apart crosscut the limestone sequences, whereas fault spacing in the Bonaventure Formation is on the order of 500 m. A value of 0 was assigned for areas where faults are absent or at least 20 m apart. A value of 1 was assigned to zones that are 5 to 20 m from a fault, 2 if the fault are only 1 to 5 m apart, and 3 for the fault zone itself (Table 4).

Discussion and conclusion

The erosion vulnerability index for limestone cliffs fluctuates between 7 and 14, but is typically around 7 for most of the coast (Fig. 10). Analysis of the vulnerability diagrams for the region reveals that major weaknesses relate mainly to the structural characteristics (a maximum value of 3 has been attributed to the dip, and the number of fractures is very high, with an attributed value of 3) and, to a lesser extent, the environmental conditions (especially the degree of sea attack; Table 5; Figure 10).

Table 5. *Values assigned to each erosional parameter for selected rock types in the Baie des Chaleurs study area*

Localization	*Lithology*	*Faults*	*Number of fractures*	*Number of the fractures networks*	*Dipping*	*Schistosity*	*Homogeneity of the stratification*	*Matrix*	*Porosity*	*Influence of the waves*	*Existence of groundwater*	*Total*
Gascon/East	Limestone	0	2	2	3	0	1	0	0	1	0	9
Gascon/West	Limestone	0	2	1	3	0	0	0	0	1	0	7
Port-Daniel/West	Limestone	1	2	1	3	0	0	0	0	1	0	7
Port-Daniel/Mcginis	Limestone	0	1	1	3	0	0	0	0	2	0	7
Percé/Murphy Cr.	Limestone	1	3	3	3	0	0	0	0	2	0	12
Percé/Indian pointe	Limestone	1	3	3	3	0	2	1	0	1	0	14
Percé/West	Sandstone	0	2	2	0	0	0	3	1	2.5	2	12.5
Ste-Thérese-de-Gaspé	Sandstone	0	2	2	0	0	0	3	1	1	1	10
Cap d'Espoir	Sandstone	0	2	2	0	0	0	3	1	1	1	10
Caplan/Saint-Siméon	Sandstone	0	2	2	3	0	0	3	1	1	1	13
Newport East	Shist	0	2	2	3	3	0	1	3	1	1	16
Newport West	Quartzite	0	1	1	3	0	0	0	0	2	0	7
St-Georges/tête d'indien	Conglomerate	1	1.5	2.5	1	0	1.5	3	1	2	0	15.5
Percé/Coin du Banc	Conglomerate	0	0	0	3	0	0	3	1	1	1.5	9.5
Percé/West	Conglomerate	0	1.5	1.5	0	0	0	3	1	2.5	1.5	11
Newport Centre	Conglomerate	0	0	0	0	0	0	3	1	2	0	6

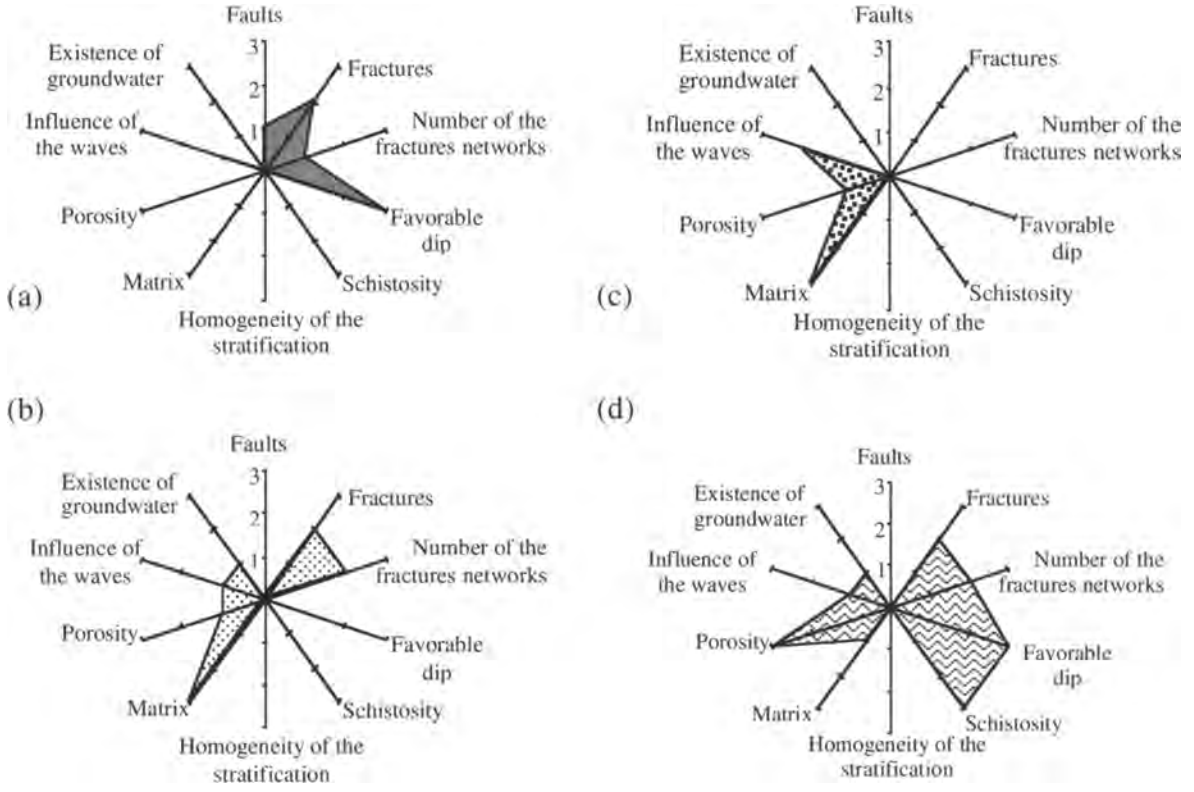

Fig. 11. (a) Typical limestone cliff (Port-Daniel). Erosion here is related to layer-slip (bed on bed; structural context), falling blocks and attack by the sea (small basal notches, abrasion and cleaning of debris at the bottom of the cliffs). This type of rock assemblage is generally unaffected by continuous processes (cryoclasty, haloclasty, etc.); (b) Typical sandstone cliff (Carboniferous). This assemblage of sandstone and siltstone is characterized by several factors that affect rock integrity and the rocks are consequently vulnerable to almost all processes resulting in both continuous and discontinuous erosion. Almost 60% of the coastline is marked by this type of cliff (structure/lithology); (c) Typical conglomerate sequence (Carboniferous). Conglomerate sequences are typically interstratified with sandstone; they have few weaknesses and are not easily affected by weakening factors. When in a basal position and interstratified with sandstone, the rate of retreat is considerably reduced. When forming the upper part of the cliff, they fall by blocks according to the joint pattern (overhangs); (d) Typical schist cliff (Precambrian) characterized by several weakening factors, including structural (well-developed schistosity and highly fractured), environmental (in contact with the sea) and microscopic (high porosity). The rocks are vulnerable to almost all erosional processes resulting in both continuous and discontinuous erosion. Layer-slip (bed on bed) and overhang collapse are the most significant modes of retreat.

In the case of the Maquereau Group (interlayered schist and quartzite), the index varies between 7 and 16. Quartzite layers are generally quite resistant (index = 7), but the highly porous schist layers are clearly more susceptible (index = 16; Table 5 and Figure 10).

Vulnerability diagrams for the limestone, quartzite and schist units of the Chaleurs, and Maquereau groups and the Indian, Murphy Creek and White Head formations clearly demonstrate the importance of structure (steep dip: >45°; high number of fractures: >20/m^3; Fig. 11a and d). The main process for retreat in these cases is sliding, locally accompanied by rockfalls. The influence of sea action on these cliffs is minimal, and groundwater was not observed. Freeze–thaw processes operate mainly along fractures, but laboratory experiments confirmed that limestone in particular, with its low porosity, high percentage of cement and lack of schistosity, is not very susceptible to erosional processes that operate at the microstructural scale, such as freeze–thaw, salt weathering and wetting–drying. The average retreat for these areas, based on calculated estimates and direct measurements, is 0.1 m/year for limestone and quartzites. The retreat of limestone cliffs is therefore attributed to sliding and block falls (Figs 10 and 11a and d).

The erosional vulnerability index for the sandstone cliffs in the study area varies between 10 and 12.5, with 80% of the cliffs having an index generally around 11. Vulnerability

diagrams reveal that these rocks are susceptible to almost all erosional parameters. Apart from several structural aspects (number of fractures exceeding 50/m^3) and lithological weaknesses (high porosity, low percentage of matrix or cement; Table 5), the influence of the environmental parameters can also be discerned. In particular, wave exposure (numerous basal notches), abrasion and dislocation by sea ice, and the presence of groundwater all contribute significantly to erosion (Fig. 11b). The vulnerability diagrams also reflect the experimental results that show how strongly the Bonaventure sandstones react to freeze–thaw and salt weathering processes. Rates of retreat (up to 0.36 m/year; average of 0.2–0.3 m/year) are accordingly among the most rapid for the study area.

Conglomeratic units have erosion vulnerability indexes that vary between 6 and 15.5. Most conglomerates, and especially those of the Bonaventure Formation, display few weaknesses (vulnerabities = 6; Fig. 11c). The average global retreat, in the Baie des Chaleurs area, during the last decade was 0.03–0.4 m/year (1990 to 2000), and the calculated average is 0.05 m/year based on both measurements and calculated estimates. These rates, however, should be applied with caution since conglomerate units tend to fail as blocks measuring 2 to 10 m^3 in volume, especially when this lithology is at the top of the cliff. For example, the conglomerates in the Coin du Banc region exhibit weaknesses at the lithological and structural level that can result in mass movements on the order of 15 m per event (frequency unknown). These landslides play a stabilizing role by temporarily protecting the base of the cliff from erosional processes such as wave action and sea ice abrasion. Overall, conglomerates are among the most resistant lithologies, especially when the cliff is lithologically homogeneous and not very high (3 to 5 m). The contrast in erosion rates between sandstone and conglomerate largely determines the shape of the shoreline: the bays are dominated by sandstone, whereas the headlands are generally underlain by conglomerate (Fig. 10).

The stability of coastal cliffs at Baie des Chaleurs is determined by complex interactions between many parameters, as is true for many other areas (cf. Suzuki 1982; Trenhaile 1987; Tsujimoto 1987; Sunamura 1992; Belov *et al.* 1999; Benumof & Griggs 1999). In this region, stability is governed by relationships between physical rock properties (matrix/cement and porosity), structures (dip, fractures, fault, schistosity and homogeneity of the stratification), and the environmental context (groundwater, wave and sea ice). The vulnerability diagrams, which enable us to easily visualize the most dominant weaknesses of a cliff section and consequently identify the probable erosion processes, is based on many macroscopic features that are easily observed in the field. Nevertheless, the difficulty of obtaining a precise estimate for the annual rate of retreat due to episodic losses led the authors to propose a moderate-term (50 year) management and follow-up plan for coastal erosion. Data for several variables, including cliff vulnerability, lithological strength and estimated rate of retreat, were georeferenced and integrated into the 'Gaspesian Erosion Project', part of the Geographic Information System (GIS) database of the Baie des Chaleurs area. The Gaspesian Erosion Project currently contains eight themes: topography, hydrography, coastline, basal notch characteristics (size), mass movements (types and characteristics), retreat estimate (ten-year period), and measured retreat using archived data. Roads, buildings and territorial limits are additional features that could be added in the future. Each of the themes is linked to an attribute table, and every georeferenced point is characterized.

Acknowledgements. The authors are grateful to Dr Cheryl Hapke and Dr Alan S. Trenhaile for detailed and valuable reviews and critiques of the paper. This research was made possible thanks to the FCAR fund of the Québec government. We thank them. We also thank the members of the geochemistry laboratory of the École des Mines (France), Jean-Claude Ozouf of the CNRS and Mr Steve Otis, development manager in the Baie des Chaleurs.

References

ALLISON, R. J. 1989. Rates and mechanisms of change in hard rock coastal cliffs. *Zeitschrift fur Geomorphologie*, **Supplement Band 73**, 125–138.

ANGLIN, F. M., WETMILLER, R. J., HORNER, R. B., ROGERS, G. C. &. DRYSDALE, J. A. 1993. *Seismicity Map of Canada*, Natural Resources Canada.

BELOV, A. P., DAVIES, P. & WILLIAMS, A. T. 1999. Mathematical Modelling of Basal Coastal Cliff Erosion in Uniform Strata: A Theoretical Approach. *Journal of Geology*, **107**, 99–109.

BENUMOF, B. T. & GRIGGS, G. B. 1999. The relationship Between Coastal Cliff Erosion Rates and the Mechanisms/Variables That Affect Seacliff Retreat in San Diego County, California. *Shore and Beach*, **67**, 4, 29–41.

BOUCHARD, S. 1991. Stabilité des ouvrages miniers. Editions Odile Germain, Québec.

BRADLEY, W. C., HUTTON, J. T. & TWIDALE, C. R. 1978. Role of salts in development of granitic tafoni, South Australia. *Journal of Geology*, **18**, 623–628.

BRISEBOIS, D. & BRUN, J. 1994. La plate-forme du Saint-Laurent et les Appalaches. *Géologie du Québec*, **1**, 95–120.

BRISEBOIS, D., LACHAMBRE, G. & PICHE, G. 1991. Carte géologique de la péninsule de la Gaspésie. Ministère des Ressources Naturelles, DV 91–21.

BUDETTA, P., GALIETTA, G. & SANTO, A. 2000. A methodology for the study of the relation betwen coastal cliff erosion and the mechanical strengh of soils and rock masses. *Engineering Geology*, **56**, 243–256.

CARDINAL, A. 1967. Inventaire des algues marines benthiques de la Baie des Chaleurs et de la Baie de Gaspé (Québec). I. Phéophycées. *Naturaliste Canadien*, **94**, 233–271.

CARTER, D. & DROUIN, M. 1973*a*. Dynamique des glaces le long des rives du Saint-Laurent. Étude des rives du Saint-Laurent. Rapport du Ministère des travaux publics.

CARTER, D. & DROUIN, M. 1973*b*. Action de la glace sur les ouvrages maritimes. Etude des rives du Saint-Laurent. Rapport du Ministère des travaux publics.

COUTARD, J. P. 1995. Les effets du gel sur la paroi calcaire du centre

de géomorphologie du CNRS à Caen – Hivers 1980–1981 à 1986–1987. *Bulletin de la Société linnéenne de Normandie*, **116**, 25–39.

DAIGNEAULT, M. 2001. *Processus d'altération/érosion à l'interface océan/continent/ atmosphère: aspects quantitatifs et semi-quantitatifs. Exemple des littoraux de l'Est du Canada (Gaspésie)*. Thèse de Doctorat de l'Ecole des Mines de Saint-Etienne, France.

DIONNE, J. C. 1970. Aspects morpho-sédimentologiques du glaciel en particulier des côtes du Saint-Laurent. Rapport Environnement Canada QFX-9.

DIONNE, J. C. 1974. Bibliographie annotée sur les aspects géologiques du glaciels, Québec. Rapport Environnement Canada LAU-X-9.

DYKE, A. S. & PREST, V. K. 1987. Late Wisconsinan and Holocene history of the Laurentide ice sheet. *Géographie physique et Quaternaire*, **41**, 237–263.

EMERY, K. O. & KUHN, G. G. 1982. Sea cliffs: their processes, profiles and classification. *Geological Society of America*, **93**, 644–654.

ENVIRONNEMENT CANADA (Région du Québec) 1994. Les cartes climatologiques du Saint-Laurent (Fleuve et Golfe). World Wide Web Address: *http://www.qc.ec.gc.ca/atmos/cartes/*

ENVIRONNEMENT CANADA 1998. Normales climatiques au Canada 1961–1990: Station CHARLO A 47°59′-N 66°20′-O. World Wide Web Address: *http://www.cmc.ec.gc.ca/climate/normals/NBC003.HTM*

HAMES, V., LAUTRIDOU, J.-P., OOZER, A. & PISSART, A. 1987. Variations dilatométriques de roches soumises à des cycles humidification/séchage. *Géographie physique et Quaternaire*, **60**, 345–354.

HAYASHI, M. 1966. Strengh and dilatancy of brittle joint mass: the extreme value stochastic and anisotropic failure mechanism. *Proceeding of the 1st International Congress of the International Society of Rock Mechanics*, **1**, 275–302.

HOCQ, M. & MARTINEAU, G. 1994. Le Quaternaire. *In*: Géologie du Québec, *Les Publications du Québec*, 121–128.

LACROIX, G. & FILTEAU, G. 1969. Les fluctuations quantitatives du zooplancton de la Baie des Chaleurs (golfe Saint-Laurent). I Conditions hydroclimatiques et analyse volumétrique. *Naturaliste Canadien*, **96**, 359–397.

LEBUIS, J. & DAVID, P. P. 1977. La stratigraphie et les événements du Quaternaire de la partie occidentale de la Gaspésie. *Géographie physique et Quaternaire*, **31**, 275–296.

MALO, M. 1994. Analyse structurale des grandes failles acadienne de la Gaspésie. *La Revue Géologique du Québec*, **1**, 21–23.

MARQUIS, R. 1994. Introduction (synthèse des articles présentés dans ce volume). *La Revue Géologique du Québec*, **1**, 5.

MOIGN, A. 1966. Formes sous-marines et littorales de la Baie du Roi, Spitsberg. *Bulletin de l'Association Géographique Française*, **342**, 11–24.

MORNEAU, F., MICHAUD, M., LECOURS, F., CÔTÉ, L. & ROY, D. 2001. *Projets de protection des berges le long de la route 132 autour de la péninsule gaspésienne*. Rapport du Gouvernement du Québec.

MCGERRIGLE, H. W. 1968. The geologic history of the Percé area. Geological Services, Quebec department of natural ressources, P.G.2.

OZOUF, J.-C. 1987. Comparaison de gélifracts naturels de grèzes charentaises et de gélifracts fabriqués. *Thèse de Doctorat de l'Université de Caen, France.*

PISSART, A. & LAUTRIDOU, J. P. 1983. Variation de longueur de cylindres de pierres de Caen (calcaire bathonien) sous l'effet de séchage et d'humidification. *Zeitschrift fur Geomorphologie*, **Supplement Band 49**, 111–116.

PRICK, A. 1996. *La désagrégation mécanique des roches par le gel et l'haloclastie*. PhD thesis, Université de Liège, Belgique.

PRICK, A. 1999. *Étude de la cryoclastie et de l'haloclastie par méthode dilatométrique*. Académie Royale de Belgique.

REID, A., THIBAULT, D., MICHAUD, L., LE GROS, M. & ROSS, N. 1990. *Etude sur la protection du littoral de la Gaspésie et des Iles-de-la-Madeleine*. Projet no: 7430-01-01-00118-00.

REMY, J.-M. 1993. *Influence de la structure du milieu poreux carbonaté sur les transferts d'eau et les changements de phase eau-glace. Application à la durabilité au gel de roches calcaires de Lorraine*. Thèse de Doctorat de l'Institut National Polytechnique de Lorraine, Nancy, France.

SELBY, M. J. 1980. A rock mass strength classification for geomorphic purposes: with tests from Antarctica and New Zealand. *Zeitschrift fur Geomorphologie*, **24**, 31–51.

ST-JULIEN, P., SLIVITZKY, A. & FEININGER, T. 1983. A deep structural profile across the Appalachians of southern Québec. Dans Contributions to the tectonics and geophysics of mountain chains. *Geological Society of America*, **158**, 103–111.

SUNAMURA, T. 1992. *Geomorphology of rocky coasts*. Wiley, Chichester.

SUZUKI, T. 1982. Rate of lateral planation by Iwaki River, Japan. *Transactions of the Japanese Geomorphological Union*, **3**, 1–24.

TREMBLAY, P. & BOURQUE, P. A. 1991. *Géologie du Sud du Québec, du Bas-Saint-Laurent et de la Gaspésie*. Ministère de l'Énergie et des Ressources du Québec, GT 91–03.

TRENHAILE, A. S. 1987. *The Geomorphology of Rock Coasts*. Oxford University Press, Oxford.

TRENHAILE, A. S. & MERCAN, D.W. 1984. Frost weathering and the saturation of coastal rocks. *Earth Surface Processes and Landforms*, **9**, 321–331.

TSUJIMOTO, H. 1987. Dynamic conditions for shore platform initiation. *Science Reports of the Institute of Geoscience, University of Tsukuba*, **A8**, 45–93.

WHALLEY, W. B. 1984. *Rockfalls. Mass Movements on Slopes*, Wiley, Chichester, 217–256.

WILLIAMS, H. 1979. Appalachian orogen in Canada. *Journal Canadien des Sciences de la Terre*, **16**, 792–807.

Index

Page numbers in *italic* refer to figures, page numbers in **bold** refer to tables.

abrasion 110, 111, 153
  ice floes 153, *154*
  shingle 131
    experiments 132–138
Acadian unit, Gaspesian Peninsula 150, 151
aerial photography
  calibration 64
  fracture analysis 60
    data analysis 66–68
  fracture density 64, 66, 67
  French National Geographic Institute 141, *142*
    photogrammetric analysis 142–147
  pre-1986 data analysis 68
air compression 110
Anglo-Paris Basin 14, 37
Anse à Beaufils 158
Antifer 59, 141, 145, 146
Ault 59
Ault-Onival 140

Baie des Chaleurs 149, **151**
  erosion rates 151–153, **152**
Barrois' Sponge Bed 26–27
bathymetry, English Channel 103, 105
beach, raised 24
Beach Erosion of the Rives-Manche (BERM) Project 1, 139
beach platform *see* shore platforms
beaches, sedimentary balance 145, 146
Beachy Head 3, 4, *6*, 9, *11*
  1999 collapse 20–21, 29, 39, *42*, 57, 95–96
  complex cliff failure 17–21, *18*
Beachy Head Anticline 4, *5*, 17
bed sheer stress 110
Belle Tout Beds 9, 11
Bénouville 48, 49
Birling Gap 20, 24
  2001 collapse *42*
Birling Gap Syncline *5*, 9
Black Rock Raised Beach 24
blockwork structures 121, 122, 129
Bois de Cise 37, 59, *63*, 141
Bonaventure Formation 151, 153, 157–161, *162*, 163, 166
bottom-up failure 9, 11, 20, 29
Brazilian Crushing Strength 78
breaker height 123
breaker types 123, 124
breaking, perfect 111, 113
breakwaters 122, 124
Brighton
  Elephant Beds 24
  Marina 24, 29, 77
  Raised Beach 24
bulking 28, 39, 86

Campanian
  Normandy cliffs, flint content 141, 145
  Sussex cliffs *5*
Canada, Baie des Chaleurs, coastal cliff erosion 149
Cap d'Ailly 141
Cap d'Antifer 140
Cap d'Espoir 158
Carboniferous sedimentary unit, Gaspesian Peninsula 150, 151–153
Castrum 5, 22
caves 16, 21, 22, *23*, 29, 37, 94, 111, *112*
cement 159
Cenomanian, Normandy cliffs, flint content 141, 145
Chaleurs Group 153, 155, 157, 161, *162*, 163, 165
chalk
  degraded 24, 28, 83
  density 75, 77, 79, 82
  hardness classification *76*
  lithostratigraphic units *4*, 6
    Normandy 35, *38*, *147*
  moisture content 75–77, 79, 83
  physical properties 75–86, *84*
  porosity 82, *83*, 94
  strength 84
    tests 77–81
  weathering 24
chalk flow 20, 21, 26–28, 95
chatter marks 136
chert 131
clay-with-flints 3, 22, 48
cliff base erosion 111
cliff collapse
  classification 5, 9, **10**, **25**, 38
  French coast 38, **40**, **41**, *42*
    field observation 69–71, *72*
    pre-1986 aerial photo data 68, *69*, *72*
    scale 38
  frequency 28
  geohazards 7, **25**
  identification 5, **9**
  large scale 43
  magnitude 5, **9**, 28, 38
  medium scale 44
  small scale 44
  summary 25
  Sussex Chalk 7, *8*, **25**, *42*
  triggering mechanisms 48
  very large scale 39, 94
  volume estimation 39, 86, 92
  wave attack 100
cliff evolution 33, 141
cliff failure
  Beachy Head type 17
  Birling Gap 24, *42*
  complex 17, *46*, 47
  contributing factors
    cliff height 4, 7, 15, 93
    climate 94
    faults 5
    folds 5

cliff failure (*cont.*)
contributing factors (*cont.*)
joints 94
marine 109
Cow Gap 22
dry valley-fills 24
failure surface 26
Holywell type 12, *15*
Joss Bay type 3, 26, 45
mechanisms 3, 4
Newhaven Castle Hill 22
Peacehaven type *14*, 15
plane and wedge 12–16, 20, 22, 28, 45
Seaford Head 22
Seven Sisters type 9
simple vertical 9, *12*, *13*, 22, 45, *46*
sliding failure type 45, *46*
undefined failure type 47
cliff retreat 29, 33, 48, 57, 90, 109
Baie des Chaleurs 149, 151–153
photogrammetric analysis 141–147
cliff slabbing 28
cliff trimming 29
climate *26*, 29, 48, 49, *51*, 83, 85, 99
coastal evolution, quantification 141
coastal management 99, 139
coastal protection 29, 139
shingle bars 131
coastal structures, wave damage 121
Coin du Banc 153, 161, *163*, **164**, 166
conglomerate 161, **164**, 165
erosion rate 151–153
vulnerability index 166
Coniacian, Normandy cliffs, flint content 141, *143*, 145
Contrat de Plan Interrégional du Bassin de Paris (CPIBP) 139
Cow Gap, Eastbourne 22
cracks, wave pressure propagation 113, 121, 122, 127
Craie de Rouen *see* Rouen Chalk
Cretaceous, Upper, lithostratigraphy 3, *4*, 34
Criel sur Mer 59
Cuckmere Haven 11
Cuckmere River 5, 24
Culver Chalk Formation 3, *5*, 16, 22, 28, 29, *36*, 84

debris run-out 9, 27, 39, 44, 89
Beachy Head 17, 20
Newhaven Castle Hill 22
Went Hill 91–96
Dieppe 48, 59, 141, 145, 146
dip, effect on stability 161
dissolution pipes 20, 22, *23*, 24, 29, 37, 49
drought 49

Eletot 37, 59, 141
English Channel
study area *34*
wave data 100–103
wave energy modelling 101–107
erosion
basal 26, 29, 52, 54, 111, *112*
ice blocks 153, *154*
macroscopic episodic 151
dislocation by sea ice 151
mass movement 151, 153
marine 12, 20, 21, 24, 26, 29, 48, 49, 109–119, *123*
effect of debris run-out 17
river 24
subaerial 109, 110, 119
vulnerability mapping 156–166
erosion rates 29, 33, 99, 122
erosional parameters 156, **158**, **164**
dip of strata 161
effect of wave action 157
faults 161
fractures 161
homogeneity of stratification 160
percentage of matrix/cement 159
porosity 158
presence of groundwater 157
schistosity 160
Etretat 141, 146

fahrböschung *21*, 89
failure *see* cliff failure
faults
effects on erosional vulnerability 161
normal 59, 60, 63, 64, *112*
Seven Sisters 9
strike–slip 5
Fécamp 35, 37, 59, *112*, 141, 145, 146
flint 131, 139
abrasion rates 136, 138
characteristics 137
strength 81, **82**
flint bands 35, 59
flint content of cliffs 141, 145
flow mechanisms 95
flow slide 27–28, 95
flume 113
folding, influence on cliff failure 28
folds 5
Forillon Formation 155
fracture analysis, multiscale 58
fracture density, French coast 64, 66–68, *67*, 72
fracture filling 16, 44
sheet-flint filled 16
fracture patterns *36*, 37, *39*, 60, 94, 154, 9, 16, *see also* joint sets
fractures 57
effect on erosional vulnerability 161
effects of wave pressure 113
French coast 37
aerial photograph analysis 60–69
field observation 69
orientation 37, 59, **60**, 64
typology *39*, 58, **61**
strata bound 59
stress-release 59
synsedimentary 59
freeze-thaw cycle 83, 149, 150, 154–155, 157, 165
French cliffs
coastal erosion management 139
instability 33
late Cretaceous succession 34
retreat 141–147
Friar's Bay Anticline *5*
frost *see* freeze-thaw cycle

Gascon 163
Gaspé Sandstone Sequence 153, 155, 159, 161
Gaspesian Erosion Project 166
Gaspesian Peninsula
  cliff erosion 149
  geology 150–151
Gault 3, 22
geohazards 3, 5, 7, *8*, **9**, **25**
  classification **10**
geology, Sussex cliffs 3
geomorphology, chalk cliffs *6*, *7*, 109–110
Glauconitic Marl 22
Glynde Marl 14
Grande Dalles, 2001 collapse 39, *42*, 45, 48, 49
Greensand, Upper 22
Grey Chalk Subgroup 14, 17
groundwater 37, 157
Gun Gardens 17, 20
gypsum precipitation 84

H/L value 89, 95
hazard identification 5
hazard mapping 1, 6, **10**, 99
Head Ledge 17, 22
hill wash 24
Holywell Cliffs 12, *15*
Holywell Nodular Chalk Formation 12, 14, *15*, 17, 20, *36*
  France 35, 37
Hope Gap 22, 24
hydraulic action 111
hydraulic model tests 124

ice, sea, effect on cliffs 149, 151, 153
ice blocks, collapse 153, *154*
ice floes 149, 153
ice heave 83
ice walls, collapse 153, *154*
Indian Point Formation 155, 157, 160, 161, *162*, 163, 165
Intact Dry Density (IDD) 75, *76*
Iribarren number 123

Jevington Fault *5*, 22
joint sets
  open conjugate 14
  steeply inclined conjugate 11, 12–16, *16*, 20, 22, 28
  vertical 9, *12*, 20
  see also fracture patterns
joint spacing 122, 153
joints 59
  wave impact 121
Joss Bay 3, 26

karst features
  France 37, 49
  Sussex 22

Lancing Flint Band 28
landslides, rotational 22
Le Tilleul 37, 59
Le Tréport 47, 141, 145, 146
Lewes Nodular Chalk Formation 9, 20, 22, *36*
  France 35, 37
limestone 155, 159, 161, 163, **164**
  erosion rate 151–153
  vulnerability index 165
lithostratigraphy *4*, 34, *38*
loess 3, 24, 141
longshore drift 131, 139, 145

macro tidal effects 113
Major Fracture Type (MFT) 66–68
mapping, geohazard 1, 6, **10**, 99
Maquereau Group 151, 153, 155, *159*, 160, 161, 165
Margate Chalk 26
marl seams 22, 28, 35, 59
mass movement 153
master-joints 59, 60, 63, 64
matrix 159
mean drop gradient 89
Melbourne Rock 14, 20
micro-organisms 110
mineral precipitation 84
modelling
  mathematical, wave energy 99, 101–107
  tidal effects on cliff 113
  wave impact pressure propagation 124
mudslides 22, 28
Murphy Creek Formation 151, 157, 163, 165

Natural Moisture Content (NMC) 75, *76*
New Pit Chalk Formation 14, 20, *36*
  France 35, 37
Newhaven Castle Hill 22
Newhaven Chalk Formation *5*, *7*, 29, *36*
  France 35, 37
  P-wave velocity profile 84, *85*, *86*
  plane and wedge failure 15, 16
Newhaven Fault *5*
Newhaven Syncline 2, *5*, 28, 29
Normandy cliffs
  cliff retreat 143–147
  flint abrasion rates 134–138
  flint content 141, 145
  fracture analysis 57
Normandy, Haute, chalk lithology 35, 140–141, 146
notch, wave-cut 20, 26, 29, 52, 54, 111, *112*, 157, 160, *162*, 163

Old Nore Beds 77
Old Steine Anticline *5*, 29
Ouse River 5
overhangs 9, 52, 153, 154

Palaeogene deposits 22, 29, 141
Peacehaven Cliffs 15–16
  2001 collapse *14*, *42*, 45
Peacehaven Coast Protection Works 29, 84, *86*
Penly 141
Percé Point 151, 158, 161, 163
periglacial processes 24, 28
Petites Dalles 37, 45, 48, 59
photogrammetric analysis 142–147
photogrammetric surveys (IGN) 139
Picardy cliffs
  chalk lithology 35, 140–141
  cliff retreat 143–147

Plenus Marls 14, 17, 18, 20
Point Load Test (PLT) 77
pore water
  chemistry 84
  pressure 95
porosity 94, 158
Port-Daniel 163, 165
Portobello 28, 29
postcards, Seven Sisters cliff fall 1914 *91*, *92*, *93*
Pourville 48, 141
Puys 141
  Lewes Chalk *13*
    2000 collapse 39, *42*, 45, 49, *53*, 57

quartzite 150–153, 155, 161, 165
Quaternary
  periglacial processes 24, 28, 29
    clay-with-flints 3
Quebec Ministry of Transport 149
Quiberville 141
Quiberville, Newhaven Chalk *16*, 59

rainfall 29, 48, 49, *51*, *52*, 94
raised beach, Brighton 24
ravelling 29
river terrace deposits, Cuckmere 24
ROCC (Risk of Cliff Collapse) Project 1, 33, 99
  database 2, 6, 24, **40**, **41**
rock disintegration experiments 154–156
rock mass character 6, 9, **25**, 81, 84
rock mass data 6
rock slope failure 7
rock strength 122
Rouen Chalk 35, *36*, 37
run-out *see* debris run-out

Sainflou model 115, 119
St Aubin, Seaford Chalk *13*
St Martin Plage, New Pit Chalk *16*, 47
St Pierre en Port *13*, 59, *71*
St Valéry en Caux 37, 45, 141, 145, 146
  2001 collapse *42*
salt precipitation 84, *85*, 110
salt weathering 110, 111, 154–155
sandstone 161, **164**
  erosion rate 151–153
  vulnerability index 165–166
Santonian
  Normandy cliffs, flint content 141, *143*, 145
  Sussex cliffs *5*
Saturation Moisture Content (SMC) *76*, 77
scan-line surveys 6
scars 39, 44, 45, 57
schist 150–153, 155, 160, **164**, 165
schistosity 160
sea bed slope 123
sea level rise 29, 99
Seaford Chalk Formation 4, *5*, *7*, 9, *11*, 20, *36*, 77, 83
  France 35, 37
Seaford Head 22, *23*
Seaford Head Anticline 5
Seaford Syncline *5*
sediment, metastable 24
sediment accumulation 117
sedimentary balance 145, 146
Senneville sur Fécamp , New Pit Chalk *16*, 59
Seven Sisters 9, *12*, 45, 90
  1914 collapse 89, 91–96
  erosion 90
sheet flints 16, 22, 24
shingle
  bars 131
  movement 131
    experiments 132–138
  potential production 145, 146
  role in erosion 113, 116, 119
Shooters Bottom 9, *11*
shore platforms 24, 59, 131
  erosion 110, 111, 117–118
shoreline evolution surveys 139
siltstone 155, 160
solifluction 24
Sotteville 141
spalling 7, 11, 14, 22, 28
Splash Point 28
springs 37
storm prediction 99
storm surges 111
strata-bound fractures 59
stratification, homogeneity 160
stratigraphy
  chalk *4*, 34
    Haute Normandy 146
stress release fractures 59
sturzstrom 95
surf similarity parameter 123
Sussex cliffs
  collapse hazards *8*, **25**
  flint abrasion rates 134–138
  late Cretaeous succession 3, *4*, *5*
synsedimentary fractures 59, 64, 66

Taconian unit, Gaspesian Peninsula 150, 151
Telscombe Cliffs 29
tension crack 9, 26, 89
tides 94, 110, 111
  macro tidal effects 111, 113
toe erosion 117, 121
top-down failure 9, 11
Total Fracture Type (TFT) 66–67
tumbling, flint shingle abrasion experiments 132–138
Turonian
  Normandy cliffs, flint content 141, *143*, 145
  Sussex cliffs *5*

undercutting *123*
Undrained Triaxial Test 80, **82**, 85
Uniaxial Compressive Strength (UCS) 79

valley-fill 24
valleys, dry 'hanging' 24, 90, 140
Valpollet, Seaford Chalk *13*
Veules-les-Roses, Newhaven Chalk *16*, 37, 48, *112*
Veulettes sur Mer, Seaford Chalk *13*, 37
  2001 collapse 39, *42*
vulnerability diagrams 156

water depth 111
water hammer 110
water layer weathering 110
wave, breaking 111, 122, 123
wave action 49, 111, 123, 157
wave data, English Channel 100, *102*
wave dissipation 118
wave energy
  distribution 103, 109
  modelling 99, 101–107
Wave Energy Risk Factor 103
wave flume 113
wave height *104*, **104**, *105*
wave impact pressure propagation 113, 121, 124, 125
wave measurement 113
wave pressure 111, 115–116
wave reflection 111, 117
wave shock 110
wave tank 124
wave-cut notch 26, 29, 52, 54
wave-cut platform 19, 20, 24, 28, 110
  Beachy Head 20
weathering 21, 24, 29, 83, 84
  subaerial 110
wedge action 111
Went Hill, Seven Sisters 91–96
West Melbury Marly Chalk Formation 17, 22
wetting-drying 49, 110, 154–155, 165
White Chalk Subgroup 20
White Head Formation 153, 155, 157, *159*, 161, *162*, 163, 165

Yport, 2001 collapse 37, 48, *53*, 57

Zig Zag Chalk Formation 17, 20, *36*